Performance Analysis of MIMO Relay Networks with Beamforming

by

Hyunjun Kim

A Dissertation Presented in Partial Fulfillment
of the Requirements for the Degree
Doctor of Philosophy

Approved July 2012 by the
Graduate Supervisory Committee:

Cihan Tepedelenlioglu, Chair
Tolga M. Duman
Yu Hui
Junshan Zhang

ARIZONA STATE UNIVERSITY

August 2012

ABSTRACT

This dissertation considers two different kinds of two-hop multiple-input multiple-output (MIMO) relay networks with beamforming (BF). First, "one-way" amplify-and-forward (AF) and decode-and-forward (DF) MIMO BF relay networks are considered, in which the relay amplifies or decodes the received signal from the source and forwards it to the destination, respectively, where all nodes beamform with multiple antennas to obtain gains in performance with reduced power consumption. A direct link from source to destination is included in performance analysis. Novel systematic upper-bounds and lower-bounds to average bit or symbol error rates (BERs or SERs) are proposed. Second, "two-way" AF MIMO BF relay networks are investigated, in which two sources exchange their data through a relay, to improve the spectral efficiency compared with one-way relay networks. Novel unified performance analysis is carried out for five different relaying schemes using two, three, and four time slots in sum-BER, the sum of two BERs at both sources, in two-way relay networks with and without direct links.

For both kinds of relay networks, when any node is beamforming simultaneously to two nodes (i.e. from source to relay and destination in one-way relay networks, and from relay to both sources in two-way relay networks), the selection of the BF coefficients at a beamforming node becomes a challenging problem since it has to balance the needs of both receiving nodes. Although this "BF optimization" is performed for BER, SER, and sum-BER in this dissertation, the solution for optimal BF coefficients not only is difficult to implement, it also does not lend itself to performance analysis because the optimal BF coefficients cannot be expressed in closed-form. Therefore, the performance of optimal schemes through bounds, as well as suboptimal ones

such as strong-path BF, which beamforms to the stronger path of two links based on their received signal-to-noise ratios (SNRs), is provided for BERs or SERs, for the first time. Since different channel state information (CSI) assumptions at the source, relay, and destination provide different error performance, various CSI assumptions are also considered.

To

my wife, Jungae An, and my daughters, Minhye Kim and Minseo Kim,

for their love and support

ACKNOWLEDGEMENTS

Ever since I started studying at Arizona State University (ASU), I have been indebted to many people for their advice, guidance, and support. This dissertation is dedicated to all of them.

First of all, I would like to express my deepest appreciation to my ideal advisor Dr. Cihan Tepedelenlioğlu for his advice and patience during the course of my Ph.D. research. His coaching with criticism, open-mindedness, and understanding has made me progress to this end in a delightful manner. His enthusiasm towards work and insights in research have made him a creative role model for me. I would also like to express my appreciation to my former advisor Dr. Tolga M. Duman for his priceless advice since the beginning of my Ph.D. studies.

Second, I would like to show my sincere thanks to my committee members as well: Dr. Tolga M. Duman, Dr. Joseph Y. Hui, and Dr. Junshan Zhang. Their encouragement and support have played an important role in my Ph.D. dissertation. My appreciation also goes to my colleagues, with whom it has been the most pleasant journey in my life. In particular, Yuan Zhang and Mahesh Banavar have been of huge help in my Ph.D. research.

Finally, I would love to extend my warmest gratitude to my family: My wife, Jungae An, and my children, Minhye Kim and Minseo Kim, who have always been my source of joy and strength. I will never forget their love and support, but I doubt that I will ever be able to convey my appreciation fully to them. I also wish to thank my mother-in-law and sisters-in-law, who have provided my family with all kinds of help and support during my graduate studies.

TABLE OF CONTENTS

LIST OF TABLES

LIST OF FIGURES

Chapter 1

Introduction

In this chapter, background preliminaries for this dissertation are briefly described, which are multiple antenna systems, cooperative diversity systems, and performance metrics. Contributions of this dissertation are listed with their organization as well.

1.1 Background

Wireless communications is one of the fastest growing industries over the last decades. The recent number of cellular and wireless network users worldwide indicates rapid growth of business in wireless systems. Nowadays, wireless users require more applications, such as peer-to-peer (P2P) file sharing, online gaming, and multimedia. At the same time, there exists increasing user demand for more bandwidth, broader coverage, and better mobility support, which establishes a trend of significant increase in traffic volume in wireless networks. To support users' demand for high data rates in a reliable manner, one solution is to consider spatial diversity using multiple antennas at the transmitter and receiver, and cooperative diversity using using relays between the transmitter and receiver, which are considered throughout the dissertation.

1.1.1 MIMO Systems

Systems using multiple antennas at the transmitter and receiver are referred to as multiple-input multiple-output (MIMO) systems, illustrated in Figure 1.1. MIMO antenna systems take advantage of the spatial diversity to combat a severe fading environment due to their excellent link reliability [1]

since the first paper was presented by Winters in 1987 [2]. MIMO systems' high throughput with reliability, spectral efficiency, and degrees of freedom makes them a powerful candidate of the 4^{th} generation (4G) wireless communications standards [3]. All 4G candidates such as long term evolution advanced (LTE-Advanced) and worldwide inter-operability for microwave access (WiMAX) (i.e. IEEE 802.16m) adopt MIMO [4] to achieve peak data rates of 100 Mbps for high mobility and 1 Gbps for low mobility, according to the international mobile telecommunications advanced (IMT-Advanced) requirements [5].

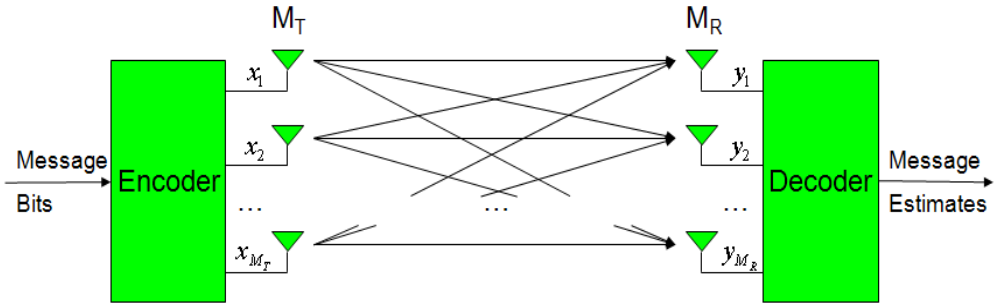

Figure 1.1: A Simple Block Diagram of a MIMO System.

The combination of maximum ratio transmission (MRT) beamforming (BF) [6], and maximum ratio combining (MRC) beamforming [7] is one simple way to achieve spatial diversity if full channel state information (CSI) is available at the transmitter and receiver for the MIMO antenna technology. Since BF produces or receives a narrow wireless beam, it requires less power for the same distance compared to a single antenna system, creates or receives less interference to or from others, and increases reliability for transmission or reception. Various BF techniques are considered and deployed with MIMO using multiple directional antenna elements to utilize BF advantages in wireless standards such as wireless local area network (WLAN) (i.e. IEEE 802.11n) [8], LTE-Advanced [9], and WiMAX [10].

1.1.2 Cooperative Diversity Systems

To support tremendous wireless traffic volume with high reliability and broader coverage, cooperative diversity schemes, using relays between the source and destination, have been widely investigated because of their spatial diversity and extensive coverage with reduced power consumption [11–13], which are also referred as to relay networks.

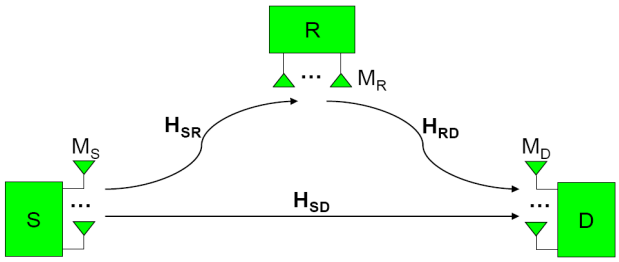

Figure 1.2: A Two-Hop One-way Relay Network using Multiple Antennas.

1.1.2.1 One-way Relay Networks

Figure 1.2 shows a two-hop one-way relay network using multiple antennas at all nodes. Amplify-and-forward or decode-and-forward (AF/DF) one-way relaying using two time slots is known to offer gains in performance when the destination keeps apart from the source, in which the relay and destination receive the transmitted signal from the source in the first time slot, and the relay amplifies or decodes and forwards the transmitted signal, and the destination receives the relayed signal while the source remains silent in the second time slot [11–13]. To support IMT-Advanced data rate requirements, 4G networks should reduce the cell sizes to decrease power consumption compared with existing systems (i.e. 3^{rd} generation (3G) networks). Additionally, high speed features cannot be valid indoors because of building penetration

loss [14]. To overcome these problems, 4G standards such as LTE-Advanced and WiMAX support AF/DF multi-hop relay systems to extend service area and to improve data rates indoors [15–18].

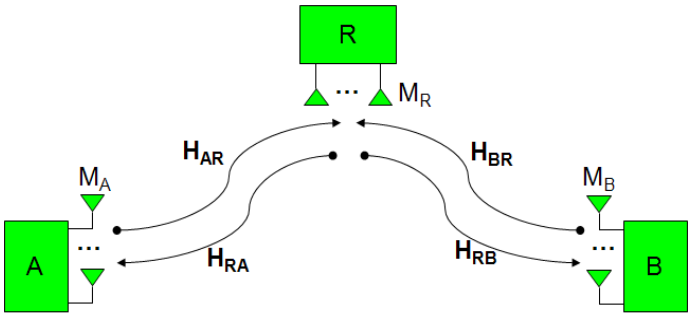

Figure 1.3: A Two-Hop Two-Way Relay Network using Multiple Antennas.

1.1.2.2 Two-way Relay Networks

Even though one-way relaying provides spatial diversity and extensive coverage with reduced power consumption, it causes a spectral loss due to more use of time slots. To improve the spectral efficiency in two time slots, two-way relaying is suggested as illustrated in Figure 1.3, in which two sources transmit simultaneously their signals to the relay in the first time slot (i.e. multiple access phase), and the relay amplifies or decodes transmitted signals and forwards the combined signals to the sources in the second time slot (i.e. broadcast phase) [19–21]. Unlike one-way relay networks, however, one problem of this two-slot two-way network is that it cannot utilize the full potential of relay networks by neglecting possible direct links. To exploit the presence of direct links in two-way relay networks as illustrated in Figure 1.4, three or four time slots are necessary, which is discussed in this dissertation. Relay architectures including one-way and two-way relaying are investigated using

the present standards such as LTE-Advanced and WiMAX in the literature to deploy relays efficiently in cellular systems [22, 23].

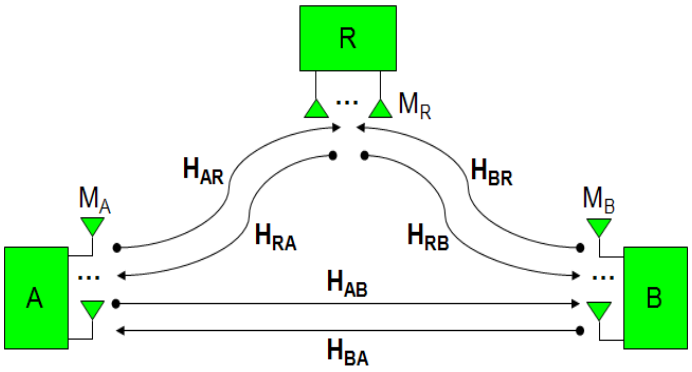

Figure 1.4: A Two-hop Two-Way Relay Network using Multiple Antennas with Direct Links.

1.1.3 Performance Metrics

Regardless of systems, theoreticians in wireless communications have presented their systems' performance in the form of closed-form expressions. To provide results in closed-form, the performance metrics of interest should be clearly defined. Since the advent of wireless communications, one of the performance metrics of interest has been the average probability of error, which can be either a bit error rate (BER) or symbol error rate (SER) averaged across fading channels. When memoryless modulated signals are transmitted and corrupted over an additive white Gaussian noise (AWGN) channel, the instantaneous error rate can be represented, or approximated by the well-known Gaussian Q-function, in which the performance of communication systems depends solely on the received signal-to-noise ratio (SNR). In addition, if a physical phenomenon such as signal attenuation by lossy channels is considered, the attenuated signal passed through the channel affects the performance

of communication systems. Hence, the additive noise and signal fading play a major role in the performance of communication systems [7, 24–26].

The main interest of this dissertation is the average probability of error defined as follows:

$$P_E = \mathbb{E}_X \left[aQ\left(\sqrt{2bX}\right)\right] = \int_0^\infty aQ\left(\sqrt{2bx}\right) f_X(x)dx, \tag{1.1}$$

where $Q(x) := \left(1/\sqrt{2\pi}\right)\int_x^\infty e^{-y^2/2}dy$ [7,24–26], $\mathbb{E}_X[\cdot]$ denotes expectation with respect to X, a and b are modulation related positive constants, and P_E could be either BER or SER by depending on the choice of a and b. For example, $a = 1$ and $b = 1$ provide exact SER for binary phase shift keying (BPSK), while $a = 2$ and $b = \sin^2(\pi/M)$ and $a = 4\left(1 - 1/\sqrt{M}\right)$ and $b = 3/(2(M - 1))$ provide tight SER approximations for M-ary PSK (M-PSK) and M-ary quadrature amplitude modulation (M-QAM), respectively [7, 24, 27]. Since the tightness of these approximations for different values of a and b are well-studied in the literature, equation (1.1) is used as the metric of the average probability of error throughout the dissertation. For another performance metric of average error rates, sum-BER, sum of BERs at destination nodes, is considered, since there are two receiving nodes and the worse one dominates the sum in two-way relay networks. Sum-BER is defined as follows:

$$P_b = \frac{1}{\log_2(M)}\int_0^\infty aQ\left(\sqrt{2bx}\right)\left(f_{X_1}(x) + f_{X_2}(x)\right)dx. \tag{1.2}$$

Communication systems are designed to transmit various information from sources to destinations. The channel capacity quantifies the maximum data rates of information transmitted over the channels with arbitrary low error probability. Therefore, the channel capacity is another excellent performance metric of communication systems. Especially, the ergodic capacity can be considered when the channel is ergodic over AWGN, in which the channel coefficients vary in time and they can be averaged over their statistics with

coding with large blocks of data [7, 24, 28]. If the channel is random and ergodic and the CSI is known at the receiver only, the MIMO channel capacity with the equal transmit power allocation technique is given by

$$C = \mathbb{E}_H \left[\log \left(\det \left(\mathbf{I}_{M_R} + \frac{\rho}{M_T} \mathbf{H}^H \mathbf{H} \right) \right) \right], \tag{1.3}$$

where M_T and M_R are the number of transmit and receive antennas, respectively, ρ is average transmit SNR, and $(\cdot)^H$ represents a complex Hermitian. Based on this ergodic capacity, maximum ergodic sum-rate for two-way relay networks is defined as follows:

$$R = \frac{1}{T} \int_0^\infty \log_2(1+x) \left(f_{X_1}(x) + f_{X_2}(x) \right) dx, \tag{1.4}$$

where T is the number of time slots used.

1.2 Contributions of Dissertation

In this dissertation, we have considered two different kinds of two-hop MIMO relay networks with BF. First, one-way AF and DF MIMO BF relay networks are considered, in which the relay amplifies or decodes the received signal from the source and forwards it to the destination, respectively, where all nodes conduct BF with multiple antennas to obtain gains in performance with reduced power consumption when the destination keeps apart from the source. A direct link from source to destination is included in performance analysis since there are no existing closed-form expressions for BERs or SERs, which are provided herein using novel proposed systematic upper-bounds and lower-bounds. Second, two-way AF MIMO BF relay networks are investigated, in which two sources exchange their data through a relay, to improve the spectral efficiency compared with one-way relay networks. Novel unified performance analysis is carried out for various different relaying schemes using two, three,

and four time slots in sum-BER, the sum of two BERs at both sources, in two-way relay networks with and without direct links.

For both kinds of relay networks, when beamforming to two nodes simultaneously (i.e. from source to relay and destination in one-way relay networks, and from relay to both sources in two-way relay networks), the selection of the BF coefficients at a beamforming node becomes a challenging problem since it has to balance the needs of both receiving nodes. Although this BF optimization is discussed for BER, SER, and sum-BER in this dissertation, the solution for optimal BF coefficients not only is difficult to implement, it also does not lend itself to performance analysis because the optimal BF coefficients cannot be expressed in closed-form. Therefore, the performance of optimal schemes through bounds, as well as suboptimal ones such as strong-path BF, which beamforms to the stronger path of two links based on their received SNRs, is provided for BERs or SERs, for the first time. Since different CSI assumptions at the source, relay, and destination provide different error performance, various CSI assumptions are also considered.

Based on published literature, our contributions can be listed in three categories, one-way relay networks, average performance bounds, and two-way relay networks. For one-way relay networks, our contributions are as follows:

- Strong-path BF, the source beamforms to the stronger of $S \rightarrow D$ and $S \rightarrow R \rightarrow D$, is analyzed in AF/DF MIMO one-way relay networks with both known and unknown CSI assumptions, for the first time, and we show that it outperforms the optimized BF performance at high SNR.

- When the CSI on $S \rightarrow R$ and $R \rightarrow D$ is unknown at the destination and source, respectively, a novel selection relaying that does not require threshold optimization is presented.

- A novel combined lower-bound is investigated for AF/DF MIMO BF relaying networks with known CSI of the relay link at the source and destination, and we show that the lower-bound is achievable at the expense of a rate penalty.

- New high SNR performance is analyzed for lower-bound and strong-path BF with AF MIMO one-way relay networks.

For average performance bounds, our contributions can be listed as follows:

- Novel average performance bounds are obtained for systems with instantaneous SNRs given by a sum of N statistically independent (but not necessarily identically distributed) non-negative random variables (RVs) by the product of single integral expressions using the arithmetic mean (AM) and geometric mean (GM) inequality.

- The tightness of the bounds is evaluated analytically at high SNR, and the SNR gap between the bounds and the true error rate is shown to go to zero as the number of RVs N increases.

- Tight closed-form combined expressions for AF relay networks with multiple relays and AF MIMO BF relay networks with multiple antennas are obtained, for the first time in the literature.

- The mathematical technique used to obtain the bounds is applied to non-Gaussian Middleton's class-A noise, for the first time.

For two-way relay networks, this dissertation contributes as follows:

- Novel closed-form sum-BER expressions are presented in a unified framework for AF MIMO two-way relaying protocols with BF.
- This is the first dissertation dealing with performance analysis of AF MIMO two-way relay networks using BF with multiple relay antennas, to the best of our knowledge.
- Two novel two-way relaying protocols are proposed using three or four time slots, and we show that two proposed protocols outperform existing protocols in sum-BER at high-SNR.
- New closed-form high-SNR sum-BER performance is provided in a single expression for five AF MIMO BF two-way relaying protocols. A novel analytical high-SNR gap expression between the five different protocols is provided.
- Novel unified average combined sum-BER approximations in closed-form for AF MIMO BF two-way relay networks including direct links.
- New unified combined high SNR performance is presented for AF MIMO BF two-way relay networks including direct links.
- This dissertation is first literature applying the theory of stochastic orders to compare two average sum-BERs and sum-rates for AF MIMO BF two-way relay networks with and without direct links.

1.3 Dissertation Organization

The remainder of this dissertation is organized as follows. In Chapter 2, strong-path BF as a sub-optimal scheme is analyzed, in which the source beamforms to the stronger of the direct and relay links depending on their received SNRs at the destination, in AF/DF MIMO fixed one-way relay networks when the CSI of the relay link is both known and unknown at the source and destination. Novel upper-bounds for strong-path BF are presented when the CSI of the relay is known at the source and destination. A new selection relaying scheme with strong-path BF is proposed when the CSI of the relay link is not fully known at the source and destination. High SNR performance is also analyzed for AF relay networks to simplify the strong-path BF performance via diversity and array gain expressions. Performance comparisons are presented among these schemes with simulation and analytical results.

In Chapter 3, a novel lower-bound of AF/DF MIMO relay networks is presented with known CSI of the relay link at the source and destination. It is shown that the lower-bound is achievable at the expense of a rate penalty, and the achievable scheme using three time slots is analyzed for AF/DF MIMO fixed two-hop relay networks. When the CSI of the relay link is not known at the source and destination, selection relaying is considered. High SNR performance is analyzed for AF relay networks to simplify the lower-bound via diversity and array gain expressions. The optimal SNR threshold is analyzed for selection relaying. Comparisons are presented between strong-path BF and selection relaying with a corresponding lower-bound using simulation and analytical results.

In Chapter 4, novel average BER/SER bounds are obtained for systems with instantaneous SNRs given by a sum of N statistically independent non-negative random variables (RVs). Their tightness is quantified analytically at high SNR by calculating the SNR gap, and shown to be within $O(1/N)$ of the true value. The bounds are most useful when the distribution of the sum is intractable, since they do not require finding the combined probability density functions (PDFs) or cumulative distribution functions (CDFs) of the sum. The bounds are illustrated with the MRC, the combined average performance for AF relay networks using multiple relays, and AF MIMO single relay systems with BF using multiple antennas at the source, relay, and destination. In addition, applicability of the bounds to non-Gaussian noise is addressed, and the tightness of the bounds is confirmed graphically.

In Chapter 5, unified performance analysis is conducted for AF MIMO BF two-way relay networks with five different relaying protocols. Two novel relaying protocols are introduced using three and four time slots suitable for BF over the existing relaying protocols. As a result, unified CDFs are provided for unified RVs attained from the five different relaying protocols, and the closed-form unified sum-BER expression is obtained. Due to simplicity, high SNR performance expressions are presented for sum-BER, and the analytical high-SNR gap expression is provided. BF optimization is also discussed for sum-BER since multiple antennas are used at all nodes. We investigate the performance of the five protocols using the metric of sum-BER, and show that the proposed three-slot and four-slot protocols outperform the existing two-slot, three-slot, four-slot protocols in sum-BER for some practical scenarios with beamforming, while the two-slot protocol is better than the proposed protocols when a single relay antenna is used.

In Chapter 6, unified performance analysis and stochastic ordering have been carried out for AF MIMO BF two-way relay networks with direct links in Rayleigh fading. Novel average combined sum-BER performance is provided in closed-form with a simple expression for three different protocols. New unified high SNR performance is also presented for its simplicity, and all performance is compared by simulations. In addition, Stochastic ordering of average sum-BER and maximum sum-rate is presented using the unified expressions of AF MIMO BF two-way relay networks with and without direct links. It can be seen that all protocols with direct links dominate the two-slot protocol without direct links, and the four-slot protocol outperforms other protocols at high-SNR when direct links cannot contribute much to the total performance if average transmit SNRs are unbalanced, whereas the three-slot protocol outperforms other protocols at high-SNR otherwise. In addition, stochastic ordering can compare two average quantities even when the average performance is not tractable in closed-form, and it is shown that a large Los parameter K can provide better performance in sum-BER and sum-rate for all two-way relay protocols.

Finally, Chapter 7 concludes this dissertation based on the results obtained from Chapter 2 to Chapter 6.

Chapter 2

Performance Analysis of AF/DF MIMO Relay Networks with Strong-Path Beamforming

Two-hop multiple-input multiple-output (MIMO) relay networks with beamforming (BF) are considered such as Figure 2.1, in which a source node transmits its signals to a destination node aided by a relay node, when the source and destination conduct BF with multiple antennas, to obtain gains in performance with reduced power consumption if the destination keeps apart from the source. Amplify-and-forward (AF) and decode-and-forward (DF) relaying schemes are considered, in which the relay amplifies or decodes the received signals from the source and forwards them to the destination, respectively.

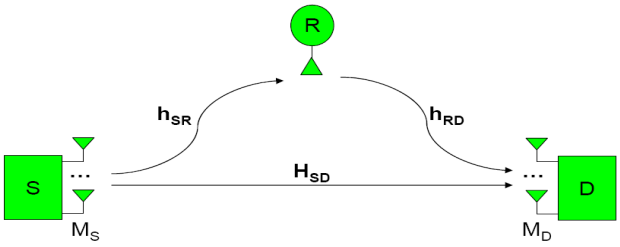

Figure 2.1: Relay Network System Model.

When BF to both relay and destination, the selection of the BF coefficients at the source becomes a challenging problem since the source has to balance the needs of the relay and destination, which is called BF optimization. However, the solution for optimal BF coefficients not only is difficult to implement, it also does not lend itself to performance analysis because the optimal BF coefficients cannot be expressed in closed-form. Therefore, the performance of optimal schemes through suboptimal ones such as strong-path BF

is provided in bit or symbol error rates (BERs/SERs), for the first time. Since different channel state information (CSI) assumptions at the source, relay, and destination provide different error performance, various CSI assumptions are also considered.

In this chapter, strong-path BF, which beamforms from the source to the stronger path of direct and dual-hop relay links based on their received signal-to-noise ratios (SNRs) at the destination, is analyzed in AF/DF MIMO fixed one-way relay networks with both known and unknown CSI assumptions. BF in AF/DF relay networks has been studied in the following works. A closed-form lower-bound of an AF relay link is provided for a single relay antenna with multiple source and destination antennas in [29]. A BER expression is presented for a MIMO link in [30]. Combined optimized BF performance is given by using the finite Grassmannian BF vectors in [31].

In BF relay networks, the beamformer at the source has to be selected depending on the channels of the direct and relay links. An optimal BF vector is acquired by using the gradient ascent method with finite Grassmannian initial points maximizing combined received SNR, resulting in a complex non-convex iterative problem [31]. It is of interest to investigate BF schemes that are simple to implement and novel analytical upper-bounds for AF/DF relay networks since there is no a closed-form solution of the optimized BF scheme in [31]. In strong-path BF, only one BF vector for a stronger path is used for direct and relay links based on their received SNRs. Strong-path BF has been introduced without analysis in [31], which we provide herein. When the CSI on $S \rightarrow R$ and $R \rightarrow D$ is unknown at the destination and source, respectively, a novel selection relaying scheme that does not require threshold optimization is adopted, and compared with our extension of traditional selection relaying

schemes with a threshold [11]. In addition, high SNR performance is analyzed since the strong-path BF performance are complicated and cannot be written in closed-form.

2.1 System Model

Figure 2.1 shows the system which consists of a source S, a relay R, and a destination D. The source and destination are equipped with multiple antennas M_S and M_D while the relay uses a single antenna. The half-duplex scenario with a two-slot scheme is considered, in which the relay and destination receive the transmitted signal from the source in the first time slot, and the relay amplifies/decodes and forwards the transmitted signal from the source and the destination receives the relayed signal while the source remains silent in the second time slot [11].

All CSI is assumed to be known to connected nodes. For example, $\mathbf{H}_{SD}$ is known only to the source and destination but not to the relay. The exception is knowledge of $\mathbf{h}_{RD}$ at the source and of $\mathbf{h}_{SR}$ at the destination, whose presence or absence is both considered herein. The BF vector is chosen based on if the relay link or the direct link is better in terms of the instantaneous received SNR.

The received signals using MRT and MRC of the direct and relay links at the destination for AF relaying are as follows:

$$y_{SD} = \sqrt{\rho_{SD}}\mathbf{c}_{SD}^H\mathbf{H}_{SD}\mathbf{f}_{SD}x + \mathbf{c}_{SD}^H\mathbf{n}_{SD} \tag{2.1}$$

$$\begin{aligned} y_{SRD} = &\frac{\sqrt{\rho_{SR}\rho_{RD}}\mathbf{c}_{RD}^H\mathbf{h}_{RD}f_{RD}c_{SR}^*\mathbf{h}_{SR}^T\mathbf{f}_{SR}x}{\sqrt{1+\rho_{SR}\|\mathbf{h}_{SR}^T\mathbf{f}_{SR}\|^2}} \\ &+ \frac{\sqrt{\rho_{RD}}\mathbf{c}_{RD}^H\mathbf{h}_{RD}f_{RD}c_{SR}^*n_{SR}}{\sqrt{1+\rho_{SR}\|\mathbf{h}_{SR}^T\mathbf{f}_{SR}\|^2}} + \mathbf{c}_{RD}^H\mathbf{n}_{RD}, \end{aligned} \tag{2.2}$$

where ρ_{SD}, ρ_{SR}, and ρ_{RD} are average transmit SNRs, $\mathbf{c}_{SD}$ $(M_D \times 1)$, c_{SR} (1×1), and $\mathbf{c}_{RD}$ $(M_D \times 1)$ are MRC combining weight vectors or scalars with Euclidean norm 1; $\mathbf{H}_{SD}$ $(M_D \times M_S)$, $\mathbf{h}_{SR}$ $(M_S \times 1)$, and $\mathbf{h}_{RD}$ $(M_D \times 1)$ are channel coefficient matrices or vectors, assumed to be i.i.d. $CN(0,1)$; $\mathbf{f}_{SD}$ $(M_S \times 1)$, $\mathbf{f}_{SR}$ $(M_S \times 1)$, and f_{RD} (1×1) are BF vectors or scalars with norm 1; $x \in \{\pm 1\}$ is BPSK with $\mathbb{E}[|x|^2] = 1$ and $\mathbb{E}[x] = 0$, $\mathbf{n}_{SD}$ $(M_D \times 1)$, n_{SR} (1×1), and $\mathbf{n}_{RD}$ $(M_D \times 1)$ are noise vectors or scalars distributed $CN(0, \mathbf{I})$ where $\mathbf{I}$ is the identity matrix, $(\cdot)^H$ denotes a vector Hermitian, $(\cdot)^*$ represents a complex conjugate, and $(\cdot)^T$ denotes a vector transpose. Variables c_{SR}, f_{RD}, and n_{SR} are scalars since the relay has a single antenna, which means there is no BF at the relay.

The received signals using MRT and MRC of the direct and relay links at the destination for DF relaying are as follows:

$$y_{SD} = \sqrt{\rho_{SD}}\mathbf{c}_{SD}^H \mathbf{H}_{SD}\mathbf{f}_{SD}x + \mathbf{c}_{SD}^H \mathbf{n}_{SD} \tag{2.3}$$

$$y_{SRD} = \sqrt{\rho_{RD}}\mathbf{c}_{RD}^H \mathbf{h}_{RD} f_{RD}\hat{x} + \mathbf{c}_{RD}^H \mathbf{n}_{RD}, \tag{2.4}$$

where $\hat{x}$ is the maximum likelihood (ML) decoded symbol from $y_{SR} = \sqrt{\rho_{SR}}$ $c_{SR}^* \mathbf{h}_{SR}\mathbf{f}_{SR}x + c_{SR}^* \mathbf{n}_{SR}$ at the first time slot.

The combined received signals for AF and DF relaying using equations (2.1)-(2.4) can be written as

$$y = a_{SD}\, y_{SD} + a_{SRD}\, y_{SRD}, \tag{2.5}$$

where a_{SD} and a_{SRD} are combining weights for specific optimization criteria. The minimum mean square error (MMSE) criterion [24, 31, 32] is used for AF relaying. Recall from [24, 31, 32] that the MMSE coefficient for a_{SD} is $\sqrt{P}/N$ where P is the signal power and N is the aggregate noise power in equations (2.1) and (2.3). Similarly, a_{SRD} can be obtained from equations (2.2) and

(2.4). For DF relaying, cooperative MRC (CMRC) [33] criterion is used to find a_{SD} and a_{SRD}.

2.2 Performance Analysis

To avoid the complex non-convex optimization problem to solve for a combined BF as in [31], strong-path BF will be considered, in which the source beamforms to the stronger path of direct and relay links based on their instantaneous received SNRs. More specifically, the BF vector is chosen based on stronger instantaneous received SNR between direct and relay links.

Therefore, if $\gamma_{SD} > \gamma_{SRD}$, $\mathbf{f}_{SD} = \mathbf{f}_{SR} = \mathbf{v}_{SD}$, which is the strongest right singular vector of $\mathbf{H}_{SD}$; otherwise $\mathbf{f}_{SD} = \mathbf{f}_{SR} = \mathbf{v}_{SR}$, which is $\mathbf{h}_{SR}/\|\mathbf{h}_{SR}\|$. For combining vectors, if $\gamma_{SD} > \gamma_{SRD}$, $\mathbf{c}_{SD} = \mathbf{u}_{SD}$, the strongest left singular vector of $\mathbf{H}_{SD}$, and $\mathbf{c}_{RD} = \mathbf{u}_{RD}$, the strongest left singular vector of $\mathbf{h}_{RD}$, otherwise $\mathbf{c}_{SD} = \mathbf{H}_{SD}\mathbf{v}_{SR}/\|\mathbf{H}_{SD}\mathbf{v}_{SR}\|$ and $\mathbf{c}_{RD} = \mathbf{u}_{RD}$.

2.2.1 Known $\mathbf{h}_{RD}$ at S and $\mathbf{h}_{SR}$ at D

Using equations (2.1) and (2.2), if $\gamma_{SD} > \gamma_{SRD}$, the received signals at the destination are given by

$$y_{SD} = \sqrt{\rho_{SD}}\|\mathbf{H}_{SD}\mathbf{v}_{SD}\|x + \mathbf{u}_{SD}^H\mathbf{n}_{SD} \tag{2.6}$$

$$y_{SRD} = \frac{\sqrt{\rho_{SR}\rho_{RD}}\|\mathbf{h}_{RD}\|\|\mathbf{h}_{SR}^T\mathbf{v}_{SD}\|x}{\sqrt{1+\rho_{SR}\|\mathbf{h}_{SR}^T\mathbf{v}_{SD}\|^2}} + \frac{\sqrt{\rho_{RD}}\|\mathbf{h}_{RD}\|n_{SR}}{\sqrt{1+\rho_{SR}\|\mathbf{h}_{SR}^T\mathbf{v}_{SD}\|^2}} + \mathbf{u}_{RD}^H\mathbf{n}_{RD}. \tag{2.7}$$

Similarly, if $\gamma_{SD} \leq \gamma_{SRD}$, we have

$$y_{SD} = \sqrt{\rho_{SD}}\|\mathbf{H}_{SD}\mathbf{v}_{SR}\|x + \frac{(\mathbf{H}_{SD}\mathbf{v}_{SR})^H}{\|\mathbf{H}_{SD}\mathbf{v}_{SR}\|}\mathbf{n}_{SD} \tag{2.8}$$

$$y_{SRD} = \frac{\sqrt{\rho_{SR}\rho_{RD}}\|\mathbf{h}_{RD}\|\|\mathbf{h}_{SR}^T\mathbf{v}_{SR}\|x}{\sqrt{1+\rho_{SR}\|\mathbf{h}_{SR}^T\mathbf{v}_{SR}\|^2}} + \frac{\sqrt{\rho_{RD}}\|\mathbf{h}_{RD}\|n_{SR}}{\sqrt{1+\rho_{SR}\|\mathbf{h}_{SR}^T\mathbf{v}_{SR}\|^2}} + \mathbf{u}_{RD}^H\mathbf{n}_{RD}. \tag{2.9}$$

If the MMSE criterion is used to combine signals for equations (2.6)-(2.9) when $\mathbf{h}_{SR}$ and $\mathbf{h}_{RD}$ are known at D and S, respectively, the total instantaneous received SNR for the strong-path BF AF relaying can be represented by

$$\gamma = \begin{cases} \gamma_{SD} + \gamma'_{SRD}, & \gamma_{SD} > \gamma_{SRD} \\ \gamma'_{SD} + \gamma_{SRD}, & \gamma_{SD} \leq \gamma_{SRD} \end{cases}, \tag{2.10}$$

where $\gamma_{SD} = \rho_{SD}\|\mathbf{H}_{SD}\mathbf{v}_{SD}\|^2$, $\gamma'_{SRD} = \gamma'_{SR}\gamma_{RD}/\left(1+\gamma'_{SR}+\gamma_{RD}\right)$, $\gamma'_{SR} = \rho_{SR}$ $\|\mathbf{h}_{SR}^T\mathbf{v}_{SD}\|^2$, $\gamma_{RD} = \rho_{RD}\|\mathbf{h}_{RD}\|^2$, $\gamma'_{SD} = \rho_{SD}\|\mathbf{H}_{SD}\mathbf{v}_{SR}\|^2$, $\gamma_{SR} = \rho_{SR}\|\mathbf{h}_{SR}^T\mathbf{v}_{SR}\|^2$, and $\gamma_{SRD} = \gamma_{SR}\gamma_{RD}/\left(1+\gamma_{SR}+\gamma_{RD}\right)$. To recall our notation, primes (i.e. γ'_{SD}, γ'_{SR}, and γ'_{SRD}) indicate instantaneous SNRs with unmatched beamformers. A BF vector is "matched" when it is the strongest right singular vector of the corresponding channel.

Therefore, the instantaneous BER using BPSK is given by

$$\begin{aligned} P_E^{SBAF} = {} & P_r\left(\gamma_{SD} > \gamma_{SRD}\right) Q\left(\sqrt{2\left(\gamma_{SD}+\gamma'_{SRD}\right)}\right) I(\gamma_{SD} > \gamma_{SRD}) \\ & + P_r\left(\gamma_{SD} \leq \gamma_{SRD}\right) Q\left(\sqrt{2\left(\gamma'_{SD}+\gamma_{SRD}\right)}\right) I(\gamma_{SD} \leq \gamma_{SRD}), \end{aligned} \tag{2.11}$$

where $I(\cdot)$ is an indicator function. From equation (2.11), an analytical upper-bound can be obtained if the indicator functions are removed. Using Craig's formula for $Q(\cdot)$ functions, the average BER using BPSK is upper-bounded by

$$\begin{aligned} P_E \leq {} & P_r\left(\gamma_{SD} > \gamma_{SRD}\right) \frac{1}{\pi}\int_0^{\pi/2} \mathbb{E}\left[e^{-\frac{\gamma_{SD}}{\sin^2\theta}}\right] \mathbb{E}\left[e^{-\frac{\gamma'_{SRD}}{\sin^2\theta}}\right] d\theta \\ & + P_r\left(\gamma_{SD} \leq \gamma_{SRD}\right) \frac{1}{\pi}\int_0^{\pi/2} \mathbb{E}\left[e^{-\frac{\gamma'_{SD}}{\sin^2\theta}}\right] \mathbb{E}\left[e^{-\frac{\gamma_{SRD}}{\sin^2\theta}}\right] d\theta. \end{aligned} \tag{2.12}$$

The first expectation of equation (2.12), $\mathbb{E}\left[e^{-\gamma_{SD}/\sin^2\theta}\right]$, can be derived as (please see details in Appendix 2.1)

$$\mathbb{E}\left[e^{-\frac{\gamma_{SD}}{\sin^2\theta}}\right] = \sum_{n=1}^{M_D} \sum_{m=M_S-M_D}^{(M_S+M_D)n-2n^2} d_{n,m}\left(\frac{\sin^2\theta}{\sin^2\theta + \frac{\rho_{SD}}{n}}\right)^{m+1}, \tag{2.13}$$

where $d_{n,m}$ are coefficients given by [30, eqn. (24)], and Tables 2.1-2.3 provide typical coefficients. The third expectation of equation (2.12), $\mathbb{E}\left[e^{-\gamma'_{SD}/\sin^2\theta}\right]$, can be derived as (please see details in Appendix 2.2)

$$\mathbb{E}\left[e^{-\frac{\gamma'_{SD}}{\sin^2\theta}}\right] = \left(\frac{\sin^2\theta}{\rho_{SD}+\sin^2\theta}\right)^{M_D}. \tag{2.14}$$

Since integrals cannot be expressed in closed-form, the second and fourth expectations of equation (2.12), $\mathbb{E}\left[e^{-\gamma'_{SRD}/\sin^2\theta}\right]$ and $\mathbb{E}\left[e^{-\gamma_{SRD}/\sin^2\theta}\right]$, can be directly evaluated numerically by integrating with the corresponding PDFs. The PDF of γ'_{SRD}, $f_{\gamma'_{SRD}}(x)$, is given in Appendix 2.3, and that of γ_{SRD}, $f_{\gamma_{SRD}}(x)$, is given in [29, eqn. (12)]. Therefore, equation (2.11) can be upper-bounded once equations (2.13) and (2.14) are substituted for equation (2.12), along with $\mathbb{E}\left[e^{-\gamma'_{SRD}/\sin^2\theta}\right]$ and $\mathbb{E}\left[e^{-\gamma_{SRD}/\sin^2\theta}\right]$.

Table 2.1: The Coefficients $d_{n,m}$ for $(M_S, M_D) = (1,1), (2,1), (3,1), (4,1)$, and $(2,2)$

(M_S, M_D)	(1, 1)	(2, 1)	(3, 1)	(4, 1)	(2, 2)	
	n = 1	n = 2	n = 3	n = 4	n = 1	n = 2
m = 0	1	1	1	1	2	-1
m = 1					-2	
m = 2					2	
m = 3						
m = 4						

Table 2.2: The Coefficients $d_{n,m}$ for $(M_S, M_D) = (3,2), (4,2)$, and $(3,3)$

(M_S, M_D)	(3, 2)		(4, 2)		(3, 3)		
	n = 1	n = 2	n = 1	n = 2	n = 1	n = 2	n = 3
m = 0					3	-3	1
m = 1	3	-3/4			-6	3/2	
m = 2	-4	-1/4	4	-1/2	12	-3/4	
m = 3	3		-6	-3/8	-12	-3/8	
m = 4			4	-1/8	6	-3/8	

Table 2.3: The Coefficients $d_{n,m}$ for $(M_S, M_D) = (4, 3)$ and $(4, 4)$

(M_S, M_D)	(4, 3)			(4, 4)			
	n = 1	n = 2	n = 3	n = 1	n = 2	n = 3	n = 4
m = 0				4	-6	4	-1
m = 1	6	-3	2/3	-12	6	-4/3	
m = 2	-16	1	8/27	36	-6	4/9	
m = 3	27	3/8	1/27	-68	1	28/81	
m = 4	-24	-3/4		84	-1	92/243	
m = 5	10	-5/32		-60	5/2	100/729	
m = 6		-15/32		20	-5/2	20/729	
m = 7					35/32		
m = 8					-35/32		

Similarly, based on the combined signal for strong-path BF DF relaying, when $\mathbf{h}_{SR}$ and $\mathbf{h}_{RD}$ are known at D and S, respectively, the total received SNR can be represented by

$$\gamma = \begin{cases} \frac{\left(\gamma_{SD}/\sqrt{\rho_{SD}} \pm \gamma'_{eq}/\sqrt{\rho_{RD}}\right)^2}{\gamma_{SD}/\rho_{SD} + \gamma'^2_{eq}/(\rho_{RD}\gamma_{RD})}, & \gamma_{SD} > \gamma_{SRD} \\ \frac{\left(\gamma'_{SD}/\sqrt{\rho_{SD}} \pm \gamma_{eq}/\sqrt{\rho_{RD}}\right)^2}{\gamma'_{SD}/\rho_{SD} + \gamma^2_{eq}/(\rho_{RD}\gamma_{RD})}, & \gamma_{SD} \leq \gamma_{SRD} \end{cases}, \tag{2.15}$$

where $\gamma_{eq} = \left[Q^{-1}\left(\left(1 - P_{SR}\right) P_{RD} + P_{SR}\left(1 - P_{RD}\right)\right)\right]/2$, $P_{SR} = Q\left(\sqrt{2\gamma_{SR}}\right)$, $P_{RD} = Q\left(\sqrt{2\gamma_{RD}}\right)$, $\gamma'_{eq} = \left[Q^{-1}\left(\left(1 - P'_{SR}\right) P_{RD} + P'_{SR}\left(1 - P_{RD}\right)\right)\right]/2$, $P'_{SR} = Q\left(\sqrt{2\gamma'_{SR}}\right)$, and $\pm$ is used for $\hat{x} = x$ or $\hat{x} = -x$ from equation (2.4). Sub-optimal CMRC of [33] is used instead of ML since its performance is very similar to that of ML at high SNR.

Similar to equation (2.11) for AF relaying, if the indicator functions are removed, the instantaneous BER using BPSK can be upper-bounded by

$$\begin{aligned} P_E^{SBDF} \leq\ & P_r\left(\gamma_{SD} > \gamma_{SRD}\right)\left[\left(1 - P'_{SR}\right) Q\left(\sqrt{2\gamma_{\hat{x}=x}}\right) + P'_{SR} Q\left(\sqrt{2\gamma_{\hat{x}=-x}}\right)\right] \\ & + P_r\left(\gamma_{SD} \leq \gamma_{SRD}\right)\left[\left(1 - P_{SR}\right) Q\left(\sqrt{2\gamma'_{\hat{x}=x}}\right) + P_{SR} Q\left(\sqrt{2\gamma'_{\hat{x}=-x}}\right)\right], \end{aligned} \tag{2.16}$$

where $\gamma_{\hat{x}=-x}$ and $\gamma'_{\hat{x}=-x}$ are the total received SNRs when $\gamma_{SD} > \gamma_{SRD}$ and $\gamma_{SD} \leq \gamma_{SRD}$ for $\hat{x} = -x$ from equation (2.15), respectively. The average BER

can be obtained by averaging the instantaneous BER over γ_{SD}, γ_{SR}, γ_{RD}, γ'_{SD}, and γ'_{SR} numerically.

2.2.2 Unknown $\mathbf{h}_{RD}$ at S and $\mathbf{h}_{SR}$ at D: New Selection Relaying with Strong-Path BF

If $\mathbf{h}_{RD}$ and $\mathbf{h}_{SR}$ are unknown at the source and destination, respectively, the most practical approach is selection relaying [11]. In traditional selection relaying with single antennas using no BF, the relay transmits the amplified signal to the destination if the received SNR of the $S \rightarrow R$ exceeds a predetermined threshold, and the source retransmits the signal otherwise in the second time slot. In the presence of beamforming, this can be extended where the relay transmits its signal only when it exceeds a threshold. Since the optimization of such a threshold requires numerical techniques, however, we seek a selection relaying approach that does not require a threshold. In our proposed selection relaying with strong-path BF, the relay transmits the amplified signal to the destination if $\gamma_{SD} \leq \gamma_{SR}$ (i.e. if the strong-path is through the relay), and the source retransmits the signal otherwise in the second time slot. The advantages of the strong-path selection relaying are that it is simple to implement and does not require a threshold.

The source determines the BF vector based on the effective received SNRs over the channels, $\mathbf{H}_{SD}$ and $\mathbf{h}_{SR}$, and the destination combines received signals based on the received SNRs of $\mathbf{H}_{SD}$ and $\mathbf{h}_{RD}$ since $\mathbf{h}_{RD}$ and $\mathbf{h}_{SR}$ are unknown at the source and destination, respectively. Therefore, if $\gamma_{SD} > \gamma_{SR}$, $\mathbf{f}_{SD} = \mathbf{f}_{SR} = \mathbf{v}_{SD}$, which is the strongest right singular vector of $\mathbf{H}_{SD}$; otherwise $\mathbf{f}_{SD} = \mathbf{f}_{SR} = \mathbf{v}_{SR}$, which is $\mathbf{h}_{SR}/\|\mathbf{h}_{SR}\|$. For combining vectors, if $\gamma_{SD} > \gamma_{RD}$, $\mathbf{c}_{SD} = \mathbf{u}_{SD}$ and $\mathbf{c}_{RD} = \mathbf{u}_{RD}$, otherwise $\mathbf{c}_{SD} = \mathbf{H}_{SD}\mathbf{v}_{SR}/\|\mathbf{H}_{SD}\mathbf{v}_{SR}\|$

and $\mathbf{c}_{RD} = \mathbf{u}_{RD}$. Note that this scheme does not require knowledge of $\mathbf{h}_{RD}$ and $\mathbf{h}_{SR}$ at the source and destination, respectively.

To characterize performance, if $\gamma_{SD} > \gamma_{SR}$, the source transmits twice over two consecutive time slots, where on both slots $\mathbf{v}_{SD}$ is used for BF and $\mathbf{u}_{SD}$ is used for combining:

$$y_{SD} = \sqrt{\rho_{SD}}\|\mathbf{H}_{SD}\mathbf{v}_{SD}\|x + \mathbf{u}_{SD}^H\mathbf{n}_{SD}, \tag{2.17}$$

and the relay never transmits the amplified signals in this case. If $\gamma_{SD} \leq \gamma_{SR}$, $\mathbf{v}_{SR}$ is used for BF and $\mathbf{H}_{SD}\mathbf{v}_{SR}/\|\mathbf{H}_{SD}\mathbf{v}_{SR}\|$ and $\mathbf{u}_{RD}$ are used for combining so that

$$y_{SD} = \sqrt{\rho_{SD}}\|\mathbf{H}_{SD}\mathbf{v}_{SR}\|^2 x + \frac{(\mathbf{H}_{SD}\mathbf{v}_{SR})^H}{\|\mathbf{H}_{SD}\mathbf{v}_{SR}\|}\mathbf{n}_{SD} \tag{2.18}$$

$$y_{SRD} = \frac{\sqrt{\rho_{SR}\rho_{RD}}\|\mathbf{h}_{RD}\|\|\mathbf{h}_{SR}^T\mathbf{v}_{SR}\|x}{\sqrt{1+\rho_{SR}\|\mathbf{h}_{SR}^T\mathbf{v}_{SR}\|^2}} + \frac{\sqrt{\rho_{RD}}\|\mathbf{h}_{RD}\|n_{SR}}{\sqrt{1+\rho_{SR}\|\mathbf{h}_{SR}^T\mathbf{v}_{SR}\|^2}} + \mathbf{u}_{RD}^H\mathbf{n}_{RD}. \tag{2.19}$$

If the MMSE criterion is used to combine signals for equations (2.17)-(2.19), the total instantaneous received SNR for the strong-path BF selection relaying can be represented by

$$\gamma = \begin{cases} 2\gamma_{SD}, & \gamma_{SD} > \gamma_{SR} \\ \frac{\left(\gamma'_{SD}\sqrt{1+\gamma_{SR}}+\gamma_{RD}\sqrt{\gamma_{SR}}\right)^2}{(1+\gamma_{SR})\left(\gamma'_{SD}+\gamma_{RD}\right)+\gamma_{RD}^2}, & \gamma_{SD} \leq \gamma_{SR} \end{cases}, \tag{2.20}$$

where $\gamma_{SD} = \rho_{SD}\|\mathbf{H}_{SD}\mathbf{v}_{SD}\|^2$, $\gamma'_{SD} = \rho_{SD}\|\mathbf{H}_{SD}\mathbf{v}_{SR}\|^2$, $\gamma_{SR} = \rho_{SR}\|\mathbf{h}_{SR}^T\mathbf{v}_{SR}\|^2$, and $\gamma_{RD} = \rho_{RD}\|\mathbf{h}_{RD}\|^2$. Therefore, the instantaneous BER for strong-path BF selection relaying using BPSK is upper-bounded by

$$\begin{aligned} P_E^{SRAF} \leq\ & P_r\left(\gamma_{SD} > \gamma_{SR}\right) Q\left(\sqrt{4\gamma_{SD}}\right) \\ & + P_r\left(\gamma_{SD} \leq \gamma_{SR}\right) Q\left(\frac{\sqrt{2}\left(\gamma'_{SD}\sqrt{1+\gamma_{SR}}+\gamma_{RD}\sqrt{\gamma_{SR}}\right)}{\sqrt{(1+\gamma_{SR})\left(\gamma'_{SD}+\gamma_{RD}\right)+\gamma_{RD}^2}}\right). \end{aligned} \tag{2.21}$$

Similarly, based on the combined signal for DF relaying, if $\mathbf{h}_{SR}$ and $\mathbf{h}_{RD}$ are unknown at D and S, respectively, the total received SNR can be

represented by

$$\gamma = \begin{cases} 2\gamma_{SD}, & \gamma_{SD} > \gamma_{SRD} \\ \frac{\gamma'_{SD} \pm \gamma_{RD}}{\sqrt{\gamma'_{SD} + \gamma_{RD}}}, & \gamma_{SD} \leq \gamma_{SRD} \end{cases} . \tag{2.22}$$

The instantaneous BER using BPSK can also be upper-bounded by

$$\begin{aligned} P_E^{SRDF} \leq & P_r\left(\gamma_{SD} > \gamma_{SRD}\right) Q\left(\sqrt{2\gamma_{SD}}\right) \\ & + P_r\left(\gamma_{SD} \leq \gamma_{SRD}\right) \left[\left(1 - P_{SR}\right) Q\left(\sqrt{2\gamma_{\hat{x}=x}}\right) + P_{SR} Q\left(\sqrt{2\gamma_{\hat{x}=-x}}\right)\right]. \end{aligned} \tag{2.23}$$

Note that all variables in equations (2.21) and (2.23) are channel dependent, which makes averaging analytically intractable. However, the average BER can be obtained by averaging the instantaneous BER in equations (2.21) and (2.23) over γ_{SD}, γ_{SR}, γ_{RD}, and γ'_{SD} numerically.

2.3 High SNR Analysis for AF Strong-Path BF

Simple high SNR performance for AF strong-path BF is now considered to further simplify equations (2.12)-(2.14). The approximation uses the PDFs of γ_{SD}, γ_{SRD}, γ'_{SD}, and γ'_{SRD}, and shows that they satisfy the assumptions given in [34], which provides a systematic method for high SNR analysis. Based on [34], the average BER of an uncoded system using BPSK can be approximated by

$$P_E = \left(\rho G_c\right)^{-G_d} + o\left(\rho^{-G_d}\right) \tag{2.24}$$

as $\rho \to \infty$, where $G_c = 2\left(\sqrt{\pi}(t+1)\right)^{1/(t+1)} / \left(2^t \alpha \Gamma(t+3/2)\right)^{1/(t+1)}$ is the coding, or array gain, ρ is the average transmit SNR, $G_d = t + 1$ is the diversity order, t is the first nonzero derivative order of the PDF of a channel dependent random variable λ at the origin.

This random variable is proportional to the instantaneous SNR as $\gamma = \rho\lambda$, and $\alpha = f_\lambda^{(t)}(0)/t! \neq 0$. The average SNR ρ may be ρ_{SR} with ρ_{SD} and ρ_{RD}

which are constant multiples of ρ_{SR}, and λ may be either $\lambda_{SD} := \gamma_{SD}/\rho_{SR}$ or $\lambda_{SRD} := \gamma_{SRD}/\rho_{SR}$ in the sequel. Therefore, equation (2.24) can be calculated once t and α are found using the corresponding PDFs. The array and diversity gains, G_c and G_d, in equation (2.24) are found for the direct and multi-hop links separately, and then they are combined to obtain high SNR performance for the whole system. High SNR performance for AF strong-path BF can be obtained once t and α are found using PDFs of $\lambda_{SD} := \gamma_{SD}/\rho_{SR}$, $\lambda'_{SD} := \gamma'_{SD}/\rho_{SR}$, $\Lambda_{SRD} := \Gamma_{SRD}/\rho_{SR}$, and $\Lambda'_{SRD} := \Gamma'_{SRD}/\rho_{SR}$, where we recall that $\Gamma_{SRD} = \gamma_{SR}\gamma_{RD}/\left(\gamma_{SR} + \gamma_{RD}\right)$ and $\Gamma'_{SRD} = \gamma'_{SR}\gamma_{RD}/\left(\gamma'_{SR} + \gamma_{RD}\right)$.

For the direct link, the PDFs of λ_{SD} and λ'_{SD} are used to find t_{SD}, t'_{SD}, and α_{SD}. In this case, $t_{SD} = M_S \cdot M_D - 1$ since the diversity order of the direct link using MRT with MRC when $\gamma_{SD} > \gamma_{SRD}$ is given by $M_S \cdot M_D$ [6]. Similarly $t'_{SD} = M_D - 1$ since when $\gamma_{SD} \leq \gamma_{SRD}$ the diversity order is M_D. In the latter case, the BF vector is not matched with the direct link. The t_{SD} order derivative of the PDF of λ_{SD} evaluated at the origin is given in Appendix 2.4. The t'_{SD} order derivative of the PDF of λ'_{SD} evaluated at the origin is obtained by $\left(\rho_{SR}/\rho_{SD}\right)^{M_D}$ (please see details in Appendix 2.5). Therefore, both derivatives of λ_{SD} and λ'_{SD} evaluated at the origin are as follows:

$$f_{\lambda_{SD}}^{(t_{SD})}(0) = \sum_{n=1}^{M_D} \sum_{m=M_S-M_D}^{(M_S+M_D)n-2n^2} d_{n,m} \binom{t_{SD}}{m} (-1)^{t_{SD}+m} \left(\frac{n\rho_{SR}}{\rho_{SD}}\right)^{t_{SD}+1} \tag{2.25}$$

$$f_{\lambda'_{SD}}^{(t'_{SD})}(0) = \left(\frac{\rho_{SR}}{\rho_{SD}}\right)^{M_D}. \tag{2.26}$$

Henceforth, α_{SD} can be obtained using equations (2.25) and (2.26)

$$\alpha_{SD} = \begin{cases} \frac{f_{\lambda_{SD}}^{(t_{SD})}(0)}{(M_S \cdot M_D - 1)!}, & \gamma_{SD} > \gamma_{SRD} \\ \frac{f_{\lambda'_{SD}}^{(t'_{SD})}(0)}{(M_D - 1)!}, & \gamma_{SD} \leq \gamma_{SRD} \end{cases}. \tag{2.27}$$

For the relay link, the PDFs of Λ_{SRD} and Λ'_{SRD} can be used to find t_{SRD}, t'_{SRD}, and α_{SRD}. Since the diversity order of the relay link using MRT with

MRC when $\gamma_{SD} > \gamma_{SRD}$ is given by 1, $t'_{SRD} = 0$. In this case, the BF vector is not matched with the relay link. We have $t_{SRD} = \min(M_S, M_D) - 1$ since the diversity order of the relay link using MRT with MRC when $\gamma_{SD} \leq \gamma_{SRD}$ is given by $\min(M_S, M_D)$ [35]. The t_{SRD} order derivative of the PDF of Λ_{SRD} evaluated at the origin can be obtained by removing antenna correlation factors from [35, eqn. (28)]. The t'_{SRD} order derivative of the PDF of Λ'_{SRD} evaluated at the origin can be obtained once $M_S = 1$ is substituted for the t_{SRD} order derivative of the PDF of Λ_{SRD} evaluated at the origin. Therefore, we have

$$f_{\Lambda'_{SRD}}^{(t'_{SRD})}(0) = \begin{cases} 1, & M_S < M_D \quad or \quad M_S > M_D > 1 \\ \left(\frac{\rho_{SR}}{\rho_{RD}}\right) + 1, & M_S = M_D \quad or \quad M_S > M_D = 1 \end{cases} \tag{2.28}$$

$$f_{\Lambda_{SRD}}^{(t_{SRD})}(0) = \begin{cases} \left(\frac{\rho_{SR}}{\rho_{RD}}\right)^{M_D}, & M_S > M_D \\ 1, & M_S < M_D \\ \left(\frac{\rho_{SR}}{\rho_{RD}}\right)^{M_D} + 1, & M_S = M_D \end{cases} . \tag{2.29}$$

Putting them together, α_{SRD} can be obtained using equations (2.28) and (2.29)

$$\alpha_{SRD} = \begin{cases} f_{\Lambda'_{SRD}}^{(t'_{SRD})}(0), & \gamma_{SD} > \gamma_{SRD} \\ \frac{f_{\Lambda_{SRD}}^{(t_{SRD})}(0)}{(\min(M_S, M_D)-1)!}, & \gamma_{SD} \leq \gamma_{SRD} \end{cases} . \tag{2.30}$$

For the combined link, the diversity order is $M_S \cdot M_D + 1$ if $\gamma_{SD} > \gamma_{SRD}$ because the received SNR of the combined link is $\gamma_{SD} + \gamma'_{SRD}$, and it is $M_D + \min(M_S, M_D)$ if $\gamma_{SD} \leq \gamma_{SRD}$ because that of the combined link is $\gamma'_{SD} + \gamma_{SRD}$. The final combined α_C is given by using equations (2.25), (2.26), (2.28) and (2.29).

$$\alpha_C = \begin{cases} \frac{f_{\lambda_{SD}}^{(t_{SD})}(0) \cdot f_{\Lambda'_{SRD}}^{(t'_{SRD})}(0)}{(M_S \cdot M_D)!}, & \gamma_{SD} > \gamma_{SRD} \\ \frac{f_{\lambda'_{SD}}^{(t'_{SD})}(0) \cdot f_{\Lambda_{SRD}}^{(t_{SRD})}(0)}{(M_D + \min(M_S, M_D)-1)!}, & \gamma_{SD} \leq \gamma_{SRD} \end{cases} . \tag{2.31}$$

Based on α_C in equation (2.31), the combined link high SNR performance for the strong-path BF can be obtained when $M_S \cdot M_D + 1 > M_D + \min(M_S, M_D)$

as

$$G_d^{SB} = \min(M_S \cdot M_D + 1, M_D + \min(M_S, M_D)) = M_D + \min(M_S, M_D) \tag{2.32}$$

$$G_c^{SB} = [P_r(\gamma_{SD} \leq \gamma_{SRD}) \left(\frac{f_{\lambda'_{SD}}^{(M_D-1)}(0) \cdot f_{\Lambda_{SRD}}^{(\min(M_S,M_D)-1)}(0)\Gamma\left(M_D + \min(M_S, M_D) + \frac{1}{2}\right)}{2\sqrt{\pi}(M_D + \min(M_S, M_D))!} \right)]^{-1/G_d^{SB}}. \tag{2.33}$$

The combined link high SNR performance for the strong-path BF can be obtained when $M_S \cdot M_D + 1 = M_D + \min(M_S, M_D)$, where G_d^{SB} is in equation (2.32) and

$$G_c^{SB} = [P_r(\gamma_{SD} \leq \gamma_{SRD}) \left(\frac{f_{\lambda'_{SD}}^{(M_D-1)}(0) \cdot f_{\Lambda_{SRD}}^{(\min(M_S,M_D)-1)}(0)\Gamma\left(M_D + \min(M_S, M_D) + \frac{1}{2}\right)}{2\sqrt{\pi}(M_D + \min(M_S, M_D))!} \right) + P_r(\gamma_{SD} > \gamma_{SRD}) \left(\frac{f_{\lambda_{SD}}^{(M_S \cdot M_D - 1)}(0) \cdot f_{\Lambda'_{SRD}}^{(0)}(0)\Gamma\left(M_S \cdot M_D + \frac{3}{2}\right)}{2\sqrt{\pi}(M_S \cdot M_D + 1)!} \right)]^{-1/G_d^{SB}}, \tag{2.34}$$

which is the same as equation (2.33) except the final term that is present when $M_S \cdot M_D + 1 = M_D + \min(M_S, M_D)$.

In this case, full diversity order cannot be achieved since all potential resources of the system are not used as compared with the lower-bound obtained by the three-slot scheme. For special cases, if $M_S = 1$ with arbitrary M_D, the diversity order of strong-path BF is $M_D + 1$. If $M_D = 1$ with arbitrary M_S, when $P_r(\gamma_{SD} > \gamma_{SRD}) \approx 1$ which occurs if both M_S and M_D are bigger than 1, strong-path BF diversity is close to optimal. For example, the diversity order of strong-path BF at high SNR when $M_D = 1$ with arbitrary M_S is 2 but the diversity order for the lower-bound is $M_S + 1$. From equation (2.32), it is clear that the diversity order of strong-path BF is dominated by

the two-hop relay link. Therefore, the role of the relay in improving performance for strong-path BF is in increasing the array gain in equations (2.33) and (2.34), and in improving performance at low SNRs.

2.4 Simulation Results

The relationships among the average SNR values are chosen as $\rho_{SR} = \rho_{RD}$ and ρ_{SD} dB $= \rho_{SR}$ dB $- 30\log_{10}(2)$, which corresponds to the relay located in the mid-point of the S and D in a simplified path-loss model [7, p.46] with path-loss exponent of 3 (i.e. the "mid-point relay model"). Alternatively, we also consider $\rho_{SR} = \rho_{RD} = \rho_{SD}$ which is the "equidistant relay model". In Monte-Carlo simulations, the transmitted symbol is BPSK modulated with unit power, and the channel is 100-symbol block fading with $(M_S, M_D) = (2, 2)$ or (4,4). MRC with MMSE combining is used for AF relaying, and MRC with CMRC combining is used for DF relaying.

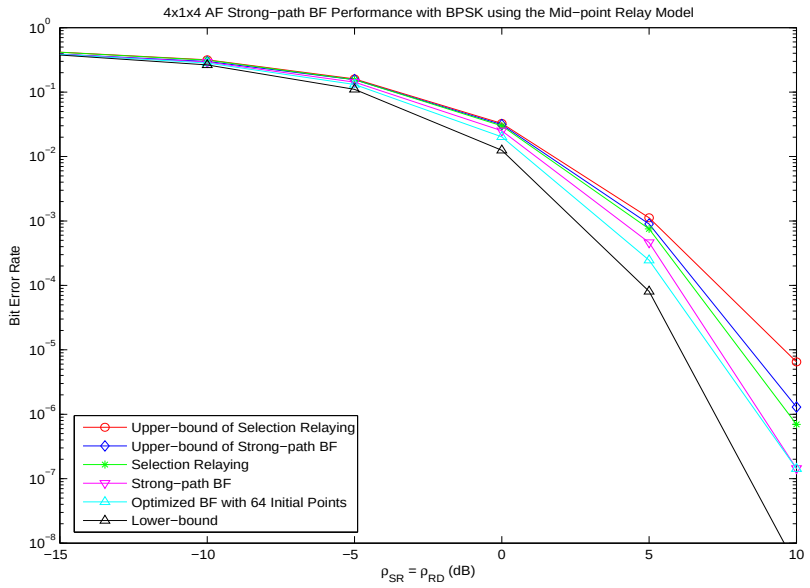

Figure 2.2: $4 \times 1 \times 4$ AF Strong-Path BF Performance with BPSK using the Mid-Point Relay Model.

For illustration of our high SNR results, we select $\rho_{SR} = \rho_{RD} = \rho_{SD} \rightarrow \infty$ even though our analysis applies to nonequal average SNRs as well. The combined optimized BF performance from [31] and the lower-bound obtained by using two different BF vectors "matched" with the relay and direct links, respectively are included as benchmarks. For BF optimization, 64 Grassmannian vectors [36] are used as initial points for the gradient ascent algorithm.

2.4.1 AF/DF Strong-Path BF

This section shows AF/DF strong-path BF performance from Section 2.2, and all CSI is assumed to be known at the source and destination. Figure 2.2 shows $4 \times 1 \times 4$ AF strong-path BF performance with BPSK using the mid-point relay model. The upper-bound of strong-path BF is from equation (2.12) and its actual performance is from equation (2.11). The upper-bound of selection relaying is from equation (2.21) and its actual performance is from equation (2.21) with the indicator functions. Strong-path BF performance is 1.9 dB worse than the ideal lower-bound, 0.1 dB worse than optimized BF performance, and 1 dB better than selection relaying performance at the rate 10^{-6}. The upper-bounds are 1.1 dB and 1.9 dB worse than their actual performance at the rate 10^{-5}.

Figure 2.3 shows $4 \times 1 \times 4$ DF strong-path BF performance with BPSK using the mid-point relay model. The upper-bound of strong-path BF is from equation (2.16) and its actual performance is from equation (2.16) with the indicator functions. The upper-bound of selection relaying is from equation (2.23) and its actual performance is from equation (2.23) with the indicator functions. Strong-path BF performance is 1.2 dB worse than the ideal lower-bound and 0.4 dB better than selection relaying performance at the rate 10^{-6}.

The upper-bounds are 1.4 dB and 2.5 dB worse than their actual performance at the rate 10^{-5}.

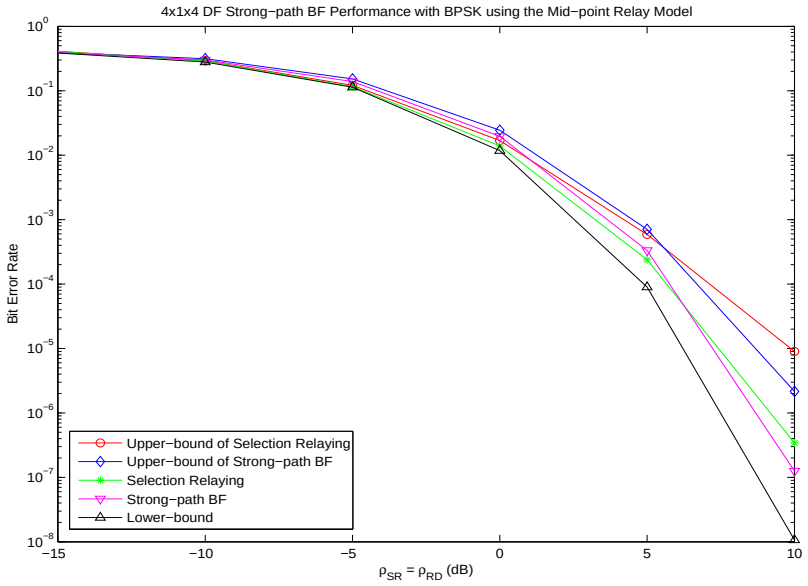

Figure 2.3: $4 \times 1 \times 4$ DF Strong-Path BF Performance with BPSK using the Mid-Point Relay Model

2.4.2 AF/DF Selection Relaying for Strong-Path BF

This section shows selection relaying with strong-path BF performance from Section 2.2, where $\mathbf{h}_{RD}$ and $\mathbf{h}_{SR}$ are assumed to be unknown at the source and destination, respectively. Our extension of traditional selection relaying as well as hybrid selection relaying, in which the relay transmits the amplified signal to the destination if $\gamma_{SD} \leq \gamma_{SR}$ and $\gamma_{SR} > T$ where T is the predetermined optimized threshold, and the source retransmits the signal otherwise in the second time slot (i.e. no relaying if $\gamma_{SD} > \gamma_{SR}$), is illustrated by simulations. Even though the hybrid selection relaying slightly outperforms the traditional and strong-path selection relaying, it requires threshold optimization.

Figure 2.4 shows performance comparisons among $4 \times 1 \times 4$ traditional, strong-path, hybrid selection relaying schemes using the mid-point relay model. The combined AF optimized BF performance with 64 initial points is obtained by Monte-Carlo simulations. AF/DF strong-path selection relaying performance is obtained by averaging the analytical SNR expression from equations (2.21) and (2.23) with the indicator functions, respectively. The performance of traditional and hybrid selection relaying, which rely on threshold optimization, illustrates that the gains due to the presence of a threshold are negligible. This motivates the merits of the proposed threshold-free selection approach. AF/DF strong-path selection relaying performance is about 1 dB and 0.5 dB worse than the AF optimized BF performance, respectively, at 10^{-6}. The novel strong-path selection relaying scheme does not require threshold optimization and its performance is similar to other schemes which require threshold optimization.

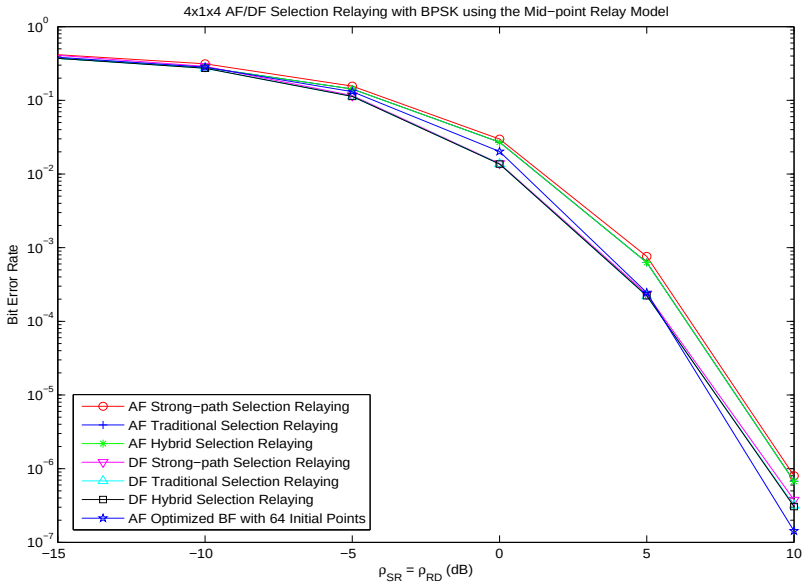

Figure 2.4: $4 \times 1 \times 4$ Selection Relaying with Strong-Path BF Performance with BPSK using the Mid-Point Relay Model.

Based on Monte-Carlo simulation results, the actual strong-path BF performance is very close to the optimized BF performance and ideal lower-bounds even though its upper-bound seems loose when path-loss exists. However, the upper-bounds are very tight to actual performance at high SNR. In addition, availability of the CSI at the source and destination is very crucial in performance.

2.4.3 High SNR Analysis for AF Strong-Path BF

This section shows high SNR performance for strong-path BF from Section 2.3, and all CSI is assumed to be known at the source and destination. Figure 2.5 shows $4 \times 1 \times 4$ strong-path BF performance with BPSK using the mid-point relay model. The combined optimized BF performance with 64 initial points of [31] is obtained by Monte-Carlo simulations. The upper-bound of strong-path BF is attained analytically from equation (2.12). The strong-path BF performance is acquired by averaging the analytical SNR expression from equation (2.11), and is seen to be very close to the optimized BF performance at 10^{-7} and the upper-bound of strong-path BF is about 1.4 dB worse than strong-path BF performance at 10^{-6}. The optimized BF performance is better than strong-path BF performance at low SNR but close to or slightly worse than strong-path BF performance at high SNR, due to the fact that the gradient search algorithm used in the optimized scheme is not guaranteed to converge to the optimum point.

Figure 2.5 shows $2 \times 1 \times 2$ high SNR performance for strong-path BF with BPSK using the equidistant relay model with $\rho_{SR} = \rho_{RD} = \rho_{SD}$. The strong-path BF performance is acquired by averaging the analytical SNR expression from equation (2.11). The upper-bound of the combined link from

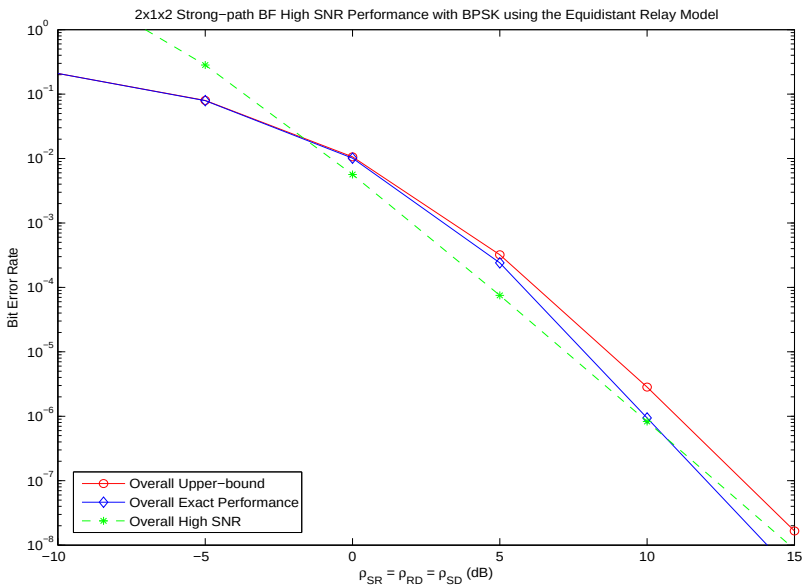

Figure 2.5: $2 \times 1 \times 2$ High SNR Performance for Strong-Path BF with BPSK using the Equidistant Relay Model.

equation (2.12) and high SNR performance for the combined link from equations (2.25)-(2.34) are obtained analytically and they match well at high SNR. The combined upper-bound is about 1 dB worse than the combined strong-path BF performance at 10^{-6}. The performance is dominated by the two-hop relay link at high SNR but by the direct link at low SNR. Using the mid-point relay model, since the BF vector is usually chosen for the relay link at low SNR and for the direct link at high SNR, the relay contributes to the combined performance more at low SNR than at high SNR because the relay link performance dominates the combined performance at low SNR.

Table 2.4: Summary of AF/DF BF Relaying Categories

Categories	CSI Assumptions	BF from S	Combining at D
Strong-Path BF	All Known	1 Stronger	MMSE/CMRC
Selection Relaying	Some Unknown	1 Stronger	MMSE/CMRC

2.5 Chapter Summary

Strong-path BF in AF/DF MIMO fixed relay networks has been investigated with an i.i.d. Rayleigh fading channel. Table 2.4 shows the summary of assumptions and uses for AF/DF relaying categories with BF in the chapter. Two categories are explored with both fully known and partially known CSI of the relay link at the source and destination in AF/DF MIMO relay networks. Novel upper-bounds are presented for AF/DF relaying with known and unknown CSI of the relay link at the source and destination. This chapter also adopts a new selection relaying if the CSI of the relay link is unknown at the source and destination. For strong-path BF, only a single BF vector is allowed for both direct and relay links. For selection relaying for strong-path BF, a single BF vector is allowed with partial CSI known at the source and destination. About the combining scheme at the destination, MRC with MMSE or MRC with CMRC is used for AF/DF relaying schemes. In addition, high SNR performance analysis is also conducted to simplify the BER expressions.

Strong-path BF is a simple approach that avoids complex iterative techniques for calculating the beamformer and can be matched to different CSI assumptions. Based on analytical and simulation results, strong-path BF performance is very similar to the optimized BF scheme of [31]. Gaps between the lower-bound and strong-path BF performance are within 2 dB at 10^{-7}. In addition, proposed strong-path selection relaying performance is about 1 dB worse than the optimized BF performance at high SNR and does not require threshold optimization. Strong-path BF performance does have a diversity order that is the same as that of the lower-bound when $M_S = 1$, and is close

when $M_D = 1$. The relay contributes to the combined performance more at low SNR than at high SNR since the relay link performance dominates the combined performance at low SNR in the mid-point relay model.

Appendix 2.1: Derivation of Equation (2.13)

This appendix derives equation (2.13), which is the first expectation of equation (2.12). Equation (2.13) can be calculated by

$$\begin{aligned}\mathbb{E}\left[e^{-\frac{\gamma_{SD}}{\sin^2\theta}}\right] &= \int_0^\infty e^{-\frac{x}{\sin^2\theta}} f_{\gamma_{SD}}(x)dx \\ &= \int_0^\infty e^{-\frac{x}{\sin^2\theta}} \sum_{n=1}^{M_D} \sum_{m=M_S-M_D}^{(M_S+M_D)n-2n^2} d_{n,m} \frac{n^{m+1}x^m e^{-\frac{nx}{\rho_{SD}}}}{m!\rho_{SD}^{m+1}} dx,\end{aligned} \tag{2.35}$$

where $f_{\gamma_{SD}}(x)$ is the PDF of γ_{SD}, which will be derived in the next paragraph. Using $\int_0^\infty x^n e^{-\mu x}dx = n!\mu^{-n-1}$ [37, p.340] for equation (2.35), equation (2.13) can be obtained.

The derivation of $f_{\gamma_{SD}}(x)$ is following. From [30, eqn. (23)], the PDF of γ_{SD} can be directly obtained by using the PDF of $\Lambda_{SD} := \gamma_{SD}/\rho_{SD}$ based on $f_Y(y) = f_X\left(y/\rho_{SD}\right)/\rho_{SD}$ [38, p.131] as

$$f_{\gamma_{SD}}(x) = \sum_{n=1}^{M_D} \sum_{m=M_S-M_D}^{(M_S+M_D)n-2n^2} d_{n,m} \frac{n^{m+1}x^m e^{-\frac{nx}{\rho_{SD}}}}{\rho_{SD}^{m+1}m!}, \quad x > 0. \tag{2.36}$$

Appendix 2.2: Derivation of Equation (2.14)

This appendix derives $\mathbb{E}\left[e^{-\gamma'_{SD}/\sin^2\theta}\right]$ of equation (2.14). Since the BF vector is not matched with the channel $\mathbf{H}_{SD}$, the PDF can be written as

$$f_{\gamma'_{SD}}(x) = \frac{x^{M_D-1}e^{-\frac{x}{\rho_{SD}}}}{(M_D-1)!\rho_{SD}^{M_D}}, \quad x \geq 0. \tag{2.37}$$

By the definition of the expectation,

$$\mathbb{E}\left[e^{-\frac{\gamma'_{SD}}{\sin^2\theta}}\right] = \int_0^\infty e^{-\frac{x}{\sin^2\theta}} \frac{x^{M_D-1}e^{-\frac{x}{\rho_{SD}}}}{(M_D-1)!\rho_{SD}^{M_D}} dx. \tag{2.38}$$

If $\int_0^\infty x^n e^{-\mu x}dx = n!\mu^{-n-1}$ is used for equation (2.38), equation (2.14) can be obtained.

Appendix 2.3: Derivation of the PDF of γ'_{SRD}

This appendix derives the PDF of γ'_{SRD}. Since the BF vector is not matched with the channel $\mathbf{h}_{SR}$ and there is no BF for the channel $\mathbf{h}_{RD}$, the CDFs and PDFs can be written as followings:

$$F_{\gamma'_{SR}}(x) = 1 - e^{-\frac{x}{\rho_{SR}}}, \quad x \geq 0 \tag{2.39}$$

$$f_{\gamma'_{SR}}(x) = \frac{1}{\rho_{SR}} e^{-\frac{x}{\rho_{SR}}}, \quad x \geq 0 \tag{2.40}$$

$$F_{\gamma_{RD}}(x) = 1 - e^{-\frac{x}{\rho_{RD}}} \sum_{p=0}^{M_D-1} \frac{\left(\frac{x}{\rho_{RD}}\right)^p}{p!}, \quad x \geq 0 \tag{2.41}$$

$$f_{\gamma_{RD}}(x) = \frac{x^{M_D-1} e^{-\frac{x}{\rho_{RD}}}}{(M_D-1)!\rho_{RD}^{M_D}}, \quad x \geq 0. \tag{2.42}$$

Based on the equations (2.39)-(2.42), if the derivation procedures in Appendix of [29] is followed using $\int_0^\infty x^{\nu-1} e^{-\frac{\beta}{x}-\gamma x} dx = 2\left(\frac{\beta}{\gamma}\right)^{\frac{\nu}{2}} K_\nu\left(2\sqrt{\beta\gamma}\right)$ [37, p.368] for $\gamma'_{SRD} = \gamma'_{SR}\gamma_{RD}/\left(1+\gamma'_{SR}+\gamma_{RD}\right)$, the CDF of γ'_{SRD} can be obtained by

$$\begin{aligned} F_{\gamma'_{SRD}}(x) = 1 - & \frac{2e^{-x\left(\frac{1}{\rho_{SR}}+\frac{1}{\rho_{RD}}\right)}\sqrt{\frac{\rho_{RD}}{\rho_{SR}}} x^{M_D-\frac{1}{2}}\sqrt{x+1}}{(M_D-1)!\rho_{RD}^{M_D}} \\ & \sum_{q=0}^{M_D-1} \binom{M_D-1}{q} \left(\frac{\rho_{RD}(x^2+x)}{\rho_{SR}x^2}\right)^{q/2} K_{q+1}\left(2\sqrt{\frac{x^2+x}{\rho_{SR}\rho_{RD}}}\right). \end{aligned} \tag{2.43}$$

If equation (2.43) is taken derivative with respect to x, the PDF of γ'_{SRD} can be obtained by

$$\begin{aligned} f_{\gamma'_{SRD}}(x) = & -\frac{2e^{-x\left(\frac{1}{\rho_{SR}}+\frac{1}{\rho_{RD}}\right)}\sqrt{\frac{\rho_{RD}}{\rho_{SR}}} x^{M_D-\frac{3}{2}}}{(M_D-1)!\rho_{RD}^{M_D}\sqrt{x+1}} \sum_{q=0}^{M_D-1} \binom{M_D-1}{q} \left(\frac{\rho_{RD}(1+x)}{\rho_{SR}x}\right)^{q/2} \\ & \left[K_{q+1}\left(2\sqrt{\frac{x^2+x}{\rho_{SR}\rho_{RD}}}\right)\left(\left(-\frac{1}{\rho_{SR}}-\frac{1}{\rho_{RD}}+M_D+q+1\right)x+M_D\right.\right. \\ & \left.\left.-\left(\frac{1}{\rho_{SR}}+\frac{1}{\rho_{RD}}\right)x^2\right)-(2x+1)\sqrt{\frac{x^2+x}{\rho_{SR}\rho_{RD}}}K_{q+2}\left(2\sqrt{\frac{x^2+x}{\rho_{SR}\rho_{RD}}}\right)\right], \quad x \geq 0. \end{aligned} \tag{2.44}$$

Appendix 2.4: Derivation of $f_{\lambda_{SD}}^{(t_{SD})}(0)$

This appendix derives $f_{\lambda_{SD}}^{(t_{SD})}(0)$ for equation (2.25). From [30, eqn. (23)], the PDF of Λ_{SD} is used to obtain that of $\lambda_{SD} := \gamma_{SD}/\rho_{SR} = \rho_{SD}\Lambda_{SD}/\rho_{SR}$ using $f_{\lambda_{SD}}(y) = \rho_{SR} f_{\Lambda_{SD}}\left(y\rho_{SR}/\rho_{SD}\right)/\rho_{SD}$ by

$$f_{\lambda_{SD}}(x) = \sum_{n=1}^{M_D} \sum_{m=M_S-M_D}^{(M_S+M_D)n-2n^2} d_{n,m} \frac{\left(\frac{n\rho_{SR}}{\rho_{SD}}\right)^{m+1} x^m e^{-\frac{nx\rho_{SR}}{\rho_{SD}}}}{m!}, \quad x > 0. \tag{2.45}$$

If the t_{SD} order derivative is taken for equation (2.45) with respect to x,

$$\begin{aligned} f_{\lambda_{SD}}^{(t_{SD})}(x) = \sum_{n=1}^{M_D} \sum_{m=M_S-M_D}^{(M_S+M_D)n-2n^2} & d_{n,m} \binom{t_{SD}}{m} e^{-\frac{nx\rho_{SR}}{\rho_{SD}}} \\ & \sum_{k=0}^{m} C_k \left(-1\right)^{t_{SD}+m+k} \left(\frac{n\rho_{SR}}{\rho_{SD}}\right)^{t_{SD}+k+1} x^k, \end{aligned} \tag{2.46}$$

where $C_0 = 1$ and C_k is any real coefficient. Once equation (2.46) is evaluated at the origin, equation (2.25) can be obtained.

Appendix 2.5: Derivation of $f_{\lambda'_{SD}}^{(t'_{SD})}(0)$

This appendix derives $f_{\lambda'_{SD}}^{(t'_{SD})}(0)$ for equation (2.26). The PDF of λ'_{SD} is given by

$$f_{\lambda'_{SD}}(x) = \frac{x^{M_D-1} e^{\frac{-x\rho_{SR}}{\rho_{SD}}}}{\left(\frac{\rho_{SD}}{\rho_{SR}}\right)^{M_D} (M_D-1)!}, \quad x \geq 0, \tag{2.47}$$

which can be derived from $f_{\gamma'_{SD}}(x) = x^{M_D-1}e^{-x/\rho_{SD}}/(\rho_{SD}^{M_D}(M_D-1)!),\ x > 0$ using $f_{\lambda'_{SD}}(y) = \rho_{SR} f_{\gamma'_{SD}}\left(y\rho_{SR}/\rho_{SD}\right)/\rho_{SD}$ since $\lambda'_{SD} := \gamma'_{SD}/\rho_{SR} = \rho_{SD}\Lambda'_{SD}/\rho_{SR}$. If the t'_{SD} order derivative is taken for equation (2.47) with respect to x,

$$f_{\lambda'_{SD}}^{(t'_{SD})}(x) = \sum_{k=0}^{t'_{SD}} \binom{t'_{SD}}{k} \frac{(-1)^k e^{-\frac{x\rho_{SR}}{\rho_{SD}}} x^{M_D-(t'_{SD}-k+1)}}{\left(\frac{\rho_{SD}}{\rho_{SR}}\right)^{M_D+k} \left(M_D-(t'_{SD}-k+1)\right)!}. \tag{2.48}$$

Once equation (2.48) is evaluated at the origin, $\left(\rho_{SR}/\rho_{SD}\right)^{M_D}$ can be obtained.

Chapter 3

Performance Analysis of AF/DF MIMO Relay Networks with Beamforming using Multiple Relay Antennas

Two-hop multiple-input multiple-output (MIMO) relay networks with beamforming (BF) are considered such as Figure 3.1, in which a source node transmits its signals to a destination node aided by a relay node, when all nodes conduct BF with multiple antennas, to obtain gains in performance with reduced power consumption if the destination keeps apart from the source. Amplify-and-forward (AF) and decode-and-forward (DF) relaying schemes are considered, in which the relay amplifies or decodes the received signals from the source and forwards them to the destination, respectively. Even though their distance is far, the direct link from source to destination is included in performance analysis since there are no existing closed-form expressions for bit or symbol error rates (BERs/SERs), which are provided herein using a novel proposed systematic upper-bound.

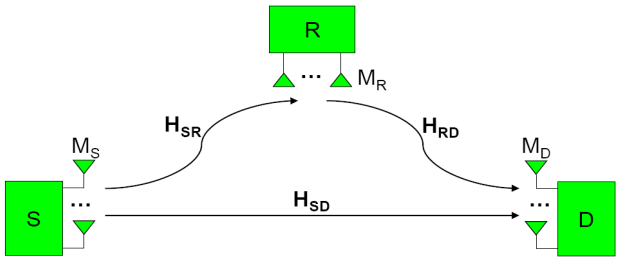

Figure 3.1: The System Model of Two-Hop Relay Networks.

When BF to both relay and destination, the selection of the BF coefficients at the source becomes a challenging problem since the source has to balance the needs of the relay and destination, which is called BF optimization. However, the solution for optimal BF coefficients not only is difficult

to implement, it also does not lend itself to performance analysis because the optimal BF coefficients cannot be expressed in closed-form. Therefore, the performance of optimal schemes through bounds is provided in BERs/SERs, for the first time.

In this chapter, the half-duplex scenario is considered with a two-slot scheme, and the combined BER or SER performance of relay networks with BF is analyzed for the first time, to the best of our knowledge. A novel combined lower-bound is investigated for an AF/DF BF relaying scheme with known CSI of the relay link at the source and destination. The lower-bound is obtained by using two different BF vectors "matched" with the relay and direct links, respectively. A BF vector is matched when it is the strongest right singular vector of the corresponding channel. It is found that the lower-bound is achievable at the expense of a rate penalty. The lower-bound and its achievable scheme are analyzed with the relay using a single antenna in first two sections, and the lower-bound is analyzed with the relay with multiple antennas in the following section.

A closed-form performance with a corresponding SNR distribution is provided for only the multi-hop portion of an AF relay network with a single relay antenna and multiple source and destination antennas in [29] and [35]. Similar work is done with four equivalent systems for a dual-hop AF relay network in [39]. These schemes, however, do not utilize the relay network's full potential as they exclude the direct link. A general BF structure of the optimal relay amplifying matrix is derived for AF MIMO relay systems with a direct link in [40]. On the other hand, a closed-form BER expression is presented in [30] for a direct point-to-point MIMO link, where the number of transmit antennas is no less than the number of receive antennas.

Optimized combined BF for AF relaying is shown to lead to a non-convex problem and is solved using a gradient ascent algorithm with a finite number of Grassmannian BF vectors for initial starting points when all CSI is known at the source and destination in [31]. This solution not only is difficult to implement, it also does not lend itself to BER or SER analysis because the optimal BF coefficients cannot be expressed in closed-form. In the view of this background, it is desirable to analyze the BER performance of optimal schemes through bounds in relay networks.

3.1 System Model

Figure 3.1 shows the two-hop AF MIMO relay system, which consists of a source S, a relay R, and a destination D. All nodes are equipped with multiple antennas, M_S, M_R, and M_D, respectively, and $\mathbf{H}_{SD}$, $\mathbf{H}_{SR}$, and $\mathbf{H}_{RD}$ are channel matrices connecting the nodes, which are assumed to be statistically independent. The half-duplex time division multiple access (TDMA) scenario is considered with the two-slot scheme, in which the relay and destination receive the transmitted signal from the source in the first time slot, and the relay amplifies and forwards the transmitted signal and the destination receives the relayed signal while the source remains silent in the second time slot [11]. Unless otherwise stated, all CSI is assumed to be known only to connected nodes. For example, $\mathbf{H}_{SD}$ is known only to the source and destination, but not to the relay. The exception is knowledge of $\mathbf{H}_{RD}$ at the source and of $\mathbf{H}_{SR}$ at the destination, whose presence or absence is both considered herein.

The received signals using MRT and MRC via the direct and relay links at the destination for AF relaying are as follows:

$$y_{SD} = \sqrt{\rho_{SD}}\mathbf{c}_{SD}^H \mathbf{H}_{SD}\mathbf{f}_{SD}x + \mathbf{c}_{SD}^H \mathbf{n}_{SD} \tag{3.1}$$

$$\begin{aligned} y_{SRD} = &\frac{\sqrt{\rho_{SR}\rho_{RD}}\mathbf{c}_{RD}^H \mathbf{H}_{RD}\mathbf{f}_{RD}\mathbf{c}_{SR}^H \mathbf{H}_{SR}\mathbf{f}_{SR}x}{\sqrt{1+\rho_{SR}\|\mathbf{H}_{SR}\mathbf{f}_{SR}\|^2}} \\ &+ \frac{\sqrt{\rho_{RD}}\mathbf{c}_{RD}^H \mathbf{H}_{RD}\mathbf{f}_{RD}\mathbf{c}_{SR}^H \mathbf{n}_{SR}}{\sqrt{1+\rho_{SR}\|\mathbf{H}_{SR}\mathbf{f}_{SR}\|^2}} + \mathbf{c}_{RD}^H \mathbf{n}_{RD}, \end{aligned} \tag{3.2}$$

where ρ_{SD}, ρ_{SR}, and ρ_{RD} are average transmit SNRs; $\mathbf{H}_{SD}$ $(M_D \times M_S)$, $\mathbf{H}_{SR}$ $(M_R \times M_S)$, and $\mathbf{H}_{RD}$ $(M_D \times M_R)$ are channel coefficient matrices, assumed to be i.i.d. according to $CN(0,1)$; $\mathbf{f}_{SD}$ $(M_S \times 1)$, $\mathbf{f}_{SR}$ $(M_S \times 1)$[1], and $\mathbf{f}_{RD}$ $(M_R \times 1)$ are BF vectors with norm 1 obtained as the strongest right singular vectors of corresponding channel coefficient matrices; $\mathbf{c}_{SD}$ $(M_D \times 1)$, $\mathbf{c}_{SR}$ $(M_R \times 1)$, and $\mathbf{c}_{RD}$ $(M_D \times 1)$ are combining weight vectors with norm 1 obtained as the strongest left singular vectors of corresponding channel coefficient matrices; x is transmitted symbol with $\mathbb{E}[|x|^2] = 1$ and $\mathbb{E}[x] = 0$; $\mathbf{n}_{SD}$ $(M_D \times 1)$, $\mathbf{n}_{SR}$ $(M_R \times 1)$, and $\mathbf{n}_{RD}$ $(M_D \times 1)$ are noise according to $CN(0, \mathbf{I})$, where I is the identity matrix; and $(\cdot)^H$ denotes a vector Hermitian.

The received signals using MRT and MRC of the direct and relay links at the destination for DF relaying are as follows:

$$y_{SD} = \sqrt{\rho_{SD}}\mathbf{c}_{SD}^H \mathbf{H}_{SD}\mathbf{f}_{SD}x + \mathbf{c}_{SD}^H \mathbf{n}_{SD} \tag{3.3}$$

$$y_{SRD} = \sqrt{\rho_{RD}}\mathbf{c}_{RD}^H \mathbf{H}_{RD}\mathbf{f}_{RD}\hat{x} + \mathbf{c}_{RD}^H \mathbf{n}_{RD}, \tag{3.4}$$

where $\hat{x}$ is the ML decoded symbol from $y_{SR} = \sqrt{\rho_{SR}}\mathbf{c}_{SR}^H \mathbf{H}_{SR}\mathbf{f}_{SR}x + \mathbf{c}_{SR}^H \mathbf{n}_{SR}$ at the first time slot.

Using equations (3.1)-(3.4), the combined received signals for AF and DF relaying can be written as

$$y = a_{SD}\, y_{SD} + a_{SRD}\, y_{SRD}, \tag{3.5}$$

[1]Clearly, $\mathbf{f}_{SD} = \mathbf{f}_{SR}$ for realizable two-slot schemes, but we allow them to be different for the purpose of deriving lower-bounds.

where a_{SD} and a_{SRD} are combining weights for specific optimization criteria. The MMSE criterion [24,31,32] is used to find a_{SD} and a_{SRD} for AF relaying, and CMRC is used to find them for DF relaying.

3.2 Performance Analysis for Two-Slot Lower-Bounds with $M_R = 1$

Using a single antenna at R (i.e. $M_R = 1$, the focus of this section is on schemes that use two time slots: $S \rightarrow R$ and $S \rightarrow D$ in the first time slot, and $R \rightarrow D$ in the second time slot. Since the first time slot involves beamforming to both the relay and the destination (i.e. $\mathbf{f}_{SD} = \mathbf{f}_{SR}$), the optimization of the BF is nontrivial and cannot be expressed in closed-form [31]. To find a universal performance bound for the two-slot scheme with BF, two distinct BF vectors are allowed from the source to the relay and destination, respectively. Since a single antenna is used, two channel coefficient matrices (i.e. $\mathbf{H}_{SR}$ and $\mathbf{H}_{RD}$) should be notated with channel coefficient vectors such as $\mathbf{h}_{SR}$ ($M_S \times 1$) and $\mathbf{h}_{RD}$ ($M_D \times 1$). Therefore, to find a lower-bound, $\mathbf{f}_{SD} = \mathbf{v}_{SD}$ and $\mathbf{f}_{SR} = \mathbf{v}_{SR}$ are chosen with $\mathbf{v}_{SD}$ being the strongest right singular vector of $\mathbf{H}_{SD}$ and $\mathbf{v}_{SR} = \mathbf{h}_{SR}/\|\mathbf{h}_{SR}\|$, respectively, for equations (3.1) and (3.2). In addition, $\mathbf{c}_{SD} = \mathbf{u}_{SD}$ and $\mathbf{c}_{RD} = \mathbf{u}_{RD}$ where $\mathbf{u}_{SD}$ is the strongest left singular vector of $\mathbf{H}_{SD}$ and $\mathbf{u}_{RD} = \mathbf{h}_{RD}/\|\mathbf{h}_{RD}\|$.

The simplest way to attain the lower-bound for the two-slot scheme is to use a three-slot scheme: The destination receives the transmitted signal from the source while the relay remains silent in the first time slot; the relay receives the transmitted signal from the source in the second time slot; the destination receives the relayed signal from the relay while the source remains silent in the third time slot. The three-slot scheme, however, has a spectral efficiency that is 2/3 of the two-slot scheme. Attaining the lower-bound with

the three-slot scheme is possible with the same power per bit as the two-slot scheme but it has a loss in spectral efficiency. When this loss is not acceptable, then the forthcoming lower-bound expression is still useful in bounding the performance of the best two-slot scheme for any choice of BF.

3.2.1 AF Lower-Bound

If $\mathbf{v}_{SD}$ and $\mathbf{v}_{SR}$ are used for BF vectors and $\mathbf{u}_{SD}$ and $\mathbf{u}_{RD}$ are used as combining vectors in equations (3.1) and (3.2)

$$y_{SD} = \sqrt{\rho_{SD}}\|\mathbf{H}_{SD}\mathbf{v}_{SD}\|x + \mathbf{u}_{SD}^H\mathbf{n}_{SD} \tag{3.6}$$

$$y_{SRD} = \frac{\sqrt{\rho_{SR}\rho_{RD}}\|\mathbf{h}_{RD}\|\|\mathbf{h}_{SR}^T\mathbf{v}_{SR}\|x}{\sqrt{1+\rho_{SR}\|\mathbf{h}_{SR}^T\mathbf{v}_{SR}\|^2}} + \frac{\sqrt{\rho_{RD}}\|\mathbf{h}_{RD}\|n_{SR}}{\sqrt{1+\rho_{SR}\|\mathbf{h}_{SR}^T\mathbf{v}_{SR}\|^2}} + \mathbf{u}_{RD}^H\mathbf{n}_{RD}. \tag{3.7}$$

If the MMSE criterion is used to combine signals from equations (3.6) and (3.7) when all CSI is known at the source and destination, the total instantaneous received SNR can be represented by

$$\gamma = \gamma_{SD} + \gamma_{SRD} = \gamma_{SD} + \frac{\gamma_{SR}\gamma_{RD}}{1+\gamma_{SR}+\gamma_{RD}}, \tag{3.8}$$

where $\gamma_{SD} = \rho_{SD}\|\mathbf{H}_{SD}\mathbf{v}_{SD}\|^2$ is the instantaneous received SNR of the direct link, γ_{SRD} is that of the two-hop relay link, $\gamma_{SR} = \rho_{SR}\|\mathbf{h}_{SR}^T\mathbf{v}_{SR}\|^2 = \rho_{SR}\|\mathbf{h}_{SR}\|^2$, and $\gamma_{RD} = \rho_{RD}\|\mathbf{h}_{RD}\|^2$.

Using Craig's formula [7] based on equation (3.8), the average BER using BPSK can be written as

$$P_E = \frac{1}{\pi}\int_0^{\pi/2} \mathbb{E}\left[e^{-\frac{\gamma_{SD}}{\sin^2\theta}}\right]\mathbb{E}\left[e^{-\frac{\gamma_{SRD}}{\sin^2\theta}}\right]d\theta. \tag{3.9}$$

The first expectation in equation (3.9) can be derived as (please see details in Appendix 3.1)

$$\mathbb{E}\left[e^{-\frac{\gamma_{SD}}{\sin^2\theta}}\right] = \sum_{n=1}^{M_D}\sum_{m=M_S-M_D}^{(M_S+M_D)n-2n^2} d_{n,m}\left(\frac{\sin^2\theta}{\sin^2\theta+\frac{\rho_{SD}}{n}}\right)^{m+1}, \tag{3.10}$$

where $d_{n,m}$ are coefficients given by [30, eqn. (24)], and Tables 2.1-2.3 provide typical coefficients. A closed-form solution of the second expectation in equation (3.9) is not tractable but it can be lower-bounded by removing the 1 in the denominator of the last term in equation (3.8), which yields the following bound (please see details in Appendix 3.2):

$$\mathbb{E}\left[e^{-\frac{\gamma_{SRD}}{\sin^2\theta}}\right] \geq 1 - \frac{2\sqrt{\frac{\rho_{RD}}{\rho_{SR}}}}{(M_D-1)!\rho_{RD}^{M_D}\sin^2\theta}\sum_{p=0}^{M_S-1}\frac{1}{p!}\left(\frac{1}{\rho_{SR}\rho_{RD}}\right)^{p/2}\sum_{u=0}^{p}\sum_{q=0}^{M_D-1}\binom{M_D-1}{q}$$
$$\binom{p}{u}\left(\frac{\rho_{RD}}{\rho_{SR}}\right)^{u/2+q/2}\frac{\sqrt{\pi}\left(\frac{4}{\sqrt{\rho_{SR}\rho_{RD}}}\right)^{q+u-p+1}\Gamma(M_D+q+u+2)\Gamma(M_D+2p-q-u)}{\left(\frac{1}{\sin^2\theta}+\frac{1}{\rho_{SR}}+\frac{1}{\rho_{RD}}+\frac{2}{\sqrt{\rho_{SR}\rho_{RD}}}\right)^{M_D+q+u+2}\Gamma\left(M_D+p+\frac{3}{2}\right)}$$
$${}_2F_1\left(M_D+q+u+2, q+u-p+\frac{3}{2}; M_D+p+\frac{3}{2}; \frac{\frac{1}{\sin^2\theta}+\frac{1}{\rho_{SR}}+\frac{1}{\rho_{RD}}-\frac{2}{\sqrt{\rho_{SR}\rho_{RD}}}}{\frac{1}{\sin^2\theta}+\frac{1}{\rho_{SR}}+\frac{1}{\rho_{RD}}+\frac{2}{\sqrt{\rho_{SR}\rho_{RD}}}}\right), \tag{3.11}$$

where ${}_2F_1(\alpha,\beta;\gamma;z)$ is the Gauss hypergeometric function [37]. Therefore, equation (3.9) can be lower-bounded once equations (3.10) and (3.11) are substituted.

3.2.2 High SNR Analysis for AF Lower-Bound

Simple high SNR performance for the lower-bound is now considered to further simplify equations (3.9)-(3.11). The approximation uses the PDFs of γ_{SD} and γ_{SRD} and shows that they satisfy the assumptions given in [34], which provides a systematic method for high SNR analysis. Based on [34], the average BER of an uncoded system using BPSK can be approximated by

$$P_E = (\rho G_c)^{-G_d} + o\left(\rho^{-G_d}\right) \tag{3.12}$$

as $\rho \to \infty$, where $G_c = 2\left(\sqrt{\pi}(t+1)\right)^{1/(t+1)} / \left(2^t\alpha\Gamma(t+3/2)\right)^{1/(t+1)}$ is the array gain, ρ is the average transmit SNR, $G_d = t+1$ is the diversity order, t is the first nonzero derivative order of the PDF of a channel dependent random variable λ at the origin. This random variable is proportional to the instanta-

neous SNR as $\gamma = \rho\lambda$, and $\alpha = f_{\lambda}^{(t)}(0)/t! \neq 0$. The average SNR ρ may be ρ_{SR} with ρ_{SD} and ρ_{RD} which are constant multiples of ρ_{SR}, and λ may be either $\lambda_{SD} := \gamma_{SD}/\rho_{SR}$ or $\lambda_{SRD} := \gamma_{SRD}/\rho_{SR}$ in the sequel. Therefore, equation (3.12) can be calculated once t and α are found using PDFs of λ_{SD} and λ_{SRD}. The array and diversity gains, G_c and G_d, in equation (3.12) are found for the direct and multi-hop links separately, and then they are combined to obtain high SNR performance for the whole system.

For the direct link, the PDF of λ_{SD}, given by Appendix 3.3, is used to find t_{SD}, the first nonzero derivative order of the PDF of λ_{SD}, and $\alpha_{SD} = f_{\lambda_{SD}}^{(t_{SD})}(0)/t_{SD}!$. In this case, $t_{SD} = M_S \cdot M_D - 1$ since the diversity order of MIMO MRT with MRC is given by $M_S \cdot M_D$ [6]. If the t_{SD} order derivative of the PDF of λ_{SD} is evaluated at the origin, the following can be obtained (please see details in Appendix 3.3)

$$f_{\lambda_{SD}}^{(t_{SD})}(0) = \sum_{n=1}^{M_D} \sum_{m=M_S-M_D}^{(M_S+M_D)n-2n^2} d_{n,m} \binom{t_{SD}}{m} (-1)^{t_{SD}+m} \left(\frac{n\rho_{SR}}{\rho_{SD}}\right)^{t_{SD}+1}. \quad (3.13)$$

Based on equation (3.13), α_{SD} can be acquired by

$$\alpha_{SD} = \frac{f_{\lambda_{SD}}^{(t_{SD})}(0)}{(M_S \cdot M_D - 1)!}. \quad (3.14)$$

For the relay link, the PDF of $\Lambda_{SRD} = \Gamma_{SRD}/\rho_{SR}$, where $\Gamma_{SRD} = \gamma_{SR}\gamma_{RD}/(\gamma_{SR} + \gamma_{RD})$ given in [29, eqn. (12)], can be used to find t_{SRD} and α_{SRD} because the instantaneous SNRs Γ_{SRD} and γ_{SRD} are equivalent at high average SNR since they differ by a constant term in the denominator of equation (3.8). Since the diversity order of the relay link is given by $\min(M_S, M_D)$ in [35], $t_{SRD} = \min(M_S, M_D) - 1$. The t_{SRD} order derivative of the PDF of Λ_{SRD} evaluated at the origin can be obtained by removing antenna correlation

factors from [35, eqn. (28)] as follows:

$$f_{\Lambda_{SRD}}^{(t_{SRD})}(0) = \begin{cases} \left(\frac{\rho_{SR}}{\rho_{RD}}\right)^{M_D}, & M_S > M_D \\ 1, & M_S < M_D \\ \left(\frac{\rho_{SR}}{\rho_{RD}}\right)^{M_D} + 1, & M_S = M_D \end{cases} . \tag{3.15}$$

Based on equation (3.15), α_{SRD} can be written as

$$\alpha_{SRD} = \frac{f_{\Lambda_{SRD}}^{(t_{SRD})}(0)}{(\min(M_S, M_D) - 1)!} = \begin{cases} \frac{\left(\frac{\rho_{SR}}{\rho_{RD}}\right)^{M_D}}{(M_D-1)!}, & M_S > M_D \\ \frac{1}{(M_S-1)!}, & M_S < M_D \\ \frac{\left(\frac{\rho_{SR}}{\rho_{RD}}\right)^{M_D}+1}{(M_D-1)!}, & M_S = M_D \end{cases} . \tag{3.16}$$

For the combined link, the PDF of $\gamma_{SD} + \Gamma_{SRD}$ is a convolution of $f_{\gamma_{SD}}(x)$ and $f_{\Gamma_{SRD}}(x)$, which is difficult to obtain in closed-form. Instead of using the PDF of $\gamma_{SD} + \Gamma_{SRD}$, an alternate approach is used to find t_C and α_C for the combined link. We have $t_C = M_S \cdot M_D + \min(M_S, M_D) - 1$ since the diversity order of the combined link is $M_S \cdot M_D + \min(M_S, M_D)$, which is the sum of the diversity orders of the direct and relay links because the received SNR of the combined link is $\gamma_{SD} + \Gamma_{SRD}$. To find $f_{\lambda_{SD}+\Lambda_{SRD}}^{(t_C)}(0)$, the product of $f_{\lambda_{SD}}^{(t_{SD})}(0)$ and $f_{\Lambda_{SRD}}^{(t_{SRD})}(0)$ can be used, which is shown in Appendix 3.4. Therefore, the final combined α_C is given by using equations (3.13) and (3.15)

$$\alpha_C = \frac{f_{\lambda_{SD}}^{(t_{SD})}(0) \cdot f_{\Lambda_{SRD}}^{(t_{SRD})}(0)}{(M_S \cdot M_D + \min(M_S, M_D) - 1)!}. \tag{3.17}$$

Based on α_C and t_C, G_d and G_c can be substituted as explained after equation (3.12). The combined link high SNR performance for the lower-bound can be obtained by

$$G_d^{LB} = M_S \cdot M_D + \min(M_S, M_D) \tag{3.18}$$

$$G_c^{LB} = 2\left(\frac{2^{G_d^{LB}-1}\alpha_C \Gamma\left(G_d^{LB} + \frac{1}{2}\right)}{\sqrt{\pi} G_d^{LB}}\right)^{-\frac{1}{G_d^{LB}}} . \tag{3.19}$$

Since all potential resources of the relay network are used, full diversity order is achieved.

3.2.3 DF Lower-Bound

If $\mathbf{v}_{SD}$, $\mathbf{v}_{SR}$, and $\mathbf{v}_{RD}$ are used for BF vectors and $\mathbf{u}_{SD}$, $\mathbf{u}_{SR}$, and $\mathbf{u}_{RD}$ are used as combining vectors in equations (3.3) and (3.4),

$$y_{SD} = \sqrt{\rho_{SD}}\mathbf{u}_{SD}^H \mathbf{H}_{SD}\mathbf{v}_{SD}x + \mathbf{u}_{SD}^H \mathbf{n}_{SD} \tag{3.20}$$

$$y_{SRD} = \sqrt{\rho_{RD}}\mathbf{u}_{RD}^H \mathbf{H}_{RD}\mathbf{v}_{RD}\hat{x} + \mathbf{u}_{RD}^H \mathbf{n}_{RD}, \tag{3.21}$$

where $\hat{x}$ is the ML decoded symbol from $y_{SR} = \sqrt{\rho_{SR}}\mathbf{u}_{SR}^H \mathbf{H}_{SR}\mathbf{v}_{SR}x + \mathbf{u}_{SR}^H \mathbf{n}_{SR}$.

If the CMRC criterion is used to combine signals from equations (3.20) and (3.21) when all CSI is known at the source and destination, the total instantaneous received SNR can be represented by

$$\gamma = \begin{cases} \frac{\left(\gamma_{SD}/\sqrt{\rho_{SD}} + \gamma_{eq}/\sqrt{\rho_{RD}}\right)^2}{\gamma_{SD}/\rho_{SD} + \gamma_{eq}^2/(\rho_{RD}\gamma_{RD})}, & \hat{x} = x \\ \frac{\left(\gamma_{SD}/\sqrt{\rho_{SD}} - \gamma_{eq}/\sqrt{\rho_{RD}}\right)^2}{\gamma_{SD}/\rho_{SD} + \gamma_{eq}^2/(\rho_{RD}\gamma_{RD})}, & \hat{x} = -x \end{cases}, \tag{3.22}$$

where $\gamma_{eq} = [Q^{-1}((1 - P_{SR})P_{RD} + P_{SR}(1 - P_{RD}))]/2$, $P_{SR} = Q(\sqrt{2\gamma_{SR}})$, and $P_{RD} = Q(\sqrt{2\gamma_{RD}})$ when the sub-optimal CMRC combining scheme [33] is used. CMRC is used instead of ML [41] because CMRC is much simpler than ML and the performance of it is very similar to that of ML at high SNR. The instantaneous BER using BPSK is given by

$$P_E^{DFLB} = (1 - P_{SR})\, Q\left(\sqrt{2\gamma_{\hat{x}=x}}\right) + P_{SR} Q\left(\sqrt{2\gamma_{\hat{x}=-x}}\right). \tag{3.23}$$

The average BER can be obtained by averaging the instantaneous BER over γ_{SD}, γ_{SR}, and γ_{RD} numerically.

3.3 Performance Analysis for the Three-Slot Scheme with $M_R = 1$

The half-duplex scenario is considered with a three-slot scheme, in which the relay and destination receive the transmitted signal from the source

with a BF vector matched with the direct link ($S \rightarrow D$) in the first time slot; the relay and destination receive the transmitted signal from the source with a BF vector matched with the relay link ($S \rightarrow R$) in the second time slot; the destination receives the relayed signal from the relay while the source remains silent in the third time slot [42]. Figure 3.2 shows the three-slot relaying scheme. We assume that a block of signals is transmitted from the source and relay for each time slot, so that all channels are considered to be statistically independent even if same channels are used consecutively.

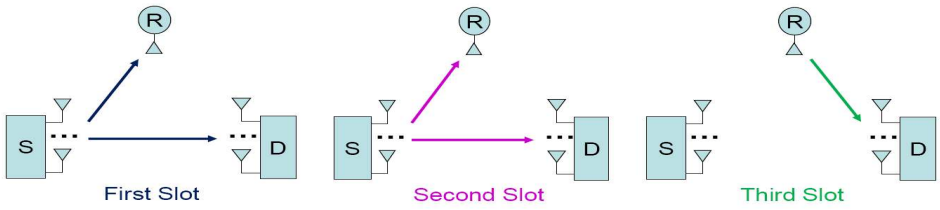

Figure 3.2: The Three-Slot Scheme.

The received signals using MRT and MRC at the destination and relay via the first, second, and third time slots are as follows:

$$y_{SD,1} = \sqrt{\rho_{SD}}\mathbf{c}_{SD,1}^H \mathbf{H}_{SD,1}\mathbf{f}_{SD}x + \mathbf{c}_{SD,1}^H \mathbf{n}_{SD,1} \tag{3.24}$$

$$y_{SR,1} = \sqrt{\rho_{SR}}c_{SR,1}^* \mathbf{h}_{SR,1}^T \mathbf{f}_{SD}x + c_{SR,1}^* n_{SR,1} \tag{3.25}$$

$$y_{SD,2} = \sqrt{\rho_{SD}}\mathbf{c}_{SD,2}^H \mathbf{H}_{SD,2}\mathbf{f}_{SR}x + \mathbf{c}_{SD,2}^H \mathbf{n}_{SD,2} \tag{3.26}$$

$$y_{SR,2} = \sqrt{\rho_{SR}}c_{SR,2}^* \mathbf{h}_{SR,2}^T \mathbf{f}_{SR}x + c_{SR,2}^* n_{SR,2} \tag{3.27}$$

$$y_{SRD} = \sqrt{\rho_{RD}}\mathbf{c}_{RD}^H \mathbf{h}_{RD} f_{RD} w y_{SR} + \mathbf{c}_{RD}^H \mathbf{n}_{RD}, \tag{3.28}$$

where $\mathbf{c}_{SD,1}$ ($M_D \times 1$), $\mathbf{c}_{SD,2}$ ($M_D \times 1$), $c_{SR,1}$ (1×1), $c_{SR,2}$ (1×1), and $\mathbf{c}_{RD}$ ($M_D \times 1$) are MRC combining weight vectors or scalars with Euclidean norm 1; $\mathbf{H}_{SD,1}$ ($M_D \times M_S$), $\mathbf{H}_{SD,2}$ ($M_D \times M_S$), $\mathbf{h}_{SR,1}$ ($M_S \times 1$), $\mathbf{h}_{SR,2}$ ($M_S \times 1$), and $\mathbf{h}_{RD}$ ($M_D \times 1$) are channel coefficient matrices or vectors, assumed to be i.i.d.

$CN(0,1)$; $\mathbf{n}_{SD,1}$ $(M_D \times 1)$, $\mathbf{n}_{SD,2}$ $(M_D \times 1)$, $n_{SR,1}$ (1×1), $n_{SR,2}$ (1×1), and $\mathbf{n}_{RD}$ $(M_D \times 1)$ are noise vectors or scalars distributed $CN(0, \mathbf{I})$ where $\mathbf{I}$ is the identity matrix; w is a normalization weight scalar,

$$1/\sqrt{\rho_{SR}^2 \left(\|\mathbf{h}_{SR,1}^T \mathbf{f}_{SD}\|^2 + \|\mathbf{h}_{SR,2}^T \mathbf{f}_{SR}\|^2\right)^2 + \rho_{SR} \left(\|\mathbf{h}_{SR,1}^T \mathbf{f}_{SD}\|^2 + \|\mathbf{h}_{SR,2}^T \mathbf{f}_{SR}\|^2\right)},$$

y_{SR} is the aggregated received signal combining equations (3.25) and (3.27) at the relay given below.

Using equations (3.24)-(3.27), the combined received signals using the minimum mean square error (MMSE) criterion [24, 31, 32] at the destination and relay can be written as follows:

$$\begin{aligned} y_{SD} = {} & \rho_{SD} |\mathbf{c}_{SD,1}^H \mathbf{H}_{SD,1} \mathbf{f}_{SD}| \mathbf{c}_{SD,1}^H \mathbf{H}_{SD,1} \mathbf{f}_{SD} x + \sqrt{\rho_{SD}} |\mathbf{c}_{SD,1}^H \mathbf{H}_{SD,1} \mathbf{f}_{SD}| \mathbf{c}_{SD,1}^H \mathbf{n}_{SD,1} \\ & + \rho_{SD} |\mathbf{c}_{SD,2}^H \mathbf{H}_{SD,2} \mathbf{f}_{SR}| \mathbf{c}_{SD,2}^H \mathbf{H}_{SD,2} \mathbf{f}_{SR} x + \sqrt{\rho_{SD}} |\mathbf{c}_{SD,2}^H \mathbf{H}_{SD,2} \mathbf{f}_{SR}| \mathbf{c}_{SD,2}^H \mathbf{n}_{SD,2} \end{aligned} \tag{3.29}$$

$$\begin{aligned} y_{SR} = {} & \rho_{SR} |c_{SR,1}^* \mathbf{h}_{SR,1}^T \mathbf{f}_{SD}| c_{SR,1}^* \mathbf{h}_{SR,1}^T \mathbf{f}_{SD} x + \sqrt{\rho_{SR}} |c_{SR,1}^* \mathbf{h}_{SR,1}^T \mathbf{f}_{SD}| c_{SR,1}^* n_{SR,1} \\ & + \rho_{SR} |c_{SR,2}^* \mathbf{h}_{SR,2}^T \mathbf{f}_{SR}| c_{SR,2}^* \mathbf{h}_{SR,2}^T \mathbf{f}_{SR} x + \sqrt{\rho_{SR}} |c_{SR,2}^* \mathbf{h}_{SR,2}^T \mathbf{f}_{SR}| c_{SR,2}^* n_{SR,2}. \end{aligned} \tag{3.30}$$

Recall from [24, 31, 32] that the MMSE coefficient is $\sqrt{P}/N$ where P is the aggregate signal power and N is the aggregate noise power from equations (3.24)-(3.27). Before relaying the combined received signals to the destination, the relay normalizes them to make ρ_{RD} represent an average transmit SNR at the relay. After three time slots, therefore, the received signals at the destination via the relay and direct links are given by equations (3.28) and (3.29), respectively.

3.3.1 Performance Analysis

For better performance with no spectral loss, our work focuses on schemes that use three time slots: $S \rightarrow R$ and $S \rightarrow D$ with a BF vector

matched with $S \rightarrow D$ in the first time; $S \rightarrow R$ and $S \rightarrow D$ with another BF vector matched with $S \rightarrow R$ in the second time slot; $R \rightarrow D$ in the third time slot. The three-slot scheme is a natural extension of the two-slot scheme, in which $S \rightarrow R$ and $S \rightarrow D$ in the first time slot and $R \rightarrow D$ in the second time slot [11], and strong-path BF, which beamforms to the stronger path of direct and relay links based on their instantaneous received SNR's [43].

Even though the two-slot scheme allows two distinct BF vectors from the source to the relay and destination, respectively, to find a universal performance bound, the three-slot scheme can use two different BF vectors naturally during the first and second time slots. Therefore, determining the BF vectors is not an issue in the three-slot scheme. For BF vectors, $\mathbf{f}_{SD}$ is chosen with $\mathbf{v}_{SD}$, the strongest right singular vector of $\mathbf{H}_{SD,1}$, and $\mathbf{f}_{SR}$ is chosen with $\mathbf{v}_{SR} = \mathbf{h}_{SR}/\|\mathbf{h}_{SR}\|$ for equations (3.24)-(3.30). For combining vectors, in addition, $\mathbf{c}_{SD,1}$ is used with $\mathbf{u}_{SD,1}$, the strongest left singular vector of $\mathbf{H}_{SD,1}$, $\mathbf{c}_{SD,2}$ is used with $\mathbf{u}_{SD,2} = \mathbf{H}_{SD,2}\mathbf{f}_{SR}/\|\mathbf{H}_{SD,2}\mathbf{f}_{SR}\|$, and $\mathbf{c}_{RD}$ is used with $\mathbf{u}_{RD} = \mathbf{h}_{RD}/\|\mathbf{h}_{RD}\|$.

If $\mathbf{v}_{SD}$ and $\mathbf{v}_{SR}$ are used for BF vectors and $\mathbf{u}_{SD,1}$, $\mathbf{u}_{SD,2}$ and $\mathbf{u}_{RD}$ are used as combining vectors in equations (3.24)-(3.30), the received signals through all three time slots can be written as follows:

$$\begin{aligned} y_{SD} = {} & \rho_{SD}\left(\|\mathbf{H}_{SD,1}\mathbf{v}_{SD}\|^2 + \|\mathbf{H}_{SD,2}\mathbf{v}_{SR}\|^2\right)x \\ & + \sqrt{\rho_{SD}}\left(\|\mathbf{H}_{SD,1}\mathbf{v}_{SD}\|\mathbf{u}_{SD,1}^H\mathbf{n}_{SD,1} + \|\mathbf{H}_{SD,2}\mathbf{v}_{SR}\|\mathbf{u}_{SD,2}^H\mathbf{n}_{SD,2}\right) \end{aligned} \tag{3.31}$$

$$\begin{aligned} y_{SR} = {} & \rho_{SR}\left(\|\mathbf{h}_{SR,1}^T\mathbf{v}_{SD}\|^2 + \|\mathbf{h}_{SR,2}^T\mathbf{v}_{SR}\|^2\right)x \\ & + \sqrt{\rho_{SR}}\left(\|\mathbf{h}_{SR,1}^T\mathbf{v}_{SD}\|n_{SR,1} + \|\mathbf{h}_{SR,2}^T\mathbf{v}_{SR}\|n_{SR,2}\right) \end{aligned} \tag{3.32}$$

$$y_{SRD} = \sqrt{\rho_{RD}}w\|\mathbf{h}_{RD}\|y_{SR} + \mathbf{u}_{RD}^H\mathbf{n}_{RD}, \tag{3.33}$$

where w is obtained with $\mathbf{v}_{SD}$ and $\mathbf{v}_{SR}$.

If the MMSE criterion is used to combine signals from equations (3.31) and (3.33) when all CSI is known at the source and destination, the total instantaneous received SNR can be represented by

$$\gamma = \gamma_{SD} + \gamma_{SRD} = \Gamma_{SD} + \Gamma'_{SD} + \frac{(\Gamma_{SR} + \Gamma'_{SR})\,\Gamma_{RD}}{1 + (\Gamma_{SR} + \Gamma'_{SR}) + \Gamma_{RD}}, \tag{3.34}$$

where $\gamma_{SD} := \Gamma_{SD} + \Gamma'_{SD}$, $\Gamma_{SD} = \rho_{SD}\|\mathbf{H}_{SD,1}\mathbf{v}_{SD}\|^2$, $\Gamma'_{SD} = \rho_{SD}\|\mathbf{H}_{SD,2}\mathbf{v}_{SR}\|^2$, $\Gamma_{SR} = \rho_{SR}\|\mathbf{h}_{SR}\|^2$, $\Gamma'_{SR} = \rho_{SR}\|\mathbf{h}_{SR}^T\mathbf{v}_{SD}\|^2$, $\Gamma_{RD} = \rho_{RD}\|\mathbf{h}_{RD}\|^2$, and $\gamma_{SRD} := (\Gamma_{SR} + \Gamma'_{SR})\,\Gamma_{RD}/\,(1 + (\Gamma_{SR} + \Gamma'_{SR}) + \Gamma_{RD})$. Note that primes (i.e. Γ'_{SD} and Γ'_{SR}) indicate instantaneous received SNR's with unmatched beamformers. We also define $\gamma^+_{SD} = \rho_{SD}\|\mathbf{H}^+_{SD}\mathbf{v}^+_{SD}\|^2$, a received SNR when $M_S + 1$ source antennas are used for BF via the direct link, where $\mathbf{H}^+_{SD}$ $(M_D \times (M_S + 1))$ is a channel coefficient matrix assumed to be i.i.d. $CN(0, 1)$ and $\mathbf{v}^+_{SD}$ is the strongest right singular vector of $\mathbf{H}^+_{SD}$ since the SER performance using γ^+_{SD} provides an upper-bound for the SER performance using γ_{SD}.

Based on an SER expression, $P_E = \mathbb{E}\left[aQ\left(\sqrt{2b\gamma}\right)\right]$ where a and b are modulation related constants (i.e. $a = 1, b = 1$ for BPSK and approximately $a = 2, b = \sin^2(\pi/M)$ for M-ary PSK) and γ is an instantaneous received SNR, [eqn. (20)] [44] presents a simple SER approximation as

$$P_E = \frac{a\sqrt{b}}{2\sqrt{\pi}} \int_0^\infty \frac{e^{-bx}}{\sqrt{x}} F_\gamma(x)dx. \tag{3.35}$$

When the CDF's of γ^+_{SD} and $\Gamma_{SRD} := (\Gamma_{SR} + \Gamma'_{SR})\,\Gamma_{RD}/\,((\Gamma_{SR} + \Gamma'_{SR}) + \Gamma_{RD})$ are substituted to equation (3.35), the average SER's for the direct and relay links are as follows (please see details in Appendix 3.5):

$$P_{E,SD} \le \frac{a}{2} - \sum_{n=1}^{M_D} \sum_{m=M_S-M_D+1}^{(M_S+M_D+1)n-2n^2} \sum_{k=0}^{m} \frac{a\sqrt{b}\,d_{n,m+1}\,n^k(2k-1)!!}{2^{k+1}k!\rho_{SD}^k\left(b + \frac{n}{\rho_{SD}}\right)^{k+\frac{1}{2}}} \tag{3.36}$$

$$P_{E,SRD} \geq \frac{a}{2} - \frac{a\sqrt{b}\sqrt{\frac{\rho_{RD}}{\rho_{SR}}}}{(M_D-1)!\rho_{RD}^{M_D}} \sum_{p=0}^{M_S} \frac{1}{p!} \left(\frac{1}{\rho_{SR}\rho_{RD}}\right)^{\frac{p}{2}} \sum_{q=0}^{M_D+p-1} \binom{M_D+p-1}{q} \left(\frac{\rho_{RD}}{\rho_{SR}}\right)^{\frac{q}{2}}$$
$$\frac{\left(\frac{4}{\sqrt{\rho_{SR}\rho_{RD}}}\right)^{q-p+1}}{\left(b+\frac{1}{\rho_{SR}}+\frac{1}{\rho_{RD}}+\frac{2}{\sqrt{\rho_{SR}\rho_{RD}}}\right)^{M_D+q+\frac{3}{2}}} \frac{\Gamma(M_D+q+\frac{3}{2})\Gamma(M_D+2p-q-\frac{1}{2})}{\Gamma(M_D+p+1)}$$
$${}_2F_1\left(M_D+q+\frac{3}{2}, q-p+\frac{3}{2}; M_D+p+1; \frac{b+\frac{1}{\rho_{SR}}+\frac{1}{\rho_{RD}}-\frac{2}{\sqrt{\rho_{SR}\rho_{RD}}}}{b+\frac{1}{\rho_{SR}}+\frac{1}{\rho_{RD}}+\frac{2}{\sqrt{\rho_{SR}\rho_{RD}}}}\right), \tag{3.37}$$

where $d_{n,m}$ is the coefficient given by [30, eqn. (24)], !! denotes the double factorial defined in [37], and ${}_2F_1(\alpha,\beta;\gamma;z)$ is the Gauss hypergeometric function in [37]. Note that $P_{E,SD}$ is upper-bounded by using γ_{SD}^{+} instead of γ_{SD} since it is intractable to obtain the CDF and PDF of γ_{SD}. Note also that $P_{E,SRD}$ is lower-bounded by removing the 1 in the denominator of γ_{SRD} since an SER closed-form solution is not tractable with γ_{SRD} even though the CDF and PDF of γ_{SRD} are obtained and used to find numerical solutions. Both upper-bound and lower-bound are tight to the exact SER performance, and enough to show the superiority of the three-slot scheme over the two-slot scheme in SER performance at high SNR.

Based on the total instantaneous received SNR given in equation (3.34), the average combined SER using Craig's formula [7] can be written as

$$P_E = \frac{1}{\pi} \int_0^{\frac{(M-1)\pi}{M}} \mathbb{E}\left[e^{-\frac{g\gamma_{SD}}{\sin^2\theta}}\right] \mathbb{E}\left[e^{-\frac{g\gamma_{SRD}}{\sin^2\theta}}\right] d\theta, \tag{3.38}$$

where $g = \sin^2(\pi/M)$ for M-ary PSK including BPSK. A closed-form solution of the first expectation in equation (3.38) is not tractable but it can be upper-bounded by using γ_{SD}^{+} instead of γ_{SD} (please see details in Appendix 3.6):

$$\mathbb{E}\left[e^{-\frac{g\gamma_{SD}}{\sin^2\theta}}\right] \leq \sum_{n=1}^{M_D} \sum_{m=M_S-M_D+1}^{(M_S+M_D+1)n-2n^2} d_{n,m+1} \left(\frac{\sin^2\theta}{\sin^2\theta+\frac{g\rho_{SD}}{n}}\right)^{m+1}. \tag{3.39}$$

A closed-form solution of the second expectation in equation (3.38) is not obtainable, but it can be lower-bounded by removing the 1 in the denominator

of γ_{SRD} similar to equation (3.37) as follows (please see details also in Appendix 3.6):

$$\mathbb{E}\left[e^{-\frac{g\gamma_{SRD}}{\sin^2\theta}}\right] \geq 1 - \frac{2g\sqrt{\frac{\rho_{RD}}{\rho_{SR}}}}{(M_D-1)!\rho_{RD}^{M_D}\sin^2\theta}\sum_{p=0}^{M_S}\frac{1}{p!}\left(\frac{1}{\rho_{SR}\rho_{RD}}\right)^{\frac{p}{2}}\sum_{q=0}^{M_D+p-1}\binom{M_D+p-1}{q}$$
$$\frac{\sqrt{\pi}\left(\frac{\rho_{RD}}{\rho_{SR}}\right)^{q/2}\left(\frac{4}{\sqrt{\rho_{SR}\rho_{RD}}}\right)^{q-p+1}}{\left(\frac{g}{\sin^2\theta}+\frac{1}{\rho_{SR}}+\frac{1}{\rho_{RD}}+\frac{2}{\sqrt{\rho_{SR}\rho_{RD}}}\right)^{M_D+q+2}}\frac{\Gamma(M_D+q+2)\Gamma(M_D+2p-q)}{\Gamma\left(M_D+p+\frac{3}{2}\right)}$$
$$ {}_2F_1\left(M_D+q+2, q-p+\frac{3}{2}; M_D+p+\frac{3}{2}; \frac{\frac{g}{\sin^2\theta}+\frac{1}{\rho_{SR}}+\frac{1}{\rho_{RD}}-\frac{2}{\sqrt{\rho_{SR}\rho_{RD}}}}{\frac{g}{\sin^2\theta}+\frac{1}{\rho_{SR}}+\frac{1}{\rho_{RD}}+\frac{2}{\sqrt{\rho_{SR}\rho_{RD}}}}\right). \tag{3.40}$$

Therefore, equation (3.38) can be upper-bounded once equations (3.39) and (3.40) are substituted. Instead of the upper-bound, however, the exact solution of equation (3.38) can be also obtained by averaging $aQ\left(\sqrt{2b\left(\gamma_{SD}+\gamma_{SRD}\right)}\right)$ numerically.

3.3.2 High SNR Analysis

Simple high SNR performance is now considered to simplify equations (3.36)-(3.40). The approximation uses PDF's of γ_{SD}^{+} and Γ_{SRD}, and we check that both PDF's satisfy the assumptions given in [34], which provides a systematic method for high SNR analysis. Based on [34], the average SER of an uncoded system can be approximated by

$$P_E = (2b\rho G_a)^{-G_d} + o\left(\rho^{-G_d}\right) \tag{3.41}$$

as $\rho \to \infty$, where $G_a = \left(\left(\sqrt{\pi}(t+1)\right)/\left(a2^t\alpha\Gamma(t+3/2)\right)\right)^{1/(t+1)}$ is the array gain, ρ is the average transmit SNR, $G_d = t+1$ is the diversity order, t is the first nonzero derivative order of the PDF of a channel dependent random variable λ at the origin, and a and b are modulation specific positive constants from the instantaneous SER, $P_E(\lambda) = aQ\left(\sqrt{2b\rho\lambda}\right)$. This random variable, λ, is proportional to the instantaneous SNR as $\gamma = \rho\lambda$, and $\alpha = f_{\lambda}^{(t)}(0)/t! \neq 0$.

The average transmit SNR ρ may be ρ_{SR} with ρ_{SD} and ρ_{RD} which are constant multiples of ρ_{SR}, and channel dependent random variable λ may be either $\lambda_{SD} := \gamma^{+}_{SD}/\rho_{SR}$ or $\lambda_{SRD} := \Gamma_{SRD}/\rho_{SR}$ in the sequel. Therefore, equation (3.41) can be calculated once t and α are found using the PDF's of λ_{SD} and λ_{SRD}. The array and diversity gains, G_a and G_d, in equation (3.41) are found for the direct and relay links separately, and then they are combined to obtain high SNR performance for the whole system.

For the direct link, the PDF of λ_{SD}, given by Appendix 3.7, is used to find t_{SD}, the first nonzero derivative order of the PDF of λ_{SD}, and $\alpha_{SD} = f^{(t_{SD})}_{\lambda_{SD}}(0)/t_{SD}!$. In this case, $t_{SD} = (M_S+1)\cdot M_D - 1$ since the diversity order of the direct link using MRT with MRC is given by $(M_S+1)\cdot M_D$ because the received SNR of the direct link is $\Gamma_{SD} + \Gamma'_{SD}$. If the t_{SD} order derivative of the PDF of λ_{SD} is evaluated at the origin, the following can be obtained (please see details in Appendix 3.7)

$$f^{(t_{SD})}_{\lambda_{SD}}(0) = \sum_{n=1}^{M_D} \sum_{m=M_S-M_D+1}^{(M_S+M_D+1)n-2n^2} d_{n,m+1} \binom{t_{SD}}{m} (-1)^{t_{SD}+m} \left(\frac{n\rho_{SR}}{\rho_{SD}}\right)^{t_{SD}+1}. \quad (3.42)$$

Based on equation (3.42), α_{SD} can be acquired by

$$\alpha_{SD} = \frac{f^{(t_{SD})}_{\lambda_{SD}}(0)}{((M_S+1)\cdot M_D - 1)!}. \quad (3.43)$$

Therefore, the direct link high SNR performance can be obtained as follows:

$$P_{E,SD} \leq (2b\rho_{SR}G_{a,SD})^{-G_{d,SD}} + o\left(\rho_{SR}^{-G_{d,SD}}\right) \quad (3.44)$$

$$G_{d,SD} = (M_S+1)\cdot M_D \quad (3.45)$$

$$G_{a,SD} = \left(\frac{a2^{G_{d,SD}-1}\alpha_{SD}\Gamma\left(G_{d,SD}+\frac{1}{2}\right)}{\sqrt{\pi}G_{d,SD}}\right)^{-\frac{1}{G_{d,SD}}}. \quad (3.46)$$

For the relay link, the PDF of $\lambda_{SRD} := \Gamma_{SRD}/\rho_{SR}$, where Γ_{SRD} is defined just after equation (3.35), can be used to find t_{SRD} and α_{SRD} because the instantaneous SNR's Γ_{SRD} and γ_{SRD} are equivalent at high average SNR

since they differ by a constant term in the denominator of equation (3.34). Since the diversity order of the relay link is given by $\min(M_S+1, M_D)$, $t_{SRD} = \min(M_S+1, M_D) - 1$ because the received SNR of the first hop of the relay link is $\Gamma_{SR} + \Gamma'_{SR}$. The t_{SRD} order derivative of the PDF of λ_{SRD} evaluated at the origin can be obtained by extending the number of source antennas by 1 and removing antenna correlation factors from [35, eqn. (28)] as follows:

$$f_{\lambda_{SRD}}^{(t_{SRD})}(0) = \begin{cases} \left(\frac{\rho_{SR}}{\rho_{RD}}\right)^{M_D}, & M_S+1 > M_D \\ 1, & M_S+1 < M_D \\ \left(\frac{\rho_{SR}}{\rho_{RD}}\right)^{M_D} + 1, & M_S+1 = M_D \end{cases} . \tag{3.47}$$

Based on equation (3.47), α_{SRD} can be written as

$$\alpha_{SRD} = \frac{f_{\lambda_{SRD}}^{(t_{SRD})}(0)}{(\min(M_S+1, M_D)-1)!} = \begin{cases} \frac{\left(\frac{\rho_{SR}}{\rho_{RD}}\right)^{M_D}}{(M_D-1)!}, & M_S+1 > M_D \\ \frac{1}{M_S!}, & M_S+1 < M_D \\ \frac{\left(\frac{\rho_{SR}}{\rho_{RD}}\right)^{M_D}+1}{(M_D-1)!}, & M_S+1 = M_D \end{cases} . \tag{3.48}$$

Therefore, the relay link high SNR performance can be obtained as follows:

$$P_{E,SRD} = (2b\rho_{SR}G_{a,SRD})^{-G_{d,SRD}} + o\left(\rho_{SR}^{-G_{d,SRD}}\right) \tag{3.49}$$

$$G_{d,SRD} = \min(M_S+1, M_D) \tag{3.50}$$

$$G_{a,SRD} = \left(\frac{a2^{G_{d,SRD}-1}\alpha_{SRD}\Gamma\left(G_{d,SRD}+\frac{1}{2}\right)}{\sqrt{\pi}G_{d,SRD}}\right)^{-\frac{1}{G_{d,SRD}}} . \tag{3.51}$$

Instead of using the PDF of $\gamma_{SD}^{+} + \Gamma_{SRD}$, an alternate approach is used to find t_C and α_C for the combined link. We have $t_C = (M_S+1)\cdot M_D + \min(M_S+1, M_D) - 1$ since the diversity order of the combined link is $(M_S+1)\cdot M_D + \min(M_S+1, M_D)$, which is the sum of the diversity orders of the direct and relay links because the received SNR of the combined link is $\gamma_{SD}^{+} + \Gamma_{SRD}$. To find $f_{\lambda_{SD}+\lambda_{SRD}}^{(t_C)}(0)$, the product of $f_{\lambda_{SD}}^{(t_{SD})}(0)$ and $f_{\lambda_{SRD}}^{(t_{SRD})}(0)$ can be used, which is shown in Appendix 3.4. Therefore, the final combined

α_C is given by using equations (3.42) and (3.47)

$$\alpha_C = \frac{f_{\lambda_{SD}}^{(t_{SD})}(0) \cdot f_{\Lambda_{SRD}}^{(t_{SRD})}(0)}{((M_S+1)\cdot M_D + \min(M_S+1, M_D) - 1)!}. \tag{3.52}$$

Based on α_C and t_C, G_d and G_a can be substituted as explained after equation (3.41). The combined link high SNR performance can be obtained as follows:

$$P_E \leq (2b\rho_{SR}G_a)^{-G_d} + o\left(\rho_{SR}^{-G_d}\right) \tag{3.53}$$

$$G_d = (M_S+1)\cdot M_D + \min(M_S+1, M_D) \tag{3.54}$$

$$G_a = \left(\frac{a2^{G_d-1}\alpha_C\Gamma\left(G_d+\frac{1}{2}\right)}{\sqrt{\pi}G_d}\right)^{-\frac{1}{G_d}}. \tag{3.55}$$

Since all potential resources of the relay network are used, full diversity orders are achieved from the direct, relay, and combined links.

3.3.3 Selection Relaying with BF

If $\mathbf{h}_{RD}$ and $\mathbf{h}_{SR}$ are unknown at the source and destination, respectively, the most practical approach is selection relaying [11]. In traditional selection relaying with single antennas, the relay transmits the amplified signal to the destination if the received SNR of the $S \rightarrow R$ exceeds a predetermined threshold. In the presence of beamforming using three time slots, this can be extended where the relay transmits its aggregated amplified signal with BF only when it exceeds the threshold. Therefore, if the received SNR for the first two time slots, $\Gamma_{SR} + \Gamma'_{SR}$, exceeds the threshold at the relay, the relay transmits the aggregated amplified signal, and the source retransmits the signal with a matched BF vector otherwise in the third time slot.

The source determines the BF vectors based on the channels, $\mathbf{H}_{SD}$ and $\mathbf{h}_{SR}$, and the destination combines received signals based on the received SNR's of $\mathbf{H}_{SD}$ and $\mathbf{h}_{RD}$ since $\mathbf{h}_{RD}$ and $\mathbf{h}_{SR}$ are unknown at the source and destination,

respectively. Therefore, if $\Gamma_{SR} + \Gamma'_{SR} > T$ where T is the predetermined threshold, $\mathbf{f}_{SD}$ is chosen with $\mathbf{v}_{SD}$, the strongest right singular vector of $\mathbf{H}_{SD,1}$, and $\mathbf{f}_{SR}$ is chosen with $\mathbf{v}_{SR} = \mathbf{h}_{SR}/\|\mathbf{h}_{SR}\|$ for equations (3.24)-(3.30). For combining, $\mathbf{c}_{SD,1}$ is used with $\mathbf{u}_{SD,1}$, the strongest left singular vector of $\mathbf{H}_{SD,1}$, $\mathbf{c}_{SD,2}$ is used with $\mathbf{u}_{SD,2} = \mathbf{H}_{SD,2}\mathbf{f}_{SR}/\|\mathbf{H}_{SD,2}\mathbf{f}_{SR}\|$, and $\mathbf{c}_{RD}$ is used with $\mathbf{u}_{RD} = \mathbf{h}_{RD}/\|\mathbf{h}_{RD}\|$. If $\Gamma_{SR} + \Gamma'_{SR} \leq T$, $\mathbf{v}_{SD,3}$, the strongest right singular vector of $\mathbf{H}_{SD,3}$, is used for the BF vector, and $\mathbf{u}_{SD,3}$, the strongest left singular vector of $\mathbf{H}_{SD,3}$, is used for the combining vector in the third time slot. Note that this scheme does not require knowledge of $\mathbf{h}_{RD}$ and $\mathbf{h}_{SR}$ at the source and destination, respectively.

To characterize performance, if $\Gamma_{SR} + \Gamma'_{SR} \leq T$, note that the source transmits three times with three distinct BF vectors over three statistically independent consecutive time slots, and the relay never transmits the aggregated amplified signals in this case. For the first two time slots, $\mathbf{v}_{SD}$ and $\mathbf{v}_{SR}$ are used for the BF vectors, and $\mathbf{u}_{SD,1}$ and $\mathbf{u}_{SD,2}$ are used for combining vectors. For the third time slot, $\mathbf{v}_{SD,3}$ and $\mathbf{u}_{SD,3}$ are used for the BF and combining vectors, respectively:

$$y_{SD,1} = \sqrt{\rho_{SD}}\mathbf{u}_{SD,1}^H \mathbf{H}_{SD,1}\mathbf{v}_{SD}x + \mathbf{u}_{SD,1}^H \mathbf{n}_{SD,1} \tag{3.56}$$

$$y_{SD,2} = \sqrt{\rho_{SD}}\mathbf{u}_{SD,2}^H \mathbf{H}_{SD,2}\mathbf{v}_{SR}x + \mathbf{u}_{SD,2}^H \mathbf{n}_{SD,2} \tag{3.57}$$

$$y_{SD,3} = \sqrt{\rho_{SD}}\mathbf{u}_{SD,3}^H \mathbf{H}_{SD,3}\mathbf{v}_{SD,3}x + \mathbf{u}_{SD,3}^H \mathbf{n}_{SD,3}. \tag{3.58}$$

If $\Gamma_{SR} + \Gamma'_{SR} > T$, $\mathbf{v}_{SD}$ and $\mathbf{v}_{SR}$ are used for the BF vectors, and $\mathbf{u}_{SD,1}$, $\mathbf{u}_{SD,2}$, and $\mathbf{u}_{RD}$ are used for the combining vectors:

$$\begin{aligned} y_{SD} = {} & \rho_{SD}\left(\|\mathbf{H}_{SD,1}\mathbf{v}_{SD}\|^2 + \|\mathbf{H}_{SD,2}\mathbf{v}_{SR}\|^2\right)x \\ & + \sqrt{\rho_{SD}}\left(\|\mathbf{H}_{SD,1}\mathbf{v}_{SD}\|\mathbf{u}_{SD,1}^H\mathbf{n}_{SD,1} + \|\mathbf{H}_{SD,2}\mathbf{v}_{SR}\|\mathbf{u}_{SD,2}^H\mathbf{n}_{SD,2}\right) \end{aligned} \tag{3.59}$$

$$\begin{aligned} y_{SR} = {} & \rho_{SR}\left(\|\mathbf{h}_{SR,1}^T\mathbf{v}_{SD}\|^2 + \|\mathbf{h}_{SR,2}^T\mathbf{v}_{SR}\|^2\right)x \\ & + \sqrt{\rho_{SR}}\left(\|\mathbf{h}_{SR,1}^T\mathbf{v}_{SD}\|n_{SR,1} + \|\mathbf{h}_{SR,2}^T\mathbf{v}_{SR}\|n_{SR,2}\right) \end{aligned} \tag{3.60}$$

$$y_{SRD} = \sqrt{\rho_{RD}} w \|\mathbf{h}_{RD}\| y_{SR} + \mathbf{u}_{RD}^H \mathbf{n}_{RD}, \tag{3.61}$$

where w is obtained with $\mathbf{v}_{SD}$ and $\mathbf{v}_{SR}$. Note that the received signal equations (3.59)-(3.61) when $\Gamma_{SR}+\Gamma'_{SR} > T$ are exactly same as equations (3.31)-(3.33).

If the MMSE criterion is used to combine signals, given by equations (3.56)-(3.61), for both cases separately, the total instantaneous received SNR for selection relaying can be represented by

$$\gamma = \begin{cases} 2\Gamma_{SD} + \Gamma'_{SD}, & \Gamma_{SR}+\Gamma'_{SR} \le T \\ \frac{\left(\left(\Gamma_{SD}+\Gamma'_{SD}\right)\sqrt{1+\left(\Gamma_{SR}+\Gamma'_{SR}\right)}+\Gamma_{RD}\sqrt{\left(\Gamma_{SR}+\Gamma'_{SR}\right)}\right)^2}{\left(1+\left(\Gamma_{SR}+\Gamma'_{SR}\right)\right)\left(\left(\Gamma_{SD}+\Gamma'_{SD}\right)+\Gamma_{RD}\right)+\Gamma_{RD}^2}, & \Gamma_{SR}+\Gamma'_{SR} > T \end{cases}, \tag{3.62}$$

where $\Gamma_{SD} = \rho_{SD}\|\mathbf{H}_{SD,1}\mathbf{v}_{SD}\|^2$, $\Gamma_{SR} = \rho_{SR}\|\mathbf{h}_{SR,2}^T\mathbf{v}_{SR}\|^2$, $\Gamma_{RD} = \rho_{RD}\|\mathbf{h}_{RD}\|^2$, and $\Gamma'_{SR} = \rho_{SR}\|\mathbf{h}_{SR,1}^T\mathbf{v}_{SD}\|^2$. Therefore, the instantaneous SER for selection relaying is approximately given by

$$\begin{aligned} P_E^{SR} &= P_r\left(\Gamma_{SR}+\Gamma'_{SR} \le T\right) aQ\left(\sqrt{2b\left(2\Gamma_{SD}+\Gamma'_{SD}\right)}\right) \\ &\quad + P_r\left(\Gamma_{SR}+\Gamma'_{SR} > T\right) I\left(\Gamma_{SR}+\Gamma'_{SR} > T\right) \\ &\quad aQ\left(\frac{\sqrt{2b}\left(\left(\Gamma_{SD}+\Gamma'_{SD}\right)\sqrt{1+\left(\Gamma_{SR}+\Gamma'_{SR}\right)}+\Gamma_{RD}\sqrt{\left(\Gamma_{SR}+\Gamma'_{SR}\right)}\right)}{\sqrt{\left(1+\left(\Gamma_{SR}+\Gamma'_{SR}\right)\right)\left(\left(\Gamma_{SD}+\Gamma'_{SD}\right)+\Gamma_{RD}\right)+\Gamma_{RD}^2}}\right), \end{aligned} \tag{3.63}$$

where $P_r\left(\Gamma_{SR}+\Gamma'_{SR} \le T\right) = 1-e^{-T/\rho_{SR}}\sum_{u=0}^{M_S}\left(T/\rho_{SR}\right)^u/u!$, $P_r\left(\Gamma_{SR}+\Gamma'_{SR} > T\right) = 1 - P_r\left(\Gamma_{SR}+\Gamma'_{SR} \le T\right)$, and $I(\cdot)$ is an indicator function.

Note that all variables in equation (3.63) are channel dependent, which makes averaging analytically intractable. However, the average SER can be obtained by averaging the instantaneous SER in equation (3.63) over Γ_{SD}, Γ_{SR}, Γ_{RD}, and Γ'_{SR} numerically. Based on equation (3.63), we can also find numerically the optimal threshold T_{opt} using the following optimization:

$$\begin{aligned} &\text{minimize} \quad \mathbb{E}\left[P_E^{SR}\right] \\ &\text{subject to} \quad T \ge 0. \end{aligned} \tag{3.64}$$

3.4 Performance Analysis for Two-Slot Lower-Bounds with Multiple Relay Antennas

To obtain the lower-bound on performance, two different BF vectors are used from the source to the relay and destination, respectively. Therefore, $\mathbf{f}_{SD}$ is the strongest right singular vector of $\mathbf{H}_{SD}$, and $\mathbf{f}_{SR}$ is the strongest right singular vector of $\mathbf{H}_{SR}$ for equations (3.1) and (3.2).

3.4.1 Performance Analysis

If the MMSE criterion is used to combine signals from equations (3.1) and (3.2) when all CSI is known at the source and destination, the total instantaneous received SNR can be represented by

$$\gamma = \gamma_{SD} + \frac{\gamma_{SR}\gamma_{RD}}{1 + \gamma_{SR} + \gamma_{RD}}, \tag{3.65}$$

where $\gamma_{SD} = \rho_{SD}\|\mathbf{H}_{SD}\mathbf{f}_{SD}\|^2$, $\gamma_{SR} = \rho_{SR}\|\mathbf{H}_{SR}\mathbf{f}_{SR}\|^2$, $\gamma_{RD} = \rho_{RD}\|\mathbf{H}_{RD}\mathbf{f}_{RD}\|^2$, and $\gamma_{SRD} := \gamma_{SR}\gamma_{RD}/(1 + \gamma_{SR} + \gamma_{RD})$.

From an average SER approximation, $P_E = \mathbb{E}\left[aQ\left(\sqrt{2b\gamma}\right)\right]$, where a and b are modulation related constants (i.e. approximately $a = 1, b = 1$ for BPSK, $a = 2, b = \sin^2(\pi/M)$ for M-ary PSK, and $a = 4, b = 3/(2(M-1))$ for M-ary QAM) and γ is an instantaneous received SNR, reference [44, eqn. (20)] presents a simple average SER approximation as

$$P_E = \frac{a\sqrt{b}}{2\sqrt{\pi}} \int_0^\infty \frac{e^{-bx}}{\sqrt{x}} F_\gamma(x) dx, \tag{3.66}$$

where $F_\gamma(x)$ is the cumulative distribution function (CDF) of γ.

If the CDFs of γ_{SD} and $\Gamma_{SRD} := \gamma_{SR}\gamma_{RD}/\left(\gamma_{SR} + \gamma_{RD}\right)$ obtained by upper-bounding equation (3.65) are substituted to equation (3.66), respectively, the approximate average SERs for the direct and relay links can be

obtained as follows (please see details in Appendix 3.8):

$$P_{E,SD} = \frac{a}{2} - \sum_{n=1}^{M_D} \sum_{m=M_S-M_D}^{(M_S+M_D)n-2n^2} \sum_{k=0}^{m} \frac{a\sqrt{b} d_{n,m} n^k (2k-1)!!}{2^{k+1} k! \rho_{SD}^k \left(b + \frac{n}{\rho_{SD}}\right)^{k+\frac{1}{2}}} \tag{3.67}$$

$$\begin{aligned} P_{E,SRD} \geq \frac{a}{2} - \sum_{n=1}^{M_R} \sum_{m=M_S-M_R}^{(M_S+M_R)n-2n^2} \sum_{k=0}^{m} \sum_{i=1}^{M_R} \sum_{j=M_D-M_R}^{(M_D+M_R)i-2i^2} \sum_{p=0}^{k+j} \binom{k+j}{p} \\ \frac{a\sqrt{b} d_{n,m} d_{i,j} n^{\frac{k+p+1}{2}} i^{\frac{2j+k-p+1}{2}}}{k! j! \rho_{SR}^{\frac{k+p+1}{2}} \rho_{RD}^{\frac{2j+k-p+1}{2}}} \frac{\left(4\sqrt{\frac{ni}{\rho_{SR}\rho_{RD}}}\right)^{p-k+1}}{\left(b + \frac{n}{\rho_{SR}} + \frac{i}{\rho_{RD}} + 2\sqrt{\frac{ni}{\rho_{SR}\rho_{RD}}}\right)^{p+j+\frac{5}{2}}} \\ \frac{\Gamma\left(j+p+\frac{5}{2}\right)\Gamma\left(j+2k-p+\frac{1}{2}\right)}{\Gamma(k+j+2)} \\ {}_2F_1\left(j+p+\frac{5}{2}, p-k+\frac{3}{2}; k+j+2; \frac{b + \frac{n}{\rho_{SR}} + \frac{i}{\rho_{RD}} - 2\sqrt{\frac{ni}{\rho_{SR}\rho_{RD}}}}{b + \frac{n}{\rho_{SR}} + \frac{i}{\rho_{RD}} + 2\sqrt{\frac{ni}{\rho_{SR}\rho_{RD}}}}\right), \end{aligned} \tag{3.68}$$

where $d_{n,m}$ are coefficients given by [30, eqn. (24)], !! denotes double factorial defined in [37], and ${}_2F_1(\alpha, \beta; \gamma; z)$ is the Gauss hypergeometric function in [37, p.1005]. Note that $P_{E,SRD}$ is lower-bounded by removing the 1 in the denominator of γ_{SRD} in equation (3.65). Note also that equations (3.67) and (3.68) are valid when $M_S \geq M_D$, $M_S \geq M_R$, and $M_D \geq M_R$ and are also valid if M_S, M_R, and M_D are switched each other otherwise. This is true for all cases about the number of antennas in the sequel.

For the combined instantaneous received SNR, $\gamma = \gamma_{SD} + \gamma_{SRD}$, the following average SER upper-bound expression is used.

$$P_E \leq \frac{a\sqrt{b}}{2\sqrt{2\pi}} \int_0^\infty \frac{e^{-bx}}{\sqrt[4]{x}} F_{\gamma_{SRD}}(x) dx \int_0^\infty \frac{e^{-by}}{\sqrt[4]{y}} f_{\gamma_{SD}}(y) dy, \tag{3.69}$$

where $\sqrt[4]{x}$ is the fourth root of x, $F_{\gamma_{SRD}}(x)$ is the CDF of γ_{SRD}, and $f_{\gamma_{SD}}(y)$ is the probability density function (PDF) of γ_{SD}. Equality holds when γ_{SD} is equal to γ_{SRD} since the relationship between the arithmetic and geometric means are used.

If the PDF of γ_{SD} and the CDF of Γ_{SRD} are substituted to equation (8), the approximate combined average SER can be obtained as follows:

$$P_E \approx \frac{a\sqrt{b}}{2\sqrt{2\pi}} \left[\sum_{n=1}^{M_D} \sum_{m=M_S-M_D}^{(M_S+M_D)n-2n^2} \sum_{k=0}^{m} \frac{d_{n,m} n^{m+1} \Gamma\left(m+\frac{3}{4}\right)}{m! \rho_{SD}^{m+1} \left(b+\frac{n}{\rho_{SD}}\right)^{m+\frac{3}{4}}} \right]$$
$$\left[\frac{\Gamma\left(\frac{3}{4}\right)}{b^{\frac{3}{4}}} - \sum_{n=1}^{M_R} \sum_{m=M_S-M_R}^{(M_S+M_R)n-2n^2} \sum_{k=0}^{m} \sum_{i=1}^{M_R} \sum_{j=M_D-M_R}^{(M_D+M_R)i-2i^2} \sum_{p=0}^{k+j} \binom{k+j}{p} \right.$$
$$\frac{2 d_{n,m} d_{i,j} n^{\frac{k+p+1}{2}} i^{\frac{2j+k-p+1}{2}}}{k! j! \rho_{SR}^{\frac{k+p+1}{2}} \rho_{RD}^{\frac{2j+k-p+1}{2}}} \frac{\sqrt{\pi} \left(4\sqrt{\frac{ni}{\rho_{SR}\rho_{RD}}}\right)^{p-k+1}}{\left(b+\frac{n}{\rho_{SR}}+\frac{i}{\rho_{RD}}+2\sqrt{\frac{ni}{\rho_{SR}\rho_{RD}}}\right)^{p+j+\frac{11}{4}}} \tag{3.70}$$
$$\frac{\Gamma\left(j+p+\frac{11}{4}\right)\Gamma\left(j+2k-p+\frac{3}{4}\right)}{\Gamma\left(k+j+\frac{9}{4}\right)}$$
$$\left. {}_2F_1\left(j+p+\frac{11}{4}, p-k+\frac{3}{2}; k+j+\frac{9}{4}; \frac{b+\frac{n}{\rho_{SR}}+\frac{i}{\rho_{RD}}-2\sqrt{\frac{ni}{\rho_{SR}\rho_{RD}}}}{b+\frac{n}{\rho_{SR}}+\frac{i}{\rho_{RD}}+2\sqrt{\frac{ni}{\rho_{SR}\rho_{RD}}}}\right) \right].$$

Note that equation (3.70) is a combined link average SER approximation since equation (3.69) gives an SER upper-bound for the overall system and using Γ_{SRD} provides a lower-bound on performance for the relay link. Indeed, since equation (3.70) is the upper-bound of lower-bound of actual SER performance, it provides a very tight approximation to actual SER performance for the entire SNR region except at very low SNR.

3.4.2 High SNR Analysis

Simple high SNR performance is now considered to simplify equations (3.67), (3.68), and (3.70). The approximation uses the PDFs of $\lambda_{SD} := \gamma_{SD}/\rho_{SR}$ and $\lambda_{SRD} := \Gamma_{SRD}/\rho_{SR}$, and both PDFs are checked to satisfy the assumptions given in [34], which provides a systematic method for high SNR analysis. Based on [34], the average SER of an uncoded system can be approximated by

$$P_E = (2b\rho G_a)^{-G_d} + o\left(\rho^{-G_d}\right) \tag{3.71}$$

as $\rho \to \infty$, where ρ is the average transmit SNR, $G_d = t + 1$ is the diversity order, $G_a = \left(\left(\sqrt{\pi}(t+1)\right) / \left(a 2^t \alpha \Gamma(t + 3/2)\right)\right)^{1/(t+1)}$ is the array gain, t is the first nonzero derivative order of the PDF of a channel dependent random variable λ at the origin, and a and b are modulation specific positive constants from the instantaneous SER, $P_E(\lambda) = aQ\left(\sqrt{2b\rho\lambda}\right)$. This random variable, λ, is proportional to the instantaneous SNR as $\gamma = \rho\lambda$, and $\alpha = f_{\lambda}^{(t)}(0)/t! \neq 0$.

In this chapter, the average transmit SNR ρ may be ρ_{SR} with ρ_{SD} and ρ_{RD} which are constant multiples of ρ_{SR}, and channel dependent random variable λ may be either λ_{SD} or λ_{SRD} in the sequel. Therefore, equation (3.71) can be calculated once t and α are found using the PDFs of λ_{SD} and λ_{SRD}. The array and diversity gains, G_a and G_d, in equation (3.71) are found for the direct and relay links separately, and then they are combined to obtain high SNR performance for the whole system.

For the direct link, the PDF of λ_{SD} is used to find t_{SD}, the first nonzero derivative order of the PDF of λ_{SD}, and $\alpha_{SD} = f_{\lambda_{SD}}^{(t_{SD})}(0)/t_{SD}!$. In this case, $t_{SD} = M_S \cdot M_D - 1$ since the diversity order of MIMO MRT with MRC is given by $M_S \cdot M_D$ [6]. If the t_{SD} order derivative of the PDF of λ_{SD} is evaluated at the origin, the following can be obtained

$$f_{\lambda_{SD}}^{(t_{SD})}(0) = \sum_{n=1}^{M_D} \sum_{m=M_S-M_D}^{(M_S+M_D)n-2n^2} \binom{t_{SD}}{m} (-1)^{t_{SD}+m} d_{n,m} \left(\frac{n\rho_{SR}}{\rho_{SD}}\right)^{t_{SD}+1}. \quad (3.72)$$

Based on equation (3.72), α_{SD} can be acquired by

$$\alpha_{SD} = \frac{f_{\lambda_{SD}}^{(t_{SD})}(0)}{(M_S \cdot M_D - 1)!}. \quad (3.73)$$

For the relay link, the PDF of λ_{SRD} can be used to find t_{SRD} and α_{SRD} because the instantaneous SNR's, Γ_{SRD} and γ_{SRD}, are equivalent at high average SNR since they differ by a constant term in the denominator of equation (3.65). Since the diversity order of the relay link is given by

$\min\{M_S \cdot M_R, M_R \cdot M_D\}$ [35], $t_{SRD} = \min\{M_S \cdot M_R, M_R \cdot M_D\} - 1$. The t_{SRD} order derivative of the PDF of λ_{SRD} evaluated at the origin can be obtained as follows:

$$f_{\lambda_{SRD}}^{(t_{SRD})}(0) = \begin{cases} f_{\lambda_{RD}}^{(t_{RD})}(0), & M_S > M_D \\ f_{\lambda_{SR}}^{(t_{SR})}(0), & M_S < M_D \\ f_{\lambda_{SR}}^{(t_{SR})}(0) + f_{\lambda_{RD}}^{(t_{RD})}(0), & M_S = M_D \end{cases}, \tag{3.74}$$

where $t_{SR} = M_S \cdot M_R - 1$, $t_{RD} = M_R \cdot M_D - 1$, $\lambda_{SR} := \gamma_{SR}/\rho_{SR}$, $\lambda_{RD} := \gamma_{RD}/\rho_{SR}$, and $f_{\lambda_{SR}}^{(t_{SR})}(0)$ and $f_{\lambda_{RD}}^{(t_{RD})}(0)$ are given as follows:

$$f_{\lambda_{SR}}^{(t_{SR})}(0) = \sum_{n=1}^{M_R} \sum_{m=M_S-M_R}^{(M_S+M_R)n-2n^2} \binom{t_{SR}}{m} (-1)^{t_{SR}+m} d_{n,m} n^{t_{SR}+1} \tag{3.75}$$

$$f_{\lambda_{RD}}^{(t_{RD})}(0) = \sum_{n=1}^{M_R} \sum_{m=M_D-M_R}^{(M_R+M_D)n-2n^2} \binom{t_{SD}}{m} (-1)^{t_{RD}+m} d_{n,m} \left(\frac{n\rho_{SR}}{\rho_{RD}}\right)^{t_{RD}+1}. \tag{3.76}$$

Based on equation (3.74), α_{SRD} can be written as

$$\alpha_{SRD} = \frac{f_{\lambda_{SRD}}^{(t_{SRD})}(0)}{(\min\{M_S \cdot M_R, M_R \cdot M_D\} - 1)!} \tag{3.77}$$

For the combined link, the PDF of $\gamma_{SD} + \Gamma_{SRD}$ is a convolution of $f_{\gamma_{SD}}(x)$ and $f_{\Gamma_{SRD}}(x)$, which is difficult to obtain in closed-form. Instead of using the PDF of $\gamma_{SD}+\Gamma_{SRD}$, an alternate approach is used to find t_C and α_C for the combined link. We have $t_C = M_S \cdot M_D + \min\{M_S \cdot M_R, M_R \cdot M_D\} - 1$ since the diversity order of the combined link is $M_S \cdot M_D + \min\{M_S \cdot M_R, M_R \cdot M_D\}$, which is the sum of the diversity orders of the direct and relay links because the received SNR of the combined link is $\gamma_{SD} + \Gamma_{SRD}$. To find $f_{\lambda_{SD}+\lambda_{SRD}}^{(t_C)}(0)$, the product of $f_{\lambda_{SD}}^{(t_{SD})}(0)$ and $f_{\lambda_{SRD}}^{(t_{SRD})}(0)$ can be used. Therefore, the final combined α_C is given by using equations (3.72) and (3.74)

$$\alpha_C = \frac{f_{\lambda_{SD}}^{(t_{SD})}(0) \cdot f_{\lambda_{SRD}}^{(t_{SRD})}(0)}{(M_S \cdot M_D + \min\{M_S \cdot M_R, M_R \cdot M_D\} - 1)!}. \tag{3.78}$$

Based on α_C and t_C, G_d and G_c can be substituted as explained after equation (3.71). The combined link high SNR performance can be obtained by

$$P_E = (2b\rho_{SR}G_a)^{-G_d} + o\left(\rho_{SR}^{-G_d}\right) \tag{3.79}$$

$$G_d = M_S \cdot M_D + \min\{M_S \cdot M_R, M_R \cdot M_D\} \tag{3.80}$$

$$G_a = \left(\frac{a2^{G_d-1}\alpha_C\Gamma\left(G_d+\frac{1}{2}\right)}{\sqrt{\pi}G_d}\right)^{-\frac{1}{G_d}}. \tag{3.81}$$

Since all potential resources of the relay network are used, the lower-bound can achieve full diversity order, $M_S \cdot M_D + \min\{M_S \cdot M_R, M_R \cdot M_D\}$. Using t_{SD}, t_{SRD}, and equations (3.72) and (3.74), high SNR performance for the direct and relay links can be expressed as equations (3.79)-(3.81) as well.

3.5 Simulation Results

The relationships among the average SNR values are chosen as $\rho_{SR} = \rho_{RD}$ and ρ_{SD} dB $= \rho_{SR}$ dB $- 30\log_{10}(2)$, which corresponds to the relay located in the mid-point of the S and D in a simplified path-loss model [7, p.46] with path-loss exponent of 3 (i.e. the "mid-point relay model"). Alternatively, we also consider $\rho_{SR} = \rho_{RD} = \rho_{SD}$ which is the "equidistant relay model". In Monte-Carlo simulations, the transmitted symbol is BPSK, QPSK, or 8-PSK modulated with unit power, and the channel is 100-symbol block fading with $(M_S, M_R, M_D) = (2,1,2)$, (2,2,2), or (4,1,4). MRC with MMSE combining is used for all relaying schemes. For illustration of our high SNR results, we select $\rho_{SR} = \rho_{RD} = \rho_{SD} \to \infty$ even though our analysis applies to nonequal average SNRs as well. The combined optimized BF performance from [31] is included as a benchmark. For BF optimization, 8 and 64 Grassmannian vectors [36] are used as initial points for the gradient ascent algorithm for 2 and 4 source antennas, respectively. Limited feedback performance is also included using the 8 and 64 Grassmannian BF vectors. For limited feedback

implementations, once actual BF coefficients are obtained at the destination, they are compared with Grassmannian vectors in the pre-designed codebook. The index of the closest vector in Euclidean distance is then sent to the source.

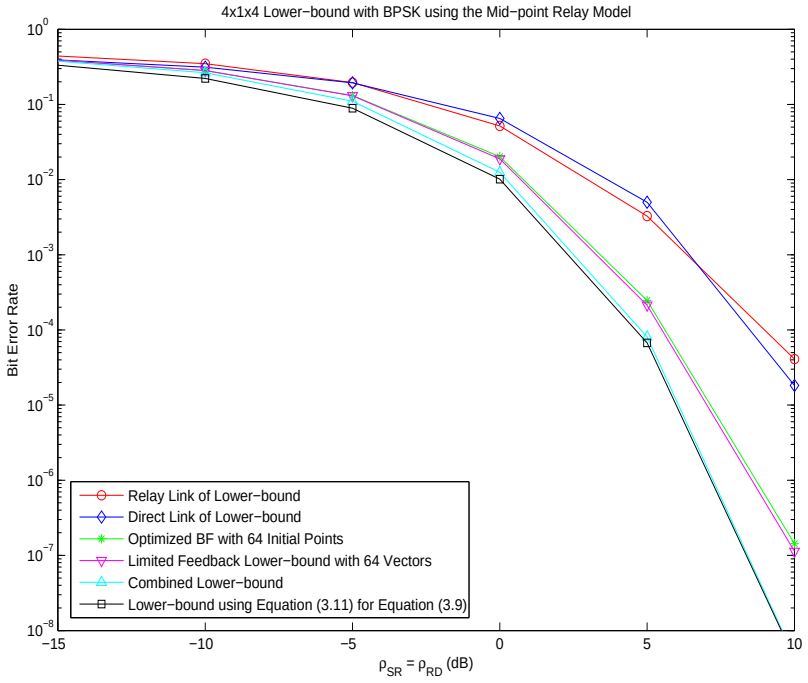

Figure 3.3: $4 \times 1 \times 4$ Lower-Bound with BPSK using the Mid-Point Relay Model.

3.5.1 Performance Analysis for Two-Slot Lower-Bounds with $M_R = 1$

Figure 3.3 shows the lower-bound using the mid-point relay model for a $4 \times 1 \times 4$ system. The combined optimized BF performance with 64 initial points and the lower-bound using limited feedback with 64 BF vectors from [31] are illustrated by Monte-Carlo simulations. The lower-bound including the performance of the direct and relay links from equation (3.9) and its lower-bound using equation (3.11) for equation (3.9) are presented analytically. The lower-bound in equation (3.9) is about 1.9 dB better than the optimized BF

performance at 10^{-7}, and the lower-bound in equation (3.9) and its lower-bound using equation (3.11) for equation (3.9) are very tight at high SNR. The lower-bound using limited feedback is similar to or a little better than the optimized BF performance. In the mid-point relay model, the relay link performance dominates the combined performance at low SNR whereas the direct link performance dominates the combined performance at high SNR.

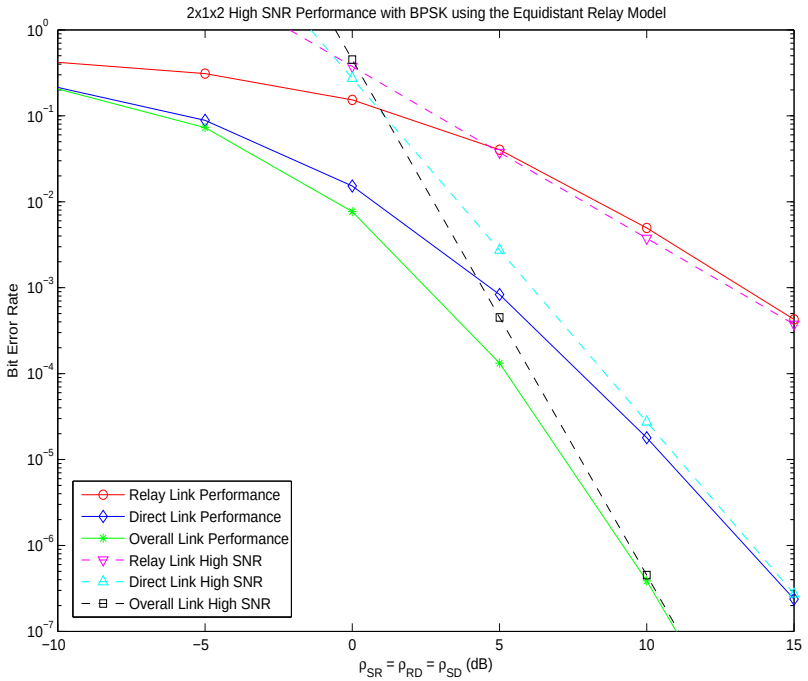

Figure 3.4: $2 \times 1 \times 2$ High SNR Performance with BPSK using the Equidistant Relay Model.

Figure 3.4 shows the high SNR performance with BPSK for a $2 \times 1 \times 2$ lower-bound using the equidistant relay model. The lower-bound for relay, direct, and combined links from equation (3.9) and high SNR performance for the lower-bound of relay, direct, and combined links from equations (3.12)-(3.19) are obtained analytically, and they match well at high SNR. It is seen that the direct link performance dominates the relay link performance for the

entire SNR range. As seen in Figure 3.3, however, if the mid-point relay model is used, the relay link performance dominates the direct link performance at low SNR. Note that, for the high SNR approximation of the lower-bound to be tight, the equidistant relay model in Figure 3.4 requires higher SNR compared with the mid-point relay model in Figure 3.3.

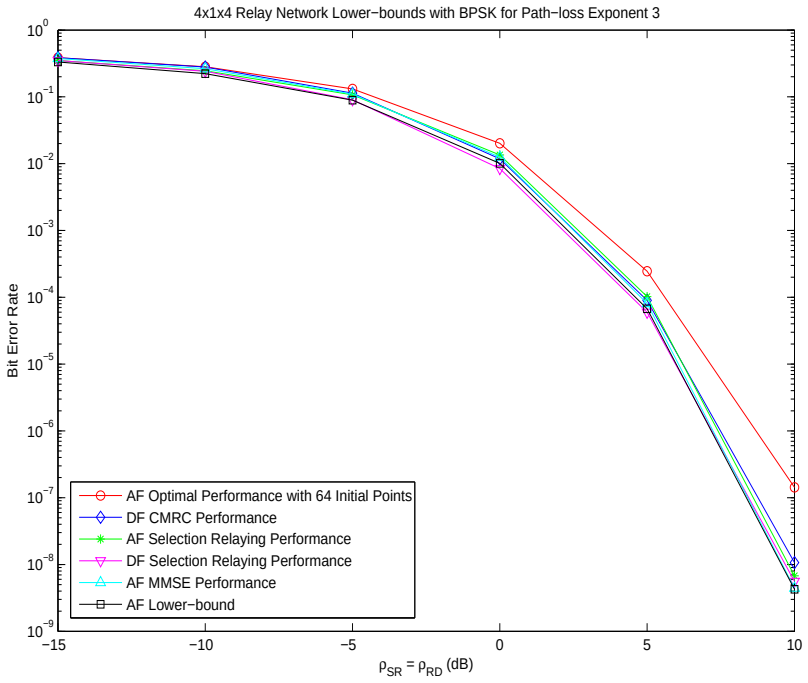

Figure 3.5: $4 \times 1 \times 4$ AF/DF Relay Network Performance with BPSK using the Mid-Point Relay Model.

Figure 3.5 shows $4 \times 1 \times 4$ AF/DF relay network performance with BPSK using the mid-point relay model. For $4 \times 1 \times 4$, most schemes are about 1.2-1.7 dB better than the optimized scheme in performance at 10^{-7}. Strong-path BF performance is similar to the optimized performance at 10^{-7}. The lower-bound of AF MMSE is very tight to AF MMSE performance. AF schemes are a little better than DF schemes in lower-bounds at high SNR.

Based on simulations, all lower-bounds are better than the optimized performance, and the strong-path BF with AF MMSE is similar to or even better than the optimized performance when the path-loss exists. In general, AF schemes are better than DF schemes at high SNR even though DF schemes are slightly better than AF schemes at low SNR, in error performance.

3.5.2 Performance Analysis for the Three-Slot Scheme with $M_R = 1$

As explained in advance, the transmit SNR is normalized with respect to the number of message bits. For example, therefore, if the two-slot scheme with BPSK uses the transmit SNR 1, then the three-slot scheme with BPSK does the transmit SNR 2/3. Therefore, the X-axis in figures represents SNR per message bit for two-slot schemes, and the three-slot scheme uses less SNR than the SNR represented on X-axis for fair comparisons. For illustration of high SNR results, we use the equidistant relay model to show clearly the diversity order of the relay system even though our analysis applies to any relay models as well. The combined optimized BF performance from [31], the strong-path BF performance from [42], and the lower-bound of the two-slot scheme are included as benchmarks. Unless otherwise stated, the benchmarks use two time slots with BPSK or QPSK, and the three-slot schemes do QPSK or 8-PSK. Two-slot schemes with BPSK are compared with three-slot schemes with QPSK, and two-slot schemes with QPSK are compared with three-slot schemes with 8-PSK. For BF optimization, 8 Grassmannian vectors [36] are used as initial points for the gradient ascent algorithm.

Figure 3.6 shows the three-slot scheme performance with QPSK using the mid-point relay model for a $2 \times 1 \times 2$ system. All exact performance for the direct, relay, and combined links is averaged from $aQ\left(\sqrt{2b\gamma_{SD}}\right)$,

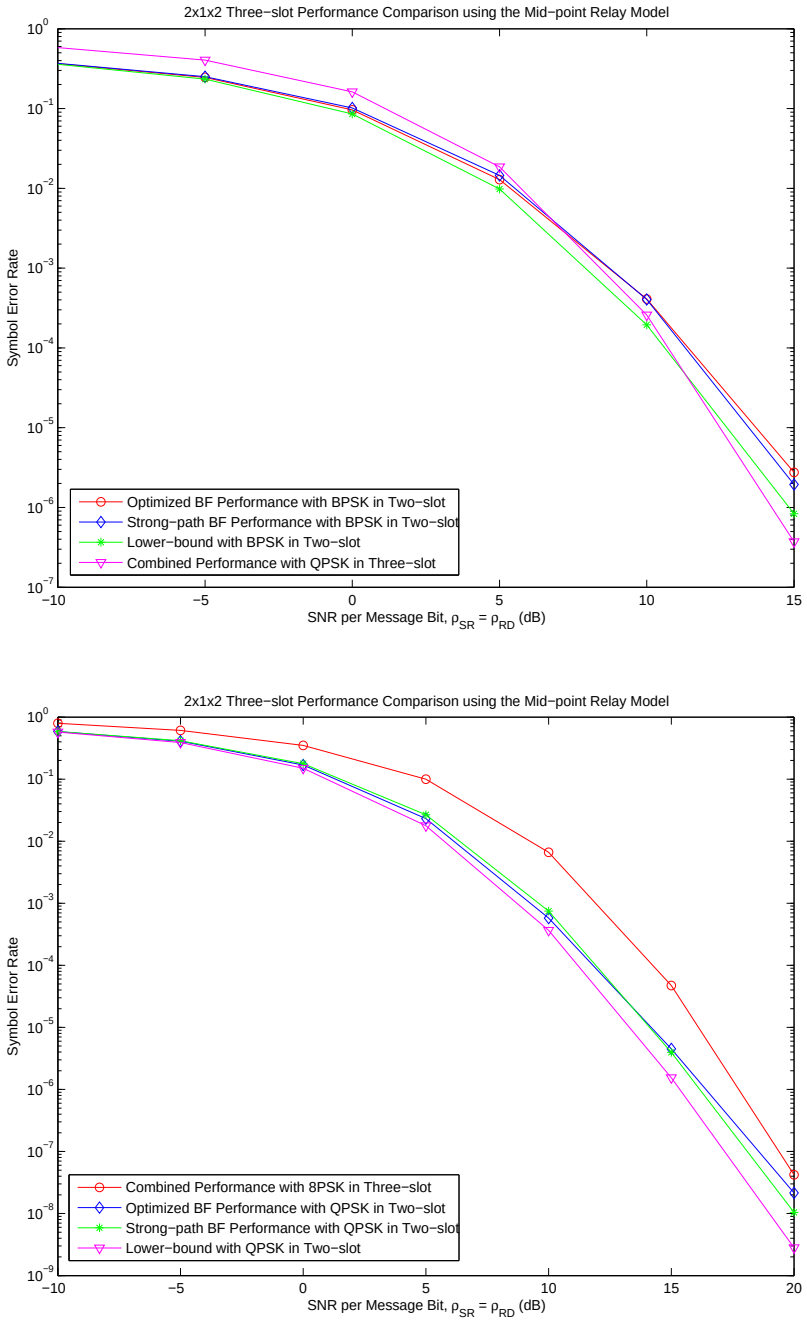

Figure 3.6: $2 \times 1 \times 2$ Three-Slot Scheme Performance Comparison using the Mid-Point Relay Model.

$aQ\left(\sqrt{2b\gamma_{SRD}}\right)$, and $aQ\left(\sqrt{2b\left(\gamma_{SD}+\gamma_{SRD}\right)}\right)$, respectively. The direct link upper-bound is from equation (3.36), the relay link lower-bound is from equation (3.37), and the combined link upper-bound is from equations (3.38)-(3.40). It shows that the lower-bound and upper-bound are tight to the exact performance, and the relay link outperforms the direct link at low SNR whereas the direct link outperforms the relay link at high SNR in the mid-point relay model.

Figure 3.7 shows the $2 \times 1 \times 2$ three-slot scheme performance comparison using the mid-point relay model. While the combined optimized BF performance using 8 initial points from [31] is illustrated by a Monte-Carlo simulation, all other performance is presented analytically. The strong-path BF performance is averaged from equation (7) of [43], and the combined lower-bound of the two-slot scheme is from equation (7) of [42]. The combined three-slot scheme performance is from equations (3.38)-(3.40).

The three-slot scheme performance with QPSK are about 1.8 dB better than the optimized BF performance with BPSK, about 1.4 dB better than the strong-path BF performance with BPSK, and about 0.6 dB better than the lower-bound of the two-slot scheme with BPSK at 10^{-6} even though all two-slot scheme performance is better than the three-slot scheme performance at low SNR. This means that the three-slot scheme with QPSK can transmit 1/3 factor more message bits with better performance than the two-slot schemes with BPSK at high SNR. Meanwhile, the three-slot scheme performance with 8-PSK are about 0.8 dB worse than the optimized BF performance with QPSK, about 1.3 dB worse than the strong-path BF performance with QPSK, and about 2.2 dB worse than the lower-bound of the two-slot scheme with QPSK at 10^{-7} even though the performance gaps become smaller and

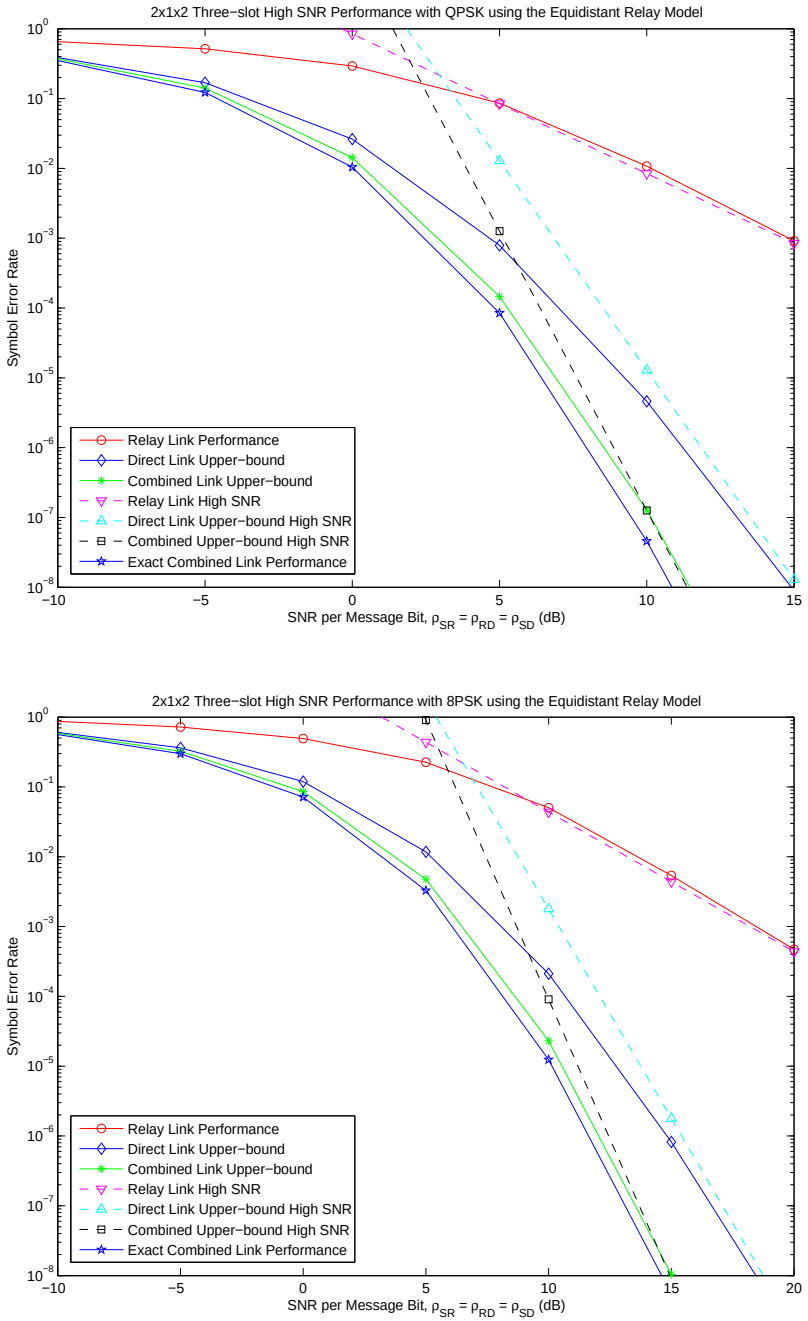

Figure 3.7: $2 \times 1 \times 2$ Three-Slot Scheme High SNR Performance using the Equidistant Relay Model.

the three-slot scheme performance becomes finally better than the two-slot scheme performance as SNR goes to high. Note that the lower-bound of the two-slot scheme is an unachievable bound, and the optimized BF and the strong-path BF are reasonable schemes using two time slots. It is recognizable that the three-slot scheme performance is much better than the two-slot scheme performance with same modulation if rate loss is acceptable.

Figure 3.8 shows the high SNR performance comparison for a $2 \times 1 \times 2$ system using the equidistant relay model. The strong-path BF performance is same as Figure 3.7, and its high SNR performance is from equations (2.24)-(2.34). The combined lower-bound of the two-slot scheme is from equation (7) of [42], and its high SNR performance is from equation (14) of [42]. The combined three-slot scheme performance is same as Figures 3.6 and 3.7, and its high SNR performance is from equation (3.53). The three-slot scheme high SNR performance with QPSK is about 1.9 dB better than the high SNR performance of the two-slot lower-bound with BPSK and about 3.3 dB better than the strong-path BF high SNR performance with BPSK at 10^{-8}. On the other hand, the three-slot scheme high SNR performance with 8-PSK is about 0.35 dB better than the strong-path BF high SNR performance with QPSK and about 1 dB worse than the high SNR performance of the two-slot lower-bound with QPSK at 10^{-9}. Note that the three-slot scheme needs more SNR to outperform the two-slot scheme in the second illustration even though the three-slot scheme with 8-PSK dominates the two-slot lower-bound with QPSK at 20 dB. In any cases, the comparison illustrations confirm that the three-slot scheme can transmit more or same message bits with better performance than the two-slot scheme at high SNR.

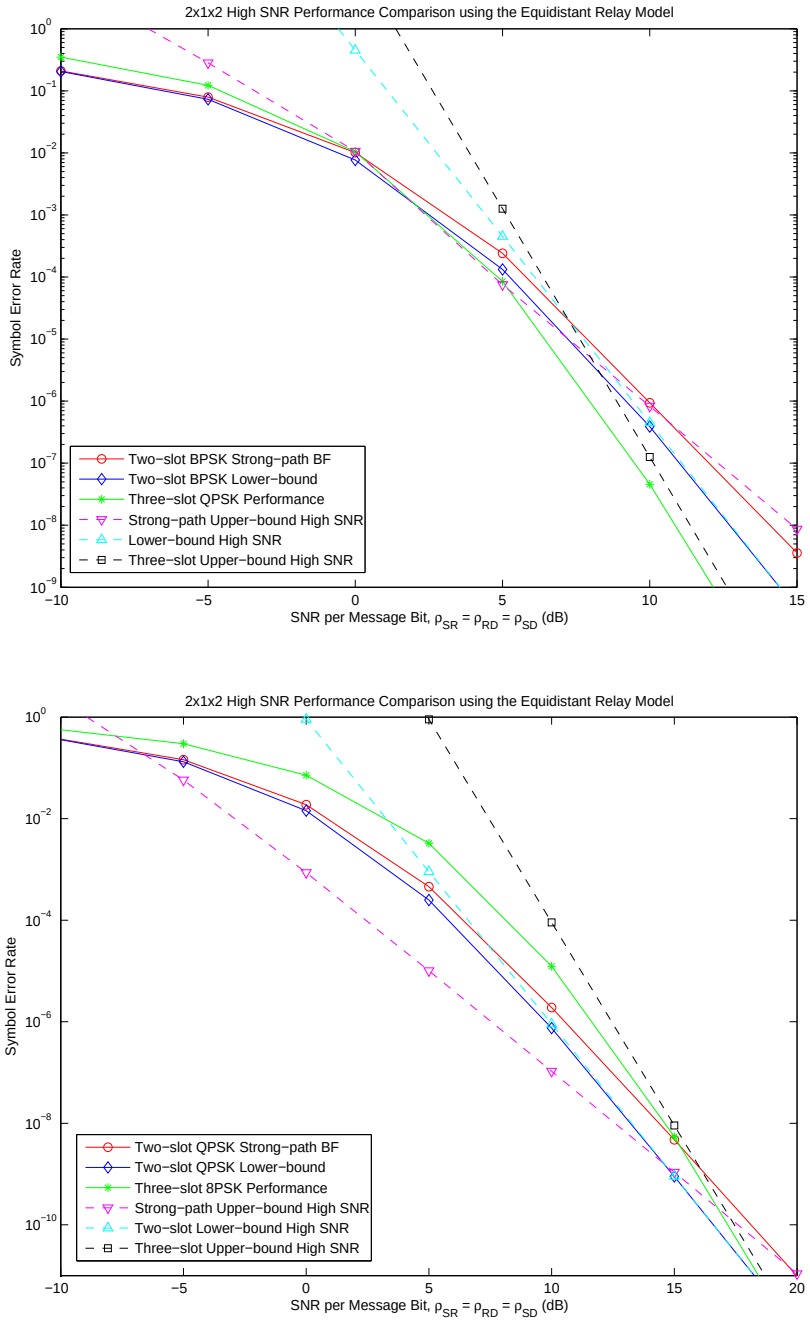

Figure 3.8: $2 \times 1 \times 2$ High SNR Performance Comparison using the Equidistant Relay Model.

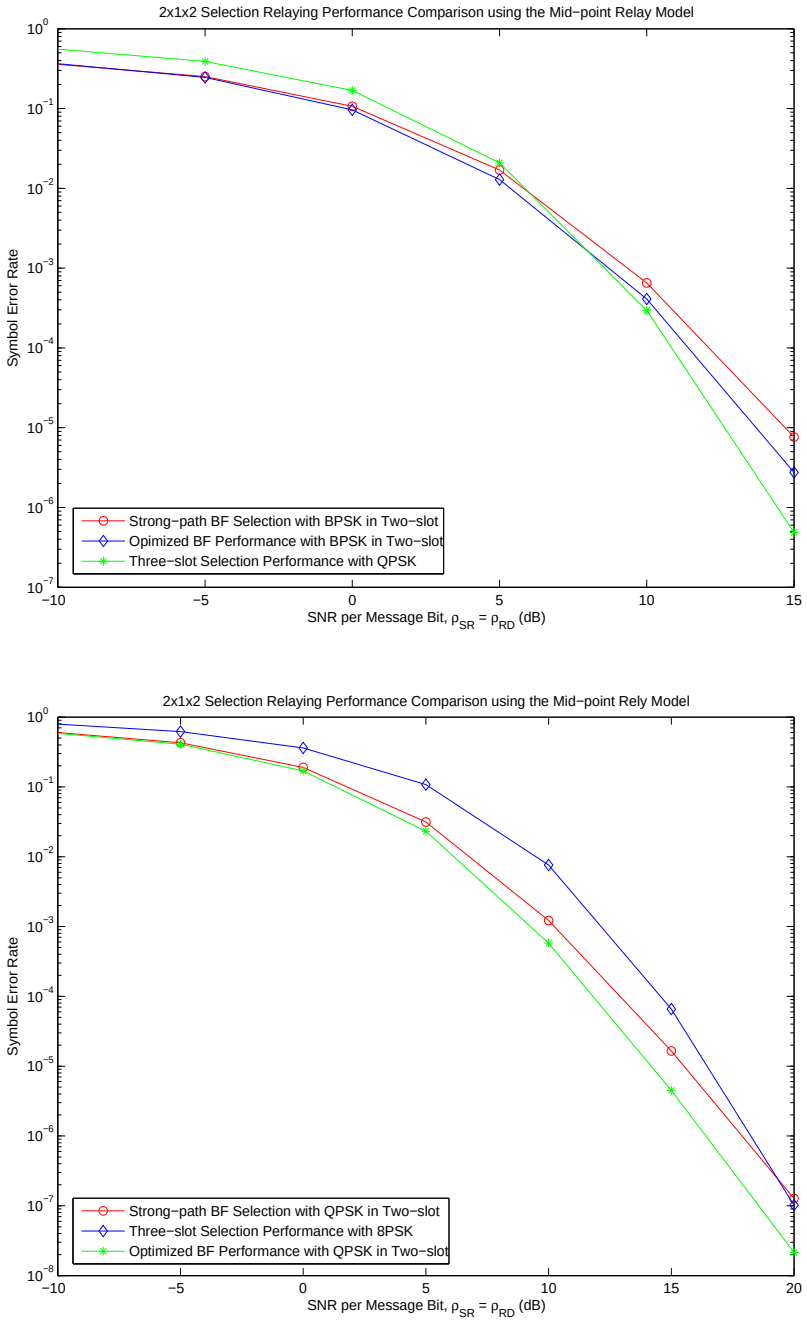

Figure 3.9: $2 \times 1 \times 2$ Selection Relaying Performance Comparison using the Mid-Point Relay Model.

This subsection shows the three-slot scheme selection relaying performance from Section 3.3.3, where $\mathbf{h}_{RD}$ and $\mathbf{h}_{SR}$ are assumed to be unknown at the source and destination, respectively. Our extension of traditional selection relaying with BF using three time slots, in which the relay transmits the aggregated amplified signal to the destination if $\Gamma_{SR} + \Gamma'_{SR} > T$, and the source retransmits the signal otherwise in the third time slot (i.e. no relaying if $\Gamma_{SR} + \Gamma'_{SR} \leq T$), is illustrated by simulations.

Figure 3.9 shows the $2 \times 1 \times 2$ selection relaying performance comparison among the two-slot and three-slot schemes using the mid-point relay model. The combined optimized BF performance is from Figure 3.7, and the strong-path BF selection relaying performance using the two-slot scheme is averaged from equation (16) of [45]. The three-slot selection relaying performance is averaged from equation (3.63) with numerically optimized thresholds from equation (3.64). The three-slot selection relaying performance with QPSK is about 2.8 dB better than the strong-path BF selection relaying performance with BPSK, about 1.6 dB better than the optimized BF performance with BPSK at 10^{-6}. Therefore, the three-slot selection relaying with QPSK can also transmit 1/3 factor more message bits with better performance than the two-slot schemes with BPSK at high SNR. Similarly, the three-slot selection relaying performance with 8-PSK is about 0.3 dB better than the strong-path BF selection relaying performance with QPSK, about 1.4 dB worse than the optimized BF performance with QPSK at 10^{-7} even though the performance gaps become smaller and the three-slot performance becomes finally better than the two-slot scheme performance as SNR goes to high. Note that $\mathbf{h}_{RD}$ and $\mathbf{h}_{SR}$ are unknown at the source and destination for selection relaying, and they are known to the optimized BF scheme.

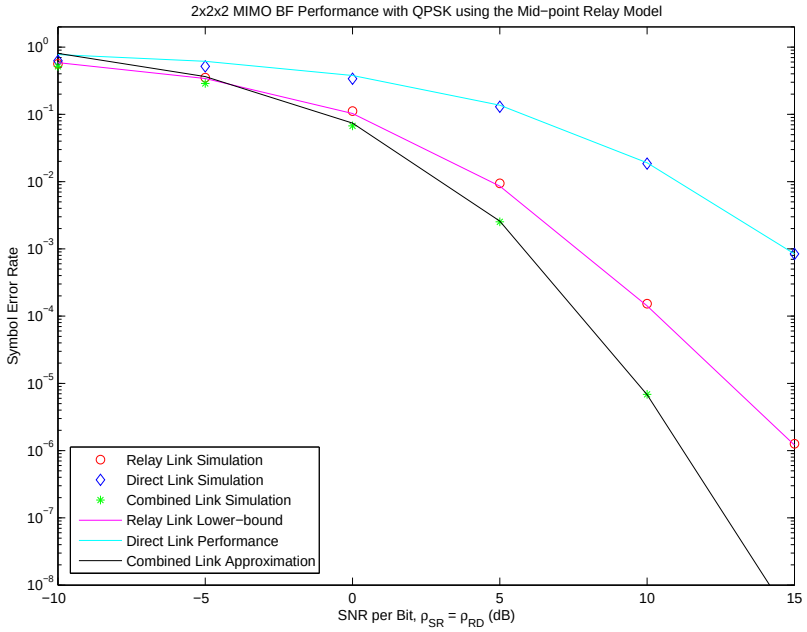

Figure 3.10: $2\times2\times2$ MIMO BF Performance with QPSK using the Mid-Point Relay Model.

3.5.3 Performance Analysis for Two-Slot Lower-Bounds with Multiple Relay Antennas

Figure 3.10 shows $2 \times 2 \times 2$ MIMO BF performance with QPSK using the mid-point relay model. From Figure 3.10, simulations mean Monte-Carlo simulations, and the performance for the direct, relay, and combined links is from equations (3.67), (3.68), and (3.70), respectively. The direct link performance, the relay link lower-bound, and the combined link approximation match well with their corresponding simulations. Note that the combined link approximation is obtained using two different BF vectors from the source to the relay and destination, respectively.

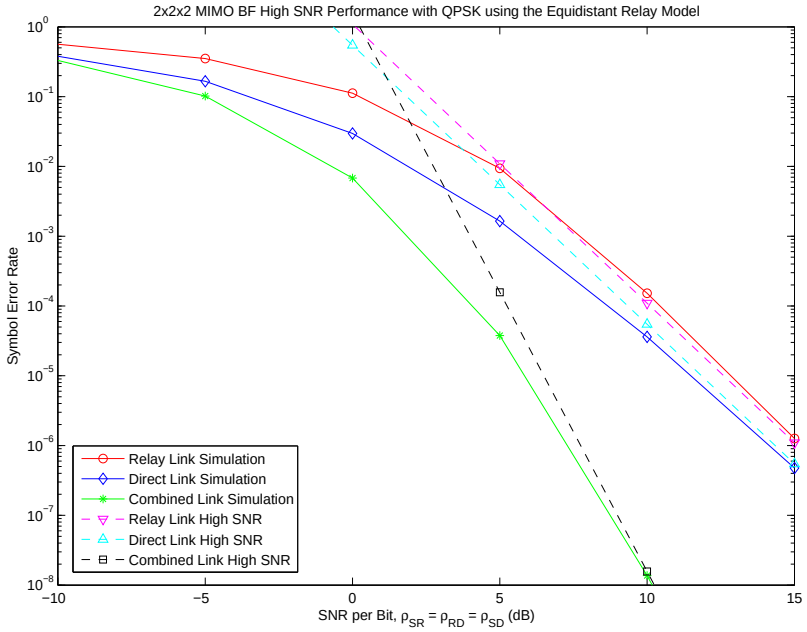

Figure 3.11: $2 \times 2 \times 2$ MIMO BF High SNR Performance with QPSK using the Equidistant Relay Model.

Figure 3.11 shows $2 \times 2 \times 2$ MIMO BF high SNR performance with QPSK using the equidistant relay model. The high SNR performance for the direct, relay, and combined links is from equations (3.73), (3.77), and (3.79), respectively. Even though final high SNR results are omitted for the direct and relay links, they can be obtained using t_{SD}, t_{SRD}, and equations (3.73) and (3.77). All high SNR performance matches well with their simulations. The diversity orders of the direct, relay, and combined links are 4, 4, and 8, respectively.

Figure 3.12 shows $2 \times 2 \times 2$ MIMO BF performance comparison with QPSK using two relay models, the mid-point and equidistant relay models. The system's lower-bounds and optimized BF performance are from Monte-Carlo simulations. Their performance gaps are about 1 dB at the error rate

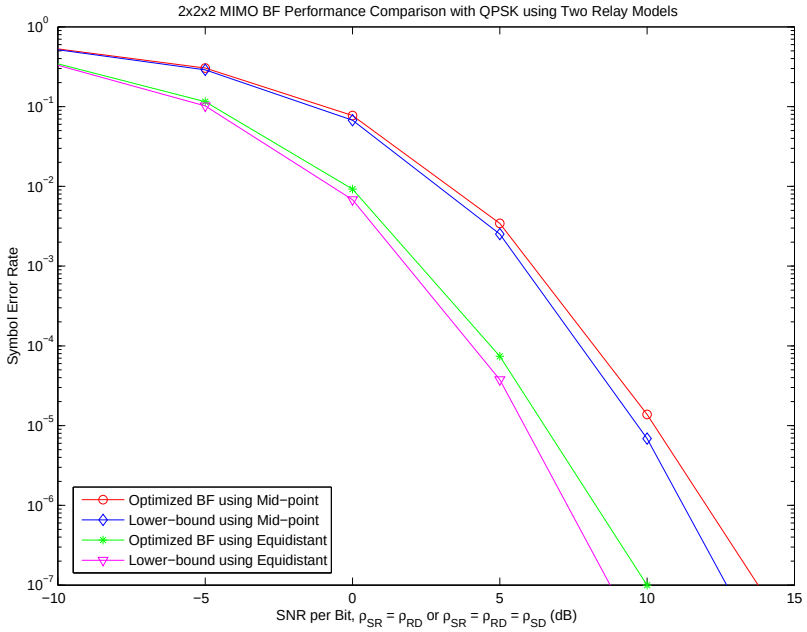

Figure 3.12: $2 \times 2 \times 2$ MIMO BF Performance Comparison with QPSK using Two Relay Models.

10^{-7} for both relay models. That is why the lower-bound of the system is useful. Note that the diversity order of optimized BF performance is not same as that of the lower-bound. In addition, note also that the lower-bound is actual performance when the number of source antennas, M_S, is 1.

Table 3.1: Summary of Relaying Categories with BF

Categories	CSI Assumption	BF	Combining
Three-Slot	All CSI	2 Vectors	MMSE/CMRC
Lower-Bound	All CSI	2 Vectors	MMSE/CMRC
Strong-Path	All CSI	1 Vector	MMSE/CMRC
Selection	Partial CSI	1 Vector	MMSE/CMRC
Three-Slot Selection	Partial CSI	2 Vectors	MMSE/CMRC

3.6 Chapter Summary

Table 3.1 shows the summary of assumptions and uses for AF/DF relaying categories in this chapter. Two categories are explored with both fully known and partially known CSI of the relay link at the source and destination. First, we have investigated combined lower-bounds in AF/DF MIMO BF fixed two-hop relay networks using a single relay antenna with an i.i.d. Rayleigh fading channel. Novel lower-bounds using BF are presented for AF/DF relaying with known CSI of the relay link at the source and destination. Lower-bounds are obtained by using two different BF vectors matched with the relay and direct links, respectively, and are achievable at the expense of a rate penalty using the proposed three-slot scheme.

Lower-bounds are meaningful due to tight closed-forms to possible performance since finding the optimal BF using the two-slot scheme is a complex non-convex optimization problem and there is no way to obtain a closed-form solution. This chapter adopts selection relaying if some CSI of the relay link is unknown at the source and destination. The optimal SNR threshold is analyzed and used for selection relaying. High SNR performance analysis is also done in AF relay networks. We show performance comparisons among strong-path BF and optimized BF with a corresponding lower-bound.

Based on analytical and simulation results, all lower-bounds are better than the optimized performance, and AF schemes are better than DF schemes at high SNR even though DF schemes are a little better than AF schemes at low SNR. Lower-bounds are useful benchmarks in best performance even though they have a drawback in spectral efficiency. In addition, availability of the CSI at the source and destination is crucial in performance.

Second, AF MIMO fixed two-hop relay networks using a single relay antenna with BF using three time slots have been investigated with i.i.d. Rayleigh fading channels. For the three-slot scheme, two different BF vectors are used separately for both direct and relay links using distinct time slots with full CSI at the source and destination. After signals with a BF vector matched with the direct link are transmitted, signals with another BF vector matched with the relay link are transmitted. Once the relay combines both signals, it transmits aggregated amplified signals to the destination in the third time slot. If partial CSI is available at the source and destination, the three-slot selection relaying scheme with BF is used to obtain a full available diversity. MRC with MMSE is used for combining for all relaying schemes. In addition, high SNR performance analysis is also conducted to simplify the SER expressions. For comparisons, Table 3.1 also shows the summary of assumptions and uses for AF relaying categories for two-slot schemes in [42, 43].

The three-slot scheme is investigated to explore new relaying schemes which are easy to implement, are analyzable in closed-form, and have better performance than two-slot scheme without rate penalty. Even though the relay contributes to the combined performance more at low SNR than at high SNR, since the relay link performance dominates the direct performance at low SNR in the mid-point relay model, the three-slot scheme achieves full diversity order of $(M_S+1)\cdot M_D+\min(M_S+1, M_D)$ when perfect CSI is available at the source and destination. As a consequence, the three-slot scheme can transmit more or same message bits with better performance than the two-slot scheme at high SNR. Adaptive modulation and BF schemes can be considered for the two-slot and three-slot relaying schemes since the three-slot schemes are not always better in SER performance with no rate penalty.

Based on analytical and simulation results using the mid-point and equidistant relay models, the three-slot scheme performance with QPSK are about 1.8 dB better than the optimized BF performance with BPSK, about 1.4 dB better than the strong-path BF performance with BPSK, and about 0.6 dB better than the lower-bound of the two-slot scheme with BPSK at 10^{-6} even though all two-slot scheme performance is better than the three-slot scheme performance at low SNR. The three-slot scheme high SNR performance with QPSK is about 1.9 dB better than the high SNR performance of the two-slot lower-bound with BPSK and about 3.3 dB better than the strong-path BF high SNR performance with BPSK at 10^{-8}. The three-slot scheme selection relaying performance with QPSK is about 2.8 dB better than the strong-path BF selection relaying performance with BPSK, about 1.6 dB better than the optimized BF performance with BPSK at 10^{-6}. Even though the three-slot scheme performance with 8-PSK requires more SNR to dominate the two-slot scheme performance with QPSK, similar phenomena happen at high SNR. Therefore, although all two-slot scheme performance is better than the three-slot scheme performance at low SNR, the three-slot schemes become better in SER performance as SNR goes high.

Finally, the combined lower-bound is investigated in MIMO BF AF fixed two-hop relay networks using multiple relay antennas with i.i.d. Rayleigh fading channels. A novel lower-bound using MIMO BF is presented for AF relaying using multiple antennas at the source, relay, and destination when all CSI of the relay link is known at the source and destination. The lower-bound is obtained by using two different BF vectors matched with the relay and direct links, respectively. It is achievable using a three-slot scheme, and is a lower-bound for two-slot schemes.

Based on analytical and simulation results, all performance analysis matches with Monte-Carlo simulations, and the systems's lower-bound is about 1 dB difference compared with the optimal BF performance at the error rate 10^{-7} for both mid-point and equidistant relay models. The lower-bound is meaningful due to a tight closed-form to possible performance since finding the optimal BF using the two-slot scheme is a complex non-convex optimization problem, and there is no way to obtain a closed-form solution. Finally, note that the lower-bound reduces to the actual performance when the number of source antennas, M_S, is 1.

Appendix 3.1: Derivation of Equation (3.10)

This appendix derives equation (3.10), which is the first expectation of equation (3.9). Equation (3.10) can be calculated by

$$\begin{aligned}\mathbb{E}\left[e^{-\frac{\gamma_{SD}}{\sin^2\theta}}\right] &= \int_0^\infty e^{-\frac{x}{\sin^2\theta}} f_{\gamma_{SD}}(x)dx \\ &= \int_0^\infty e^{-\frac{x}{\sin^2\theta}} \sum_{n=1}^{M_D} \sum_{m=M_S-M_D}^{(M_S+M_D)n-2n^2} d_{n,m} \frac{n^{m+1}x^m e^{-\frac{nx}{\rho_{SD}}}}{m!\rho_{SD}^{m+1}} dx,\end{aligned} \tag{3.82}$$

where $f_{\gamma_{SD}}(x)$ is the PDF of γ_{SD}, which will be derived in the next paragraph. Using $\int_0^\infty x^n e^{-\mu x}dx = n!\mu^{-n-1}$ [37, p.340] for equation (3.82), equation (3.10) can be obtained.

The derivation of $f_{\gamma_{SD}}(x)$ is following. From [30, eqn. (23)], the PDF of γ_{SD} can be directly obtained by using the PDF of $\Lambda_{SD} := \gamma_{SD}/\rho_{SD}$ based on $f_Y(y) = f_X\left(y/\rho_{SD}\right)/\rho_{SD}$ [38, p.131] as

$$f_{\gamma_{SD}}(x) = \sum_{n=1}^{M_D} \sum_{m=M_S-M_D}^{(M_S+M_D)n-2n^2} d_{n,m} \frac{n^{m+1}x^m e^{-\frac{nx}{\rho_{SD}}}}{\rho_{SD}^{m+1}m!}, \quad x > 0. \tag{3.83}$$

Appendix 3.2: Derivation of Equation (3.11)

This appendix derives equation (3.11), which is the second expectation of equation (3.9). Equation (3.11) can be calculated by using the integration-

by-parts method [46], which is $P_E = -\int_0^\infty \left(dP_E(\gamma)/d\gamma\right) F_\gamma(\gamma) d\gamma$, where P_E is the average BER, $P_E(\gamma)$ is the instantaneous BER, and $F_\gamma(\gamma)$ is the cumulative distribution function (CDF) of γ.

$$\mathbb{E}\left[e^{-\frac{\gamma_{SRD}}{\sin^2\theta}}\right] \geq \int_0^\infty \frac{1}{\sin^2\theta} e^{-\frac{x}{\sin^2\theta}} F_{\Gamma_{SRD}}(x) dx = \int_0^\infty \frac{1}{\sin^2\theta} e^{-\frac{x}{\sin^2\theta}} dx$$
$$- \int_0^\infty \frac{e^{-\frac{x}{\sin^2\theta}}}{\sin^2\theta} \frac{2e^{-x\left(\frac{1}{\rho_{SR}}+\frac{1}{\rho_{RD}}\right)} \sqrt{\frac{\rho_{RD}}{\rho_{SR}}} x^{M_D}}{M_D! \rho_{RD}^{M_D}} \sum_{p=0}^{M_S-1} \frac{1}{p!} \left(\frac{x^2}{\rho_{SR}\rho_{RD}}\right)^{p/2}$$
$$\sum_{u=0}^{p} \binom{p}{u} \left(\frac{\rho_{RD}}{\rho_{SR}}\right)^{u/2} \sum_{q=0}^{M_D-1} \binom{M_D-1}{q} \left(\frac{\rho_{RD}}{\rho_{SR}}\right)^{q/2} K_{q+u-p+1}\left(\frac{2x}{\sqrt{\rho_{SR}\rho_{RD}}}\right) dx, \tag{3.84}$$

where $F_{\Gamma_{SRD}}(x)$ is the CDF of $\Gamma_{SRD} = \gamma_{SR}\gamma_{RD}/\left(\gamma_{SR}+\gamma_{RD}\right)$, which is given by [29], and $K_\nu(x)$ is the modified Bessel function of the second kind.

Using $\int_0^\infty x^{\mu-1} e^{-\alpha x} K_\nu(\beta x) dx = \sqrt{\pi}(2\beta)^\nu \Gamma(\mu+\nu)\Gamma(\mu-\nu)/\left((\alpha+\beta)^{\mu+\nu}\right.$ $\left.\Gamma(\mu+1/2)\right)_2 F_1\left(\mu+\nu, \nu+1/2; \mu+1/2; (\alpha-\beta)/(\alpha+\beta)\right)$ [37, p.700] for equation (3.84), equation (3.11) can be obtained.

Appendix 3.3: Derivation of Equation (3.13)

This appendix derives $f_{\lambda_{SD}}^{(t_{SD})}(0)$ for equation (3.13). From [30, eqn. (23)], the PDF of Λ_{SD} is used to obtain that of $\lambda_{SD} := \gamma_{SD}/\rho_{SR} = \rho_{SD}\Lambda_{SD}/\rho_{SR}$ using $f_{\lambda_{SD}}(y) = \rho_{SR} f_{\Lambda_{SD}}\left(y\rho_{SR}/\rho_{SD}\right)/\rho_{SD}$ by

$$f_{\lambda_{SD}}(x) = \sum_{n=1}^{M_D} \sum_{m=M_S-M_D}^{(M_S+M_D)n-2n^2} d_{n,m} \frac{\left(\frac{n\rho_{SR}}{\rho_{SD}}\right)^{m+1} x^m e^{-\frac{nx\rho_{SR}}{\rho_{SD}}}}{m!}, \quad x > 0. \tag{3.85}$$

If the t_{SD} order derivative is taken for equation (3.85) with respect to x,

$$f_{\lambda_{SD}}^{(t_{SD})}(x)$$
$$= \sum_{n=1}^{M_D} \sum_{m=M_S-M_D}^{(M_S+M_D)n-2n^2} d_{n,m} \binom{t_{SD}}{m} e^{-\frac{nx\rho_{SR}}{\rho_{SD}}} \sum_{k=0}^{m} C_k \left(-1\right)^{t_{SD}+m+k} \left(\frac{n\rho_{SR}}{\rho_{SD}}\right)^{t_{SD}+k+1} x^k, \tag{3.86}$$

where $C_0 = 1$ and C_k is any real coefficient. Once equation (3.86) is evaluated at the origin, equation (3.13) is obtained.

Appendix 3.4: Derivation of $f^{(t_C)}_{\lambda_{SD}+\Lambda_{SRD}}(0)$

This appendix derives $f^{(t_C)}_{\lambda_{SD}+\Lambda_{SRD}}(0)$ for the combined link using the PDFs of direct and relay links. A general case is shown in this appendix first and appropriate results using PDFs can be substituted for the solution. Since both PDFs satisfy the assumptions given in [34], they can be written as follows:

$$f_{\lambda_{SD}}(x) = \alpha_{SD} x^{t_{SD}} + o\left(x^{t_{SD}+\epsilon}\right) \tag{3.87}$$

$$f_{\Lambda_{SRD}}(x) = \alpha_{SRD} x^{t_{SRD}} + o\left(x^{t_{SRD}+\epsilon}\right), \tag{3.88}$$

as $x \to 0$. Using Craig's formula, the average BER using BPSK can be written as

$$P_E = \frac{1}{\pi}\int_0^{\pi/2} \mathbb{E}\left[e^{-\frac{\rho_{SR}\lambda_{SD}}{\sin^2\theta}}\right] \mathbb{E}\left[e^{-\frac{\rho_{SR}\Lambda_{SRD}}{\sin^2\theta}}\right] d\theta. \tag{3.89}$$

Using equations (3.87) and (3.88) and $\int_0^\infty x^n e^{-\mu x} dx = n!\mu^{-n-1}$, both expectations of equation (3.89) can be solved as follows:

$$\begin{aligned}\mathbb{E}\left[e^{-\frac{\rho_{SR}\lambda_{SD}}{\sin^2\theta}}\right] &= \int_0^\infty e^{-\frac{\rho_{SR}\lambda_{SD}}{\sin^2\theta}} \left[\alpha_{SD} x^{t_{SD}} + o\left(x^{t_{SD}+\epsilon}\right)\right] dx \\ &= \alpha_{SD} t_{SD}! \sin^{2(t_{SD}+1)}\theta \rho_{SR}^{-(t_{SD}+1)} + o\left(\rho_{SR}^{-(t_{SD}+1)}\right)\end{aligned} \tag{3.90}$$

$$\mathbb{E}\left[e^{-\frac{\rho_{SR}\Lambda_{SRD}}{\sin^2\theta}}\right] = \alpha_{SRD} t_{SRD}! \sin^{2(t_{SRD}+1)}\theta \rho_{SR}^{-(t_{SRD}+1)} + o\left(\rho_{SR}^{-(t_{SRD}+1)}\right). \tag{3.91}$$

Using equations (3.90) and (3.91) and $\int_0^{\pi/2} \sin^{2m} x dx = \pi(2m-1)!!/(2(2m)!!)$ of [37, p.395], where !! denotes double factorial defined in [37], equation (3.89) can be solved by

$$\begin{aligned}P_E = &\frac{\alpha_{SD}\alpha_{SRD} t_{SD}! t_{SRD}! (2(t_{SD}+t_{SRD}+2)-1)!!}{2(2(t_{SD}+t_{SRD}+2))!!} \rho_{SR}^{-(t_{SD}+t_{SRD}+2)} \\ &+ o\left(\rho_{SR}^{-(t_{SD}+t_{SRD}+2)}\right).\end{aligned} \tag{3.92}$$

Therefore, once equation (3.92) is compared with the proof result of [34, p.1391], $f^{(t_C)}_{\lambda_{SD}+\Lambda_{SRD}}(0)$ can be found by $f^{(t_{SD})}_{\lambda_{SD}}(0) \cdot f^{(t_{SRD})}_{\Lambda_{SRD}}(0)$ since α_{SD} and α_{SRD} are in a product form in equation (3.92).

Appendix 3.5: Derivations of Equations (3.36) and (3.37)

This appendix derives equations (3.36) and (3.37), which are SER representations of both the direct and relay links. From [30, eqn. (23)], the PDF of Γ_{SD} can be directly obtained by using the PDF of $\Lambda_{SD} := \Gamma_{SD}/\rho_{SD}$ based on $f_Y(y) = f_X\left(y/\rho_{SD}\right)/\rho_{SD}$ [38, p.131] as

$$f_{\Gamma_{SD}}(x) = \sum_{n=1}^{M_D} \sum_{m=M_S-M_D}^{(M_S+M_D)n-2n^2} d_{n,m} \frac{n^{m+1} x^m e^{-\frac{nx}{\rho_{SD}}}}{\rho_{SD}^{m+1} m!}, \quad x > 0. \tag{3.93}$$

Once integration is carried out over the PDF after extending the number of source antennas by 1 from equation (3.93), the CDF of γ_{SD}^{+} is obtained by

$$F_{\gamma_{SD}^{+}}(x) = 1 - \sum_{n=1}^{M_D} \sum_{m=M_S-M_D+1}^{(M_S+M_D+1)n-2n^2} d_{n,m+1} e^{\frac{-nx}{\rho_{SD}}} \sum_{k=0}^{m} \frac{(nx)^k}{k! \rho_{SD}^k}, \quad x > 0. \tag{3.94}$$

If equation (3.94) is applied to the SER expression, $P_E = a\sqrt{b}/(2\sqrt{\pi}) \int_0^\infty e^{-bx} F_\gamma(x)/\sqrt{x} dx$, equation (3.36) is obtained.

To obtain the CDF of $\Gamma_{SRD} := \left(\Gamma_{SR} + \Gamma'_{SR}\right) \Gamma_{RD} / \left(\left(\Gamma_{SR} + \Gamma'_{SR}\right) + \Gamma_{RD}\right)$, the PDF of the first hop of the relay link should be obtained first. After a convolution between $f_{\Gamma_{SR}}(x) = x^{M_S-1} e^{-x/\rho_{SR}} / \left((M_S-1)! \rho_{SR}^{M_S}\right)$ and $f_{\Gamma'_{SR}}(x) = e^{-x/\rho_{SR}}/\rho_{SR}$ is done, if procedures in [29, Appendix] are followed with Γ_{SRD}, the CDF of Γ_{SRD} is obtained as

$$\begin{aligned} F_{\Gamma_{SRD}}(x) = 1 - & \frac{2 e^{-x\left(\frac{1}{\rho_{SR}} + \frac{1}{\rho_{RD}}\right)} \sqrt{\frac{\rho_{RD}}{\rho_{SR}}} x^{M_D}}{(M_D-1)! \rho_{RD}^{M_D}} \sum_{p=0}^{M_S} \frac{1}{p!} \left(\frac{x^2}{\rho_{SR}\rho_{RD}}\right)^{\frac{p}{2}} \\ & \sum_{q=0}^{M_D+p-1} \binom{M_D+p-1}{q} \left(\frac{\rho_{RD}}{\rho_{SR}}\right)^{\frac{q}{2}} K_{q-p+1}\left(\frac{2x}{\sqrt{\rho_{SR}\rho_{RD}}}\right), \quad x \geq 0, \end{aligned} \tag{3.95}$$

where $K_\nu(x)$ is the modified Bessel function of the second kind. Similarly, equation (3.37) is obtained when the above SER expression is used for equation (3.95).

Appendix 3.6: Derivations of Equations (3.39) and (3.40)

This appendix derives equations (3.39) and (3.40), which are expectations of both the direct and relay links. From Appendix 3.5, before obtaining equation (3.94), its PDF obtained by extending the number of source antennas by 1 is

$$f_{\gamma_{SD}^{+}}(x)=\sum_{n=1}^{M_D}\sum_{m=M_S-M_D+1}^{(M_S+M_D+1)n-2n^2} d_{n,m+1}\frac{n^{m+1}x^m e^{\frac{-nx}{\rho_{SD}}}}{m!\rho_{SD}^{m+1}},\quad x>0. \tag{3.96}$$

Using the PDF, if the following expectation is calculated, then equation (3.39) can be obtained.

$$\mathbb{E}\left[e^{-\frac{g\gamma_{SD}}{\sin^2\theta}}\right]\leq\int_0^\infty e^{-\frac{gx}{\sin^2\theta}}f_{\gamma_{SD}^{+}}(x)dx. \tag{3.97}$$

Since the CDF of Γ_{SRD} is given in equation (3.95), equation (3.40) can be calculated by using the integration-by-parts method [46], which is $P_E=-\int_0^\infty\left(dP_E(\gamma)/d\gamma\right)F_\gamma(\gamma)d\gamma$, where P_E is the average SER, $P_E(\gamma)$ is the instantaneous SER, and $F_\gamma(\gamma)$ is the CDF of γ. Using the CDF given in equation (3.95) and $\int_0^\infty x^{\mu-1}e^{-\alpha x}K_\nu(\beta x)dx=\sqrt{\pi}(2\beta)^\nu\Gamma(\mu+\nu)\Gamma(\mu-\nu)/\left((\alpha+\beta)^{\mu+\nu}\right.$ $\left.\Gamma(\mu+1/2)\right){}_2F_1\left(\mu+\nu,\nu+1/2;\mu+1/2;(\alpha-\beta)/(\alpha+\beta)\right)$ [37, p.700], if the following integration is solved, equation (3.40) can be obtained.

$$\mathbb{E}\left[e^{-\frac{g\gamma_{SRD}}{\sin^2\theta}}\right]\geq\int_0^\infty\frac{g}{\sin^2\theta}e^{-\frac{gx}{\sin^2\theta}}F_{\Gamma_{SRD}}(x)dx. \tag{3.98}$$

Appendix 3.7: Derivation of Equation (3.42)

This appendix derives $f_{\lambda_{SD}}^{(t_{SD})}(0)$ for equation (3.42). From Appendix 3.6, the PDF of γ_{SD}^{+} is used to obtain that of $\lambda_{SD}:=\gamma_{SD}^{+}/\rho_{SR}=\rho_{SD}\lambda_{SD}^{+}/\rho_{SR}$ using $f_{\lambda_{SD}}(y)=\rho_{SR}f_{\lambda_{SD}^{+}}\left(y\rho_{SR}/\rho_{SD}\right)/\rho_{SD}$ by

$$f_{\lambda_{SD}}(x)=\sum_{n=1}^{M_D}\sum_{m=M_S-M_D+1}^{(M_S+M_D+1)n-2n^2} d_{n,m+1}\frac{\left(\frac{n\rho_{SR}}{\rho_{SD}}\right)^{m+1}x^m e^{-\frac{nx\rho_{SR}}{\rho_{SD}}}}{m!},\quad x>0. \tag{3.99}$$

If the t_{SD} order derivative is taken for equation (3.99) with respect to x,

$$f_{\lambda_{SD}}^{(t_{SD})}(x) = \sum_{n=1}^{M_D} \sum_{m=M_S-M_D+1}^{(M_S+M_D+1)n-2n^2} d_{n,m+1} \binom{t_{SD}}{m} e^{-\frac{nx\rho_{SR}}{\rho_{SD}}} \sum_{k=0}^{m} C_k \left(-1\right)^{t_{SD}+m+k} \left(\frac{n\rho_{SR}}{\rho_{SD}}\right)^{t_{SD}+k+1} x^k, \tag{3.100}$$

where $C_0 = 1$ and C_k is any real coefficient. Once equation (3.100) is evaluated at the origin, equation (3.42) is obtained.

Appendix 3.8: Derivation of Equations (3.67) and (3.68)

This appendix derives equations (3.67) and (3.68), which are approximate average SERs for the direct and relay links. To derive equation (3.67), $f_{\gamma_{SD}}(x)$ and $F_{\gamma_{SD}}(x)$ should be found first. From [30, eqn. (23)], the PDF of γ_{SD} can be obtained using the PDF of $\Lambda_{SD} := \gamma_{SD}/\rho_{SD}$ based on $f_Y(y) = f_X\left(y/\rho_{SD}\right)/\rho_{SD}$ [38, p.131] as

$$f_{\gamma_{SD}}(x) = \sum_{n=1}^{M_D} \sum_{m=M_S-M_D}^{(M_S+M_D)n-2n^2} \frac{d_{n,m} n^{m+1} x^m e^{-\frac{nx}{\rho_{SD}}}}{m! \rho_{SD}^{m+1}}, \; x > 0. \tag{3.101}$$

If equation (3.101) is integrated with respect to x, the CDF of γ_{SD} can be acquired by

$$F_{\gamma_{SD}}(x) = 1 - \sum_{n=1}^{M_D} \sum_{m=M_S-M_D}^{(M_S+M_D)n-2n^2} \sum_{k=0}^{m} \frac{d_{n,m} e^{-\frac{nx}{\rho_{SD}}} (nx)^k}{k! \rho_{SD}^k}, \; x > 0. \tag{3.102}$$

When equation (3.102) is substituted to equation (3.66), equation (3.67) can be obtained.

Similarly, $F_{\Gamma_{SRD}}(x)$ should be found first to derive equation (3.68). From [35, Appendix], the CDF of Γ_{SRD} can be calculated by

$$F_{\Gamma_{SRD}}(x) = 1 - \int_0^\infty \bar{F}_{\gamma_{SR}}\left(\frac{x(w+x)}{w}\right) f_{\gamma_{RD}}(w+x) dw, \tag{3.103}$$

where $\bar{F}_{\gamma_{SR}}(x) = 1 - F_{\gamma_{SR}}(x)$ and $f_{\gamma_{RD}}(x)$ are as follows:

$$\bar{F}_{\gamma_{SR}}(x) = \sum_{n=1}^{M_R} \sum_{m=M_S-M_R}^{(M_S+M_R)n-2n^2} \sum_{k=0}^{m} \frac{d_{n,m} e^{-\frac{nx}{\rho_{SR}}} (nx)^k}{k! \rho_{SR}^k}, \; x > 0. \tag{3.104}$$

$$f_{\gamma_{RD}}(x) = \sum_{i=1}^{M_R} \sum_{j=M_D-M_R}^{(M_R+M_D)i-2i^2} \frac{d_{i,j} i^{j+1} x^j e^{-\frac{ix}{\rho_{RD}}}}{j! \rho_{RD}^{m+1}}, \; x > 0. \tag{3.105}$$

Equations (3.104) and (3.105) can be derived similar to equations (3.101) and (3.102).

Once equation (3.104) and (3.105) are substituted to equation (3.103), the CDF of Γ_{SRD} can be found after mathematical calculations as follows:

$$F_{\Gamma_{SRD}}(x) = 1 - \sum_{n=1}^{M_R} \sum_{m=M_S-M_R}^{(M_S+M_R)n-2n^2} \sum_{k=0}^{m} \sum_{i=1}^{M_R} \sum_{j=M_D-M_R}^{(M_D+M_R)i-2i^2} \sum_{p=0}^{k+j} \binom{k+j}{p}$$
$$\frac{2 d_{n,m} d_{i,j} n^{\frac{k+p+1}{2}} i^{\frac{2j+k-p+1}{2}}}{k! j! \rho_{SR}^{\frac{k+p+1}{2}} \rho_{RD}^{\frac{2j+k-p+1}{2}}} x^{k+j+1} e^{-x\left(\frac{n}{\rho_{SR}} + \frac{i}{\rho_{RD}}\right)} K_{p-k+1}\left(2x\sqrt{\frac{ni}{\rho_{SR}\rho_{RD}}}\right), \; x > 0, \tag{3.106}$$

where $K_\nu(x)$ is the modified Bessel function of the second kind. Finally, when equation (3.106) is substituted to equation (3.66), equation (3.68) can be obtained.

Chapter 4

Performance Bounds on Average Error Rates using the Arithmetic-Geometric Mean Inequality

One of the performance metrics of interest in communications is the average probability of error, which can be either a bit or symbol error rate (BER/SER) averaged across fading channels. When memoryless modulated signals are transmitted and corrupted over an additive white Gaussian noise (AWGN) channel, the instantaneous error rate can be represented, or approximated by the well-known Gaussian Q-function [7,24–26]. Since the Q-function is given in an integral form, averaging it over fading channels requires alternative approaches such as Craig's formula combined with a moment generating function (MGF) approach [7, 25, 26, 30, 42, 43, 47–50], or approximations with the integration-by-parts method [35,44–46,51], which are widely used to obtain closed-form expressions.

When the instantaneous signal-to-noise ratio (SNR) is given by a sum of N statistically independent non-negative random variables (RVs) and the combined probability density function (PDF) and cumulative distribution function (CDF) are intractable, Craig's formula can be used along with the product of MGFs, which requires at least a double integral (please see details in Section 4.2). This double integral causes mathematical difficulties in obtaining closed-form expressions. As a consequence, if Craig's formula combined with a MGF approach is not solvable, the Chernoff bound [7, 24] can be considered even though its performance is far from the actual performance. We propose upper and lower-bounds, which are much tighter than the Chernoff bound and can be obtained just as simply. This approach enable us to obtain tight closed-form

combined expressions for AF relay networks with multiple relays and amplify-and-forward (AF) multiple-input multiple-output (MIMO) beamforming (BF) relay networks with multiple antennas, for the first time in the literature.

In this chapter, novel average performance bounds are obtained for systems with instantaneous SNRs given by a sum of N statistically independent (but not necessarily identically distributed) non-negative RVs by the product of single integral expressions using the arithmetic mean (AM) and geometric mean (GM) inequality. Even though the AM-GM inequality is used to find the distribution bound of a combined RV in [52, 53], it is never considered to obtain performance bounds using the product of single integrals with simple distribution functions, to the best of our knowledge. The tightness of the bounds is evaluated analytically at high SNR. The SNR gap between the bounds and the true error rate is shown to go to zero as the number of RVs N increases. The bounds are illustrated with three applications involving maximum ratio combining (MRC), AF relay networks with multiple relays, and AF relay networks with a single relay and multiple antennas. The mathematical technique used to obtain the bounds in this chapter can be applied even to some of non-Gaussian noise models, as we illustrate with Middleton's class-A noise [54].

After the problem statement is described in Section 4.1, existing techniques for calculating average performance are reviewed in Section 4.2. Novel performance bounds and their derivations are presented in Section 4.3, and the tightness of the bounds is evaluated analytically at high SNR in Section 4.4.

Applications involving MRC and relay networks are discussed in Section 4.5, and non-Gaussian additive noise is considered in Section 4.6. In Section 4.7, Monte-Carlo simulations compare the bounds with the actual performance. Finally, Section 4.8 summarizes this chapter.

Notation: $f(x) = o(g(x))$ as $x \to c$ (here c may be either 0 or ∞) means that $\lim_{x\to c} f(x)/g(x) = 0$ when $f(x)$ and $g(x)$ are positive for sufficiently small or large x. $f(x) = O(g(x))$ as $x \to c$ means that $f(x)/g(x)$ is bounded for x sufficiently close to c.

4.1 Problem Statement

Consider N statistically independent non-negative RVs and their sum $X = \sum_{i=1}^{N} X_i = \rho \sum_{i=1}^{N} \lambda_i$, where ρ is the average transmit SNR, and λ_i are channel dependent RVs. The interest of this chapter is in calculating the average probability of error:

$$P_E = \mathbb{E}_X \left[aQ\left(\sqrt{2bX}\right)\right] = \int_0^\infty aQ\left(\sqrt{2bx}\right) f_X(x)dx, \tag{4.1}$$

where $Q(x) := \left(1/\sqrt{2\pi}\right) \int_x^\infty e^{-y^2/2}dy$ [7,24–26], $\mathbb{E}_X[\cdot]$ denotes expectation with respect to X, a and b are modulation related positive constants, and P_E could be either BER or SER by depending on the choice of a and b. For example, $a = 1$ and $b = 1$ provide exact SER for binary phase shift keying (BPSK), while $a = 2$ and $b = \sin^2(\pi/M)$ and $a = 4\left(1 - 1/\sqrt{M}\right)$ and $b = 3/(2(M - 1))$ provide tight SER approximations for M-ary PSK (M-PSK) and M-ary quadrature amplitude modulation (M-QAM), respectively [7,24,27]. Since the tightness of these approximations for different values of a and b are well-studied in the literature, our focus in this chapter will be on calculating equation (4.1), and on finding tight and simple bounds on equation (4.1), in cases when the distribution of X is complicated or intractable.

4.2 Review of Existing Techniques

Craig's formula is an alternative form for the Q-function, which is often used in calculating equation (4.1) [25, 26]:

$$Q(x) = \frac{1}{\pi} \int_0^{\pi/2} e^{-x^2/\left(2\sin^2\theta\right)} d\theta. \tag{4.2}$$

Substituting into equation (4.1) we have the so-called MGF approach:

$$P_E = \frac{a}{\pi} \int_0^{\pi/2} \prod_{i=1}^{N} \left[M_{X_i}\left(-\frac{b}{\sin^2\theta} \right) \right] d\theta, \tag{4.3}$$

where $M_X(s) := \int_0^\infty f_X(x) e^{sx} dx$ is the MGF. Clearly equation (4.3) requires a double integral to obtain the average error rates.

To avoid the double integral, if the integration-by-parts method is used for equation (4.1), the following alternative equation can be attained [44]:

$$P_E = \frac{a\sqrt{b}}{2\sqrt{\pi}} \int_0^\infty \frac{e^{-bx}}{\sqrt{x}} F_X(x) dx, \tag{4.4}$$

where $F_X(x)$ is the CDF of X. In what follows, we derive tight bounds on equation (4.4) that requires less integrals than equation (4.3) even when the distribution of the sum X is intractable.

4.3 Novel Average Performance Bounds

Equation (4.3) requires a double integral, which causes mathematical difficulties in some cases. In addition, if MGFs in equation (4.3) are intractable, the average probability of error cannot be expressed in closed-form. Therefore, it is of interest to derive expressions involving both PDFs and CDFs in representing equation (4.1) with reduced number of integrals. The Chernoff bound, $Q(x) \leq \frac{1}{2} e^{-x^2/2}$, does allow tractable expressions but yields rather loose bounds. This motivates the following novel average performance bounds.

Theorem 4.1. *Let $X_i,\ \ i = 1, 2, ..., N$, be statistically independent non-negative RVs, and $X = \sum_{i=1}^{N} X_i$ be their sum. Then the average performance P_E in equation (4.1) is upper-bounded by*

$$P_E \leq \frac{a\sqrt{b}}{2\sqrt{\pi N}} \int_0^\infty \frac{e^{-bx_1}}{\sqrt[2N]{x_1}} F_{X_1}(x_1)dx_1 \left[\prod_{i=2}^{N} \left(\int_0^\infty \frac{e^{-bx_i}}{\sqrt[2N]{x_i}} f_{X_i}(x_i)dx_i \right)\right]. \tag{4.5}$$

Equivalently,

$$\begin{aligned} P_E \leq & \frac{a\sqrt{b}}{2\sqrt{\pi N}} \int_0^\infty \frac{e^{-bx_1}}{\sqrt[2N]{x_1}} F_{X_1}(x_1)dx_1 \\ & \left[\prod_{i=2}^{N} \left(\int_0^\infty \left(\frac{be^{-bx_i}}{\sqrt[2N]{x_i}} + \frac{e^{-bx_i}}{2N\ \sqrt[2N]{x_i^{2N+1}}} \right) F_{X_i}(x_i)dx_i \right)\right]. \end{aligned} \tag{4.6}$$

Proof. Please see Appendix 4.1. □

Note that both bounds are reduced to equation (4.4) with equality when $N = 1$. Note also that the products in equations (4.5) and (4.6) become the $(N-1)^{th}$ powers if $X_2, X_3, ..., X_N$ are identically distributed. Recalling that in general $X_i,\ \ i = 1, 2, ..., N$, need not be identically distributed, it is clear that X_1 should be chosen among all X_i as the one for which the integral involving the CDF is tractable in equation (4.5). For the MRC case regardless of fading models, the bounds can be obtained by using the PDF and CDF of a point-to-point single antenna system, which means that the bounds are tractable unless the point-to-point single antenna system is not solvable in closed-form.

4.3.1 Approximations Based on Theorem 4.1

In Section 4.5, we will consider applications where $F_{X_i}(x_i) = 1 - \bar{F}_{X_i}(x_i)$ is represented in terms of the complementary CDFs (CCDFs). This raises the tractability of the integral, $\int_0^\infty e^{-bx_i} / \left(2N\ \sqrt[2N]{x_i^{2N+1}}\right) dx_i$, in equation (4.6). To address this issue in a way to obtain the same diversity order as equation

(4.6), we modify the second term of the inner integral in equation (4.6) to obtain:

$$P_E \approx \frac{ab^{N-\frac{1}{2}}}{2\sqrt{\pi N}}\left(1+\frac{1}{2N}\right)^{N-1}\left[\prod_{i=1}^{N}\left(\int_0^\infty \frac{e^{-bx_i}}{\sqrt[2N]{x_i}}F_{X_i}(x_i)dx_i\right)\right]. \tag{4.7}$$

This expression makes the associated integrals more tractable in the applications we consider in Section 4.5. Note that equation (4.7) is most useful when the CDFs are written in terms of the CCDFs and the corresponding CCDFs are mathematically tractable, and equations (4.5) and (4.6) are preferable in other cases.

In addition, since the first term $be^{-bx_i}/\sqrt[2N]{x_i}$ dominates the second term $e^{-bx_i}/\left(2N\sqrt[2N]{x_i^{2N+1}}\right)$ in equation (4.6), when the term $e^{-bx_i}/\left(2N\sqrt[2N]{x_i^{2N+1}}\right)$ is removed, another approximation is given by

$$P_E \approx \frac{ab^{N-1/2}}{2\sqrt{\pi N}}\left[\prod_{i=1}^{N}\left(\int_0^\infty \frac{e^{-bx_i}}{\sqrt[2N]{x_i}}F_{X_i}(x_i)dx_i\right)\right]. \tag{4.8}$$

Based on our numerical investigations, equation (4.8) provides a lower-bound for the entire SNR region, and equation (4.7) gives an upper-bound except the low SNR region even though it is not straightforward to prove these analytically. Note that equations (4.7) and (4.8) approach to the actual performance using equation (4.1) at high SNR as $N \to \infty$. Note also that high SNR gaps using equations (4.5)-(4.8) are invariant of fading models and modulation related constants, a and b, as illustrated in Section 4.7.

4.4 Tightness of the Bounds at High SNR

We now evaluate the tightness of the bounds at high SNR using the techniques in [34]. Let $X_i = \rho\lambda_i$, and the PDFs of λ_i be given by $f_{\lambda_i}(x) = \alpha_i x^{t_i} + o\left(x^{t_i}\right)$ as $x \to 0$ where $\alpha_i = f_{\lambda_i}^{(t_i)}(0)/\Gamma(t_i+1)$, and t_i is the first non-zero derivative order for which $f_{\lambda_i}^{(t_i)}(0) \neq 0$. The expression for α_i is also valid when t_i is not an integer if fractional calculus is used [55].

To evaluate the tightness of our bounds, the exact asymptotic error rate can be obtained by assuming $f_{\lambda_i}(x) = \alpha_i x^{t_i} + o\left(x^{t_i}\right)$ and substituting in equation (4.3):

$$\begin{aligned} P_E = & \frac{a\left(\prod_{i=1}^{N}\alpha_i\Gamma(t_i+1)\right)\Gamma\left(2\sum_{i=1}^{N}(t_i+1)+1\right)}{2^{2\sum_{i=1}^{N}(t_i+1)+1}\Gamma^2\left(\sum_{i=1}^{N}(t_i+1)+1\right)}(b\rho)^{-\sum_{i=1}^{N}(t_i+1)} \\ & + o\left(\rho^{-\sum_{i=1}^{N}(t_i+1)}\right) \end{aligned} \tag{4.9}$$

as $\rho \to \infty$.

When $X_i = \rho\lambda_i$ are applied to equation (4.5), it becomes the following:

$$P_E \leq \frac{a\sqrt{b\rho}}{2\sqrt{\pi N}}\int_0^\infty \frac{e^{-b\rho x_1}}{\sqrt[2N]{x_1}}F_{\lambda_1}(x_1)dx_1\left[\prod_{i=2}^{N}\left(\int_0^\infty \frac{e^{-b\rho x_i}}{\sqrt[2N]{x_i}}f_{\lambda_i}(x_i)dx_i\right)\right]. \tag{4.10}$$

If $f_{\lambda_i}(x) = \alpha_i x^{t_i} + o\left(x^{t_i}\right)$ and $F_{\lambda_i}(x) = \alpha_i x^{t_i+1}/(t_i+1) + o\left(x^{t_i+1}\right)$ are substituted into equation (4.10), the average performance is upper-bounded by

$$\begin{aligned} P_E \leq & \frac{a\Gamma\left(t_1+2-\frac{1}{2N}\right)\alpha_1\left(\prod_{i=2}^{N}\alpha_i\Gamma\left(t_i+1-\frac{1}{2N}\right)\right)}{2(t_1+1)\sqrt{\pi N}}(b\rho)^{-\sum_{i=1}^{N}(t_i+1)} \\ & + o\left(\rho^{-\sum_{i=1}^{N}(t_i+1)}\right) \end{aligned} \tag{4.11}$$

as $\rho \to \infty$. Comparing equations (4.9) and (4.11) we see that their diversity orders are both equal and given by $\sum_{i=1}^{N}(t_i+1)$.

Using equations (4.9) and (4.11), the SNR gap for large ρ between the upper-bound and the actual performance, $10\log_{10}\left(\rho_{ub}/\rho_{ac}\right)$, can be calculated as

$$\begin{aligned} & -\frac{10}{\sum_{i=1}^{N}(t_i+1)} \\ & \log_{10}\left(\frac{(t_1+1)\sqrt{\pi N}\left(\prod_{i=1}^{N}\Gamma(t_i+1)\right)\Gamma\left(2\sum_{i=1}^{N}(t_i+1)+1\right)}{2^{2\sum_{i=1}^{N}(t_i+1)}\Gamma\left(t_1+2-\frac{1}{2N}\right)\left(\prod_{i=2}^{N}\Gamma\left(t_i+1-\frac{1}{2N}\right)\right)\Gamma^2\left(\sum_{i=1}^{N}(t_i+1)+1\right)}\right). \end{aligned} \tag{4.12}$$

Notice that the gap at high SNR is independent of the constellation size (i.e. a and b) but dependent on the number of RVs N and the diversity orders of each

RV, $t_i + 1$. Using identities, $\Gamma(x+1) = x\Gamma(x)$ and $\Gamma(2x) = 2^{2x-1}\Gamma(x)\Gamma(x + 1/2)/\sqrt{\pi}$, equation (4.12) can be approximated by $[5\log_{10}((\sum_{i=1}^{N} t_i + 1)/N)]/(\sum_{i=1}^{N} t_i + 1)$ for large N. For example, when all diversity orders are identical, $t_i = t, \;\; i = 1, 2, ..., N$, the gap becomes $[5\log_{10}(t+1)]/(N(t+1))$. Therefore, the gap at high SNR behaves like $O(1/N)$, which means the bound becomes tighter inversely with N, as $N \to \infty$. We applied the same approach to the expression in equation (4.7) with a resulting high SNR gap obtained as

$$\frac{5}{\sum_{i=1}^{N}(t_i+1)} \log_{10}\left(\frac{\left(1+\frac{1}{2N}\right)^{N-1}\Gamma\left(\sum_{i=1}^{N}(t_i+1)+1\right)\left(\prod_{i=1}^{N}\Gamma(t_i+2-\frac{1}{2N})\right)}{\sqrt{N}\Gamma\left(\sum_{i=1}^{N}(t_i+1)+\frac{1}{2}\right)\left(\prod_{i=1}^{N}\Gamma(t_i+2)\right)}\right). \tag{4.13}$$

The SNR gap using equation (4.8) can be obtained by removing $(1+1/(2N))^{N-1}$ from equation (4.13), and their gaps at high SNR behave like $O(1/N)$ when all diversity orders are identical as well. Therefore, the gaps among all the bounds and the actual performance become zero as $N \to \infty$. Note that although the bound is asymptotically tight for large N, even for $N = 2$ the gap is rather small, as illustrated in Section 4.7.

4.5 Applications of the Bounds

Three applications are considered in this section, which are receive diversity systems, relay networks with multiple relays, and relay network with multiple antennas at all nodes.

4.5.1 Receive Diversity using MRC

To show the tightness of the bounds, the well-known MRC technique [7] is presented as the first application since its exact performance is obtainable in closed-form without using the bounds. In this application, the performance expressions using equations (4.5), (4.7), and (4.8) are compared with the performance using equation (4.1).

Consider a receive diversity system, which consists of a transmitter using a single antenna and a receiver equipped with multiple (N) antennas. All CSI is assumed to be known only to the destination. The received signal using MRC at the destination is given by

$$y = \sqrt{\rho}\|\mathbf{h}\|x + \frac{\mathbf{h}^H}{\|\mathbf{h}\|}\mathbf{n}, \tag{4.14}$$

where ρ is the average transmit SNR, x is the transmitted symbol with $\mathbb{E}[x] = 0$ and $\mathbb{E}[|x|^2] = 1$, $(\cdot)^H$ and $(\cdot)^T$ represent a complex Hermitian and a vector transpose, respectively, $\mathbf{h} = [h_1 \;\; h_2 \;\; ... \;\; h_N]^T$ is the channel coefficient vector, and $\mathbf{n}$ is the noise, both having independent identically distributed (i.i.d.) $CN(0,1)$ entries.

The total instantaneous received SNR is represented by

$$\gamma := \rho\|\mathbf{h}\|^2 = \sum_{i=1}^{N} \gamma_i, \tag{4.15}$$

where $\gamma_i = \rho|h_i|^2, \;\; i = 1, 2, ..., N$. In this case, γ_i correspond to X_i and the combined RV γ is X.

4.5.1.1 Rayleigh Fading

If γ is considered as a single combined RV, a simple average performance can be obtained using equation (4.4). Since γ is χ^2 distributed with N degrees of freedom, $F_\gamma(x) = 1 - e^{-x/\rho}\sum_{p=0}^{N-1} x^p/\left(p!\rho^p\right), \; x \geq 0$ [7, p.214], substituting into equation (4.4) and using $\int_0^\infty x^{n-1/2}e^{-\mu x}dx = \sqrt{\pi}2^{-n}\mu^{-n-1/2}(2n-1)!!$ [37, p.345], the average performance can be obtained by

$$P_E = \frac{a}{2} - \sum_{p=0}^{N-1} \frac{a\sqrt{b}(2p-1)!!}{2^{p+1}p!\rho^p\left(b + \frac{1}{\rho}\right)^{p+\frac{1}{2}}}, \tag{4.16}$$

where $(2p-1)!! = 1 \cdot 3 \cdot 5 \cdot ... \cdot (2p-1)$, for $p \in \mathbb{N}$. The exact performance using equation (4.1) is the well-known expression for MRC performance in [7, 24],

and equation (4.16) can be an alternative expression and be the benchmark for the following performance bounds.

To derive the bounds or approximations we use, recall the PDF and CDF of γ_i, $f_{\gamma_i}(x) = e^{-x/\rho}/\rho, \;\; x \geq 0$ and $F_{\gamma_i}(x) = 1 - e^{-x/\rho}, \;\; x \geq 0$, respectively [7, p209]. Substituting these into equations (4.5), (4.7), and (4.8), respectively, and using the integral $\int_0^\infty x^{\nu-1}e^{-\mu x}dx = \Gamma(\nu)/\mu^\nu$ [37, p.346], the average performance is upper-bounded or approximated as

$$P_E \leq \frac{a\sqrt{b}}{2\sqrt{\pi N}} \left[\frac{\Gamma\left(1-\frac{1}{2N}\right)}{b^{1-\frac{1}{2N}}} - \frac{\Gamma\left(1-\frac{1}{2N}\right)}{\left(b+\frac{1}{\rho}\right)^{1-\frac{1}{2N}}} \right] \left[\frac{\Gamma\left(1-\frac{1}{2N}\right)}{\rho\left(b+\frac{1}{\rho}\right)^{1-\frac{1}{2N}}} \right]^{N-1} \tag{4.17}$$

$$\begin{aligned} P_E \approx & \frac{a\sqrt{b}}{2\sqrt{\pi N}} \left[\frac{\Gamma\left(1-\frac{1}{2N}\right)}{b^{1-\frac{1}{2N}}} - \frac{\Gamma\left(1-\frac{1}{2N}\right)}{\left(b+\frac{1}{\rho}\right)^{1-\frac{1}{2N}}} \right] \\ & \left(1+\frac{1}{2N}\right)^{N-1} \left[\frac{b\Gamma\left(1-\frac{1}{2N}\right)}{b^{1-\frac{1}{2N}}} - \frac{b\Gamma\left(1-\frac{1}{2N}\right)}{\left(b+\frac{1}{\rho}\right)^{1-\frac{1}{2N}}} \right]^{N-1} \end{aligned} \tag{4.18}$$

$$P_E \approx \frac{ab^{N-1/2}}{2\sqrt{\pi N}} \left[\frac{\Gamma\left(1-\frac{1}{2N}\right)}{b^{1-\frac{1}{2N}}} - \frac{\Gamma\left(1-\frac{1}{2N}\right)}{\left(b+\frac{1}{\rho}\right)^{1-\frac{1}{2N}}} \right]^{N}. \tag{4.19}$$

Equation (4.17) is an application of equation (4.5) and is provably an upper-bound at all average SNR ρ. Equation (4.18) is an approximation that is also an upper-bound except at low SNR, albeit not provably. Similarly, equation (4.19) is an approximate lower-bound for the entire SNR region. In Section 4.7, it will be seen that equations (4.17)-(4.19) with $N = 5$ are within about 0.2 dB of the exact expression in [45, eqn.(6)] at high SNR regardless of fading models and modulation schemes. High SNR performance can be obtained once $\alpha_i = 1, \;\; i = 1, 2, ..., N$ and $t_i = 0, \;\; i = 1, 2, ..., N$ are substituted into the corresponding equations such as equations (4.9) and (4.11).

4.5.1.2 Rician Fading

Similarly, the PDF and CDF of γ_i is necessary to derive the bounds or approximations in Rician fading. The PDF of γ_i is given by $f_{\gamma_i}(x) = (1+K)e^{-K-(1+K)x/\rho}\, I_0\left(2\sqrt{K(1+K)x/\rho}\right)/\rho,\ \ x \geq 0$ where K is the Rician factor (i.e. $K \geq 0$) and $I_0(\cdot)$ is the zero-th order modified Bessel function of the first kind in [25, p.23], and the CDF can be obtained as $F_{\gamma_i}(x) = 1 - Q_1\left(\sqrt{2K}, \sqrt{2(1+K)x/\rho}\right),\ \ x \geq 0$ where $Q_1(\alpha,\beta)$ is the first order Marcum Q-function [25, p.93] by integrating the PDF. Substituting these into equation (4.5), and using the integral $\int_0^\infty x^{\mu-1/2}e^{-\alpha x} I_{2\nu}\left(2\beta\sqrt{x}\right)dx = \Gamma(\mu+\nu+1/2)\beta^{-1}e^{\beta^2/2\alpha}\alpha^{-\mu} M_{-\mu,\nu}\left(\beta^2/\alpha\right)/\Gamma(2\nu+1)$ where $M_{\mu,\nu}(\cdot)$ is the Whittaker function [37, p.709], the average performance is upper-bounded as

$$\begin{aligned} P_E \leq \frac{a\sqrt{b}}{2\sqrt{\pi N}} \int_0^\infty \frac{e^{-bx}}{\sqrt[2N]{x}} \left(1 - Q_1\left(\sqrt{2K}, \sqrt{\frac{2(1+K)x}{\rho}}\right)\right) dx \\ \left[\frac{\sqrt{1+K}e^{-K}\Gamma\left(1-\frac{1}{2N}\right)}{\sqrt{\rho K}} e^{\frac{K(1+K)}{2+2b\rho+2K}} \left(b + \frac{1+K}{\rho}\right)^{-\frac{1}{2}+\frac{1}{2N}}\right. \\ \left. M_{-\frac{1}{2}+\frac{1}{2N},0}\left(\frac{K(1+K)}{1+b\rho+K}\right)\right]^{N-1}. \end{aligned} \tag{4.20}$$

Even though equation (4.20) is not a perfect closed-form expression, it is easy to evaluate numerically since there exists only a single integral for a point-to-point single antenna system. Other bounds and approximations can be evaluated numerically using the PDF and CDF. However, closed-form high SNR performance can be obtained similarly to Rayleigh fading once $\alpha_i = (1+K)e^{-K},\ \ i = 1, 2, ..., N$ and $t_i = 0,\ \ i = 1, 2, ..., N$ are used.

4.5.2 AF Relay Networks with Multiple Relays

In the second application, average performance is analyzed using equation (4.7) for AF relay networks with multiple relays equipped with a single antenna. For this case, neither Craig's formula with MGFs [47, 50] nor

approximations with the integration-by-parts method [42, 43] can provide a closed-form solution, to the best of our knowledge.

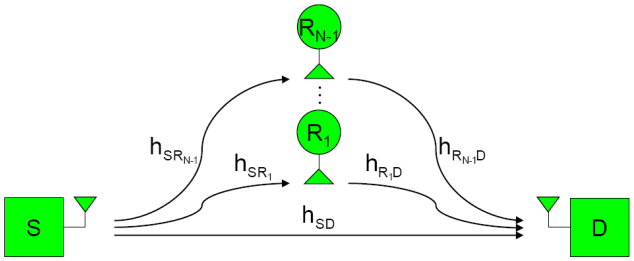

Figure 4.1: The System Model of Two-Hop Relay Networks with Multiple Relays.

Figure 4.1 shows a relay system, which consists of a source S, $N-1$ relays R_i, $i = 1, 2, ..., N-1$, and a destination D, each equipped with a single antenna. All CSI is assumed to be known to the destination and connected nodes. For example, h_{SD} is known to the source and destination, but not to the relays. The half-duplex time division multiple access (TDMA) scenario is considered with a two-slot scheme [11], in which the relays and destination receive the transmitted signal from the source in the first time slot; the destination receives the relayed signals while the source remains silent during subsequent $(N-1)$ time slots.

Reference [47] analyzes the average performance and provides four bounds for M-PSK modulation with single integrals, and are not in closed-form. Two bounds in [47] present closed-form expressions only for BPSK, which are reproduced for comparison in our simulations. For the same system model in a Nakagami-m fading environment, reference [50] provides an upper-bound on an average performance for M-PSK, but the bound contains a single integral and is not in closed-form. The authors also provide a simplified version of the bound using the Chernoff bound for one relay with BPSK in

Rayleigh fading, which is within about 2 dB of the actual performance, as seen in Section 4.6.2.

The received signals using MRC at the destination via the direct and relay links are as follows:

$$y_{SD} = \sqrt{\rho_{SD}}|h_{SD}|x + \frac{h^*_{SD}}{|h_{SD}|}n_{SD} \tag{4.21}$$

$$y_{SR_iD} = \frac{\sqrt{\rho_{SR}\rho_{RD}}|h_{SR_i}||h_{R_iD}|x}{\sqrt{1+\rho_{SR}|h_{SR_i}|^2}} + |h_{R_iD}|\frac{\sqrt{\rho_{RD}}\frac{h^*_{SR_i}}{|h_{SR_i}|}n_{SR_i}}{\sqrt{1+\rho_{SR}|h_{SR_i}|^2}} + \frac{h^*_{R_iD}}{|h_{R_iD}|}n_{R_iD}, \tag{4.22}$$

where $i = 1, 2, ..., N-1$, ρ_{SD}, ρ_{SR}, and ρ_{RD} are average transmit SNRs [1], h_{SD}, h_{SR_i}, and h_{RD} are channel coefficients, assumed to be i.i.d. $CN(0,1)$; n_{SD}, n_{SR_i}, and n_{R_iD} are noise distributed $CN(0,1)$; x is the transmitted symbol with $\mathbb{E}[x] = 0$ and $\mathbb{E}[|x|^2] = 1$, and $(\cdot)^*$ represents a complex conjugate.

Using equations (4.21) and (4.22), the combined received signal at the destination can be written as

$$y = a_{SD}\, y_{SD} + \sum_{i=1}^{N-1} a_{SR_iD}\, y_{SR_iD}, \tag{4.23}$$

where a_{SD} and a_{SR_iD} are combining weights for the minimum mean square error (MMSE) criterion [31, 42, 43, 45] in this work. Recall from the references that the MMSE coefficients are determined by $\sqrt{S_P}/N_P$, where S_P is the power of signal portions and N_P is the power of noise portions from equations (4.21) and (4.22).

If the MMSE criterion is used to combine signals from equations (4.21) and (4.22) when all CSI is known at the destination, the total instantaneous received SNR is represented by

$$\gamma = \gamma_{SD} + \sum_{i=1}^{N-1} \gamma_{SR_iD} = \gamma_{SD} + \sum_{i=1}^{N-1} \frac{\gamma_{SR_i}\gamma_{R_iD}}{1+\gamma_{SR_i}+\gamma_{R_iD}}, \tag{4.24}$$

[1] Unlike in Section 4.5.1, here we assume the average SNRs of the channels (i.e. the direct link and relay links) are different. This can be easily handled since the difference in the average SNRs can be subsumed into the channel-dependent RVs.

where $\gamma_{SD} = \rho_{SD}|h_{SD}|^2$ is the instantaneous received SNR of the direct link, γ_{SR_iD} are the instantaneous received SNRs of the two-hop relay links, $\gamma_{SR_i} = \rho_{SR}|h_{SR_i}|^2$, and $\gamma_{R_iD} = \rho_{RD}|h_{RD}|^2$. In this case, N RVs for X_i are γ_{SD} and γ_{SR_iD}, and the combined RV for X is γ. We work with a tight approximation to each term in the sum of equation (4.24) by considering $\Gamma_{SR_iD} := \gamma_{SR_i}\gamma_{R_iD}/(\gamma_{SR_i} + \gamma_{R_iD})$, which provides a performance lower-bound from the relay links. Note that both γ_{SR_iD} and Γ_{SR_iD} are equivalent at high SNR because Γ_{SR_iD} is obtained by removing the 1 in the denominator of γ_{SR_iD} in equation (4.24).

The CDF of the direct link ($S \rightarrow D$) is given by $F_{\gamma_{SD}}(x) = 1 - e^{-x/\rho_{SD}}$, $x \geq 0$ from [7, p.209], and the CDF of Γ_{SR_iD} is obtained from [45, eqn.(26)] by substituting $M_S = M_R = M_D = 1$ as

$$F_{\Gamma_{SR_iD}}(x) = 1 - \frac{2x}{\sqrt{\rho_{SR}\rho_{RD}}} e^{-x\left(\frac{1}{\rho_{SR}}+\frac{1}{\rho_{RD}}\right)} K_1\left(\frac{2x}{\sqrt{\rho_{SR}\rho_{RD}}}\right), \quad x \geq 0, \tag{4.25}$$

where $K_\nu(x)$ is the modified Bessel function of the second kind [37, p.xli]. When both CDFs are substituted to equation (4.7), and the integral $\int_0^\infty x^{\nu-1} e^{-\mu x} dx = \Gamma(\nu)/\mu^\nu$ [37, p.346] and the following integral from [37, p.700],

$$\begin{aligned} &\int_0^\infty x^{\mu-1} e^{-\alpha x} K_\nu(\beta x) dx \\ &= \frac{\sqrt{\pi}(2\beta)^\nu}{(\alpha+\beta)^{\mu+\nu}} \frac{\Gamma(\mu+\nu)\Gamma(\mu-\nu)}{\Gamma(\mu+\frac{1}{2})} {}_2F_1\left(\mu+\nu, \nu+\frac{1}{2}; \mu+\frac{1}{2}; \frac{\alpha-\beta}{\alpha+\beta}\right), \end{aligned} \tag{4.26}$$

where ${}_2F_1(\alpha, \beta; \gamma; z)$ is the Gauss hypergeometric function in [37, p.xl], are used, the average error rate is approximated by

$$\begin{aligned} P_E \approx \frac{a\sqrt{b}}{2\sqrt{\pi N}} &\left[\frac{\Gamma(C)}{b^C} - \frac{\Gamma(C)}{\left(b+\frac{1}{\rho_{SD}}\right)^C}\right] \left(1+\frac{1}{2N}\right)^{N-1} \\ &\left[\frac{b\Gamma(C)}{b^C} - \frac{8b\sqrt{\pi}\Gamma\left(3-\frac{1}{2N}\right)\Gamma(C)}{\rho_{SR}\rho_{RD}\Gamma\left(\frac{5}{2}-\frac{1}{2N}\right) B^{3-\frac{1}{2N}}} {}_2F_1\left(3-\frac{1}{2N}, \frac{3}{2}; \frac{5}{2}-\frac{1}{2N}; \frac{A}{B}\right)\right]^{N-1}, \end{aligned} \tag{4.27}$$

where $A := b + 1/\rho_{SR} + 1/\rho_{RD} - 2/\sqrt{\rho_{SR}\rho_{RD}}$, $B := b + 1/\rho_{SR} + 1/\rho_{RD} + 2/\sqrt{\rho_{SR}\rho_{RD}}$, and $C := 1 - 1/(2N)$.

Note that equation (4.27) is an approximation since the relay link performance using Γ_{SR_iD} provides a lower-bound on performance for the relay links even though equation (4.7) gives a performance upper-bound at high SNR. However, equation (4.27) actually provides a tight upper-bound at high SNR due to the tight upper-bound producing equation (4.7) since both γ_{SR_iD} and Γ_{SR_iD} from the relay link are equivalent at high SNR. Even though equation (4.27) becomes tighter to the actual performance as $N \to \infty$, it is tight even for small N (i.e. $N = 2$ or $N = 3$) as will be seen in our simulations in Section 4.7. Note also that the lower-bound using equation (4.8) can be obtained if the term $(1 + 1/(2N))^{N-1}$ is removed from equation (4.27).

4.5.3 AF MIMO Beamforming Relay Networks with Multiple Antennas

Figure 4.2 shows a two-hop MIMO relay system, which consists of a source S, a relay R, and a destination D. All nodes are equipped with multiple antennas, M_S, M_R, and M_D, respectively, and $\mathbf{H}_{SD}$, $\mathbf{H}_{SR}$, and $\mathbf{H}_{RD}$ are $M_D \times M_S$, $M_R \times M_S$, and $M_D \times M_R$ complex Gaussian channel matrices connecting the nodes, respectively, which are assumed to be statistically independent. Similar to the second application, the half-duplex TDMA scenario is considered with the two-slot scheme, where S transmits to R and D in the first time slot, and R amplifies and forwards its received signal in the second time slot while S is silent. All CSI is assumed to be known to the source, the destination, and connected nodes.

When beamforming to both relay and destination, the selection of the BF coefficients at the source becomes a challenging problem since the source

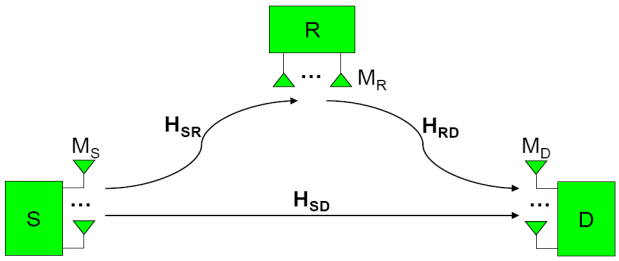

Figure 4.2: The System Model of Two-Hop MIMO Relay Networks.

has to balance the needs of the relay and destination. The optimal choice of BF by S to D might not be optimal S to R. Optimized combined BF for AF relaying is shown to lead to a non-convex problem and is solved using a gradient ascent algorithm with a finite number of Grassmannian BF vectors [36, 56] for initial starting points when all CSI is known at the source and destination in [31]. This solution not only is difficult to implement, it also does not lend itself to performance analysis because the optimal BF coefficients cannot be expressed in closed-form. In the view of this background, it is desirable to analyze the performance of optimal schemes through bounds.

In this work, the half-duplex scenario is considered with a two-slot scheme, and the combined performance of AF MIMO relay networks with BF is analyzed for the first time to the best of our knowledge. A novel combined lower-bound to any two-slot scheme is obtained by using two different BF vectors "matched" with the relay and direct links, respectively. A BF vector is matched when it is the strongest right singular vector of the corresponding channel. Since in a two-slot scheme two different BF vectors cannot be used at the same time slot, the lower-bound is achievable at the expense of a rate penalty with an extra time slot, leading to a three-slot scheme [42]. Therefore, two different BF vectors are used from the source to the relay and to the

destination, respectively, to obtain a lower-bound on performance to any two-slot scheme, or achievable performance with a three-slot scheme at a rate penalty.

Since two different BF vectors are used from the source to the relay and to the destination, respectively, the received signals using MRT and MRC via the direct and relay links at the destination are as follows:

$$y_{SD} = \sqrt{\rho_{SD}}\|\mathbf{H}_{SD}\mathbf{f}_{SD}\|x + \frac{(\mathbf{H}_{SD}\mathbf{f}_{SD})^H}{\|\mathbf{H}_{SD}\mathbf{f}_{SD}\|}\mathbf{n}_{SD} \tag{4.28}$$

$$\begin{aligned} y_{SRD} = & \frac{\sqrt{\rho_{SR}\rho_{RD}}\|\mathbf{H}_{SR}\mathbf{f}_{SR}\|\|\mathbf{H}_{RD}\mathbf{f}_{RD}\|x}{\sqrt{1+\rho_{SR}\|\mathbf{H}_{SR}\mathbf{f}_{SR}\|^2}} \\ & + \frac{\sqrt{\rho_{RD}}\|\mathbf{H}_{RD}\mathbf{f}_{RD}\|\frac{(\mathbf{H}_{SR}\mathbf{f}_{SR})^H}{\|\mathbf{H}_{SR}\mathbf{f}_{SR}\|}\mathbf{n}_{SR}}{\sqrt{1+\rho_{SR}\|\mathbf{H}_{SR}\mathbf{f}_{SR}\|^2}} + \frac{(\mathbf{H}_{RD}\mathbf{f}_{RD})^H}{\|\mathbf{H}_{RD}\mathbf{f}_{RD}\|}\mathbf{n}_{RD}, \end{aligned} \tag{4.29}$$

where ρ_{SD}, ρ_{SR}, and ρ_{RD} are average transmit SNRs; $\mathbf{H}_{SD}$ $(M_D \times M_S)$, $\mathbf{H}_{SR}$ $(M_R \times M_S)$, and $\mathbf{H}_{RD}$ $(M_D \times M_R)$ are channel coefficient matrices, assumed to be i.i.d. according to $CN(0,1)$; $\mathbf{f}_{SD}$ $(M_S \times 1)$, $\mathbf{f}_{SR}$ $(M_S \times 1)$, and $\mathbf{f}_{RD}$ $(M_R \times 1)$ are BF vectors with norm 1 obtained as the strongest right singular vectors of corresponding channel coefficient matrices; x is transmitted symbol with $\mathbb{E}[|x|^2] = 1$ and $\mathbb{E}[x] = 0$; $\mathbf{n}_{SD}$ $(M_D \times 1)$, $\mathbf{n}_{SR}$ $(M_R \times 1)$, and $\mathbf{n}_{RD}$ $(M_D \times 1)$ are noise according to $CN(0, \mathbf{I})$. Using equations (4.28) and (4.29), the combined received signal at the destination can be obtained using the MMSE coefficients such as equation (4.23).

If the MMSE criterion is used to combine signals from equations (4.28) and (4.29) when all CSI is known at the source and destination, the total instantaneous received SNR is represented by

$$\gamma = \gamma_{SD} + \gamma_{SRD} = \gamma_{SD} + \frac{\gamma_{SR}\gamma_{RD}}{1+\gamma_{SR}+\gamma_{RD}}, \tag{4.30}$$

where $\gamma_{SD} = \rho_{SD}\|\mathbf{H}_{SD}\mathbf{f}_{SD}\|^2$, $\gamma_{SR} = \rho_{SR}\|\mathbf{H}_{SR}\mathbf{f}_{SR}\|^2$, $\gamma_{RD} = \rho_{RD}\|\mathbf{H}_{RD}\mathbf{f}_{RD}\|^2$, and $\gamma_{SRD} := \gamma_{SR}\gamma_{RD}/(1+\gamma_{SR}+\gamma_{RD})$. In this case, $N = 2$ with $X_1 = \gamma_{SD}$

and $X_2 = \gamma_{SRD}$, and the combined RV $X = \gamma$. $\Gamma_{SRD} := \gamma_{SR}\gamma_{RD}/(\gamma_{SR} + \gamma_{RD})$ is used to obtain the average performance, which provides a lower-bound from the relay link. While this appears to be a special case of equation (4.24), the distributions of γ_{SR}, γ_{RD}, and γ_{SD} are much more complicated due to the MIMO nature of the system.

To obtain the combined average performance, the CDFs of γ_{SD} and Γ_{SRD} are given as follows [45, eqns. (21) and (26)]:

$$F_{\gamma_{SD}}(x) = 1 - \sum_{n=1}^{M_D} \sum_{m=M_S-M_D}^{(M_S+M_D)n-2n^2} \sum_{k=0}^{m} \frac{d_{n,m} e^{-\frac{nx}{\rho_{SD}}} (nx)^k}{k! \rho_{SD}^k}, \; x > 0 \tag{4.31}$$

$$\begin{aligned} F_{\Gamma_{SRD}}(x) = 1 - \sum_{n=1}^{M_R} \sum_{m=M_S-M_R}^{(M_S+M_R)n-2n^2} \sum_{k=0}^{m} \sum_{i=1}^{M_R} \sum_{j=M_D-M_R}^{(M_D+M_R)i-2i^2} \sum_{p=0}^{k+j} \binom{k+j}{p} \\ \frac{2 d_{n,m} d_{i,j} n^{\frac{k+p+1}{2}} i^{\frac{2j+k-p+1}{2}}}{k! j! \rho_{SR}^{\frac{k+p+1}{2}} \rho_{RD}^{\frac{2j+k-p+1}{2}}} x^{k+j+1} e^{-x\left(\frac{n}{\rho_{SR}} + \frac{i}{\rho_{RD}}\right)} \\ K_{p-k+1}\left(2x\sqrt{\frac{ni}{\rho_{SR}\rho_{RD}}}\right), \quad x > 0, \end{aligned} \tag{4.32}$$

where $d_{n,m}$ are coefficients given by [30, eqn. (24)], also provided in Tables 2.1-2.3 for completeness. Note that equations (4.31) and (4.32) are valid when $M_S \geq M_D$, $M_S \geq M_R$, and $M_D \geq M_R$ even though other cases can be easily handled with minor modifications. For example, M_S and M_D must be switched in equation (4.31) when $M_S < M_D$.

Once both CDFs are substituted into equation (4.7), and the integral $\int_0^\infty x^{\nu-1} e^{-\mu x} dx = \Gamma(\nu)/\mu^\nu$ [37, p.346] and equation (4.26) are used, the com-

bined average performance can be approximated:

$$P_E \approx \frac{5a\sqrt{b}}{8\sqrt{2\pi}} \left[\frac{\Gamma\left(\frac{3}{4}\right)}{b^{\frac{3}{4}}} - \sum_{n=1}^{M_D} \sum_{m=M_S-M_D}^{(M_S+M_D)n-2n^2} \sum_{k=0}^{m} \frac{d_{n,m} n^k \Gamma\left(k+\frac{3}{4}\right)}{k! \rho_{SD}^k \left(b+\frac{n}{\rho_{SD}}\right)^{k+\frac{3}{4}}} \right]$$
$$\left[\frac{b\Gamma\left(\frac{3}{4}\right)}{b^{\frac{3}{4}}} - \sum_{n=1}^{M_R} \sum_{m=M_S-M_R}^{(M_S+M_R)n-2n^2} \sum_{k=0}^{m} \sum_{i=1}^{M_R} \sum_{j=M_D-M_R}^{(M_D+M_R)i-2i^2} \sum_{p=0}^{k+j} \binom{k+j}{p} \right. \tag{4.33}$$
$$\frac{2bd_{n,m}d_{i,j}n^C i^G}{k!j!\rho_{SR}^C \rho_{RD}^G} \frac{\sqrt{\pi}\left(4\sqrt{\frac{ni}{\rho_{SR}\rho_{RD}}}\right)^L}{B^{p+j+\frac{11}{4}}} \frac{\Gamma\left(j+p+\frac{11}{4}\right)\Gamma\left(j+2k-p+\frac{3}{4}\right)}{\Gamma\left(k+j+\frac{9}{4}\right)}$$
$$\left. {}_2F_1\left(j+p+\frac{11}{4}, p-k+\frac{3}{2}; k+j+\frac{9}{4}; \frac{A}{B}\right) \right],$$

where $A := b + n/\rho_{SR} + i/\rho_{RD} - 2\sqrt{ni/(\rho_{SR}\rho_{RD})}$, $B := b + n/\rho_{SR} + i/\rho_{RD} + 2\sqrt{ni/(\rho_{SR}\rho_{RD})}$, $C := (k+p+1)/2$, $G := (2j+k-p+1)/2$, and $L := p-k+1$. Note that equation (4.33) is a combined link average performance approximation with the same reason for equation (4.27), which provides a very tight approximation to the 3-slot scheme performance for the entire SNR region. Note also that the lower-bound using equation (4.8) can be obtained if equation (4.33) is multiplied by 4/5.

4.5.4 Example of Non-Gaussian Noise

Even though we have assumed that the additive noise is Gaussian, the mathematical technique used to obtain the bounds in this chapter (i.e. AM and GM inequality) can also be applied to some non-Gaussian noise models such as Middleton's class-A noise [54].

We consider the same system model as Section 4.5.1 (i.e. received diversity using MRC) using Rayleigh fading with Middleton's class-A noise such as equation (1) in [54], in which the noise sample is assumed to be the superposition of a Gaussian component, g, and an impulsive component, i, with $T := \sigma_g^2/\sigma_i^2$. Even though the class-A noise is not Gaussian, it is conditionally

Gaussian, given a Poisson random variable m of parameter A, with zero mean and variance $\sigma_m^2 = \sigma^2 \left(m/(AT+A) + T/(T+1)\right)$, where σ^2 is the variance of the class-A noise. A is the impulsive index, which makes the noise impulsive if A is small (i.e. 10^{-3}). Note that we consider "Model I" in [54, eqn.(4)], in which different diversity branches are influenced by the same physical impulsive source, even though other noise models can also be considered.

Consider now N additively related statistically independent non-negative RVs over the class-A noise in Rayleigh fading environment. In this case, $\gamma_i = \rho|h_i|^2/\sigma_m^2, \;\; i = 1, 2, ..., N$ correspond to X_i and the combined RV $\gamma := \rho\|\mathbf{h}\|^2/\sigma_m^2 = \sum_{i=1}^{N} \gamma_i$ becomes X from Section II. Therefore, once the PDF and CDF of γ_i, $f_{\gamma_i}(x) = \sigma_m^2 e^{-\sigma_m^2 x/\rho}/\rho, \;\; x \geq 0$ and $F_{\gamma_i}(x) = 1 - e^{-\sigma_m^2 x/\rho}, \;\; x \geq 0$, respectively, are substituted into equations (4.5) and (4.7), respectively, and the result is averaged over σ_m^2, the average performance is upper-bounded or approximated as

$$P_E \leq \sum_{m=0}^{\infty} \frac{\alpha_m a\sqrt{b}}{2\sqrt{\pi N}} \left[\frac{\Gamma\left(1-\frac{1}{2N}\right)}{b^{1-\frac{1}{2N}}} - \frac{\Gamma\left(1-\frac{1}{2N}\right)}{\left(b+\frac{\sigma_m^2}{\rho}\right)^{1-\frac{1}{2N}}} \right] \left[\frac{\sigma_m^2 \Gamma\left(1-\frac{1}{2N}\right)}{\rho\left(b+\frac{\sigma_m^2}{\rho}\right)^{1-\frac{1}{2N}}} \right]^{N-1} \tag{4.34}$$

$$P_E \approx \sum_{m=0}^{\infty} \frac{\alpha_m a b^{N-\frac{1}{2}}}{2\sqrt{\pi N}} \left(1+\frac{1}{2N}\right)^{N-1} \left[\frac{\Gamma\left(1-\frac{1}{2N}\right)}{b^{1-\frac{1}{2N}}} - \frac{\Gamma\left(1-\frac{1}{2N}\right)}{\left(b+\frac{\sigma_m^2}{\rho}\right)^{1-\frac{1}{2N}}} \right]^{N}, \tag{4.35}$$

where $\alpha_m = e^{-A}A^m/m!$. The approximation using equation (4.8) can be obtained by removing the term $(1+1/(2N))^{N-1}$ from equation (4.35).

4.6 Numerical and Simulation Results

In Monte-Carlo or numerical simulations, the transmitted symbol is BPSK, QPSK, and 16-QAM modulated, and the channel is 100-symbol i.i.d. Rayleigh and Rician block fading (i.e. K=1). Zero mean and unit variance are used to Rayleigh fading while $\sqrt{K/2}$ mean and unit variance are used to Rician

fading. For combining signals, MRC with MMSE is used for all simulations [31, 42, 43, 45]. In relay networks, the relationships among the average SNR values are chosen as $\rho_{SR} = \rho_{RD}$ and $\rho_{SD} = 10^{(10\log_{10}(\rho_{SR})-30\log_{10}(2))/10}$, which corresponds to the relay located in the mid-point of the S and D in a simplified path-loss model [7, p.46] with path-loss exponent of 3 (i.e. the "mid-point relay model"). Alternatively, we also consider $\rho_{SR} = \rho_{RD} = \rho_{SD}$ which is the "equi-distant relay model" for high SNR analysis even though our analysis applies to other average SNR values as well. The performance of equation (4.1) is illustrated by Monte-Carlo simulations as the actual performance in the sequel. For the class-A noise, $A = 1$ and $A = 0.001$ with $T = 0.1$ are used.

4.6.1 Receive Diversity using MRC

The bound and approximations using equations (4.5), (4.7), and (4.8) are compared with the performance using equation (4.1) with the number of antennas, $(M_S, M_D) = (1, 2)$ in mixed Rayleigh-Rician fading and $(M_S, M_D) = (1, 5)$ in Rayleigh fading. To show the tightness of the bounds when the average SNR values are spread out, different average SNR values for each path are considered.

Figures 4.3 and 4.4 show the MRC performance and bounds with BPSK, QPSK, and 16-QAM using $(M_S, M_D) = (1, 2)$ in mixed Rayleigh-Rician fading when the average SNR for one path is ρ and that for other other path is various such as $\rho/10$, $\rho/100$, 10ρ, or 100ρ. Regardless of modulation schemes and SNR spreading, the bounds and approximations using equations (4.5), (4.7), and (4.8) are about 0.39 dB, 0.25 dB, and 0.23 dB apart from the actual performance at 10^{-6}, respectively, which match with high SNR performance, which is the analytical results given by Section 4.4.

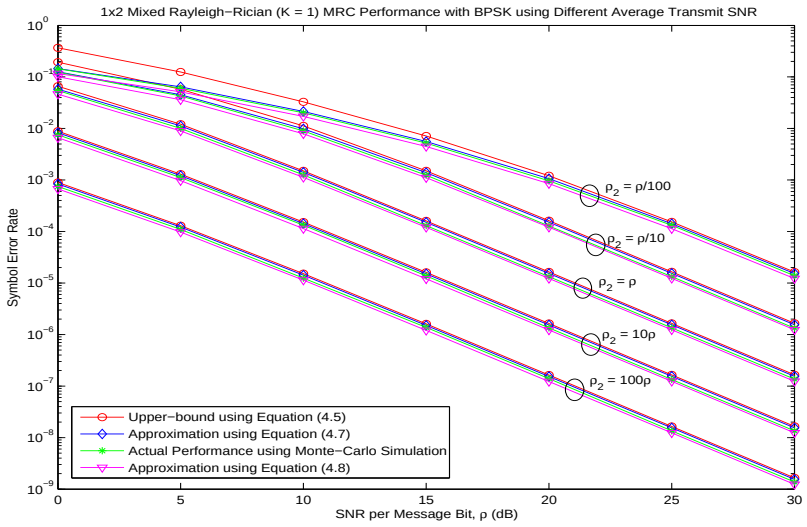

Figure 4.3: 1×2 Mixed Rayleigh-Rician MRC Performance and Bounds with BPSK using Different Average SNR.

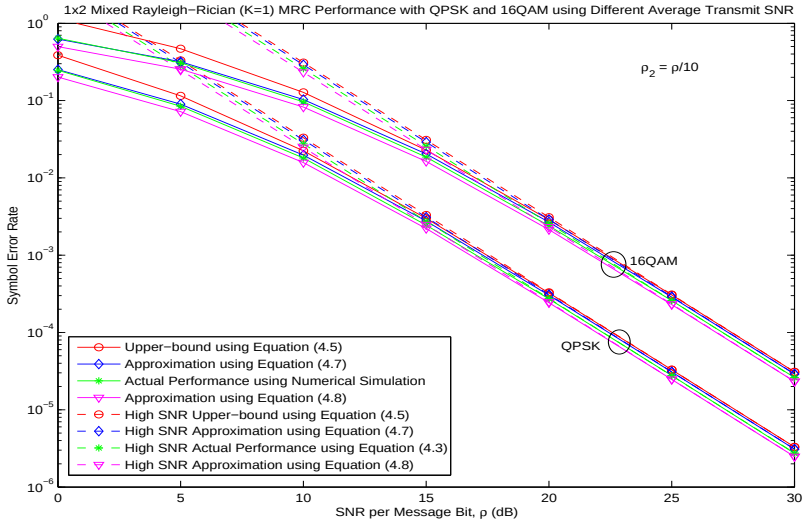

Figure 4.4: 1×2 Mixed Rayleigh-Rician MRC Performance and Bounds with QPSK and 16-QAM using Different Average SNR.

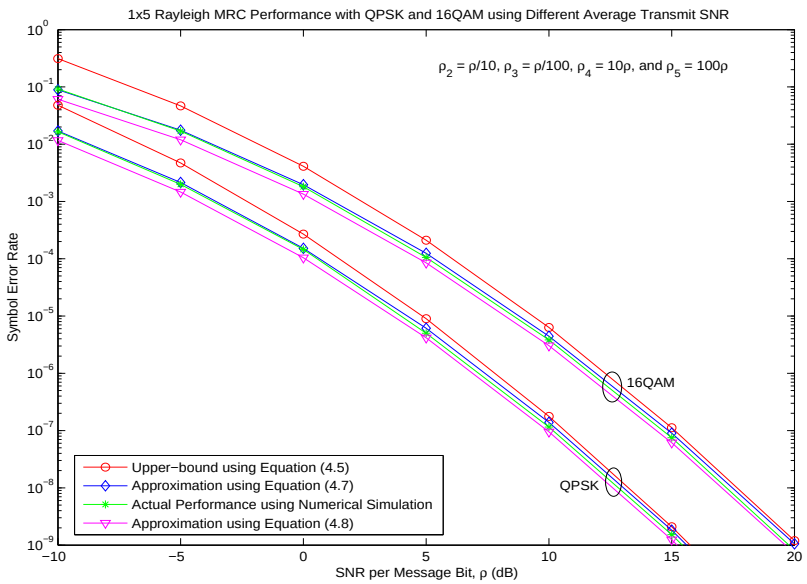

Figure 4.5: 1×5 Rayleigh MRC Performance and Bounds with QPSK and 16-QAM using Different Average SNR.

Figure 4.5 shows the MRC performance and bounds with QPSK and 16-QAM using $(M_S, M_D) = (1, 5)$ in Rayleigh fading when average SNRs from each path are ρ, $\rho/10$, $\rho/100$, 10ρ, and 100ρ, respectively. Independent of modulation schemes, the bound and approximations using equations (4.5), (4.7), and (4.8) are about 0.36 dB, 0.22 dB, and 0.2 dB apart from the actual performance at 10^{-9}, respectively, which need more SNR to obtain high SNR performance of Tables 4.1-4.3.

Figure 4.6 shows the MRC performance and bounds with BPSK using $(M_S, M_D) = (1, 2)$ in Rayleigh fading using Middleton's class-A noise (i.e. $A = 1$ and $A = 0.001$ with $T = 0.1$). The bound and approximations using equations (4.5), (4.7), and (4.8) are about 0.39 dB, 0.25 dB, and 0.23 dB apart from the actual performance at 10^{-8}. These gaps at high SNR are same as those of Gaussian noise cases.

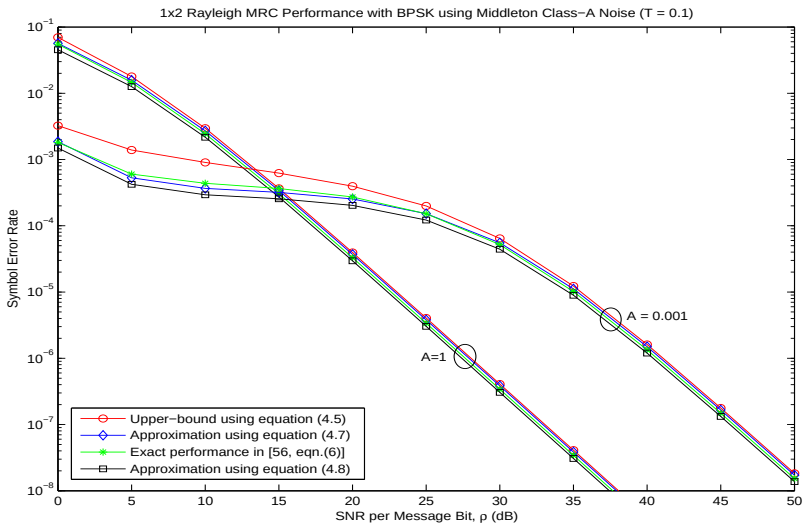

Figure 4.6: 1×2 Rayleigh MRC Performance and Bounds with BPSK using Middleton Class-A Noise.

Based on numerical evaluations and simulations, the gaps among the bounds and the actual performance using equation (4.1) become smaller as the number of antennas increases regardless of modulation schemes and SNR spreading, as predicted by equations (4.12) and (4.13). However, when an average SNR becomes low compared with the reference average SNR, the bounds or approximations become loose at low SNR even though they are still tight at high SNR.

4.6.2 AF Relay Networks with Multiple Relays

The approximations given in equations (4.7) and (4.8) are used to obtain performance for AF relay networks with multiple relays equipped with a single antenna, and it is compared with the Monte-Carlo or numerical simulations using $(M_S, M_R, M_D) = (1, 1, 1)$ with 2 or 4 relays. When average SNR values are determined, the two relay models are used; the mid-point and

equi-distant relay models. As benchmarks, the upper and lower-bounds with BPSK are included from [47, eqn.(19)].

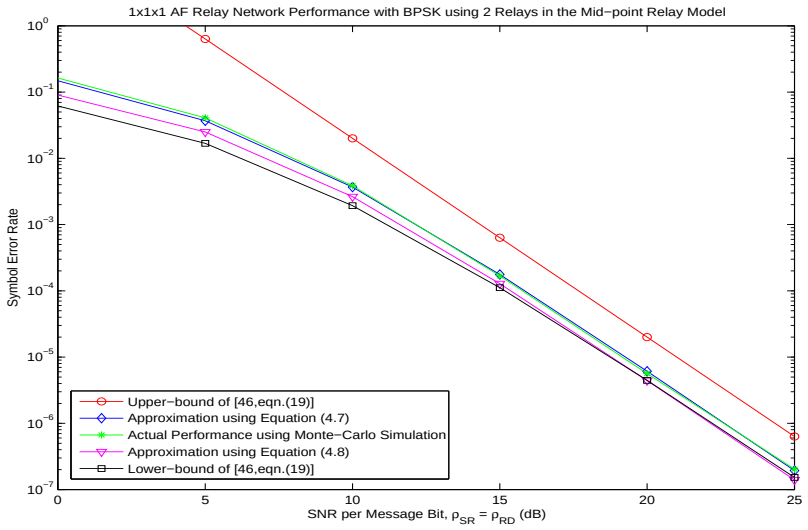

Figure 4.7: $1 \times 1 \times 1$ AF Relay Network Performance with BPSK using 2 Relays in Rayleigh Fading.

Figures 4.7 and 4.8 shows $1 \times 1 \times 1$ AF relay network performance with BPSK, QPSK, and 16-QAM using 2 relays in Rayleigh fading. The approximations using equations (4.7) and (4.8) are about 0.24 dB and 0.21 dB apart from the simulations using equation (4.1) at 10^{-6}, respectively, regardless of modulation schemes. On the other hand, the upper and lower-bounds with BPSK from [47, eqn.(19)] are about 1.8 dB and 0.4 dB apart from the simulations at 10^{-6}, respectively. High SNR analysis given by Section 4.4 matches well with the analytical results.

Figure 4.9 shows $1 \times 1 \times 1$ AF relay network performance with BPSK using 4 relays in the mid-point relay model. The approximations using equation (4.7) and (4.8) are about 0.18 dB and 0.15 dB apart from the Monte-Carlo simulations at 10^{-8}, respectively. The upper and lower-bounds from [47, eqn.(19)]

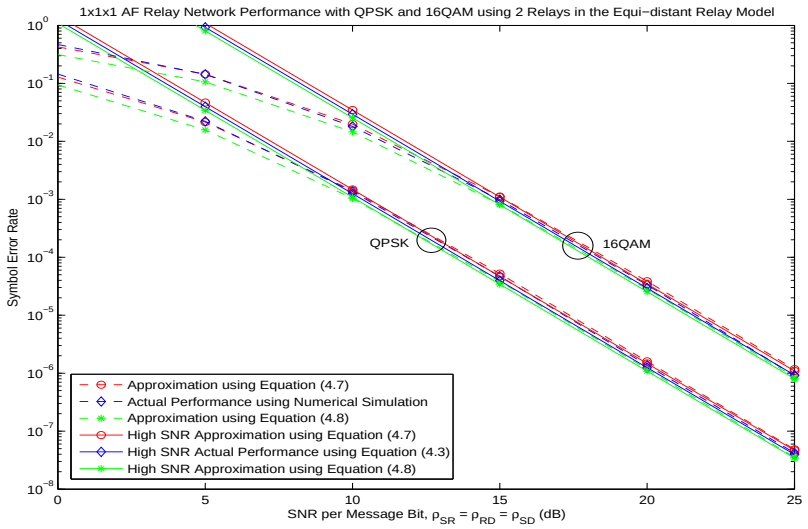

Figure 4.8: $1 \times 1 \times 1$ AF Relay Network Performance with QPSK and 16-QAM using 2 Relays in Rayleigh Fading.

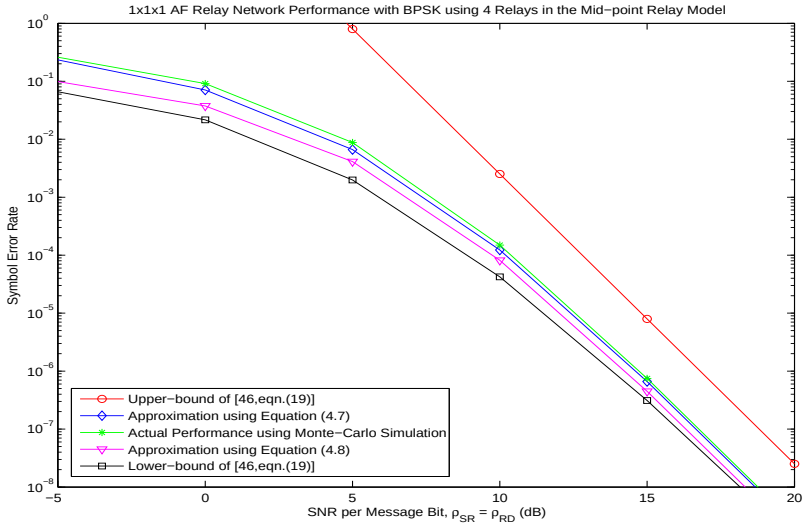

Figure 4.9: $1 \times 1 \times 1$ AF Relay Network Performance with BPSK using 4 Relays in the Mid-Point Relay Model.

are about 2.2 dB and 0.7 dB apart from the Monte-Carlo simulation at 10^{-8}, respectively. The gap between the approximation in equation (4.27) and the Monte-Carlo simulation becomes smaller as the number of relays increases, as seen in Figures 4.7-4.9.

4.6.3 AF MIMO BF Relay Networks with Multiple Antennas

The approximations given in equations (4.7) and (4.8) are also used to obtain performance of AF MIMO BF relay networks using multiple antennas at the relay, and it is compared with the simulation using $(M_S, M_R, M_D) = (2, 1, 2)$ or $(2, 2, 2)$ with a single relay. Similar to the previous example, for average SNR values, the mid-point and equi-distant relay models are used. As mentioned in Section 4.5.3, we are analyzing the performance of an ideal beamformer at S that is matched to both R and D to derive a lower-bound on any two-slot scheme. As a benchmark, the approximation using equation (4.5) from our previous work [45, eqn.(9)] is included since equation (4.33) uses equation (4.7).

Figure 4.10 shows $2 \times 1 \times 2$ AF MIMO BF relay network performance with QPSK and 16-QAM using a single relay in Rayleigh fading. The approximations using equations (4.5), (4.7), and (4.8) fit well to the simulation at high SNR, and they seem to agree with the actual performance. High SNR analysis given by Section 4.4 also matches well with the analytical results. The same trend is observed for the $2 \times 2 \times 2$ setup in Figure 4.11. The gaps among the approximations and the simulations become smaller as the number of antennas at the relay increases.

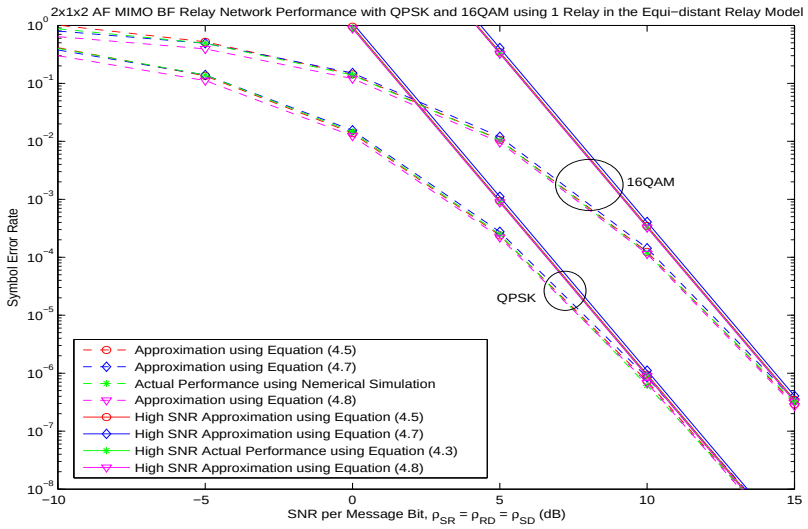

Figure 4.10: $2 \times 1 \times 2$ AF MIMO BF Relay Network Performance with QPSK and 16-QAM using 1 Relay in Rayleigh Fading.

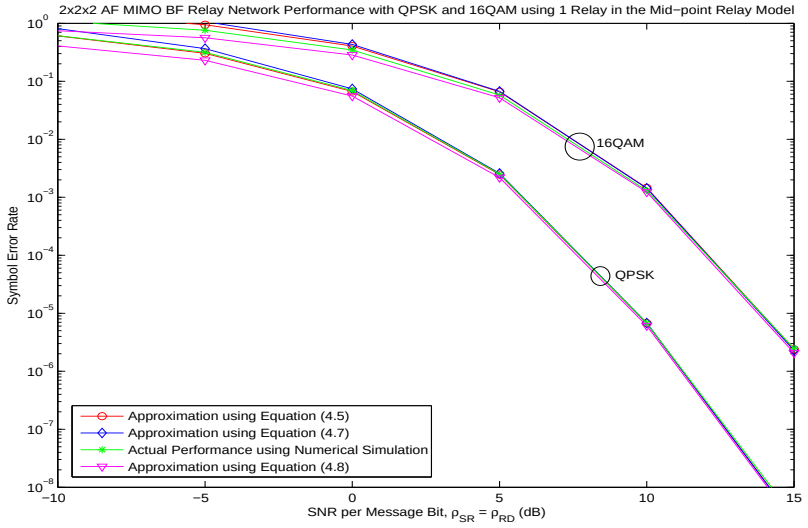

Figure 4.11: $2 \times 2 \times 2$ AF MIMO BF Relay Network Performance with QPSK and 16-QAM using 1 Relay in the Mid-Point Relay Model.

4.7 Chapter Summary

Novel average performance bounds are presented for systems with instantaneous SNRs given by a sum of N statistically independent non-negative RVs using the AM and GM inequality. The gaps among the bounds and the actual performance at high SNR are dependent on the number of RVs and the diversity orders. In particular, the tightness of the bounds is quantified analytically at high SNR, and shown to go to zero as $O(1/N)$ for large N, which is presented in Tables 4.1-4.3. Since the bounds can be used for any fading models with PDFs or CDFs available using the products of single integrals, they are simple to apply.

Table 4.1: The Analytical High SNR Gaps in dB from the Bounds to the Actual Performance for Receive Diversity Systems

Bounds	Receive Diversity with MRC		
	N = 2	N = 5	N = 10
Equation (4.5)	0.39	0.22	0.12
Equation (4.7)	0.25	0.18	0.11
Equation (4.8)	0.23	0.15	0.08

Table 4.2: The Analytical High SNR Gaps in dB from the Bounds to the Actual Performance for AF Multiple Relay Systems

Bounds	AF Multiple Relay System		
	N = 3 (2 Relays)	N = 5 (4 Relays)	N = 10 (9 Relays)
Equation (4.5)	0.32	0.22	0.12
Equation (4.7)	0.24	0.18	0.11
Equation (4.8)	0.21	0.15	0.08

The bounds are most useful when the distribution of the sum is intractable since they do not require finding the combined PDFs or CDFs of the sum. They are applied to obtain average performance in receive diversity

Table 4.3: The Analytical High SNR Gaps in dB from the Bounds to the Actual Performance for AF MIMO BF Relay Systems

Bounds	AF MIMO BF Relay System		
	N = 2 $(2 \times 1 \times 2)$	N = 2 $(2 \times 2 \times 2)$	N = 2 $(3 \times 3 \times 3)$
Equation (4.5)	0.034	0.019	0.0035
Equation (4.7)	0.149	0.105	0.05
Equation (4.8)	0.013	0.016	0.0033

using MRC to show the tightness of the bounds to the actual performance. A couple of approximations are adapted to obtain the combined average performance for AF relay networks using multiple relays equipped with a single antenna, and for AF MIMO BF single relay systems using multiple antennas at the source, relay, and destination. The gaps among the bounds and the simulations become smaller as the number of antennas and the number of relays increase. Even though the bounds are derived for AWGN, they can also be applied to some non-Gaussian noise models, as we illustrate with the class-A noise. In all the cases considered, the bounds are with a fraction of a dB of their actual values.

Appendix 4.1: Proof of Theorem 4.1

The average performance in equation (4.1) can be written as

$$P_E = \int_0^\infty \int_0^\infty ... \int_0^\infty aQ\left(\sqrt{2b\left(\sum_{i=1}^{N} x_i\right)}\right)\left(\prod_{i=1}^{N} f_{X_i}(x_i)dx_i\right), \tag{4.36}$$

where $f_{X_i}(x_i)$ are the PDFs of statistically independent non-negative RVs, X_i. To calculate equation (4.36), the first integral with respect to x_1 has to be considered at first

$$\int_0^\infty aQ\left(\sqrt{2b\left(\sum_{i=1}^{N} x_i\right)}\right) f_{X_1}(x_1)dx_1. \tag{4.37}$$

Since equation (4.37) can be solved by the integration-by-parts method, the key ingredient is the derivative of Q-function. Using the differentiation of a definite integral with respect to a parameter [37, p.21],

$$\frac{d}{d\alpha}\int_{\phi(\alpha)}^{\psi(\alpha)} f(x,\alpha)dx = \frac{d\psi}{d\alpha}f(\psi(\alpha),\alpha) - \frac{d\phi}{d\alpha}f(\phi(\alpha),\alpha) + \int_{\phi(\alpha)}^{\psi(\alpha)} \frac{\partial f}{\partial \alpha}d\alpha, \tag{4.38}$$

the derivative of Q-function is obtained by

$$\begin{aligned} &\frac{d}{dx_1}Q\left(\sqrt{2b\left(\sum_{i=1}^{N} x_i\right)}\right) \\ &= \frac{d}{dx_1}\left(\frac{1}{2} - \frac{1}{\sqrt{\pi}}\int_0^{\sqrt{b\left(\sum_{i=1}^{N} x_i\right)}} e^{-t^2}dt\right) = -\frac{\sqrt{b}e^{-b\left(\sum_{i=1}^{N} x_i\right)}}{2\sqrt{\pi\left(\sum_{i=1}^{N} x_i\right)}}. \end{aligned} \tag{4.39}$$

Therefore, the first integral with respect to x_1 of equation (4.36) is attained by the integration-by-parts method using equations (3.37) and (4.39) as

$$\int_0^{\infty} aQ\left(\sqrt{2b\left(\sum_{i=1}^{N} x_i\right)}\right) f_{X_1}(x_1)dx_1 = \int_0^{\infty} \frac{a\sqrt{b}e^{-b\left(\sum_{i=1}^{N} x_i\right)}}{2\sqrt{\pi\left(\sum_{i=1}^{N} x_i\right)}} F_{X_1}(x_1)dx_1, \tag{4.40}$$

where $F_{X_1}(x_1)$ is the CDF of X_1. Based on the first integral, equation (4.40), equation (4.36) can be rewritten as

$$P_E = \frac{a\sqrt{b}}{2\sqrt{\pi}}\int_0^{\infty}\int_0^{\infty}...\int_0^{\infty} \frac{e^{-b\left(\sum_{i=1}^{N} x_i\right)}}{\sqrt{\sum_{i=1}^{N} x_i}} F_{X_1}(x_1)dx_1 \left(\prod_{i=2}^{N} f_{X_i}(x_i)dx_i\right). \tag{4.41}$$

Using the relationship between AM and GM, $\sum_{i=1}^{N} x_i \geq N\sqrt[N]{\prod_{i=1}^{N} x_i}$, the following inequality can be obtained

$$\sqrt{\sum_{i=1}^{N} x_i} \geq \sqrt{N}\sqrt[2N]{\prod_{i=1}^{N} x_i}. \tag{4.42}$$

Once equation (4.42) is applied to equation (4.41), a novel upper-bound is obtained by equation (4.5). Equivalently, if integrals with PDFs are not tractable, equation (4.5) can be written with CDFs using the integration-by-parts method as equation (4.6).

Chapter 5

Unified Sum-BER Performance Analysis of AF MIMO Beamforming in Two-Way Relay Networks

Cooperative diversity schemes, using relays between the source and destination, have been widely investigated because of their spatial diversity and extensive coverage with reduced power consumption [11–13]. Amplify-and-forward or decode-and-forward (AF/DF) one-way relaying using two time slots is known to offer gains in performance when the destination keeps apart from the source, in which the relay and destination receive the transmitted signal from the source in the first time slot, and the relay amplifies or decodes and forwards the transmitted signal, and the destination receives the relayed signal while the source remains silent in the second time slot [11–13], referred to as one-way relaying.

Even though one-way relaying provides spatial diversity and extensive coverage with reduced power consumption, it causes a spectral loss due to more use of time slots. To improve the spectral efficiency in two time slots, two-way relaying is suggested, in which two sources transmit simultaneously their signals to the relay in the first time slot (i.e. multiple access phase), and the relay amplifies or decodes received signals and forwards the combined signals to the sources in the second time slot (i.e. broadcast phase) [19–21].

Multiple-input multiple-output (MIMO) technology has been considered as a way to combat severe fading due to its excellent link reliability based on achievable spatial diversity [1]. When multiple antennas are used, the combination of maximum ratio transmission (MRT) beamforming (BF) [6] and maximum ratio combining (MRC) beamforming [7] is one simple way to

achieve spatial diversity if full channel state information (CSI) is available at the source and destination. Since BF produces or receives a narrow wireless beam, it requires less power for the same distance compared to a single antenna system, creates or receives less interference to or from others, and increases reliability for transmission or reception. Various BF techniques are considered and deployed with MIMO using multiple directional antenna elements to utilize BF advantages in wireless standards such as wireless local area network (WLAN) (i.e. IEEE 802.11n) [8], LTE-Advanced [9], and WiMAX [10].

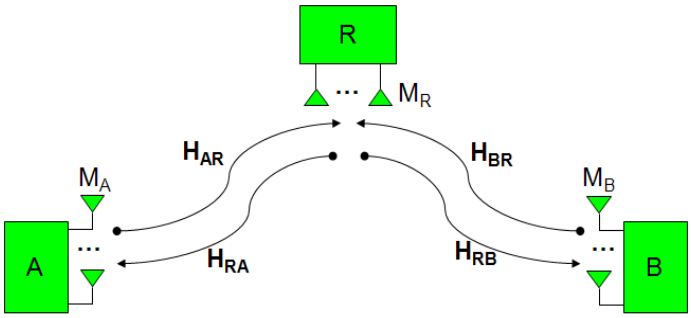

Figure 5.1: System Model of Two-Hop MIMO Two-Way Relay Networks.

When two nodes, A and B in Figure 5.1, communicate each other through the relay R, one-way relay systems using four time slots (i.e. $A \rightarrow R \rightarrow B$ and $B \rightarrow R \rightarrow A$ sequentially) can achieve less maximum ergodic sum-rate than two-way relay systems which use two or three time slots, due to more use of time slots [57]. In two-slot two-way relay networks, A and B transmit their signals to R in the first time slot, and R amplifies the added received signals and forwards them to both A and B in the second slot, while A and B transmit their signals to R in the first and second time slots, respectively, and R weighs the received signals, amplifies the added signals, and forwards them to both A and B in the third slot in three-slot two-way relay networks [19, 21, 57, 58]. Figure 5.2 illustrates five transmission schemes used in this

chapter. Even though maximum ergodic sum-rate is better for the schemes using less time slots such as the two-slot scheme, the ones using more time slots such as the three-slot scheme can be better in sum-BER since they can be good for optimization and beamforming, which are not valid for the ones using less time slots.

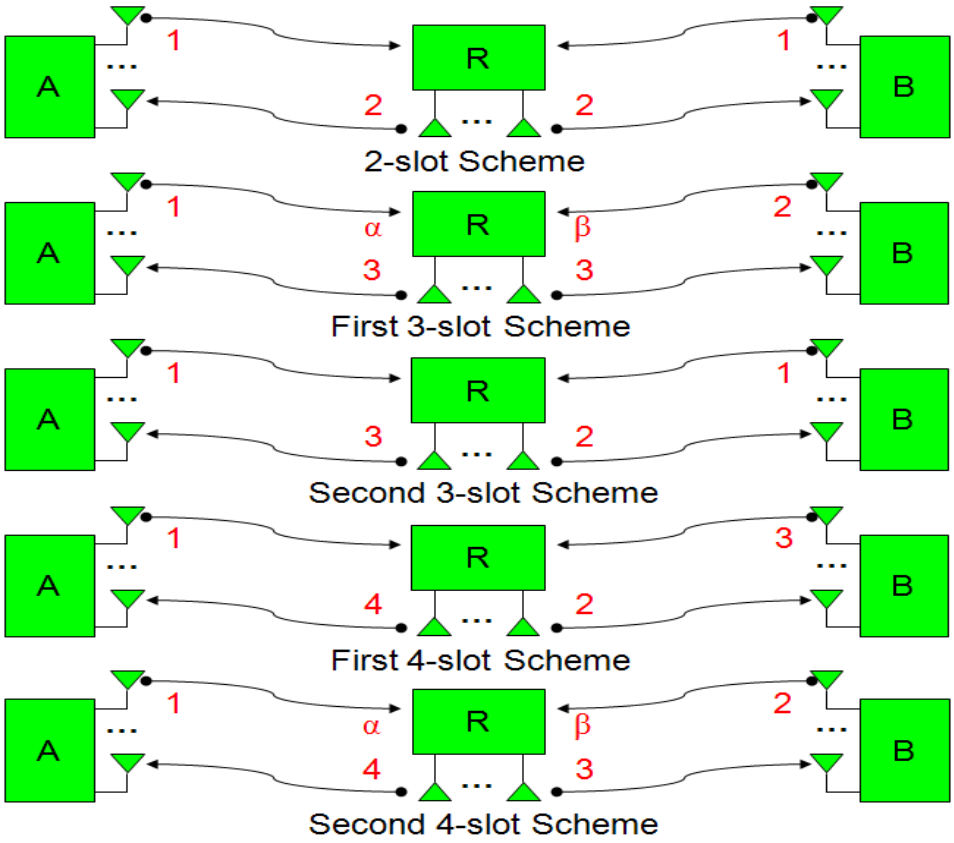

Figure 5.2: Transmission Schemes for Two-Way Relay Networks.

After AF and decode-and-forward (DF) two-way relay networks are proposed in [19], sum-bit error rate (BER) and maximum ergodic sum-rate for systems using a single antenna at all nodes are analyzed for two-way relay systems in [21, 59, 60]. Reference [21] provides closed-form sum-BER and maximum ergodic sum-rate for the two-slot, three-slot, and four-slot two-way relay systems with a single antenna at each node over Rayleigh fading, and

introduces power allocation for each received signal from A and B at R for the three-slot protocol when average transmit SNRs at A and B are sufficiently different (i.e. "unbalanced"). Reference [59] also presents sum-BER and maximum ergodic sum-rate bounds for systems using Alamouti code for the two-slot protocol when multiple antennas are used at A and B while a single antenna is used at R. Performance analysis is carried out for AF two-slot two-way relay systems with BF using a single relay antenna over Nakagami-m fading in [61]. Using multiple antennas at R, meanwhile, BF optimization for only maximum ergodic sum-rate is conducted without performance analysis for AF MIMO two-slot two-way relay systems in [62–64]. *BF optimization* is our term for simultaneous beamforming at R to both A and B. Reference [65] investigates the effects of channel estimation error at A and B for AF MIMO two-way relaying, and provides maximum ergodic sum-rate lower-bounds with imperfect channel state information (CSI) at A and B.

Based on this background, our contributions in this chapter are as follows:

- Novel closed-form sum-BER expressions are presented in a unified framework for AF MIMO two-way relaying protocols with BF.
- This is the first dissertation dealing with performance analysis of AF MIMO two-way relay networks using BF with multiple relay antennas, to the best of our knowledge.
- Two novel two-way relaying protocols are proposed using three or four time slots, and we show that two proposed protocols outperform existing protocols in sum-BER at high-SNR.

- New closed-form high-SNR sum-BER performance is provided in a single expression for five AF MIMO BF two-way relaying protocols. Based on this high-SNR analysis, an analytical high-SNR gap expression between the five different protocols is provided.

After system models are described for the five two-way relaying protocols with a single relay antenna in Section 5.1, unified performance analysis including high-SNR analysis is presented in Section 5.2. Multiple relay antennas are considered in Section 5.3, and BF optimization is discussed in Section 5.4. Numerical and Monte-Carlo simulations compare the performance of five different relaying protocols in Section 5.5. Finally, Section 5.6 summarizes this chapter.

5.1 System Model

Figure 5.1 shows a two-hop MIMO two-way relay system, which consists of two sources, which are also destinations, A and B, and a relay R. All nodes are equipped with multiple antennas, M_A, M_B, and M_R, respectively. $\mathbf{H}_{AR}$, $\mathbf{H}_{BR}$, $\mathbf{H}_{RA}$, and $\mathbf{H}_{RB}$ are $M_R \times M_A$, $M_R \times M_B$, $M_A \times M_R$, and $M_B \times M_R$ statistically independent complex Gaussian channel matrices connecting the nodes, respectively. The channel coefficients are assumed to remain static while A and B exchange their data, and channels are reciprocal in the sense that $\mathbf{H}_{RA} = \mathbf{H}_{AR}^H$ and $\mathbf{H}_{RB} = \mathbf{H}_{BR}^H$, where $(\cdot)^H$ denotes a matrix Hermitian. We assume that transmitters have knowledge only on connected nodes while receivers can access full CSI.

A half-duplex time division multiple access (TDMA) scenario is considered with five different transmission protocols, illustrated in Figure 5.2. The direct links, $A \rightarrow B$ and $B \rightarrow A$, are assumed to be negligible even though

their presence can be incorporated into our analysis. Symbols are transmitted with zero mean and unit variance, and additive noise is independent complex Gaussian with zero mean and unit variance. When multiple antennas are considered at R, BF optimization has to be conducted at R in two-slot and first three-slot protocols. We therefore first consider a single relay antenna to obtain closed-form expressions for all protocols in Section 5.2, and extend this to multiple antennas in Section 5.3. Since system models are well studied in [19, 21, 59–61], we present unified instantaneous received SNR representations for each protocol. Note that when the protocols with different number of slots are compared, transmit power is normalized so that each node uses the same power, and the constellation sizes are chosen so that the rates are fixed as well.

5.1.1 Extension of Existing Protocols

In this subsection, three two-way relaying protocols discussed in [21], where only a single antenna is considered at all nodes, are extended to using multiple antennas with BF at A and B. Note that BF optimization is not necessary even for the two-slot and first three-slot protocols when $M_R = 1$, so that performance analysis in closed-form is tractable.

5.1.1.1 Two-Slot Protocol

In the two-slot protocol, A and B transmit their signals to R using the corresponding matched BF vectors in the first time slot, and R amplifies the added signals and forwards them to A and B in the second time slot [21]. When A and B beamform in the first time slot, they use the *matched* BF vectors, the strongest right singular vectors of $\mathbf{H}_{AR}$ and $\mathbf{H}_{BR}$, denoted by $\mathbf{f}_{AR}$ and $\mathbf{f}_{BR}$, respectively.

5.1.1.2 First Three-Slot Protocol

In the first three-slot protocol, A transmits its signal to R using $\mathbf{f}_{AR}$ in the first time slot; B transmits its signal to R using $\mathbf{f}_{BR}$ in the second time slot; R weighs the received signals from A and B (i.e. with $\alpha \geq 0$ and $\beta \geq 0$ satisfying $\alpha^2 + \beta^2 = 1$), amplifies the added signals, and forwards them to A and B in the third time slot. Coefficients α and β are weights for two received signals from A and B at R, respectively, which can be determined to minimize instantaneous sum-BERs using brute force search [21]. Since there is no closed-form for α and β when instantaneous sum-BER is optimized, α and β can be chosen based on average channel statistics using our high-SNR expressions, as described in Section 5.3.2.1.

5.1.1.3 First Four-Slot Protocol (One-Way Relaying)

In the first four-slot protocol, A transmits its signal to R using $\mathbf{f}_{AR}$ in the first time slot; R amplifies the received signal and forwards it to B in the second time slot; B transmits its signal using $\mathbf{f}_{AR}$ to R in the third time slot; R amplifies the other received signal and forwards it to A in the fourth time slot. Note that transmit power normalization is required due to two transmissions at R (i.e. half of the power used by the two-slot protocol).

5.1.2 Proposed Protocols

In what follows, we propose new relaying protocols for better performance in closed-form.

5.1.2.1 Second Three-Slot Protocol

In the second three-slot protocol, A and B transmit their signals using $\mathbf{f}_{AR}$ and $\mathbf{f}_{BR}$, respectively, to R in the first time slot, R amplifies the received sum and forwards it to A and B in the second and third time slots, consecutively, and both signals are received at A and B. Since R forwards twice, transmit power normalization is required at R. To combine two received signals at the receivers, the minimum mean square error (MMSE) combining scheme is used [42, 43, 45]. Note that there is no need for combining in the existing protocols since there exists only one desired signal for them.

5.1.2.2 Second Four-Slot Protocol

The second four-slot protocol is proposed to obtain better sum-BER by taking advantage of the technique used in the first three-slot protocol, which is weighting two received signals from A and B at R with α and β, respectively. In the second four-slot protocol, A transmits its signal using $\mathbf{f}_{AR}$ to R in the first time slot; B transmits its signal using $\mathbf{f}_{BR}$ to R in the second time slot; R weighs the received signals with coefficients α and β, amplifies the weighted sum and forwards it to A and B in the third and fourth time slots, consecutively. Transmit power normalization is also required at R due to two transmissions. To combine two received signals at A and B, separately, the MMSE combining is used.

5.1.3 Unified SNR Representations for Five Different Protocols for $M_R = 1$

For the aforementioned protocols, after canceling the self-interferences, portions of received signals coming back through R induced by A and B, with

MRC and MMSE combining, the instantaneous received SNRs at A and B can be expressed, respectively, in a unified framework:

$$\gamma_{BRA} = \frac{A_{BRA}\gamma_{BR}\gamma_{RA}}{B_{BRA}\gamma_{BR} + C_{BRA}\gamma_{RA} + 1} \tag{5.1}$$

$$\gamma_{ARB} = \frac{A_{ARB}\gamma_{AR}\gamma_{RB}}{B_{ARB}\gamma_{AR} + C_{ARB}\gamma_{RB} + 1}, \tag{5.2}$$

where $\gamma_{AR} = \rho_{AR}\|\mathbf{h}_{AR}\mathbf{f}_{AR}\|^2$, $\gamma_{BR} = \rho_{BR}\|\mathbf{h}_{BR}\mathbf{f}_{BR}\|^2$, $\gamma_{RA} = \rho_{RA}\|\mathbf{h}_{RA}\|^2$, and $\gamma_{RB} = \rho_{RB}\|\mathbf{h}_{RB}\|^2$; ρ_{AR}, ρ_{BR}, ρ_{RA}, and ρ_{RB} are average transmit SNRs, where we assume $\rho_{RA} = \rho_{RB}$; $\mathbf{h}_{AR}$, $\mathbf{h}_{BR}$, $\mathbf{h}_{RA} = \mathbf{h}_{AR}^H$, and $\mathbf{h}_{RB} = \mathbf{h}_{BR}^H$ are channel coefficient vectors, assumed to be i.i.d. $CN(0,1)$; $\mathbf{f}_{AR}$ and $\mathbf{f}_{BR}$ are BF vectors with norm 1 obtained as $\mathbf{h}_{AR}^H/\|\mathbf{h}_{AR}\|$ and $\mathbf{h}_{BR}^H/\|\mathbf{h}_{BR}\|$, respectively; A_{BRA}, B_{BRA}, C_{BRA}, A_{ARB}, B_{ARB}, and C_{ARB} are non-negative constants in Table 5.1 for all five protocols. These SNR representations will be used to find distributions for performance analysis. We consider removing 1 from equations (5.1) and (5.2) to obtain closed-form sum-BER expressions, denoted respectively as Γ_{BRA} and Γ_{ARB}, which are equivalent to equations (5.1) and (5.2) at high-SNR [21, 66].

Table 5.1: The Coefficients for Equations (5.1) and (5.2) when $M_R = 1$

Constants	A_{BRA}	B_{BRA}	C_{BRA}	A_{ARB}	B_{ARB}	C_{ARB}
2-slot	1	1	$1 + \frac{\rho_{AR}}{\rho_{RA}}$	1	1	$1 + \frac{\rho_{BR}}{\rho_{RB}}$
First 3-slot	β^2	β^2	$1 + \frac{\alpha^2\rho_{AR}}{\rho_{RA}}$	α^2	α^2	$1 + \frac{\beta^2\rho_{BR}}{\rho_{RB}}$
First 4-slot	$\frac{1}{2}$	1	$\frac{1}{2}$	$\frac{1}{2}$	1	$\frac{1}{2}$
Second 3-slot	1	1	$\frac{1}{2} + \frac{\rho_{AR}}{\rho_{RA}}$	1	1	$\frac{1}{2} + \frac{\rho_{BR}}{\rho_{RB}}$
Second 4-slot	β^2	β^2	$\frac{1}{2} + \frac{\alpha^2\rho_{AR}}{\rho_{RA}}$	α^2	α^2	$\frac{1}{2} + \frac{\beta^2\rho_{BR}}{\rho_{RB}}$

5.2 Performance Analysis for $M_R = 1$

Sum-BER performance analysis including high-SNR analysis is carried out using the unified received SNR expressions. The multiple relay antenna case is described in Section 5.3.

5.2.1 Performance Metric

For the performance metric, we consider sum-BER, sum of BERs at A and B, since there are two receiving nodes and the worse one dominates the sum. Sum-BER for all protocols is defined as follows:

$$P_b = \frac{1}{\log_2(M)} \int_0^\infty aQ\left(\sqrt{2bx}\right) \left(f_{\gamma_{ARB}}(x) + f_{\gamma_{BRA}}(x)\right) dx, \tag{5.3}$$

where $Q(x) := \left(1/\sqrt{2\pi}\right) \int_x^\infty e^{-y^2/2} dy$ and a and b are modulation related positive constants. For example, $a = 1$ and $b = 1$ provide exact BER for binary phase shift keying (BPSK), while $a = 2$ and $b = \sin^2(\pi/M)$ and $a = 4\left(1 - 1/\sqrt{M}\right)$ and $b = 3/(2(M-1))$ provide tight SER approximations for M-ary PSK (M-PSK) and M-ary quadrature amplitude modulation (M-QAM), respectively.

5.2.2 Sum-BER using Unified SNR Representations

When cumulative distribution functions (CDFs) are available instead of probability density functions (PDFs), the following alternative equation can be used to calculate sum-BER.

$$\begin{aligned} P_b &= \frac{a\sqrt{b}}{2\sqrt{\pi}\log_2(M)} \int_0^\infty \frac{e^{-bx}}{\sqrt{x}} \left(F_{\gamma_{BRA}}(x) + F_{\gamma_{ARB}}(x)\right) dx \\ &\geq \frac{a\sqrt{b}}{2\sqrt{\pi}\log_2(M)} \int_0^\infty \frac{e^{-bx}}{\sqrt{x}} \left(F_{\Gamma_{BRA}}(x) + F_{\Gamma_{ARB}}(x)\right) dx. \end{aligned} \tag{5.4}$$

Note that the second line of equation (5.4) provides a lower-bound in sum-BER since the CDFs of Γ_{BRA} and Γ_{ARB}, described at the end of Section 5.1.3, are used.

To calculate sum-BER using the unified SNR representations, the distributions of equations (5.1) and (5.2) should be obtained first. Since we use the distributions of Γ_{BRA} and Γ_{ARB}, when we consider Rayleigh fading, the

distributions can be obtained as follows (please see Appendix 5.1 for derivations):

$$F_{\Gamma_{BRA}}(x) = 1 - \sum_{p=0}^{M_B-1} \sum_{k=0}^{M_A+p-1} \binom{M_A+p-1}{k} \frac{2B_{BRA}^{\frac{2M_A+p-k-1}{2}} C_{BRA}^{\frac{k+p+1}{2}}}{A_{BRA}^{M_{A+p}} p!\,(M_A-1)!\rho_{BR}^{\frac{k+p+1}{2}} \rho_{RA}^{\frac{2M_A+p-k-1}{2}}} x^{M_A+p} e^{-\frac{x}{A_{BRA}}\left(\frac{C_{BRA}}{\rho_{BR}}+\frac{B_{BRA}}{\rho_{RA}}\right)} K_{k-p+1}\left(\frac{2x}{A_{BRA}}\sqrt{\frac{B_{BRA}C_{BRA}}{\rho_{BR}\rho_{RA}}}\right), \tag{5.5}$$

$$F_{\Gamma_{ARB}}(x) = 1 - \sum_{p=0}^{M_A-1} \sum_{k=0}^{M_B+p-1} \binom{M_B+p-1}{k} \frac{2B_{ARB}^{\frac{2M_B+p-k-1}{2}} C_{ARB}^{\frac{k+p+1}{2}}}{A_{ARB}^{M_{B+p}} p!\,(M_B-1)!\rho_{AR}^{\frac{k+p+1}{2}} \rho_{RB}^{\frac{2M_B+p-k-1}{2}}} x^{M_B+p} e^{-\frac{x}{A_{ARB}}\left(\frac{C_{ARB}}{\rho_{AR}}+\frac{B_{ARB}}{\rho_{RB}}\right)} K_{k-p+1}\left(\frac{2x}{A_{ARB}}\sqrt{\frac{B_{ARB}C_{ARB}}{\rho_{AR}\rho_{RB}}}\right), \tag{5.6}$$

where $K_\nu(x)$ is the modified Bessel function of the second kind [37].

Since the CDFs of Γ_{BRA} and Γ_{ARB} are available and they are mathematically tractable, the alternative equation, equation (5.4), can be used to calculate sum-BER. As a result, once equations (5.5) and (5.6) are substituted to the second line of equation (5.4), the sum-BER can be lower-bounded in

closed-form as

$$
\begin{aligned}
P_b \geq \frac{a}{\log_2(M)} - \sum_{p=0}^{M_A-1} \sum_{k=0}^{M_B+p-1} \binom{M_B+p-1}{k} \\
\frac{a\sqrt{b} B_{ARB}^{\frac{2M_B+p-k-1}{2}} C_{ARB}^{\frac{k+p+1}{2}}}{\log_2(M) A_{ARB}^{M_B+p} p! \, (M_B-1)! \rho_{AR}^{\frac{k+p+1}{2}} \rho_{RB}^{\frac{2M_B+p-k-1}{2}}} \\
\frac{\left(\frac{4}{A_{ARB}} \sqrt{\frac{B_{ARB} C_{ARB}}{\rho_{AR}\rho_{RB}}}\right)^{k-p+1}}{\left(b + \frac{C_{ARB}}{A_{ARB}\rho_{AR}} + \frac{B_{ARB}}{A_{ARB}\rho_{RB}} + \frac{2}{A_{ARB}} \sqrt{\frac{B_{ARB} C_{ARB}}{\rho_{AR}\rho_{RB}}}\right)^{M_B+k+\frac{3}{2}}} \\
\frac{\Gamma\left(M_B+k+\frac{3}{2}\right) \Gamma\left(M_B+2p-k-\frac{1}{2}\right)}{\Gamma(M_B+p+1)} \\
{}_2F_1\left(M_B+k+\frac{3}{2}, k-p+\frac{3}{2}; M_B+p+1; \right. \\
\left. \frac{b + \frac{C_{ARB}}{A_{ARB}\rho_{AR}} + \frac{B_{ARB}}{A_{ARB}\rho_{RB}} - \frac{2}{A_{ARB}} \sqrt{\frac{B_{ARB} C_{ARB}}{\rho_{AR}\rho_{RB}}}}{b + \frac{C_{ARB}}{A_{ARB}\rho_{AR}} + \frac{B_{ARB}}{A_{ARB}\rho_{RB}} + \frac{2}{A_{ARB}} \sqrt{\frac{B_{ARB} C_{ARB}}{\rho_{AR}\rho_{RB}}}}\right) \\
- \sum_{p=0}^{M_B-1} \sum_{k=0}^{M_A+p-1} \binom{M_A+p-1}{k} \\
\frac{a\sqrt{b} B_{BRA}^{\frac{2M_A+p-k-1}{2}} C_{BRA}^{\frac{k+p+1}{2}}}{\log_2(M) A_{BRA}^{M_A+p} p! \, (M_A-1)! \rho_{BR}^{\frac{k+p+1}{2}} \rho_{RA}^{\frac{2M_A+p-k-1}{2}}} \\
\frac{\left(\frac{4}{A_{BRA}} \sqrt{\frac{B_{BRA} C_{BRA}}{\rho_{BR}\rho_{RA}}}\right)^{k-p+1}}{\left(b + \frac{C_{BRA}}{A_{BRA}\rho_{BR}} + \frac{B_{BRA}}{A_{BRA}\rho_{RA}} + \frac{2}{A_{BRA}} \sqrt{\frac{B_{BRA} C_{BRA}}{\rho_{BR}\rho_{RA}}}\right)^{M_A+k+\frac{3}{2}}} \\
\frac{\Gamma\left(M_A+k+\frac{3}{2}\right) \Gamma\left(M_A+2p-k-\frac{1}{2}\right)}{\Gamma(M_A+p+1)} \\
{}_2F_1\left(M_A+k+\frac{3}{2}, k-p+\frac{3}{2}; M_A+p+1; \right. \\
\left. \frac{b + \frac{C_{BRA}}{A_{BRA}\rho_{BR}} + \frac{B_{BRA}}{A_{BRA}\rho_{RA}} - \frac{2}{A_{BRA}} \sqrt{\frac{B_{BRA} C_{BRA}}{\rho_{BR}\rho_{RA}}}}{b + \frac{C_{BRA}}{A_{BRA}\rho_{BR}} + \frac{B_{BRA}}{A_{BRA}\rho_{RA}} + \frac{2}{A_{BRA}} \sqrt{\frac{B_{BRA} C_{BRA}}{\rho_{BR}\rho_{RA}}}}\right),
\end{aligned}
\tag{5.7}
$$

where ${}_2F_1(\alpha, \beta; \gamma; z)$ is the Gauss hypergeometric function [37, p.1005]. Note that equation (5.7) provides tight sum-BER lower-bounds for all five two-way relay protocols. To obtain equation (5.7), the following integral is used [37,

p.700]:

$$\begin{aligned}&\int_0^\infty x^{\mu-1}e^{-\alpha x}K_\nu(\beta x)dx\\&=\frac{\sqrt{\pi}\,(2\beta)^\nu}{(\alpha+\beta)^{\mu+\nu}}\frac{\Gamma(\mu+\nu)\Gamma(\mu-\nu)}{\Gamma(\mu+\frac{1}{2})}{}_2F_1\left(\mu+\nu,\nu+\frac{1}{2};\mu+\frac{1}{2};\frac{\alpha-\beta}{\alpha+\beta}\right).\end{aligned}\tag{5.8}$$

5.2.3 High-SNR Analysis for Sum-BER using Unified SNR Representations

The expression in equation (5.7) is tight at high SNR, but rather complicated. It can be simplified considerably by diversity and array gain analysis. Simple high-SNR performance is now considered to further simplify equation (5.7). The approximation uses the probability density functions (PDFs) of instantaneous SNRs normalized by the average SNR on each link defined as $\lambda_{ARB} := \Gamma_{ARB}/\rho_{AR}$ and $\lambda_{BRA} := \Gamma_{BRA}/\rho_{AR}$ where ρ_{AR} is the average transmit SNR from A to R, and both PDFs are shown satisfying the assumptions in [34], which provides a systematic method for high-SNR analysis. To simplify our analysis, we assume that ρ_{BR}, ρ_{RA}, and ρ_{RB} are constant multiples of ρ_{AR}. Based on [34, eqn.(1)], the average sum-BER of an uncoded system can be written as

$$\begin{aligned}P_b=&\frac{1}{\log_2(M)}\left((2b\rho_{AR}G_{ARB})^{-d_{ARB}}+(2b\rho_{AR}G_{BRA})^{-d_{BRA}}\right)\\&+o\left(\rho_{AR}^{-\min\{d_{ARB},d_{BRA}\}}\right),\end{aligned}\tag{5.9}$$

as $\rho_{AR}\to\infty$, where $d_{ARB}=t_{ARB}+1$ and $d_{BRA}=t_{BRA}+1$ are the diversity orders; t_{ARB} and t_{BRA} are the first nonzero derivative orders of the PDFs of channel dependent random variables, λ_{ARB} and λ_{BRA}, at the origin, respectively; $G_{ARB}=\left(\sqrt{\pi}\,(t_{ARB}+1)\,/\,(a2^{t_{ARB}}\eta_{ARB}\Gamma\,(t_{ARB}+3/2))\right)^{1/(t_{ARB}+1)}$ and $G_{BRA}=\left(\sqrt{\pi}\,(t_{BRA}+1)\,/\,(a2^{t_{BRA}}\eta_{BRA}\Gamma\,(t_{BRA}+3/2))\right)^{1/(t_{BRA}+1)}$ are the array gains; $\eta_{ARB}=f_{\lambda_{ARB}}^{(t_{ARB})}(0)/\Gamma\,(t_{ARB}+1)\neq 0$ and $\eta_{BRA}=f_{\lambda_{BRA}}^{(t_{BRA})}(0)/\Gamma\,(t_{BRA}+1)\neq 0$. The expression for η_{ARB} and η_{BRA} are also valid when t_{ARB} and t_{BRA} are not integers if fractional calculus is used [55]. Therefore, equation (5.9)

can be calculated once t_{ARB}, t_{BRA}, η_{ARB}, and η_{BRA} are found using the PDFs of λ_{ARB} and λ_{BRA}.

For the $A \to R \to B$ path, $t_{ARB} = \min\{M_A, M_B\} - 1$ since the diversity order of the $A \to R \to B$ path is $\min\{M_A, M_B\}$ [45, eqn.(16)]. The t_{ARB} order derivative of the PDF of λ_{ARB} evaluated at the origin can be obtained as (please see Appendix 5.2 for derivation)

$$f_{\lambda_{ARB}}^{(t_{ARB})}(0) = \begin{cases} f_{\lambda_{RB}}^{(t_{RB})}(0), & M_A > M_B \\ f_{\lambda_{AR}}^{(t_{AR})}(0), & M_A < M_B \\ f_{\lambda_{AR}}^{(t_{AR})}(0) + f_{\lambda_{RB}}^{(t_{RB})}(0), & M_A = M_B \end{cases}, \tag{5.10}$$

where $t_{AR} = M_A - 1$ and $t_{RB} = M_B - 1$ [45, eqn.(12)] are the first nonzero derivative orders of the PDFs of $\lambda_{AR} := \gamma_{AR}/\rho_{AR}$ and $\lambda_{RB} := \gamma_{RB}/\rho_{AR}$, at the origin, respectively;

$$f_{\lambda_{AR}}^{(t_{AR})}(0) = \left(\frac{C_{ARB}}{A_{ARB}}\right)^{t_{AR}+1} \tag{5.11}$$

$$f_{\lambda_{RB}}^{(t_{RB})}(0) = \left(\frac{B_{ARB}\rho_{AR}}{A_{ARB}\rho_{RB}}\right)^{t_{RB}+1}. \tag{5.12}$$

Therefore, η_{ARB} can be written as

$$\eta_{ARB} = \frac{f_{\lambda_{ARB}}^{(t_{ARB})}(0)}{\Gamma\left(\min\{M_A, M_B\}\right)}. \tag{5.13}$$

Similarly, for the $B \to R \to A$ path, $t_{BRA} = \min\{M_A, M_B\} - 1$ since the diversity order of the $B \to R \to A$ path is $\min\{M_A, M_B\}$. The t_{BRA} order derivative of the PDF of λ_{BRA} evaluated at the origin can be obtained as (please see Appendix 5.2 for derivation)

$$f_{\lambda_{BRA}}^{(t_{BRA})}(0) = \begin{cases} f_{\lambda_{BR}}^{(t_{BR})}(0), & M_A > M_B \\ f_{\lambda_{RA}}^{(t_{RA})}(0), & M_A < M_B \\ f_{\lambda_{BR}}^{(t_{BR})}(0) + f_{\lambda_{RA}}^{(t_{RA})}(0), & M_A = M_B \end{cases}, \tag{5.14}$$

where $t_{BR} = M_B - 1$, $t_{RA} = M_A - 1$ [45, eqn.(12)] are the first nonzero derivative orders of the PDFs of $\lambda_{BR} := \gamma_{BR}/\rho_{AR}$ and $\lambda_{RA} := \gamma_{RA}/\rho_{AR}$, at the origin, respectively;

$$f_{\lambda_{BR}}^{(t_{BR})}(0) = \left(\frac{C_{BRA}\rho_{AR}}{A_{BRA}\rho_{BR}}\right)^{t_{BR}+1} \tag{5.15}$$

$$f_{\lambda_{RA}}^{(t_{RA})}(0) = \left(\frac{B_{BRA}\rho_{AR}}{A_{BRA}\rho_{RA}}\right)^{t_{RA}+1}. \tag{5.16}$$

Therefore, η_{BRA} can be written as

$$\eta_{BRA} = \frac{f_{\lambda_{BRA}}^{(t_{BRA})}(0)}{\Gamma\left(\min\{M_A, M_B\}\right)}. \tag{5.17}$$

As a consequence, high-SNR performance can be obtained as follows:

$$P_b = \frac{1}{\log_2(M)}\left((2b\rho_{AR}G_{ARB})^{-d} + (2b\rho_{AR}G_{BRA})^{-d}\right) + o\left(\rho_{AR}^{-d}\right) \tag{5.18}$$

$$d = \min\{M_A, M_B\} \tag{5.19}$$

$$G_{ARB} = \left(\frac{a2^{d-1}\eta_{ARB}\Gamma\left(d+\frac{1}{2}\right)}{\sqrt{\pi}d}\right)^{-\frac{1}{d}} \tag{5.20}$$

$$G_{BRA} = \left(\frac{a2^{d-1}\eta_{BRA}\Gamma\left(d+\frac{1}{2}\right)}{\sqrt{\pi}d}\right)^{-\frac{1}{d}}. \tag{5.21}$$

High-SNR performance for sum-BER given in equations (5.18)-(5.21) is much simpler than the closed-form lower-bounds in equation (5.7) so that it is easy to evaluate sum-BER at high-SNR. Note that the diversity order of all five two-way relay systems is $\min\{M_A, M_B\}$, and equations (5.18)-(5.21) provide tight sum-BER lower-bounds for all five two-way relay protocols.

5.3 Multiple Antennas at R

When we consider multiple antennas at R, BF optimization at R is necessary for the two-slot and first three-slot protocols. In this case, there is no closed-form expression for performance analysis since optimal beamformers cannot be expressed in closed-form. Meanwhile, since BF optimization is

not necessary for the second three-slot, first four-slot, and second four-slot protocols, performance analysis with multiple relay antennas can be done with unified received SNRs when $M_R > 1$, which can be represented by equations (5.1) and (5.2) with the constants in Table 5.2. Note that this analysis is also applicable for the two-slot and first three-slot protocols as unattainable lower-bounds of BF optimization since two different BF vectors matched with corresponding channels are used at R to achieve the lower-bounds.

Table 5.2: The Coefficients for Equations (5.1) and (5.2) when $M_R > 1$

Constants	A_{BRA}	B_{BRA}	C_{BRA}	A_{ARB}	B_{ARB}	C_{ARB}
2-slot	1	1	$1+\frac{\rho_{AR}}{\rho_{RA}}$	1	1	$1+\frac{\rho_{BR}}{\rho_{RB}}$
First 3-slot	β^2	β^2	$1+\frac{\alpha^2\rho_{AR}}{\rho_{RA}}$	α^2	α^2	$1+\frac{\beta^2\rho_{BR}}{\rho_{RB}}$
First 4-slot	$\frac{1}{2}$	1	$\frac{1}{2}$	$\frac{1}{2}$	1	$\frac{1}{2}$
Second 3-slot	$\frac{D_{BRA,3}}{2}$	1	$\frac{1}{2}+\frac{\rho_{AR}}{\rho_{RA}}$	$\frac{D_{ARB,3}}{2}$	1	$\frac{1}{2}+\frac{\rho_{BR}}{\rho_{RB}}$
Second 4-slot	$\frac{\beta^2 D_{BRA,4}}{2}$	β^2	$\frac{1}{2}+\frac{\alpha^2\rho_{AR}}{\rho_{RA}}$	$\frac{\alpha^2 D_{ARB,4}}{2}$	α^2	$\frac{1}{2}+\frac{\beta^2\rho_{BR}}{\rho_{RB}}$

In Table 5.2, all values are exact except those denoted by $D_{ARB,3}$, $D_{BRA,3}$, $D_{ARB,4}$, and $D_{BRA,4}$, which are approximations. To clarify how the approximations in Table 5.2 can be obtained, the instantaneous received SNRs are discussed for the second three-slot protocol as an example. The instantaneous received SNRs for the second three-slot protocol at A and B are as follows:

$$\gamma_{BRA} = \gamma_{BRA,1} + \gamma_{BRA,2} = \frac{\gamma_{BR}\frac{\gamma_{RA}}{2}}{\gamma_{BR}+\gamma_{AR}+\frac{\gamma_{RA}}{2}+1} + \frac{\gamma_{BR}\frac{\gamma'_{RA}}{2}}{\gamma_{BR}+\gamma_{AR}+\frac{\gamma'_{RA}}{2}+1} \tag{5.22}$$

$$\gamma_{ARB} = \gamma_{ARB,1} + \gamma_{ARB,2} = \frac{\gamma_{AR}\frac{\gamma_{RB}}{2}}{\gamma_{AR}+\gamma_{BR}+\frac{\gamma_{RB}}{2}+1} + \frac{\gamma_{AR}\frac{\gamma'_{RB}}{2}}{\gamma_{AR}+\gamma_{BR}+\frac{\gamma'_{RB}}{2}+1}, \tag{5.23}$$

where $\gamma'_{RA} = \rho_{RA}\|\mathbf{H}_{RA}\mathbf{f}_{RB}\|^2$ and $\gamma'_{RB} = \rho_{RB}\|\mathbf{H}_{RB}\mathbf{f}_{RA}\|^2$, which are instantaneous received SNRs with *non-matched* BF vectors. Since $\gamma_{BRA,1}$ and $\gamma_{BRA,2}$ in equation (5.22) are correlated and $\gamma_{BRA,1}$ dominates $\gamma_{BRA,2}$, we approximate $\gamma_{BRA,2}$ with $\kappa\gamma_{BRA,1}$ where $\kappa := \mathbb{E}[\gamma_{BRA,2}]/\mathbb{E}[\gamma_{BRA,1}]$, so that the average values are the same: $\mathbb{E}[\gamma_{BRA,2}] = \mathbb{E}[\kappa\gamma_{BRA,1}]$. Here $0 < \kappa < 1$ since

γ_{RA} is the instantaneous SNR obtained by matched BF, whereas γ'_{RA} results when BF is not matched. This approximation is exact if $\gamma_{BRA,2}$ were a constant multiple of $\gamma_{BRA,1}$. It becomes tighter as M_R increases because κ becomes smaller as M_R increases, but it is independent of average transmit SNRs, M_A, and M_B since they do not have any effect on κ, which is checked with numerical investigations. Therefore, $\gamma_{BRA,2}$ can be absorbed in A_{BRA} as in Table 5.2, $D_{BRA,3} = 1 + \mathbb{E}[\gamma_{BRA,2}]/\mathbb{E}[\gamma_{BRA,1}]$. Note that $D_{BRA,3}$ and $D_{ARB,3} = 1 + \mathbb{E}[\gamma_{ARB,2}]/\mathbb{E}[\gamma_{ARB,1}]$ provide exact performance when $M_R = 1$ such as equations (5.7) and (5.18), and they also present a tight performance lower-bound even when $M_R > 1$, which becomes tighter as M_R increases. Similarly, $D_{ARB,4}$ and $D_{BRA,4}$ can be obtained for the second four-slot protocol.

5.3.1 Performance Analysis

We now consider performance analysis using the unified received SNRs when $M_R > 1$. Similar to obtaining equation (5.7) when $M_R = 1$, the distributions of the unified received SNRs for multiple relay antennas should be attained to calculate sum-BER for $M_R > 1$. The CDFs of Γ_{BRA} and Γ_{ARB} can be obtained as follows (please see Appendix 5.1 for derivations):

$$
\begin{aligned}
F_{\Gamma_{BRA}}(x) = 1 - \sum_{n=1}^{M_R} \sum_{m=M_B-M_R}^{(M_B+M_R)n-2n^2} \sum_{k=0}^{m} \sum_{i=1}^{M_R} \sum_{j=M_A-M_R}^{(M_A+M_R)i-2i^2} \sum_{p=0}^{k+j} \binom{k+j}{p} \\
\frac{2 d_{n,m} d_{i,j}}{k! j! \rho_{BR}^{\frac{p+k+1}{2}} \rho_R^{\frac{2j+k-p+1}{2}}} \frac{(C_{BRA} n)^{\frac{p+k+1}{2}} (B_{BRA} i)^{\frac{2j+k-p+1}{2}}}{A_{BRA}^{k+j+1}} \\
x^{k+j+1} e^{-\frac{x}{A_{BRA}} \left(\frac{C_{BRA} n}{\rho_{BR}} + \frac{B_{BRA} i}{\rho_R} \right)} K_{p-k+1} \left(\frac{2x}{A_{BRA}} \sqrt{\frac{B_{BRA} C_{BRA} n i}{\rho_{BR} \rho_R}} \right)
\end{aligned}
\tag{5.24}
$$

$$F_{\Gamma_{ARB}}(x) = 1 - \sum_{n=1}^{M_R} \sum_{m=M_A-M_R}^{(M_A+M_R)n-2n^2} \sum_{k=0}^{m} \sum_{i=1}^{M_R} \sum_{j=M_B-M_R}^{(M_B+M_R)i-2i^2} \sum_{p=0}^{k+j} \binom{k+j}{p}$$
$$\frac{2d_{n,m}d_{i,j}}{k!j!\rho_{AR}^{\frac{p+k+1}{2}}\rho_R^{\frac{2j+k-p+1}{2}}} \frac{(C_{ARB}n)^{\frac{p+k+1}{2}}(B_{ARB}i)^{\frac{2j+k-p+1}{2}}}{A_{ARB}^{k+j+1}} \tag{5.25}$$
$$x^{k+j+1}e^{-\frac{x}{A_{ARB}}\left(\frac{C_{ARB}n}{\rho_{AR}}+\frac{B_{ARB}i}{\rho_R}\right)} K_{p-k+1}\left(\frac{2x}{A_{ARB}}\sqrt{\frac{B_{ARB}C_{ARB}ni}{\rho_{AR}\rho_R}}\right),$$

where $d_{n,m}$ are coefficients given by [30, eqn.(24)], also provided in Tables 2.1-2.3 for completeness. Note that equations (5.24) and (5.25) are valid when $M_A \geq M_R$ and $M_B \geq M_R$ even though other cases can be easily handled with minor modifications. For example, M_A and M_R must be switched in equations (5.24) and (5.25) when $M_A < M_R$. Once equations (5.24) and (5.25) are substituted to the second line of equation (5.4), the sum-BER can be obtained in closed-form similar to equation (5.7), which are tight sum-BER lower-bounds for the first four-slot, second three-slot, and second four-slot protocols.

5.3.2 High-SNR Analysis

Based on the procedures in Section 5.2.3, we should calculate the t_{ARB} order derivative of the PDF of λ_{ARB} evaluated at the origin and the t_{BRA} order derivative of the PDF of λ_{BRA} evaluated at the origin to obtain high-SNR performance when $M_R > 1$. For each path, $t_{ARB} = t_{BRA} = M_R \cdot \min\{M_A, M_B\} - 1$ since the diversity order of the $A \rightarrow R \rightarrow B$ and $B \rightarrow R \rightarrow A$ paths is $M_R \cdot \min\{M_A, M_B\}$ [45, eqn.(16)]. Therefore, the t_{ARB} and t_{BRA} order derivatives of the PDFs of λ_{ARB} and λ_{BRA} evaluated at the origin, respectively, can be obtained using the following equations (please see Appendix 5.2 for derivation):

$$f_{\lambda_{AR}}^{(t_{AR})}(0) = \sum_{n=1}^{M_R} \sum_{m=M_A-M_R}^{(M_A+M_R)n-2n^2} d_{n,m}\binom{t_{AR}}{m}(-1)^{t_{AR}+m}\left(\frac{nC_{ARB}}{A_{ARB}}\right)^{t_{AR}+1} \tag{5.26}$$

$$f_{\lambda_{RB}}^{(t_{RB})}(0) = \sum_{n=1}^{M_R} \sum_{m=M_B-M_R}^{(M_B+M_R)n-2n^2} d_{n,m} \binom{t_{RB}}{m} (-1)^{t_{RB}+m} \left(\frac{n\rho_{AR} B_{ARB}}{A_{ARB}\rho_R} \right)^{t_{RB}+1} \quad (5.27)$$

$$f_{\lambda_{BR}}^{(t_{BR})}(0) = \sum_{n=1}^{M_R} \sum_{m=M_B-M_R}^{(M_B+M_R)n-2n^2} d_{n,m} \binom{t_{BR}}{m} (-1)^{t_{BR}+m} \left(\frac{n\rho_{AR} C_{BRA}}{A_{BRA}\rho_{BR}} \right)^{t_{BR}+1} \quad (5.28)$$

$$f_{\lambda_{RA}}^{(t_{RA})}(0) = \sum_{n=1}^{M_R} \sum_{m=M_A-M_R}^{(M_A+M_R)n-2n^2} d_{n,m} \binom{t_{RA}}{m} (-1)^{t_{RA}+m} \left(\frac{n\rho_{AR} B_{BRA}}{A_{BRA}\rho_R} \right)^{t_{RA}+1}, \quad (5.29)$$

where $t_{AR} = t_{RA} = M_A \cdot M_R - 1$ and $t_{BR} = t_{RB} = M_B \cdot M_R - 1$ [45, eqn.(12)]. Once equations (5.26)-(5.29) are substituted into equations (5.10) and (5.14), the resulting high-SNR performance using equations (5.18)-(5.21) and $d = M_R \cdot \min\{M_A, M_B\}$ can provide tight sum-BER lower-bounds for the second three-slot, first four-slot, and second four-slot protocols.

5.3.2.1 α-β Optimization

Following [21], it is possible determine the weighting coefficients, α and β, for the first three-slot and second four-slot protocols to minimize instantaneous sum-BERs using brute force search, which is not tractable in closed-form. However, since we are interested in high-SNR performance, we can obtain closed-form expressions using average high-SNR performance in equation (5.18), especially when $M_A = M_B = M_R = 1$ as a special case. After every variable is substituted into equation (5.18) and considering $\alpha^2 + \beta^2 = 1$, by differentiating equation (5.18) with respect to β, optimal βs for the first three-slot and second four-slot protocols can be obtained, respectively, as follows:

$$\beta_{three-slot}^2 = \frac{\sqrt{\frac{\rho_{AR}(\rho_{AR}+\rho_{RA})}{\rho_{RA}}}}{\sqrt{\frac{\rho_{AR}(\rho_{AR}+\rho_{RA})}{\rho_{RA}}} + \sqrt{\frac{\rho_{BR}(\rho_{BR}+\rho_{RB})}{\rho_{RB}}}} \quad (5.30)$$

$$\beta_{four-slot}^2 = \frac{\sqrt{\frac{\rho_{AR}(\rho_{AR}+\rho_{RA}/2)}{\rho_{RA}/2}}}{\sqrt{\frac{\rho_{AR}(\rho_{AR}+\rho_{RA}/2)}{\rho_{RA}/2}} + \sqrt{\frac{\rho_{BR}(\rho_{BR}+\rho_{RB}/2)}{\rho_{RB}/2}}} \quad (5.31)$$

Both β^2s become $\frac{1}{2}$ when $\rho_{AR} = \rho_{BR} = \rho_{RA} = \rho_{RB}$, while β^2s are bigger than $\frac{1}{2}$ when $\rho_{AR} > \rho_{BR}$, which indicates the α-β optimization is most useful when ρ_{AR} and ρ_{BR} are unbalanced. Note that these results are from average high-SNR performance, which leads to worse performance compared with numerically optimizing the instantaneous sum-BERs with respect to β. However, equations (5.30) and (5.31) do not require instantaneous channel knowledge and can be expressed in closed-form. Note that an implicit equation for optimal β is available even when multiple antennas are considered at all nodes.

5.3.2.2 Analytical Gap among Protocols at High-SNR

We now provide analytical gaps in average SNR for equal P_b between the five protocols at high-SNR. When we compare performance between two protocols, let us denote i and j for worse and better protocols in sum-BER, respectively, to make analytical gaps non-negative. Once i and j for each protocol are applied to equation (5.18) and their difference in dB is considered, the analytical gap expression can be obtained as follows:

$$\begin{aligned} 10\log_{10}\left(\frac{\rho_{AR}^{i}}{\rho_{AR}^{j}}\right) &= 10\log_{10}\left(\frac{b^j \log_2\left(M^j\right)}{b^i \log_2\left(M^i\right)}\right) \\ &\quad + \frac{10}{d}\log_{10}\left(\frac{a^i \log_2\left(M^j\right)\left(\eta_{ARB}^{i} + \eta_{BRA}^{i}\right)}{a^j \log_2\left(M^i\right)\left(\eta_{ARB}^{j} + \eta_{BRA}^{j}\right)}\right). \end{aligned} \tag{5.32}$$

Based on equation (5.32), we recognize that the analytical gap between protocols i and j depends on choice of modulation (i.e. a, b, and M), diversity order d, and average transmit SNRs and constants from Tables 5.1 and 5.2 in which need to be substituted to compute η_{ARB} and η_{BRA}.

Note that we use QPSK, 8-QAM, and 16-QAM for the two-slot, three-slot, and four-slot protocols, respectively, for rate normalization. Therefore, since a, b and M are fixed for all protocols, the analytical gap is mainly determined by the diversity order and the ratio of η_{ARB} and η_{BRA} from equations

(5.10)-(5.21) as follows:

$$\frac{\eta^i_{ARB}+\eta^i_{BRA}}{\eta^j_{ARB}+\eta^j_{BRA}}=\frac{\left(\frac{B^i_{ARB}\rho^i_{AR}}{A^i_{ARB}\rho^i_{RB}}\right)^d+\left(\frac{C^i_{ARB}}{A^i_{ARB}}\right)^d+\left(\frac{C^i_{BRA}\rho^i_{AR}}{A^i_{BRA}\rho^i_{BR}}\right)^d+\left(\frac{B^i_{BRA}\rho^i_{AR}}{A^i_{BRA}\rho^i_{RA}}\right)^d}{\left(\frac{B^j_{ARB}\rho^j_{AR}}{A^j_{ARB}\rho^j_{RB}}\right)^d+\left(\frac{C^j_{ARB}}{A^j_{ARB}}\right)^d+\left(\frac{C^j_{BRA}\rho^j_{AR}}{A^j_{BRA}\rho^j_{BR}}\right)^d+\left(\frac{B^j_{BRA}\rho^j_{AR}}{A^j_{BRA}\rho^j_{RA}}\right)^d}. \tag{5.33}$$

Therefore, the balance between ρ_{AR} and ρ_{BR} and the balance between M_A and M_B have an impact on the gap.

For example, when $\rho_{AR}=\rho_{BR}$ (i.e. balanced), the gap remains the same unless the diversity order is changed. Therefore, if M_A is fixed, the gap increases as M_B increases until M_B reaches to M_A, but it remains the same even though M_B increases after $M_A=M_B$ due to $d=M_R\cdot\min\{M_A,M_B\}$. If $\rho_{AR}\neq\rho_{BR}$ (i.e. unbalanced), α and β in η_{ARB} and η_{BRA} play important roles on the gap. When the second four-slot protocol with α-β optimization is compared with other protocols, if $\rho_{AR}>\rho_{BR}$ with $M_A=M_B$, the gap increases as ρ_{AR} increases due to the benefit of α-β optimization. However, since $\beta^2\approx 0$ when $M_A<M_B$ regardless of ρ_{AR} and ρ_{BR}, the combination of $\rho_{AR}>\rho_{BR}$ and $M_A<M_B$ removes an advantage of the α-β optimization, so that other protocols have better performance than the second four-slot protocol in this case. Therefore, the α-β optimization can be useful when $\rho_{AR}\neq\rho_{BR}$ with careful consideration of M_A and M_B.

5.4 BF Optimization

Since BF optimization is required in the two-slot and first three-slot schemes, BF optimization is discussed in this section. From the literature in [31, 63, 64], BF optimization does not seem to have an analytical solution, so we take use of relatively simple numerical methods to obtain sum-BER when BF optimization is necessary.

5.4.1 Gradient BF Optimization

For the first three-slot protocol, we should optimize only a BF vector at R suitable to both A and B for the third time slot since two separate signals are received at R in the first two time slots. Therefore, gradient BF optimization can be used for the first three-slot protocol due to its simplicity. For sum-BER, the following optimization expression can be found to obtain the optimal BF vector $\mathbf{f}_R^\star$ at R.

$$\text{minimize} \quad \left[Q\left(\sqrt{2b\gamma_{ARB}}\right) + Q\left(\sqrt{2b\gamma_{BRA}}\right)\right], \tag{5.34}$$

where

$$\gamma_{ARB} = \frac{A_{ARB}\gamma_{AR}\rho_R\|\mathbf{H}_{RB}\mathbf{f}_R\|^2}{B_{ARB}\gamma_{AR}\|\mathbf{f}_R\|^2 + \beta^2\gamma_{BR}\|\mathbf{f}_R\|^2 + \rho_R\|\mathbf{H}_{RB}\mathbf{f}_R\|^2 + \|\mathbf{f}_R\|^2}, \tag{5.35}$$

$$\gamma_{BRA} = \frac{A_{BRA}\gamma_{BR}\rho_R\|\mathbf{H}_{RA}\mathbf{f}_R\|^2}{B_{BRA}\gamma_{BR}\|\mathbf{f}_R\|^2 + \alpha^2\gamma_{AR}\|\mathbf{f}_R\|^2 + \rho_R\|\mathbf{H}_{RA}\mathbf{f}_R\|^2 + \|\mathbf{f}_R\|^2}, \tag{5.36}$$

$\rho_R := \rho_{RA} = \rho_{RB}$, and $\mathbf{f}_R$ is the complex valued optimization variable. The above non-constraint optimization problem can be solved numerically for $\mathbf{f}_R$ using the following gradient with proper line search.

$$\nabla_{\mathbf{f}_R} f(\mathbf{f}_R) = -\frac{\sqrt{b}e^{-b\gamma_{ARB}}\nabla_{\mathbf{f}_R}\gamma_{ARB}}{2\sqrt{\pi\gamma_{ARB}}} - \frac{\sqrt{b}e^{-b\gamma_{BRA}}\nabla_{\mathbf{f}_R}\gamma_{BRA}}{2\sqrt{\pi\gamma_{BRA}}}, \tag{5.37}$$

where $f(\mathbf{f}_R) = Q\left(\sqrt{2b\gamma_{ARB}}\right) + Q\left(\sqrt{2b\gamma_{BRA}}\right)$. The gradient algorithm works as described in **Algorithm 5.1**. From the algorithm, ι and ζ can be chosen as real values between 0 and 1, and t can be chosen as a positive integer. Grassmannian vectors can be obtained from the online reference [36] based on the number of antenna elements. ϵ can be an arbitrary small number (i.e. 0.001), but it should be chosen carefully since the number of iterations in the algorithm depends on $1/\epsilon$. Since the gradient algorithm finds local extreme values based on initial points, we try to find a global extreme value based on as many local extreme values as the number of given Grassmannian vectors.

Algorithm 5.1 Gradient Algorithm for BF Optimization

Given $A_{\mathrm{ARB}}, A_{\mathrm{BRA}}, B_{\mathrm{ARB}}, B_{\mathrm{BRA}}, \mathbf{H}_{\mathrm{RA}}, \mathbf{H}_{\mathrm{RB}}, \rho_{\mathrm{R}}, \gamma_{\mathrm{AR}}, \gamma_{\mathrm{BR}}$
Choose proper line search parameters ι, ζ, t, and ϵ
Initialize f_{R} with the first element of Grassmannian vectors
while Grassmannian vectors exist **do**
  Calculate $\nabla_{\mathrm{f_R}} f$ and $\|\nabla_{\mathrm{f_R}} f\|$
  while $\|\nabla_{\mathrm{f_R}} f\| > \epsilon$ **do**
    $\mathrm{f}_{\mathrm{R}} \leftarrow \mathrm{f}_{\mathrm{R}} - t\nabla_{\mathrm{f_R}} f$
    Calculate new f
    while New $f > f - \iota t\|\nabla_{\mathrm{f_R}} f\|^2$ **do**
      $t \leftarrow \zeta t$
      $\mathrm{f}_{\mathrm{R}} \leftarrow \mathrm{f}_{\mathrm{R}} - t\nabla_{\mathrm{f_R}} f$
      Calculate new f
    end while
    Calculate new $\nabla_{\mathrm{f_R}} f$ and $\|\nabla_{\mathrm{f_R}} f\|$
  end while
  Choose f_{R} maximizing f
end while

Algorithm 5.2 Iterative MSMSE Algorithm for BF Optimization

Given $\mathbf{H}_{\mathrm{AR}}, \mathbf{H}_{\mathrm{BR}}, \rho_{\mathrm{AR}}, \rho_{\mathrm{BR}}$, and ρ_{R}
Initialize f_{AR}, f_{BR}, c_{AR}, c_{BR}, $\mathbf{W}$, λ, and ITER
while AMSE $\geq \epsilon$ and $\mathrm{t} \leq$ ITER **do**
  $\mathrm{c}_{\mathrm{AR},t} \leftarrow \left[\kappa^2 \mathbf{H}_{\mathrm{AR}}^H \mathbf{W}_{t-1} \mathbf{W}_{t-1}^H \mathbf{H}_{\mathrm{AR}} + \mathbf{I}_{M_{\mathrm{A}}}\right]^{-1} \rho_{\mathrm{BR}} \kappa \mathbf{H}_{\mathrm{AR}}^H \mathbf{W}_{t-1} \mathbf{H}_{\mathrm{BR}} \mathrm{f}_{\mathrm{BR},t-1}$
  $\mathrm{c}_{\mathrm{BR},t} \leftarrow \left[\kappa^2 \mathbf{H}_{\mathrm{BR}}^H \mathbf{W}_{t-1} \mathbf{W}_{t-1}^H \mathbf{H}_{\mathrm{BR}} + \mathbf{I}_{M_{\mathrm{B}}}\right]^{-1} \rho_{\mathrm{AR}} \kappa \mathbf{H}_{\mathrm{BR}}^H \mathbf{W}_{t-1} \mathbf{H}_{\mathrm{AR}} \mathrm{f}_{\mathrm{AR},t-1}$
  $\mathrm{f}_{\mathrm{AR},t} \leftarrow \rho_{\mathrm{AR}} \kappa \mathbf{H}_{\mathrm{AR}}^H \mathbf{W}_{t-1}^H \mathbf{H}_{\mathrm{BR}} \mathrm{c}_{\mathrm{BR},t}$
  $\mathrm{f}_{\mathrm{BR},t} \leftarrow \rho_{\mathrm{BR}} \kappa \mathbf{H}_{\mathrm{BR}}^H \mathbf{W}_{t-1}^H \mathbf{H}_{\mathrm{AR}} \mathrm{c}_{\mathrm{AR},t}$
  while WMSE $\geq \epsilon$ and $\mathrm{u} \leq$ ITER **do**
    $\lambda_u \leftarrow \mathrm{tr}\left\{\mathbf{W}_{u-1}\mathbf{V} - \mathbf{W}_{u-1}\mathbf{A}\mathbf{W}_{u-1}^H\mathbf{B} - \mathbf{W}_{u-1}\mathbf{C}\mathbf{W}_{u-1}^H\mathbf{D} - \mathbf{W}_{u-1}\mathbf{W}_{u-1}^H(\mathbf{B}+\mathbf{D})\right\}$
    $\mathrm{vec}(\mathbf{W}_u) \leftarrow \left[\mathbf{B}^T \otimes \mathbf{A} + \mathbf{D}^T \otimes \mathbf{C} + (\mathbf{B}+\mathbf{D})^T \otimes \mathbf{I}_{M_{\mathrm{R}}} + \lambda_u\right]^{-1} \mathrm{vec}(\mathbf{V})$
    WMSE $\leftarrow \|\mathbf{W}_u - \mathbf{W}_{u-1}\|_F^2$
    $u \leftarrow u+1$
  end while
  $\mathbf{W}_t \leftarrow \mathbf{W}_{u-1}$
  AMSE $\leftarrow \|\mathrm{f}_{\mathrm{AR},t} - \mathrm{f}_{\mathrm{AR},t-1}\|^2 + \|\mathrm{f}_{\mathrm{BR},t} - \mathrm{f}_{\mathrm{BR},t-1}\|^2 + \|\mathrm{c}_{\mathrm{AR},t} - \mathrm{c}_{\mathrm{AR},t-1}\|^2 + \|\mathrm{c}_{\mathrm{BR},t} - \mathrm{c}_{\mathrm{BR},t-1}\|^2 + \|\mathbf{W}_t - \mathbf{W}_{t-1}\|_F^2$
  $t \leftarrow t+1$
end while

5.4.2 Iterative MSMSE BF Optimization

Meanwhile, for the two-slot protocol, we should jointly optimize BF and combining vectors at A, B and R, respectively, since two signals are received simultaneously at R in the first time slot. In this chapter, iterative minimum sum-MSE (MSMSE) BF optimization is used for the two-slot protocol, which is a combination of MSMSE algorithm in [62] and iterating algorithm in [63]. For sum-BER, since we assume that optimal $\mathbf{f}_{AR}$ and $\mathbf{f}_{BR}$ can be obtained as matched filters and optimal $\mathbf{c}_{AR}$ and $\mathbf{c}_{BR}$ can be obtained as MMSE filters, the following non-convex optimization problem can be used to obtain the optimal $\mathbf{W}$ at R (please see Appendix 5.3 for details).

$$\begin{aligned} \text{minimize} \quad & \operatorname{tr}\left\{\mathbb{E}\left[\left(y_{BRA}-\sqrt{\rho_{BR}}x_B\right)\left(y_{BRA}-\sqrt{\rho_{BR}}x_B\right)^H\right]\right\} \\ & +\operatorname{tr}\left\{\mathbb{E}\left[\left(y_{ARB}-\sqrt{\rho_{AR}}x_A\right)\left(y_{ARB}-\sqrt{\rho_{AR}}x_A\right)^H\right]\right\} \\ \text{subject to} \quad & \operatorname{tr}\left\{\mathbf{W}\mathbf{W}^H\right\}\leq 1, \end{aligned} \tag{5.38}$$

where

$$y_{BRA}=\sqrt{\rho_{BR}}\kappa\mathbf{c}_{AR}^H\mathbf{H}_{AR}^H\mathbf{W}\mathbf{H}_{BR}\mathbf{f}_{BR}x_B+\kappa\mathbf{c}_{AR}^H\mathbf{H}_{AR}^H\mathbf{W}\mathbf{n}_R+\mathbf{c}_{AR}^H\mathbf{n}_A, \tag{5.39}$$

$$y_{ARB}=\sqrt{\rho_{AR}}\kappa\mathbf{c}_{BR}^H\mathbf{H}_{BR}^H\mathbf{W}\mathbf{H}_{AR}\mathbf{f}_{AR}x_A+\kappa\mathbf{c}_{BR}^H\mathbf{H}_{BR}^H\mathbf{W}\mathbf{n}_R+\mathbf{c}_{BR}^H\mathbf{n}_B, \tag{5.40}$$

$$\kappa=\sqrt{\frac{\rho_R}{\rho_{AR}\mathbf{W}\mathbf{H}_{AR}\mathbf{f}_{AR}\mathbf{f}_{AR}^H\mathbf{H}_{AR}^H\mathbf{W}^H+\rho_{BR}\mathbf{W}\mathbf{H}_{BR}\mathbf{f}_{BR}\mathbf{f}_{BR}^H\mathbf{H}_{BR}^H\mathbf{W}^H+\mathbf{W}\mathbf{W}^H}}, \tag{5.41}$$

$\mathbf{f}_{AR}$ $(M_A\times 1)$, $\mathbf{f}_{BR}$ $(M_B\times 1)$, $\mathbf{c}_{AR}$ $(M_A\times 1)$, $\mathbf{c}_{BR}$ $(M_B\times 1)$, and $\mathbf{W}$ $(M_R\times M_R)$ are the complex valued optimization variables, $\mathbb{E}\left[x_Ax_A^*\right]=\mathbb{E}\left[x_Bx_B^*\right]=1$, $\mathbb{E}\left[\mathbf{n}_R\mathbf{n}_R^H\right]=\mathbf{I}_{M_R}$, $\mathbb{E}\left[\mathbf{n}_A\mathbf{n}_A^H\right]=\mathbf{I}_{M_A}$, $\mathbb{E}\left[\mathbf{n}_B\mathbf{n}_B^H\right]=\mathbf{I}_{M_B}$, and $*$ denotes complex conjugate.

The above optimization problem can be solved iteratively based on **Algorithm 5.2**, which uses Karush-Kuhn-Tucker (KKT) necessary conditions for optimality [62, 63, 67]. From the algorithm, ϵ can be an arbitrary

small number (i.e. 0.001), ITER can be a reasonable number of iterations (i.e. 50), $\otimes$ denotes Kronecker product, $\|\mathbf{W}\|_F$ denotes Frobenius norm of $\mathbf{W}$, $\mathrm{vec}(\mathbf{W})$ makes a column vector $\mathbf{w}$ from $\mathbf{W}$, $\mathbf{A} = \rho_{AR}\mathbf{H}_{AR}\mathbf{f}_{AR}\mathbf{f}_{AR}^H\mathbf{H}_{AR}^H$, $\mathbf{B} = \kappa^2\mathbf{H}_{BR}\mathbf{c}_{BR}\mathbf{c}_{BR}^H\mathbf{H}_{BR}^H$, $\mathbf{C} = \rho_{BR}\mathbf{H}_{BR}\mathbf{f}_{BR}\mathbf{f}_{BR}^H\mathbf{H}_{BR}^H$, $\mathbf{D} = \kappa^2\mathbf{H}_{AR}\mathbf{c}_{AR}\mathbf{c}_{AR}^H\mathbf{H}_{AR}^H$, and $\mathbf{V} = \rho_{AR}\kappa\mathbf{H}_{AR}\mathbf{f}_{AR}\mathbf{c}_{BR}^H\mathbf{H}_{BR}^H + \rho_{BR}\kappa\mathbf{H}_{BR}\mathbf{f}_{BR}\mathbf{c}_{AR}^H\mathbf{H}_{AR}^H$. Note that proper normalization is required to make ρ_{AR}, ρ_{BR}, and ρ_R represent average SNRs at each node. Note also that **Algorithm 5.2** converges to a local minimum SMSE point since the SMSE is reduced by updating the matrix $\mathbf{W}$ and vectors $\mathbf{c}_{AR}$, $\mathbf{c}_{BR}$, $\mathbf{f}_{AR}$, and $\mathbf{f}_{BR}$, and it decreases monotonically. [68].

5.5 Numerical and Simulation Results

In Monte-Carlo simulations, the transmitted symbol is QPSK, 8-QAM, or 16-QAM modulated for two-slot, three-slot, four-slot protocols, respectively, for rate normalization. Zero mean and unit variance are used to model the Rayleigh block fading channel. The distance between A and R is set as a reference d_0 whereas the distance between A and B is d. Therefore, once d_0 is determined, $10\log_{10}(\rho_{BR}) = 10\log_{10}(\rho_{AR}) - 10\gamma\log_{10}((1-d_0)/d_0)$, where γ is the path-loss exponent of the simplified path-loss model in [7]. Note that average transmit SNR is normalized in unified received SNR expressions for fair comparison among all protocols.

5.5.1 Accuracy of Analysis

This subsection shows the accuracy of our analysis in equations (5.7) and (5.18) with $M_R = 1$, and the analysis using equations (5.24)-(5.29) with $M_R > 1$. Figures 5.3 and 5.4 show $2\times1\times2$ and $2\times2\times2$ AF MIMO BF two-way relay network performance in sum-BER when both average transmit SNRs are balanced (i.e. $\rho_{AR} = \rho_{BR}$ due to $d_0 = 0.5$), respectively. All simulation curves

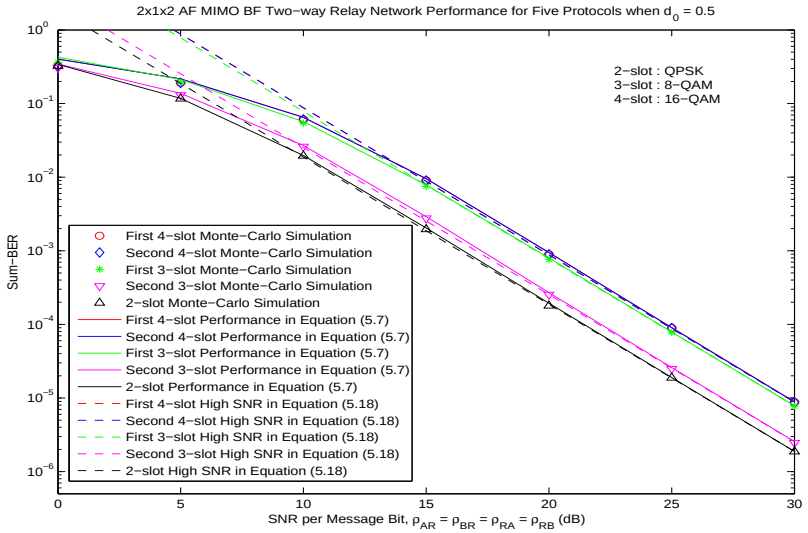

Figure 5.3: $2 \times 1 \times 2$ AF MIMO BF Two-Way Relay Network Performance in Sum-BER when $d_0 = 0.5$.

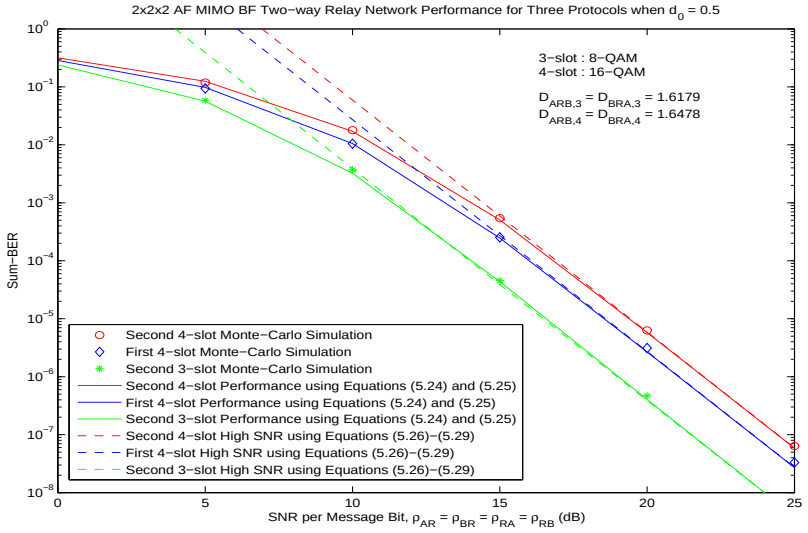

Figure 5.4: $2 \times 2 \times 2$ AF MIMO BF Two-Way Relay Network Performance in Sum-BER when $d_0 = 0.5$.

in Figures 5.3 and 5.4 are from Monte-Carlo simulations. All analytical curves of five protocols are from equation (5.7) and using equations (5.24) and (5.25) with proper constants given in Tables 5.1 and 5.2. All high-SNR analytical curves are from equation (5.18) and using equations (5.26)-(5.29) with related constants in Tables 5.1 and 5.2. Our analysis including high-SNR analysis matches exactly with Monte-Carlo simulations at high-SNR in Figures 5.3 and 5.4. Note that sum-BER performance using equation (5.7) and using equations (5.24) and (5.25) provides tight lower-bounds to equation (5.3).

5.5.2 α-β Optimization

This subsection shows α-β optimization related figures. Figure 5.5 shows the optimal average β^2 for the first three-slot and second four-slot protocols at high-SNR using equation (5.18) for $1 \times 1 \times 1$ AF two-way relay network performance with $\rho_{AR} = \rho_{RA} = \rho_{RB} = 40$ dB when average transmit SNRs are unbalanced (i.e. $\rho_{AR} \neq \rho_{BR}$ due to $d_0 \neq 0.5$) to show the accuracy of equations (5.30) and (5.31). Using the same setup, analytical results in equations (5.30) and (5.31) present $\beta^2 = 0.82915$ and $\beta^2 = 0.85159$ for the first three-slot and second four-slot protocols, respectively.

Figure 5.6 shows $2 \times 1 \times 2$ AF MIMO BF two-way relay network performance in sum-BER when average transmit SNRs are unbalanced. All simulation curves in Figure 5.6 are from numerical simulations using equation (5.3), where the optimal βs are selected based on instantaneous channel realization. All analytical curves of two protocols are from equation (5.7) with proper constants. All high-SNR analytical curves are from equation (5.18) with related constants. $\beta^2 = 0.87196$ and $\beta^2 = 0.88471$ are used for optimal values at high-SNR using equation (5.18) for the first three-slot and second

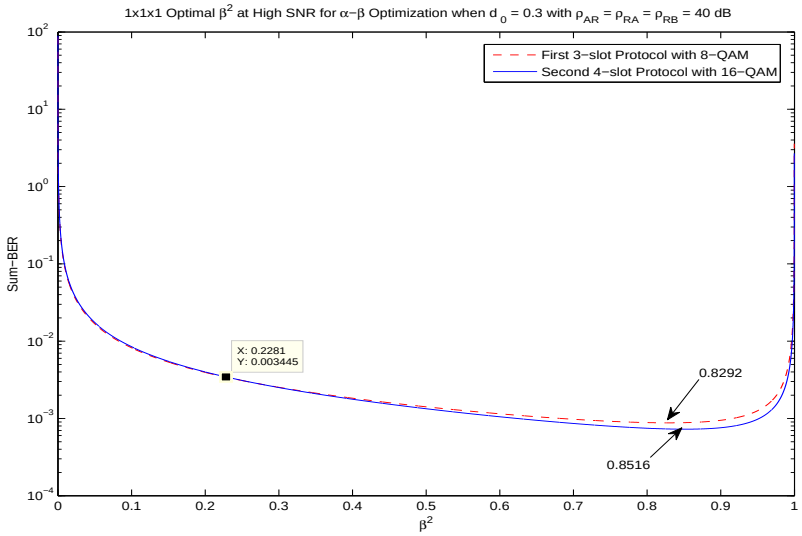

Figure 5.5: Optimal β^2 at High-SNR for $1\times1\times1$ AF Two-Way Relay Network Performance with $\rho_{AR} = 40$ dB when $d_0 = 0.3$.

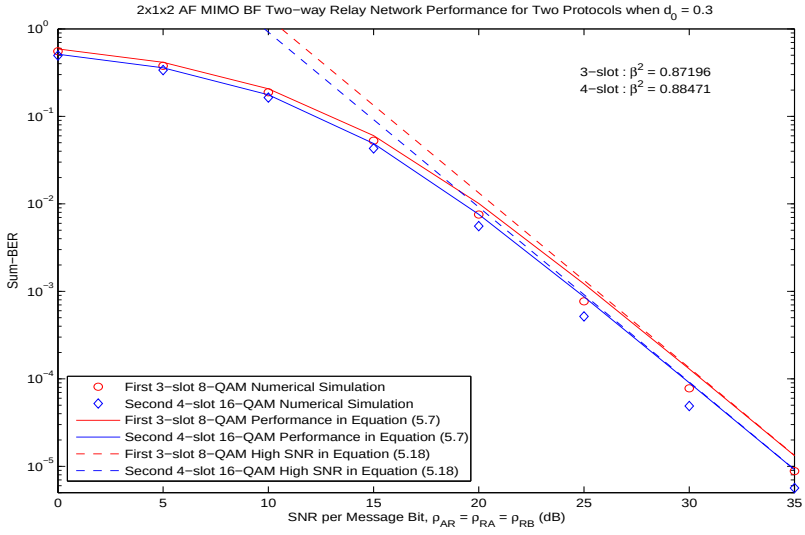

Figure 5.6: $2\times1\times2$ AF MIMO BF Two-Way Relay Network Performance in Sum-BER when $d_0 = 0.3$.

four-slot protocols, respectively. The optimal βs are chosen to minimize average high-SNR performance in our analysis. Our analysis in equation (5.7) matches exactly with high-SNR analysis in equation (5.18). However, about 1 dB gaps exist between our analysis and numerical simulations at high-SNR due to choice of optimal βs.

5.5.3 Comparisons of Protocols

This subsection compares sum-BER performance among five relaying protocols. Note that α-β optimization is performed when average transmit SNRs are unbalanced, and BF optimization, using the gradient algorithm in [31] for the first 3-slot protocol and the iterative minimum sum-MSE (MSMSE) from [62,63] for the 2-slot protocol, is conducted when multiple relay antennas are used. Figure 5.7 shows $2 \times 2 \times 2$ AF MIMO BF two-way relay network performance comparison among five protocols when average transmit SNRs are balanced. All simulation curves are from numerical simulations with Γ_{ARB} and Γ_{BRA} for fair comparison, and all analytical curves are using equations (5.24) and (5.25) with proper constants. Note that the two-slot and first three-slot protocols need to find optimal beamformers for minimum sum-BER. Our proposed three-slot protocol with normalized rate outperforms all other protocols at high-SNR in Figure 5.7.

Figure 5.8 shows $2 \times 1 \times 2$ AF MIMO BF two-way relay network performance comparison when $d_0 = 0.3$. All simulation curves are from numerical simulations using equation (5.3) with α-β optimization. All analytical curves are from equation (5.7) with proper constants. Note that the first three-slot and second four-slot protocols need to find optimal α and β satisfying $\alpha^2 + \beta^2 = 1$ for instantaneous minimum sum-BER. Our proposed four-slot

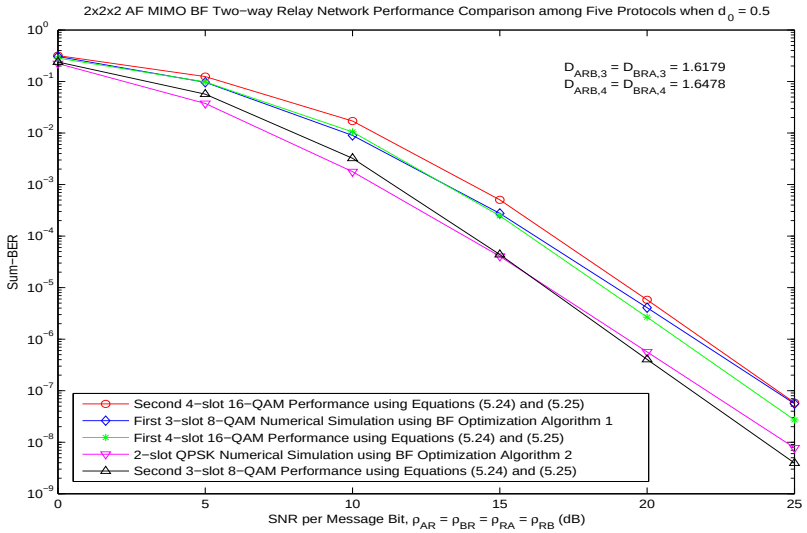

Figure 5.7: $2 \times 2 \times 2$ AF MIMO BF Two-Way Relay Network Performance in Sum-BER when $d_0 = 0.5$.

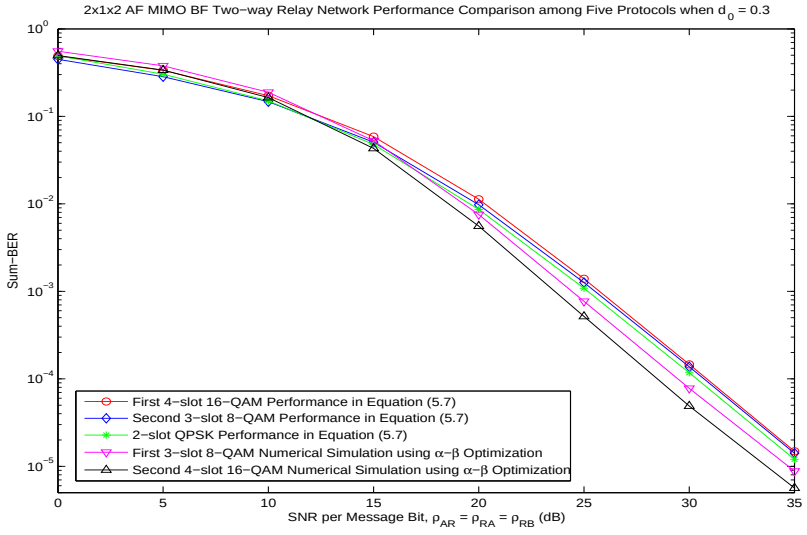

Figure 5.8: $2 \times 1 \times 2$ AF MIMO BF Two-Way Relay Network Performance Comparison when $d_0 = 0.3$.

protocol with optimal α and β and normalized rate outperforms all other protocols at high-SNR in Figure 5.8.

The analytical high-SNR gaps between five protocols for three scenarios based on equations (5.18) and (5.26)-(5.29) are given in Tables 5.3 and 5.4. All gaps are from the best protocol for each scenario in dB. For example, the best protocol in sum-BER for $2 \times 1 \times 2$ AF MIMO BF two-way relay networks when transmit SNRs are balanced is the two-slot protocol, and the gap from the two-slot protocol to the second three-slot protocol is 0.6608 dB. Note that the proposed four-slot protocol is the best protocol for $2 \times 1 \times 2$ AF MIMO BF two-way relay networks when transmit SNRs are unbalanced, and the proposed three-slot protocol is the best protocol for $2 \times 2 \times 2$ AF MIMO BF two-way relay networks when transmit SNRs are balanced.

Table 5.3: The Analytical High-SNR Gaps using Equation (5.32) between Five Protocols in dB for $2 \times 1 \times 2$ Two-Way Relaying

Balanced SNR		Unbalanced SNR	
Best Protocol	2-slot	Best Protocol	Second 4-slot
Gap to First 3-slot	3.1014	Gap to 2-slot	1.7106
Gap to Second 3-slot	0.6608	Gap to First 3-slot	0.9651
Gap to First 4-slot	3.3547	Gap to Second 3-slot	2.0607
Gap to Second 4-slot	3.3547	Gap to First 4-slot	1.1622

Table 5.4: The Analytical High-SNR Gaps using Equation (5.32) between Five Protocols in dB for $2 \times 2 \times 2$ Two-Way Relaying

Balanced SNR	
Best Protocol	Second 3-slot
Gap to 2-slot	0.8412
Gap to First 3-slot	2.9071
Gap to First 4-slot	2.1083
Gap to Second 4-slot	2.9495

5.6 Chapter Summary

Unified performance analysis has been conducted for AF MIMO BF two-way relay networks with five different relaying protocols using two, three, or four time slots. We first have introduced novel "second three-slot" and "second four-slot" protocols suitable for BF and better sum-BER performance. Novel closed-form unified sum-BER expressions have been presented with corresponding closed-form unified CDFs. Furthermore, new closed-form unified high-SNR performance expressions have been provided for simplicity and mathematical tractability, and the analytical high-SNR gap expression is provided. BF optimization is also discussed using the gradient algorithm and iterative MSMSE algorithm.

Based on analytical and simulation results, we have investigated the performance of five different protocols with two, three, or four time slots using the sum-BER metric. As a result, we can conclude that the proposed three-slot protocol outperforms all other protocols at high-SNR when multiple relay antennas are used, and the proposed four-slot protocol outperforms all other protocols at high-SNR when average transmit SNRs are unbalanced. Therefore, we can say that the proposed protocols are a good alternative to the two-slot protocol when multiple relay antennas are used and average transmit SNRs are unbalanced.

Appendix 5.1: Derivations of Equations (5.5), (5.6), (5.24), and (5.25)

This appendix derives the CDFs of Γ_{ARB} and Γ_{BRA} with a general M_R so that it covers equations (5.5), (5.6), (5.24), and (5.25). We derive the CDF of Γ_{ARB} first and discuss the CDF of Γ_{BRA} later. For the CDF of Γ_{ARB}, the following procedures can be used by the definitions of CDF and complementary

CDF (CCDF):

$$\begin{aligned} F_{\Gamma_{ARB}}(x) &= \int_0^\infty Pr\left(\frac{A_{ARB}\gamma_{AR}y}{B_{ARB}\gamma_{AR}+C_{ARB}y} \le x\right) f_{\gamma_{RB}}(y)dy \\ &= 1 - \int_{B_{ARB}x/A_{ARB}}^\infty \bar{F}_{\gamma_{AR}}\left(\frac{C_{ARB}}{A_{ARB}y - B_{ARB}x}\right) f_{\gamma_{RB}}(y)dy \\ &= 1 - \int_0^\infty \bar{F}_{\gamma_{AR}}\left(\frac{C_{ARB}x\,(w+B_{ARB}x)}{A_{ARB}w}\right) f_{\gamma_{RB}}\left(\frac{w+B_{ARB}x}{A_{ARB}}\right)\frac{dw}{A_{ARB}}, \end{aligned} \tag{5.42}$$

where $\bar{F}_{\gamma_{AR}}(x)$ is the CCDF of γ_{AR}, which $\bar{F}_{\gamma_{AR}}(x) = 1 - F_{\gamma_{AR}}(x)$. Since the CDF of γ_{AR} and the PDF of γ_{RB} are given by [45, eqns.(24)-(25)]

$$F_{\gamma_{AR}}(x) = 1 - \sum_{n=1}^{M_R}\sum_{m=M_A-M_R}^{(M_A+M_R)n-2n^2}\sum_{k=0}^{m}\frac{d_{n,m}(nx)^k e^{-nx/\rho_{AR}}}{k!\rho_{AR}^k}, \quad x>0 \tag{5.43}$$

$$f_{\gamma_{RB}}(x) = \sum_{i=1}^{M_R}\sum_{j=M_B-M_R}^{(M_B+M_R)i-2i^2}\frac{d_{i,j}i^{j+1}x^j e^{-ix/\rho_R}}{j!\rho_R^{j+1}}, \quad x>0. \tag{5.44}$$

Equation (5.25) can be acquired after complicated mathematical manipulations if equations (5.43) and (5.44) are substituted to the last line of equation (5.42). Using similar procedures, equation (5.24) can also be obtained using the corresponding constants and subscripts. Once $M_R = 1$ is applied to equations (5.24) and (5.25), equations (5.5) and (5.6) can be attained.

Appendix 5.2: Derivations of Equations (5.10), (5.14), and (5.26)-(5.29)

This appendix derives the t_{ARB} and t_{BRA} order derivatives of the PDFs of λ_{ARB} and λ_{BRA} evaluated at the origin, respectively, with a general M_R so that it covers all cases. We derive the t_{ARB} order derivative of the PDF of λ_{ARB} and evaluate it at the origin first, and then we discuss the t_{BRA} order derivative of the PDF of λ_{BRA} evaluated at the origin later. To acquire the t_{ARB} order derivative of the PDF of λ_{ARB}, we need to obtain the PDF of λ_{ARB}. Since $\lambda_{ARB} = \Gamma_{ARB}/\rho_{AR}$, we can easily find the PDF of λ_{ARB} if the PDF of Γ_{ARB} is given. From equation (5.2), Γ_{ARB} can be rewritten as

$$\begin{aligned} \Gamma_{ARB} &= \frac{A_{ARB}\gamma_{AR}\gamma_{RB}}{B_{ARB}\gamma_{AR}+C_{ARB}\gamma_{RB}} \\ &= \frac{A_{ARB}}{B_{ARB}C_{ARB}}\frac{B_{ARB}C_{ARB}\gamma_{AR}\gamma_{RB}}{B_{ARB}\gamma_{AR}+C_{ARB}\gamma_{RB}} = \frac{A_{ARB}}{B_{ARB}C_{ARB}}W, \end{aligned} \tag{5.45}$$

where $W := B_{ARB}C_{ARB}\gamma_{AR}\gamma_{RB}/\left(B_{ARB}\gamma_{AR}+C_{ARB}\gamma_{RB}\right)$, which is the received SNR of a two-hop relay system when the noise variance of the first hop is removed.

Since we consider high-SNR, W can be approximated by $\min\{B_{ARB}\gamma_{AR}, C_{ARB}\gamma_{RB}\}$ [21]. Based on the identity for the minimum of two independent RVs in [38, eqn.(6.58)], the PDF of W can be approximated at high-SNR as

$$\begin{aligned} f_W(x) &\approx f_{B_{ARB}\gamma_{AR}}(x)\bar{F}_{C_{ARB}\gamma_{RB}}(x) + f_{C_{ARB}\gamma_{RB}}(x)\bar{F}_{B_{ARB}\gamma_{AR}}(x) \\ &= \sum_{n=1}^{M_R}\sum_{m=M_A-M_R}^{(M_A+M_R)n-2n^2}\sum_{i=1}^{M_R}\sum_{j=M_B-M_R}^{(M_B+M_R)i-2i^2}\sum_{p=0}^{j} \\ &\quad \frac{d_{n,m}d_{i,j}n^{m+1}i^p x^{m+p}e^{-x\left(\frac{n}{B_{ARB}\rho_{AR}}+\frac{i}{C_{ARB}\rho_R}\right)}}{m!p!\left(B_{ARB}\rho_{AR}\right)^{m+1}\left(C_{ARB}\rho_R\right)^p} \\ &\quad + \sum_{i=1}^{M_R}\sum_{j=M_B-M_R}^{(M_B+M_R)i-2i^2}\sum_{n=1}^{M_R}\sum_{m=M_A-M_R}^{(M_A+M_R)n-2n^2}\sum_{k=0}^{m} \\ &\quad \frac{d_{n,m}d_{i,j}n^k i^{j+1}x^{k+j}e^{-x\left(\frac{n}{B_{ARB}\rho_{AR}}+\frac{i}{C_{ARB}\rho_R}\right)}}{k!j!\left(B_{ARB}\rho_{AR}\right)^k\left(C_{ARB}\rho_R\right)^{j+1}}. \end{aligned} \tag{5.46}$$

Using the identity of [38, eqn.(6.5)], the PDF of λ_{ARB} can be approximated at high-SNR as $f_{\lambda_{ARB}}(x) \approx B_{ARB}C_{ARB}\rho_{AR}f_W\left(B_{ARB}C_{ARB}\rho_{AR}x/A_{ARB}\right)/A_{ARB}$ since $\lambda_{ARB} = \Gamma_{ARB}/\rho_{AR}$. Once $f_{\lambda_{ARB}}(x)$ is differentiated t_{ARB} times and evaluated at the origin for each case (i.e. $M_A > M_B$, $M_A < M_B$, and $M_A = M_B$), the following equation can be obtained:

$$f_{\lambda_{ARB}}^{(t_{ARB})}(0) = \begin{cases} f_{\lambda_{RB}}^{(t_{RB})}(0), & M_A > M_B \\ f_{\lambda_{AR}}^{(t_{AR})}(0), & M_A < M_B \\ f_{\lambda_{AR}}^{(t_{AR})}(0) + f_{\lambda_{RB}}^{(t_{RB})}(0), & M_A = M_B \end{cases}, \tag{5.47}$$

where $f_{\lambda_{AR}}^{(t_{AR})}(0)$ and $f_{\lambda_{RB}}^{(t_{RB})}(0)$ are given in equations (5.26) and (5.27), respectively. Once $M_R = 1$ is applied to equation (5.47), equation (5.10) can be attained. Using similar procedures, equation (5.14) can be obtained.

Appendix 5.3: Derivation of Iterative MSMSE BF Optimization Algorithm

This appendix derives iterative MSMSE BF optimization algorithm (i.e. **Algorithm 5.2**) used in Section 5.4.2. When we consider the two-slot protocol using the system model in Figure 5.1, the received signals at R, A, and B, respectively, after self-interference cancelation, can be written as

$$\mathbf{y}_R = \sqrt{\rho_{AR}}\mathbf{H}_{AR}\mathbf{f}_{AR}x_A + \sqrt{\rho_{BR}}\mathbf{H}_{BR}\mathbf{f}_{BR}x_B + \mathbf{n}_R \tag{5.48}$$

$$y_{BRA} = \sqrt{\rho_{BR}}\kappa\mathbf{c}_{AR}^H\mathbf{H}_{AR}^H\mathbf{W}\mathbf{H}_{BR}\mathbf{f}_{BR}x_B + \kappa\mathbf{c}_{AR}^H\mathbf{H}_{AR}^H\mathbf{W}\mathbf{n}_R + \mathbf{c}_{AR}^H\mathbf{n}_A \tag{5.49}$$

$$y_{ARB} = \sqrt{\rho_{AR}}\kappa\mathbf{c}_{BR}^H\mathbf{H}_{BR}^H\mathbf{W}\mathbf{H}_{AR}\mathbf{f}_{AR}x_A + \kappa\mathbf{c}_{BR}^H\mathbf{H}_{BR}^H\mathbf{W}\mathbf{n}_R + \mathbf{c}_{BR}^H\mathbf{n}_B, \tag{5.50}$$

where

$$\kappa = \sqrt{\frac{\rho_R}{\rho_{AR}\mathbf{W}\mathbf{H}_{AR}\mathbf{f}_{AR}\mathbf{f}_{AR}^H\mathbf{H}_{AR}^H\mathbf{W}^H + \rho_{BR}\mathbf{W}\mathbf{H}_{BR}\mathbf{f}_{BR}\mathbf{f}_{BR}^H\mathbf{H}_{BR}^H\mathbf{W}^H + \mathbf{W}\mathbf{W}^H}}; \tag{5.51}$$

$\mathbf{c}_{AR}$ $(M_A \times 1)$ and $\mathbf{c}_{BR}$ $(M_B \times 1)$ are combining weight vectors; x_A and x_B are transmitted symbols with $\mathbb{E}[|x_A|^2] = \mathbb{E}[|x_B|^2] = 1$ and $\mathbb{E}[x_A] = \mathbb{E}[x_B] = 0$; $\mathbf{n}_R$ $(M_R \times 1)$, $\mathbf{n}_A$ $(M_A \times 1)$, and $\mathbf{n}_B$ $(M_B \times 1)$ are noise according to $CN(0, \mathbf{I})$; $\mathbf{W}$ $(M_R \times M_R)$ is the linear processing matrix, which includes the BF and combining vectors at R.

Since we are interested in sum-BER, the following sum-BER minimization problem can be obtained:

$$\begin{aligned} \text{minimize} \quad & \left[Q\left(\sqrt{2b\gamma_{ARB}}\right) + Q\left(\sqrt{2b\gamma_{BRA}}\right)\right] \\ \text{subject to} \quad & \|\mathbf{f}_{AR}\|^2 \leq 1 \\ & \|\mathbf{f}_{BR}\|^2 \leq 1 \\ & \text{tr}\left\{\mathbf{W}\mathbf{W}^H\right\} \leq 1, \end{aligned} \tag{5.52}$$

where

$$\gamma_{ARB} = \frac{\rho_{AR}\kappa^2\mathbf{c}_B^H\mathbf{H}_{BR}^H\mathbf{W}\mathbf{H}_{AR}\mathbf{f}_{AR}\mathbf{f}_{AR}^H\mathbf{H}_{AR}^H\mathbf{W}^H\mathbf{H}_{BR}\mathbf{c}_B}{\kappa^2\mathbf{c}_B^H\mathbf{H}_{BR}^H\mathbf{W}\mathbf{W}^H\mathbf{H}_{BR}\mathbf{c}_B + \mathbf{c}_B^H\mathbf{c}_B}, \tag{5.53}$$

$$\gamma_{BRA} = \frac{\rho_{BR}\kappa^2 \mathbf{c}_A^H \mathbf{H}_{AR}^H \mathbf{W} \mathbf{H}_{BR} \mathbf{f}_{BR} \mathbf{f}_{BR}^H \mathbf{H}_{BR}^H \mathbf{W}^H \mathbf{H}_{AR} \mathbf{c}_A}{\kappa^2 \mathbf{c}_A^H \mathbf{H}_{AR}^H \mathbf{W}\mathbf{W}^H \mathbf{H}_{AR} \mathbf{c}_A + \mathbf{c}_A^H \mathbf{c}_A}, \tag{5.54}$$

and $\mathrm{tr}(\mathbf{K})$ is the trace operator of matrix $\mathbf{K}$. This is not a convex problem.

To handle this non-convex problem, the problem can be simplified into following simple problems as follows:

$$\begin{aligned} \text{minimize} \quad & \left[Q\left(\sqrt{2b\gamma_{ARB}}\right) + Q\left(\sqrt{2b\gamma_{BRA}}\right) \right] \\ \text{subject to} \quad & \|\mathbf{f}_{AR}\|^2 \leq 1 \\ & \|\mathbf{f}_{BR}\|^2 \leq 1, \end{aligned} \tag{5.55}$$

when $\mathbf{c}_{AR}$, $\mathbf{c}_{BR}$, and $\mathbf{W}$ are given.

$$\text{minimize} \quad \left[Q\left(\sqrt{2b\gamma_{ARB}}\right) + Q\left(\sqrt{2b\gamma_{BRA}}\right) \right] \tag{5.56}$$

when $\mathbf{f}_{AR}$, $\mathbf{f}_{BR}$, and $\mathbf{W}$ are given.

$$\begin{aligned} \text{minimize} \quad & \left[Q\left(\sqrt{2b\gamma_{ARB}}\right) + Q\left(\sqrt{2b\gamma_{BRA}}\right) \right] \\ \text{subject to} \quad & \mathrm{tr}\left\{\mathbf{W}\mathbf{W}^H\right\} \leq 1, \end{aligned} \tag{5.57}$$

where $\mathbf{W}$ is the optimization variable when $\mathbf{f}_{AR}$, $\mathbf{f}_{BR}$, $\mathbf{c}_{AR}$, and $\mathbf{c}_{BR}$ are given. Even though this approach is sub-optimal, well-known convex results for equations (5.55) and (5.56) and necessary optimal conditions for equation (5.57) can be used.

Specifically, the solutions for equation (5.55) are well-known matched filters, $\mathbf{f}_{AR}^\star = \rho_{AR}\kappa \mathbf{H}_{AR}^H \mathbf{W}^H \mathbf{H}_{BR} \mathbf{c}_{BR}$ and $\mathbf{f}_{BR}^\star = \rho_{BR}\kappa \mathbf{H}_{BR}^H \mathbf{W}^H \mathbf{H}_{AR} \mathbf{c}_{AR}$. The solutions for equation (5.56) are well-known MMSE filters,

$$\mathbf{c}_{AR}^\star = \left[\kappa^2 \mathbf{H}_{AR}^H \mathbf{W}\mathbf{W}^H \mathbf{H}_{AR} + \mathbf{I}_{M_A}\right]^{-1} \rho_{BR}\kappa \mathbf{H}_{AR}^H \mathbf{W} \mathbf{H}_{BR} \mathbf{f}_{BR}$$

and

$$\mathbf{c}_{BR}^\star = \left[\kappa^2 \mathbf{H}_{BR}^H \mathbf{W}\mathbf{W}^H \mathbf{H}_{BR} + \mathbf{I}_{M_B}\right]^{-1} \rho_{AR}\kappa \mathbf{H}_{BR}^H \mathbf{W} \mathbf{H}_{AR} \mathbf{f}_{AR}.$$

However, since equation (5.57) is not easy to solve, we consider a minimum sum-MSE (MSMSE) problem for it as

$$\begin{aligned} \text{minimize} \quad & \operatorname{tr}\left\{\mathbb{E}\left[\left(y_{BRA}-\sqrt{\rho_{BR}}x_B\right)\left(y_{BRA}-\sqrt{\rho_{BR}}x_B\right)^H\right]\right\} \\ & +\operatorname{tr}\left\{\mathbb{E}\left[\left(y_{ARB}-\sqrt{\rho_{AR}}x_A\right)\left(y_{ARB}-\sqrt{\rho_{AR}}x_A\right)^H\right]\right\} \\ \text{subject to} \quad & \operatorname{tr}\left\{\mathbf{W}\mathbf{W}^H\right\}\leq 1, \end{aligned} \tag{5.58}$$

Even though equation (5.58) is not a convex problem, we can solve it iteratively with the Lagrange multiplier and KKT necessary conditions [67] for optimal $\mathbf{W}^\star$.

From equation (5.58), the Lagrangian function is defined by

$$\begin{aligned} & L\left(\mathbf{f}_{AR},\mathbf{f}_{BR},\mathbf{c}_{AR},\mathbf{c}_{BR},\mathbf{W}\right) \\ & := \operatorname{tr}\left\{\rho_{BR}\kappa^2\mathbf{c}_{AR}^H\mathbf{H}_{AR}^H\mathbf{W}\mathbf{H}_{BR}\mathbf{f}_{BR}\mathbf{f}_{BR}^H\mathbf{H}_{BR}^H\mathbf{W}^H\mathbf{H}_{AR}\mathbf{c}_{AR}+\mathbf{c}_{AR}^H\mathbf{c}_{AR}\right. \\ & \qquad \left.+\kappa^2\mathbf{c}_{AR}^H\mathbf{H}_{AR}^H\mathbf{W}\mathbf{W}^H\mathbf{H}_{AR}\mathbf{c}_{AR}-2\rho_{BR}\kappa\mathbf{c}_{AR}^H\mathbf{H}_{AR}^H\mathbf{W}\mathbf{H}_{BR}\mathbf{f}_{BR}+\rho_{BR}\right\} \\ & \quad +\operatorname{tr}\left\{\rho_{AR}\kappa^2\mathbf{c}_{BR}^H\mathbf{H}_{BR}^H\mathbf{W}\mathbf{H}_{AR}\mathbf{f}_{AR}\mathbf{f}_{AR}^H\mathbf{H}_{AR}^H\mathbf{W}^H\mathbf{H}_{BR}\mathbf{c}_{BR}+\mathbf{c}_{BR}^H\mathbf{c}_{BR}\right. \\ & \qquad \left.+\kappa^2\mathbf{c}_{BR}^H\mathbf{H}_{BR}^H\mathbf{W}\mathbf{W}^H\mathbf{H}_{BR}\mathbf{c}_{BR}-2\rho_{AR}\kappa\mathbf{c}_{BR}^H\mathbf{H}_{BR}^H\mathbf{W}\mathbf{H}_{AR}\mathbf{f}_{AR}+\rho_{AR}\right\} \\ & \quad +\lambda\left(\operatorname{tr}\left\{\mathbf{W}\mathbf{W}^H\right\}-1\right), \end{aligned} \tag{5.59}$$

where λ is the Lagrange multiplier. Based on KKT conditions $\nabla_{\mathbf{W}}L\left(\mathbf{f}_{AR},\mathbf{f}_{BR},\right.$ $\left.\mathbf{c}_{AR},\mathbf{c}_{BR},\mathbf{W}\right)=0$ in [67], if $\nabla_{\mathbf{X}}\operatorname{tr}\left\{\mathbf{AXB}\right\}=\mathbf{BA}$ is used, we can obtain the following crucial equation:

$$\mathbf{A}\mathbf{W}^H\mathbf{B}+\mathbf{C}\mathbf{W}^H\mathbf{D}+\mathbf{W}^H\left(\mathbf{B}+\mathbf{D}\right)+\lambda\mathbf{W}^H=\mathbf{V}, \tag{5.60}$$

where matrices $\mathbf{A}$, $\mathbf{B}$, $\mathbf{C}$, $\mathbf{D}$, and $\mathbf{V}$ are defined below equation (5.41). Once $\mathbf{W}$ is left multiplied to equation (5.60) and the trace operator is used, the Lagrange multiplier λ can be obtained as in **Algorithm 5.2** based on the power constraint. In addition, if the vector operator with $\operatorname{vec}\left(\mathbf{AXB}\right)=\left(\mathbf{B}^T\otimes\mathbf{A}\right)\operatorname{vec}\left(\mathbf{X}\right)$ is used to equation (5.60), $\operatorname{vec}\left(\mathbf{W}\right)$ can also be attained as in **Algorithm 5.2**. Therefore, if we optimize $\mathbf{f}_{AR}$, $\mathbf{f}_{BR}$, $\mathbf{c}_{AR}$, $\mathbf{c}_{BR}$, and $\mathbf{W}$ iteratively, **Algorithm 5.2** can be obtained.

Chapter 6

Unified Performance Analysis and Stochastic Ordering of AF MIMO Beamforming Two-way Relay Networks with Direct Links

Even though one-way relay networks have been widely studied due to spatial diversity and extensive coverage [11, 12], the attention of researchers has moved to two-way relay networks because of better spectral efficiency, in which two sources exchange their data through a relay in two time slots [19, 20, 57]. The "two-slot" protocol without direct links dominate other protocols (i.e. "three-slot" and "four-slot") in sum-bit error rate (BER) of two-way relay networks with normalized rate and power while the three-slot protocol is better in average sum-BER when average transmit powers from two sources are significantly different [21].

One problem of the two-slot protocol is, however, that it cannot utilize the full potential of relay networks by neglecting possible direct links due to the half duplex constraint. To exploit the presence of direct links in two-way relay networks, three or four time slots are necessary. Including direct links, reference [69] provides upper-bounds on sum-rate and outage probability with the three-slot and four-slot protocols, and reference [70] presents a mechanism combining multiuser diversity and incremental relaying, and outage analysis for multiuser two-way relay systems with the three-slot protocol.

Recently, systematic applications of stochastic ordering literature are presented for comparing physical layer communication systems [71]. Even though the theory of stochastic orders in [72] offers a wide range of framework to compare two RVs in applications of statistics, biology, economics, operations research, and reliability theory, the applications of this theory in physical

layer communication systems are very limited such as outage probability based comparisons [73,74]. Due to the lack of literature using the theory of stochastic orders in physical layer communication systems, reference [71] provides some physical layer communication examples illustrating that stochastic orders are useful in comparing systems by exploiting monotonicity, convexity, and complete monotonicity, which can be easily connected with performance metrics such as error rates and ergodic capacity.

Since the average probability of error is one of the performance metrics of interest in communications, we present novel unified average combined sum-BER approximations in closed-form for amplify-and-forward (AF) multiple-input multiple-output (MIMO) beamforming (BF) two-way relay networks including direct links with three different protocols in Rayleigh fading. New unified high signal-to-noise ratio (SNR) performance is also presented, and all performance is compared by simulations. In addition, since the authors in [71] never consider MIMO and two-way relay systems, we compare AF MIMO BF two-way relay networks using the theory of stochastic orders in terms of sum-BER and maximum sum-rate.

After system models are described for the five two-way relaying protocols with a single relay antenna in Section 6.1, unified performance analysis including high-SNR analysis is presented in Section 6.2. Multiple relay antennas are considered in Section 6.3, and numerical and Monte-Carlo simulations compare the performance of five different relaying protocols in Section 6.4. Finally, Section 6.5 summarizes this chapter.

6.1 System Model

Figure 6.1 shows a two-hop MIMO two-way relay system with direct links, which consists of two sources, which are also destinations, A and B, and a relay R. All nodes are equipped with multiple antennas, M_A, M_B, and M_R, respectively. $\mathbf{H}_{AR}$, $\mathbf{H}_{BR}$, $\mathbf{H}_{RA}$, and $\mathbf{H}_{RB}$ are $M_R \times M_A$, $M_R \times M_B$, $M_A \times M_R$, and $M_B \times M_R$ statistically independent complex Gaussian channel matrices connecting the nodes, respectively. The channel coefficients are assumed to remain static while A and B exchange their data so that $\mathbf{H}_{RA} = \mathbf{H}_{AR}^H$ and $\mathbf{H}_{RB} = \mathbf{H}_{BR}^H$, where $(\cdot)^H$ denotes a matrix Hermitian. We assume that transmitters have knowledge only on connected nodes while receivers can access full CSI.

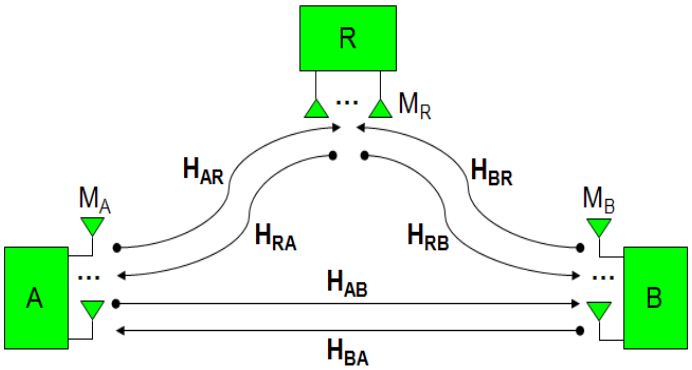

Figure 6.1: System Model of Two-Hop MIMO Two-Way Relay Networks with Direct Links.

A half-duplex time division multiple access (TDMA) scenario is considered with three different transmission protocols, illustrated in Figure 6.2. Symbols are transmitted with zero mean and unit variance, and additive noise is independent complex Gaussian with zero mean and unit variance. When multiple antennas are considered at all nodes, BF optimization has to be con-

ducted, at all nodes in the three-slot protocol but only at A and B in the first and second four-slot protocol. We therefore first consider a single antenna at all nodes to obtain closed-form expressions for all protocols in Section 6.2, and extend this to multiple antennas in Section 6.3. Since system models are well studied in [19, 21, 59–61], we present unified instantaneous received SNR representations for each protocol. Note that when the protocols with different number of slots are compared, transmit power is normalized so that each node uses the same power, and the constellation sizes are chosen so that the rates are fixed as well. Note that the two-slot and second three-slot protocols from Chapter 5 are eliminated herein since they cannot accommodate direct links in the presence of the half-duplex assumption.

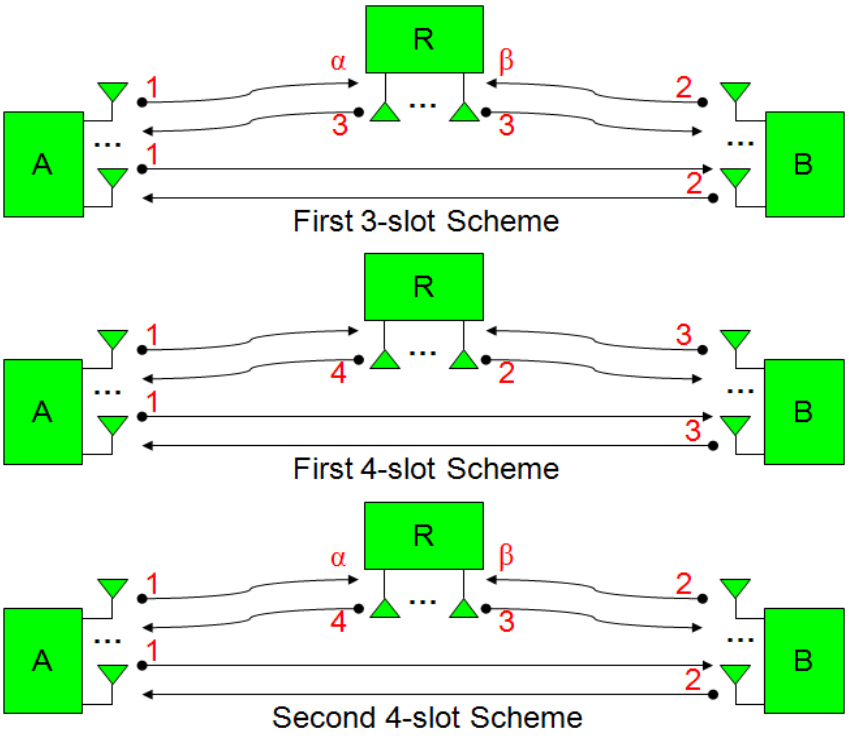

Figure 6.2: Transmission Schemes for Two-Way Relay Networks with Direct Links.

6.1.1 First Three-Slot Protocol

In the first three-slot protocol, A transmits its signal to both B and R in the first time slot; B transmits its signal to both A and R in the second time slot; R weighs the received signals from A and B (i.e. with $\alpha \geq 0$ and $\beta \geq 0$ satisfying $\alpha^2 + \beta^2 = 1$), amplifies the added signals, and forwards them to both A and B in the third time slot. To combine two received signals at A and B, separately, the MMSE combining is used [42, 43, 45]. Note that choosing coefficients α and β is well studied in Chapter 5.

6.1.2 First Four-Slot Protocol

In the first four-slot protocol, A transmits its signal to both B and R in the first time slot; R amplifies the received signal and forwards it to B in the second time slot; B transmits its signal to both A and R in the third time slot; R amplifies the other received signal and forwards it to A in the fourth time slot. Note that transmit power normalization is required due to two transmissions at R.

6.1.3 Second Four-Slot Protocol

The second four-slot protocol is proposed to obtain better sum-BER by taking advantage of the technique, which is weighting two received signals from A and B at R with α and β, respectively. In the second four-slot protocol, A transmits its signal to both B and R in the first time slot; B transmits its signal to both A and R in the second time slot; R weighs the received signals with coefficients α and β, amplifies the weighted sum and forwards it to both A and B in the third and fourth time slots, consecutively. Transmit power

normalization is also required at R due to two transmissions. To combine three received signals at A and B, separately, the MMSE combining is used.

6.1.4 Unified SNR Representations for Three Different Protocols for $M_A = M_B = M_R = 1$

For the aforementioned protocols, after canceling the self-interferences with MRC and MMSE combining, the instantaneous received SNRs at A and B can be expressed, respectively, in a unified framework:

$$\gamma_A = \gamma_{BRA} + \gamma_{BA} = \frac{A_{BRA}\gamma_{BR}\gamma_{RA}}{B_{BRA}\gamma_{BR} + C_{BRA}\gamma_{RA} + 1} + \gamma_{BA} \tag{6.1}$$

$$\gamma_B = \gamma_{ARB} + \gamma_{AB} = \frac{A_{ARB}\gamma_{AR}\gamma_{RB}}{B_{ARB}\gamma_{AR} + C_{ARB}\gamma_{RB} + 1} + \gamma_{AB}, \tag{6.2}$$

where A_{BRA}, B_{BRA}, C_{BRA}, A_{ARB}, B_{ARB}, and C_{ARB} are non-negative constants of each received SNR, given in Table 6.1; $\gamma_{AR} = \rho_{AR}|h_{AR}|^2$, $\gamma_{BR} = \rho_{BR}|h_{BR}|^2$, $\gamma_{RA} = \rho_{RA}|h_{RA}|^2$, $\gamma_{RB} = \rho_{RB}|h_{RB}|^2$, $\gamma_{AB} = \rho_{AB}|h_{AB}|^2$, and $\gamma_{BA} = \rho_{BA}|h_{BA}|^2$; ρ_{AR}, ρ_{BR}, ρ_{RA}, ρ_{RB}, ρ_{AB}, and ρ_{BA} are average transmit SNRs; h_{AR}, h_{BR}, h_{RA}, h_{RB}, h_{AB}, and h_{BA} are channel coefficients, assumed to be i.i.d. according to $CN(0,1)$; α and β are weights satisfying $\alpha^2 + \beta^2 = 1$ for two received signals from A and B at R, respectively [21]. To obtain tight bounds, we drop 1s in the denominators of both γ_{BRA} and γ_{ARB}, and denote them with Γ_{BRA} and Γ_{ARB}, respectively. Note that γ_{BRA} and γ_{ARB} are equivalent to Γ_{BRA} and Γ_{ARB}, respectively, at high SNR.

Table 6.1: The Coefficients for Equations (6.1) and (6.2) when $M_A = M_B = M_R = 1$

Constants	A_{BRA}	B_{BRA}	C_{BRA}	A_{ARB}	B_{ARB}	C_{ARB}
First three-slot	β^2	β^2	$1 + \frac{\alpha^2\rho_{AR}}{\rho_{RA}}$	α^2	α^2	$1 + \frac{\beta^2\rho_{BR}}{\rho_{RB}}$
First four-slot	$\frac{1}{2}$	1	$\frac{1}{2}$	$\frac{1}{2}$	1	$\frac{1}{2}$
Second four-slot	β^2	β^2	$\frac{1}{2} + \frac{\alpha^2\rho_{AR}}{\rho_{RA}}$	α^2	α^2	$\frac{1}{2} + \frac{\beta^2\rho_{BR}}{\rho_{RB}}$

6.2 Performance Analysis for $M_A = M_B = M_R = 1$

Sum-BER performance analysis including high-SNR analysis is carried out using the unified received SNR expressions. The multiple relay antenna case is described in Section 6.3.

6.2.1 Performance Metric

For the performance metric, we consider sum-BER, which is defined as follows for all protocols:

$$P_b = \frac{1}{\log_2(M)} \int_0^\infty aQ\left(\sqrt{2bx}\right) \left(f_{\gamma_A}(x) + f_{\gamma_B}(x)\right) dx, \tag{6.3}$$

where $Q(x) := \left(1/\sqrt{2\pi}\right) \int_x^\infty e^{-y^2/2} dy$ and a and b are modulation related positive constants. For example, $a = 1$ and $b = 1$ provide exact BER for binary phase shift keying (BPSK), while $a = 2$ and $b = \sin^2(\pi/M)$ and $a = 4\left(1 - 1/\sqrt{M}\right)$ and $b = 3/(2(M-1))$ provide tight SER approximations for M-ary PSK (M-PSK) and M-ary quadrature amplitude modulation (M-QAM), respectively.

6.2.2 Sum-BER using Unified SNR Representations

Calculating equation (6.3) using equations (6.1) and (6.2) is hard since the distributions of γ_A and γ_B are intractable. However, since the cumulative distribution functions (CDFs) of Γ_{ARB} and Γ_{BRA} and the probability density functions (PDFs) of γ_{AB} and γ_{BA} are available, the following alternative equation can be used to calculate sum-BER [66, eqn.(5)].

$$\begin{aligned} P_b \approx & \frac{a\sqrt{b}}{\log_2(M)\sqrt{8\pi}} \int_0^\infty \frac{e^{-bx_1}}{\sqrt[4]{x_1}} F_{\Gamma_{ARB}}(x_1) dx_1 \int_0^\infty \frac{e^{-bx_2}}{\sqrt[4]{x_2}} f_{\gamma_{AB}}(x_2) dx_2 \\ & + \frac{a\sqrt{b}}{\log_2(M)\sqrt{8\pi}} \int_0^\infty \frac{e^{-bx_1}}{\sqrt[4]{x_1}} F_{\Gamma_{BRA}}(x_1) dx_1 \int_0^\infty \frac{e^{-bx_2}}{\sqrt[4]{x_2}} f_{\gamma_{BA}}(x_2) dx_2. \end{aligned} \tag{6.4}$$

Note that equation (6.4) provides an approximation in sum-BER since the CDFs of Γ_{BRA} and Γ_{ARB} are used.

To calculate sum-BER using the unified SNR representations, the distributions of Γ_{ARB}, Γ_{BRA}, γ_{AB}, and γ_{BA} should be obtained first. When we consider Rayleigh fading, $f_{\gamma_{AB}}(x) = e^{-x/\rho_{AB}}/\rho_{AB}$ and $f_{\gamma_{BA}}(x) = e^{-x/\rho_{BA}}/\rho_{BA}$ are given in [7], and the CDFs of Γ_{BRA} and Γ_{ARB} can be obtained by substituting $M_A = M_B = 1$ into equations (5.5) and (5.6), respectively, as follows:

$$F_{\Gamma_{BRA}}(x) = 1 - \frac{2x}{A_{BRA}}\sqrt{\frac{B_{BRA}C_{BRA}}{\rho_{BR}\rho_{RA}}}e^{-\frac{x}{A_{BRA}}\left(\frac{C_{BRA}}{\rho_{BR}}+\frac{B_{BRA}}{\rho_{RA}}\right)} K_1\left(\frac{2x}{A_{BRA}}\sqrt{\frac{B_{BRA}C_{BRA}}{\rho_{BR}\rho_{RA}}}\right) \tag{6.5}$$

$$F_{\Gamma_{ARB}}(x) = 1 - \frac{2x}{A_{ARB}}\sqrt{\frac{B_{ARB}C_{ARB}}{\rho_{AR}\rho_{RB}}}e^{-\frac{x}{A_{ARB}}\left(\frac{C_{ARB}}{\rho_{AR}}+\frac{B_{ARB}}{\rho_{RB}}\right)} K_1\left(\frac{2x}{A_{ARB}}\sqrt{\frac{B_{ARB}C_{ARB}}{\rho_{AR}\rho_{RB}}}\right), \tag{6.6}$$

where $K_\nu(x)$ is the modified Bessel function of the second kind.

As a result, once $f_{\gamma_{AB}}(x)$, $f_{\gamma_{BA}}(x)$, and equations (6.5) and (6.6) are substituted to equation (6.4), the sum-BER can be approximated in closed-

form with the integral in equation (5.8) as

$$P_b \approx \left[\frac{\Gamma\left(\frac{3}{4}\right)}{b^{\frac{3}{4}}} - \frac{8\sqrt{\pi}B_{ARB}C_{ARB}}{A_{ARB}^2\rho_{AR}\rho_{RB}\left(b + \frac{C_{ARB}}{A_{ARB}\rho_{AR}} + \frac{B_{ARB}}{A_{ARB}\rho_{RB}} + \frac{2}{A_{ARB}}\sqrt{\frac{B_{ARB}C_{ARB}}{\rho_{AR}\rho_{RB}}}\right)^{\frac{11}{4}}} \right.$$
$$\frac{a\sqrt{b}\Gamma\left(\frac{3}{4}\right)\Gamma\left(\frac{11}{4}\right)\Gamma\left(\frac{3}{4}\right)}{\log_2(M)\rho_{AB}\sqrt{8\pi}\left(b + \frac{1}{\rho_{AB}}\right)^{\frac{3}{4}}\Gamma\left(\frac{9}{4}\right)}$$
$$\left. {}_2F_1\left(\frac{11}{4}, \frac{3}{2}; \frac{9}{4}; \frac{b + \frac{C_{ARB}}{A_{ARB}\rho_{AR}} + \frac{B_{ARB}}{A_{ARB}\rho_{RB}} - \frac{2}{A_{ARB}}\sqrt{\frac{B_{ARB}C_{ARB}}{\rho_{AR}\rho_{RB}}}}{b + \frac{C_{ARB}}{A_{ARB}\rho_{AR}} + \frac{B_{ARB}}{A_{ARB}\rho_{RB}} + \frac{2}{A_{ARB}}\sqrt{\frac{B_{ARB}C_{ARB}}{\rho_{AR}\rho_{RB}}}}\right)\right]$$
$$+ \left[\frac{\Gamma\left(\frac{3}{4}\right)}{b^{\frac{3}{4}}} - \frac{8\sqrt{\pi}B_{BRA}C_{BRA}}{A_{BRA}^2\rho_{BR}\rho_{RA}\left(b + \frac{C_{BRA}}{A_{BRA}\rho_{BR}} + \frac{B_{BRA}}{A_{BRA}\rho_{RA}} + \frac{2}{A_{BRA}}\sqrt{\frac{B_{BRA}C_{BRA}}{\rho_{BR}\rho_{RA}}}\right)^{\frac{11}{4}}} \right.$$
$$\frac{a\sqrt{b}\Gamma\left(\frac{3}{4}\right)\Gamma\left(\frac{11}{4}\right)\Gamma\left(\frac{3}{4}\right)}{\log_2(M)\rho_{BA}\sqrt{8\pi}\left(b + \frac{1}{\rho_{BA}}\right)^{\frac{3}{4}}\Gamma\left(\frac{9}{4}\right)}$$
$$\left. {}_2F_1\left(\frac{11}{4}, \frac{3}{2}; \frac{9}{4}; \frac{b + \frac{C_{BRA}}{A_{BRA}\rho_{BR}} + \frac{B_{BRA}}{A_{BRA}\rho_{RA}} - \frac{2}{A_{BRA}}\sqrt{\frac{B_{BRA}C_{BRA}}{\rho_{BR}\rho_{RA}}}}{b + \frac{C_{BRA}}{A_{BRA}\rho_{BR}} + \frac{B_{BRA}}{A_{BRA}\rho_{RA}} + \frac{2}{A_{BRA}}\sqrt{\frac{B_{BRA}C_{BRA}}{\rho_{BR}\rho_{RA}}}}\right)\right] \tag{6.7}$$

where ${}_2F_1(\alpha, \beta; \gamma; z)$ is the Gauss hypergeometric function [37, p.1005]. Note that equation (6.7) provides tight sum-BER approximations for all two-way relay protocols with direct links. Note also that equation (6.7) presents much better performance than equation (5.7) regardless of protocols due to the performance contribution from direct links. Equation (6.7) can be used to obtain equation (5.7) by removing contribution from direct links, $\Gamma(3/4) / \left(\rho_{BA}\left(b + 1/\rho_{BA}\right)^{3/4}\right)$, in the second and fourth lines of equation (6.7), when $M_A = M_B = M_R = 1$.

6.2.3 High-SNR Analysis for Sum-BER using Unified SNR Representations

Simple high-SNR performance is now considered to further simplify equation (6.7). The high SNR analysis uses the PDFs of instantaneous SNRs

normalized by the average SNR on each link defined as $\lambda_{ARB} := \Gamma_{ARB}/\rho_{AR}$, $\lambda_{BRA} := \Gamma_{BRA}/\rho_{AR}$, $\lambda_{AB} := \gamma_{AB}/\rho_{AR}$, and $\lambda_{BA} := \gamma_{BA}/\rho_{AR}$ where ρ_{AR} is the average transmit SNR from A to R, and all PDFs are shown satisfying the assumptions in [34], which provides a systematic method for high-SNR analysis. To simplify our analysis, we assume that ρ_{AB}, ρ_{BA}, ρ_{BR}, ρ_{RA}, and ρ_{RB} are constant multiples of ρ_{AR}. Based on [34, eqn.(1)], the average sum-BER of an uncoded system can be written as

$$P_b = \frac{1}{\log_2(M)} \left((2b\rho_{AR}G_A)^{-d} + (2b\rho_{AR}G_B)^{-d} \right) + o\left(\rho_{AR}^{-d}\right), \tag{6.8}$$

as $\rho_{AR} \to \infty$, where $G_A = \left(\sqrt{\pi}\,(t_A+1) \,/\, (a2^{t_A}\eta_A\Gamma\,(t_A+3/2))\right)^{1/(t_A+1)}$ and $G_B = \left(\sqrt{\pi}\,(t_B+1) \,/\, (a2^{t_B}\eta_B\Gamma\,(t_B+3/2))\right)^{1/(t_B+1)}$ are the array gains; $d = t_A+1 = t_B+1$ are the diversity orders; t_A and t_B are the first nonzero derivative orders of the PDFs of channel dependent random variables, $\lambda_{ARB}+\lambda_{AB}$ and $\lambda_{BRA}+\lambda_{BA}$, at the origin, respectively; $\eta_A = f^{(t_A)}_{\lambda_{BRA}+\lambda_{BA}}(0)/\Gamma\,(t_A+1) \neq 0$ and $\eta_B = f^{(t_B)}_{\lambda_{ARB}+\lambda_{AB}}(0)/\Gamma\,(t_B+1) \neq 0$. The expression for η_A and η_B are also valid when t_A and t_B are not integers if fractional calculus is used [55]. Therefore, equation (6.9) can be calculated once t_A, t_B, η_A, and η_B are found using the PDFs of λ_{ARB}, λ_{BRA}, λ_{AB}, and λ_{BA}.

When $M_A = M_B = M_R = 1$, $t_A = t_B = 1$ due to the diversity order $d = 2$ [45, eqn.(16)]. Therefore, based on equation (3.17) and Appendix 3.4, η_A and η_B can be written as

$$\eta_A = f_{\lambda_{BA}}(0) f_{\lambda_{BRA}}(0) = \frac{\rho_{AR}}{\rho_{BA}} \left(\frac{B_{BRA}\rho_{AR}}{A_{BRA}\rho_{RA}} + \frac{C_{BRA}\rho_{AR}}{A_{BRA}\rho_{BR}} \right) \tag{6.9}$$

$$\eta_B = f_{\lambda_{AB}}(0) f_{\lambda_{ARB}}(0) = \frac{\rho_{AR}}{\rho_{AB}} \left(\frac{B_{ARB}\rho_{AR}}{A_{ARB}\rho_{RB}} + \frac{C_{ARB}}{A_{ARB}} \right), \tag{6.10}$$

where $f_{\lambda_{ARB}}(x) = e^{-x/B_{ARB}}/B_{ARB} + \rho_{AR}e^{-\rho_{AR}x/(C_{ARB}\rho_{RB})}/\,(C_{ARB}\rho_{RB})$, $f_{\lambda_{BRA}}(x)$ $= \rho_{AR}e^{-\rho_{AR}x/(B_{BRA}\rho_{BR})}/\,(B_{BRA}\rho_{BR}) + \rho_{AR}e^{-\rho_{AR}x/(C_{BRA}\rho_{RA})}/\,(C_{BRA}\rho_{RA})$, which can be obtained by substituting $M_A = M_B = 1$ into equation (5.46), $f_{\lambda_{AB}}(x) = \rho_{AR}e^{-\rho_{AR}x/\rho_{AB}}/\rho_{AB}$, and $f_{\lambda_{BA}}(x) = \rho_{AR}e^{-\rho_{AR}x/\rho_{BA}}/\rho_{BA}$.

As a consequence, high-SNR performance can be obtained as follows:

$$P_b = \frac{1}{\log_2(M)} \left((2b\rho_{AR} G_A)^{-2} + (2b\rho_{AR} G_B)^{-2} \right) + o\left(\rho_{AR}^{-2}\right) \tag{6.11}$$

$$G_A = \left(\frac{2a\eta_A \Gamma\left(\frac{5}{2}\right)}{2\sqrt{\pi}} \right)^{-\frac{1}{2}} \tag{6.12}$$

$$G_B = \left(\frac{2a\eta_B \Gamma\left(\frac{5}{2}\right)}{2\sqrt{\pi}} \right)^{-\frac{1}{2}}. \tag{6.13}$$

High-SNR performance for sum-BER given in equations (6.11)-(6.13) is much simpler than the closed-form approximations in equation (6.7), so that it is easy to evaluate sum-BER at high-SNR. Note that the diversity order of all three two-way relay systems is 2, and equations (6.11)-(6.13) provide tight sum-BER approximations for all two-way relay protocols with direct links. Compared with equation (5.18) when $M_A = M_B = M_R = 1$, the diversity order of equation (6.11) is 2 while that of equation (5.18) is 1, which leads equation (6.11) to have better performance than equation (5.18) at high SNR.

6.2.3.1 α-β Optimization

Similar to Chapter 5, we can obtain closed-form expressions using average high-SNR performance in equation (6.11). Therefore, after every variable is substituted into equation (6.11) and considering $\alpha^2 + \beta^2 = 1$, by differentiating equation (6.11) with respect to β, optimal βs for the first three-slot and second four-slot protocols can be obtained, respectively, as follows:

$$\beta^2_{three-slot} = \frac{\sqrt{\frac{\rho_{AR}(\rho_{AR}+\rho_{RA})}{\rho_{RA}}}}{\sqrt{\frac{\rho_{AR}(\rho_{AR}+\rho_{RA})}{\rho_{RA}}} + \sqrt{\frac{\rho_{BR}(\rho_{BR}+\rho_{RB})}{\rho_{RB}}}} \tag{6.14}$$

$$\beta^2_{four-slot} = \frac{\sqrt{\frac{\rho_{AR}(\rho_{AR}+\rho_{RA}/2)}{\rho_{RA}/2}}}{\sqrt{\frac{\rho_{AR}(\rho_{AR}+\rho_{RA}/2)}{\rho_{RA}/2}} + \sqrt{\frac{\rho_{BR}(\rho_{BR}+\rho_{RB}/2)}{\rho_{RB}/2}}}, \tag{6.15}$$

which are exactly same as equations (5.30) and (5.31). Both β^2s become $\frac{1}{2}$ when $\rho_{AR} = \rho_{BR} = \rho_{RA} = \rho_{RB}$, while β^2s are bigger than $\frac{1}{2}$ when $\rho_{AR} > \rho_{BR}$,

which indicates the α-β optimization is most useful when ρ_{AR} and ρ_{BR} are unbalanced. Note that these results are from average high-SNR performance, which leads to worse performance compared with numerically optimizing the instantaneous sum-BERs with respect to β. However, equations (6.14) and (6.15) do not require instantaneous channel knowledge and can be expressed in closed-form.

6.3 Multiple Antennas at All Nodes

When we consider multiple antennas at all nodes, BF optimization is necessary, at all nodes for the first three-slot protocol but only at A and B for four-slot protocols. In this case, there is no closed-form expression for performance analysis since optimal beamformers cannot be expressed in closed-form. In addition, BF optimization is well studied in Chapter 5. Therefore, we consider lower-bounds of all protocols with direct links, where each node utilizes two distinct BF vectors *matched* with corresponding channels, to compare each other.

To clarify how Table 6.2 can be obtained, the instantaneous received SNRs are discussed for the second four-slot protocol as an example. The instantaneous received SNRs for the second four-slot protocol at A and B are as follows, respectively:

$$\gamma_{BRA} = \gamma_{BRA,1} + \gamma_{BRA,2} = \frac{\beta^2 \gamma_{BR} \frac{\gamma_{RA}}{2}}{\beta^2 \gamma_{BR} + \alpha^2 \gamma_{AR} + \frac{\gamma_{RA}}{2} + 1} + \frac{\beta^2 \gamma_{BR} \frac{\gamma'_{RA}}{2}}{\beta^2 \gamma_{BR} + \alpha^2 \gamma_{AR} + \frac{\gamma'_{RA}}{2} + 1} \tag{6.16}$$

$$\gamma_{ARB} = \gamma_{ARB,1} + \gamma_{ARB,2} = \frac{\alpha^2 \gamma_{AR} \frac{\gamma_{RB}}{2}}{\alpha^2 \gamma_{AR} + \beta^2 \gamma_{BR} + \frac{\gamma_{RB}}{2} + 1} + \frac{\alpha^2 \gamma_{AR} \frac{\gamma'_{RB}}{2}}{\alpha^2 \gamma_{AR} + \beta^2 \gamma_{BR} + \frac{\gamma'_{RB}}{2} + 1}, \tag{6.17}$$

where $\gamma'_{RA} = \rho_{RA} \|\mathbf{H}_{RA}\mathbf{f}_{RB}\|^2$ and $\gamma'_{RB} = \rho_{RB} \|\mathbf{H}_{RB}\mathbf{f}_{RA}\|^2$, which are instantaneous received SNRs with *non-matched* BF vectors. With the same rea-

son as Table 5.2, $D_{BRA,4} = 1 + \mathbb{E}[\gamma_{BRA,2}]/\mathbb{E}[\gamma_{BRA,1}]$ and $D_{ARB,4} = 1 + \mathbb{E}[\gamma_{ARB,2}]/\mathbb{E}[\gamma_{ARB,1}]$ can be obtained for the second four-slot protocol.

Table 6.2: The Coefficients for Equations (6.1) and (6.2) when Multiple Antennas are Used at All Nodes

Constants	A_{BRA}	B_{BRA}	C_{BRA}	A_{ARB}	B_{ARB}	C_{ARB}
First Three	β^2	β^2	$1+\frac{\alpha^2\rho_{AR}}{\rho_{RA}}$	α^2	α^2	$1+\frac{\beta^2\rho_{BR}}{\rho_{RB}}$
First Four	$\frac{1}{2}$	1	$\frac{1}{2}$	$\frac{1}{2}$	1	$\frac{1}{2}$
Second Four	$\frac{\beta^2 D_{BRA,4}}{2}$	β^2	$\frac{1}{2}+\frac{\alpha^2\rho_{AR}}{\rho_{RA}}$	$\frac{\alpha^2 D_{ARB,4}}{2}$	α^2	$\frac{1}{2}+\frac{\beta^2\rho_{BR}}{\rho_{RB}}$

6.3.1 Performance Analysis

We now consider performance analysis using the unified received SNRs when multiple antennas are used at all nodes. Similar to obtaining equation (6.7), the distributions of the unified received SNRs for multiple antennas at all nodes should be attained to calculate sum-BER. The CDFs of Γ_{BRA} and Γ_{ARB} can be obtained as equations (5.24) and (5.25):

$$F_{\Gamma_{BRA}}(x) = 1 - \sum_{n=1}^{M_R} \sum_{m=M_B-M_R}^{(M_B+M_R)n-2n^2} \sum_{k=0}^{m} \sum_{i=1}^{M_R} \sum_{j=M_A-M_R}^{(M_A+M_R)i-2i^2} \sum_{p=0}^{k+j} \binom{k+j}{p} \frac{2d_{n,m}d_{i,j}}{k!j!\rho_{BR}^{\frac{p+k+1}{2}}\rho_R^{\frac{2j+k-p+1}{2}}} \frac{(C_{BRA}n)^{\frac{p+k+1}{2}}(B_{BRA}i)^{\frac{2j+k-p+1}{2}}}{A_{BRA}^{k+j+1}} x^{k+j+1} e^{-\frac{x}{A_{BRA}}\left(\frac{C_{BRA}n}{\rho_{BR}}+\frac{B_{BRA}i}{\rho_R}\right)} K_{p-k+1}\left(\frac{2x}{A_{BRA}}\sqrt{\frac{B_{BRA}C_{BRA}ni}{\rho_{BR}\rho_R}}\right) \tag{6.18}$$

$$F_{\Gamma_{ARB}}(x) = 1 - \sum_{n=1}^{M_R} \sum_{m=M_A-M_R}^{(M_A+M_R)n-2n^2} \sum_{k=0}^{m} \sum_{i=1}^{M_R} \sum_{j=M_B-M_R}^{(M_B+M_R)i-2i^2} \sum_{p=0}^{k+j} \binom{k+j}{p} \frac{2d_{n,m}d_{i,j}}{k!j!\rho_{AR}^{\frac{p+k+1}{2}}\rho_R^{\frac{2j+k-p+1}{2}}} \frac{(C_{ARB}n)^{\frac{p+k+1}{2}}(B_{ARB}i)^{\frac{2j+k-p+1}{2}}}{A_{ARB}^{k+j+1}} x^{k+j+1} e^{-\frac{x}{A_{ARB}}\left(\frac{C_{ARB}n}{\rho_{AR}}+\frac{B_{ARB}i}{\rho_R}\right)} K_{p-k+1}\left(\frac{2x}{A_{ARB}}\sqrt{\frac{B_{ARB}C_{ARB}ni}{\rho_{AR}\rho_R}}\right), \tag{6.19}$$

where $d_{n,m}$ are coefficients given by [30, eqn.(24)], also provided in Tables 2.1-2.3 for completeness. Note that equations (6.18) and (6.19) are valid when

$M_A \geq M_R$ and $M_B \geq M_R$ even though other cases can be easily handled with minor modifications.

In addition, the PDFs of γ_{AB} and γ_{BA} are given as follows from equation (2.36):

$$f_{\gamma_{AB}}(x) = \sum_{n=1}^{M_B} \sum_{m=M_A-M_B}^{(M_A+M_B)n-2n^2} \frac{d_{n,m} n^{m+1} x^m e^{-\frac{nx}{\rho_{AB}}}}{m! \rho_{AB}^{m+1}} \tag{6.20}$$

$$f_{\gamma_{BA}}(x) = \sum_{n=1}^{M_A} \sum_{m=M_B-M_A}^{(M_B+M_A)n-2n^2} \frac{d_{n,m} n^{m+1} x^m e^{-\frac{nx}{\rho_{BA}}}}{m! \rho_{BA}^{m+1}} \tag{6.21}$$

Therefore, once equations (6.18)-(6.21) are substituted to equation (6.4), the sum-BER can be obtained in closed-form similar to equation (6.7), which are sum-BER lower-bounds for all protocols with direct links. When multiple antennas are used at all nodes, the performance using equations (6.18)-(6.21) is much better than that using equations (5.24) and (5.25) due to the effect of direct links.

6.3.2 High-SNR Analysis

Based on the procedures in Section 3.4.2, we should calculate the t_A order derivative of the PDF of $\lambda_{BRA} + \lambda_{BA}$ and the t_B order derivative of the PDF of $\lambda_{ARB} + \lambda_{AB}$ evaluated at the origin, both evaluated at the origin, to obtain high-SNR performance when multiple antennas are used at all nodes. Using multiple antennas, however, the PDFs of $\lambda_{BRA}+\lambda_{BA}$ and $\lambda_{ARB}+\lambda_{AB}$ are difficult to obtain in closed-form. Instead of using the PDFs of $\lambda_{BRA}+\lambda_{BA}$ and $\lambda_{ARB}+\lambda_{AB}$, an alternate approach is used to find η_A and η_B for the combined links. We have $t_A = t_B = M_R \cdot \min\{M_A, M_B\} + M_A \cdot M_B - 1$ since the diversity orders of the combined links are $M_R \cdot \min\{M_A, M_B\} + M_A \cdot M_B$ [45, eqn.(16)], which are the sums of the diversity orders of the direct and relay links. To

find $f^{(t_A)}_{\lambda_{BRA}+\lambda_{BA}}(0)$ and $f^{(t_B)}_{\lambda_{ARB}+\lambda_{AB}}(0)$, the product of $f^{(t_{BRA})}_{\lambda_{BRA}}(0)$ and $f^{(t_{BA})}_{\lambda_{BA}}(0)$ and that of $f^{(t_{ARB})}_{\lambda_{ARB}}(0)$ and $f^{(t_{AB})}_{\lambda_{AB}}(0)$ can be used, respectively.

For the $A \to R \to B$ path, $t_{ARB} = M_R \cdot \min\{M_A, M_B\} - 1$ since the diversity order of the $A \to R \to B$ path is $M_R \cdot \min\{M_A, M_B\}$ [45, eqn.(16)]. The t_{ARB} order derivative of the PDF of λ_{ARB} evaluated at the origin can be obtained as follows (Please see Appendix 5.2 for derivation):

$$f^{(t_{ARB})}_{\lambda_{ARB}}(0) = \begin{cases} f^{(t_{RB})}_{\lambda_{RB}}(0), & M_A > M_B \\ f^{(t_{AR})}_{\lambda_{AR}}(0), & M_A < M_B \\ f^{(t_{AR})}_{\lambda_{AR}}(0) + f^{(t_{RB})}_{\lambda_{RB}}(0), & M_A = M_B \end{cases}, \tag{6.22}$$

where

$$f^{(t_{AR})}_{\lambda_{AR}}(0) = \sum_{n=1}^{M_R} \sum_{m=M_A-M_R}^{(M_A+M_R)n-2n^2} d_{n,m} \binom{t_{AR}}{m} (-1)^{t_{AR}+m} \left(\frac{nC_{ARB}}{A_{ARB}}\right)^{t_{AR}+1}, \tag{6.23}$$

$$f^{(t_{RB})}_{\lambda_{RB}}(0) = \sum_{n=1}^{M_R} \sum_{m=M_B-M_R}^{(M_B+M_R)n-2n^2} d_{n,m} \binom{t_{RB}}{m} (-1)^{t_{RB}+m} \left(\frac{n\rho_{AR}B_{ARB}}{A_{ARB}\rho_R}\right)^{t_{RB}+1}, \tag{6.24}$$

and $t_{AR} = M_A \cdot M_R - 1$ and $t_{RB} = M_B \cdot M_R - 1$ [45, eqn.(12)] are the first nonzero derivative orders of the PDFs of $\lambda_{AR} := \gamma_{AR}/\rho_{AR}$ and $\lambda_{RB} := \gamma_{RB}/\rho_{AR}$, at the origin, respectively.

Similarly, for the $B \to R \to A$ path, $t_{BRA} = M_R \cdot \min\{M_A, M_B\} - 1$ since the diversity order of the $B \to R \to A$ path is $M_R \cdot \min\{M_A, M_B\}$. The t_{BRA} order derivative of the PDF of λ_{BRA} evaluated at the origin can be obtained as (please see Appendix 5.2 for derivation)

$$f^{(t_{BRA})}_{\lambda_{BRA}}(0) = \begin{cases} f^{(t_{BR})}_{\lambda_{BR}}(0), & M_A > M_B \\ f^{(t_{RA})}_{\lambda_{RA}}(0), & M_A < M_B \\ f^{(t_{BR})}_{\lambda_{BR}}(0) + f^{(t_{RA})}_{\lambda_{RA}}(0), & M_A = M_B \end{cases}, \tag{6.25}$$

where

$$f_{\lambda_{BR}}^{(t_{BR})}(0) = \sum_{n=1}^{M_R} \sum_{m=M_B-M_R}^{(M_B+M_R)n-2n^2} d_{n,m} \binom{t_{BR}}{m} (-1)^{t_{BR}+m} \left(\frac{n\rho_{AR} C_{BRA}}{A_{BRA}\rho_{BR}} \right)^{t_{BR}+1}, \tag{6.26}$$

$$f_{\lambda_{RA}}^{(t_{RA})}(0) = \sum_{n=1}^{M_R} \sum_{m=M_A-M_R}^{(M_A+M_R)n-2n^2} d_{n,m} \binom{t_{RA}}{m} (-1)^{t_{RA}+m} \left(\frac{n\rho_{AR} B_{BRA}}{A_{BRA}\rho_{R}} \right)^{t_{RA}+1}, \tag{6.27}$$

and $t_{BR} = M_B \cdot M_R - 1$, $t_{RA} = M_A \cdot M_R - 1$ [45, eqn.(12)] are the first nonzero derivative orders of the PDFs of $\lambda_{BR} := \gamma_{BR}/\rho_{AR}$ and $\lambda_{RA} := \gamma_{RA}/\rho_{AR}$, at the origin, respectively.

For the direct links, $t_{BA} = t_{AB} = M_A \cdot M_B - 1$ since the diversity orders of $B \to A$ and $A \to B$ are given by $M_A \cdot M_B$ [6]. If the t_{BA} and t_{AB} order derivatives of the PDFs of λ_{BA} and λ_{AB} are evaluated at the origin, the following can be obtained

$$f_{\lambda_{AB}}^{(t_{AB})}(0) = \sum_{n=1}^{M_B} \sum_{m=M_A-M_B}^{(M_A+M_B)n-2n^2} d_{n,m} \binom{t_{AB}}{m} (-1)^{t_{AB}+m} \left(\frac{n\rho_{AR}}{\rho_{AB}} \right)^{t_{AB}+1} \tag{6.28}$$

$$f_{\lambda_{BA}}^{(t_{BA})}(0) = \sum_{n=1}^{M_A} \sum_{m=M_B-M_A}^{(M_B+M_A)n-2n^2} d_{n,m} \binom{t_{BA}}{m} (-1)^{t_{BA}+m} \left(\frac{n\rho_{AR}}{\rho_{BA}} \right)^{t_{BA}+1}. \tag{6.29}$$

Using equations (6.22)-(6.29), therefore, the final combined η_A and η_B are given by

$$\alpha_A = \frac{f_{\lambda_{BRA}}^{(t_{BRA})}(0) \cdot f_{\lambda_{BA}}^{(t_{BA})}(0)}{\Gamma\left(M_A \cdot M_B + M_R \cdot \min\{M_A, M_B\}\right)} \tag{6.30}$$

$$\alpha_B = \frac{f_{\lambda_{ARB}}^{(t_{ARB})}(0) \cdot f_{\lambda_{AB}}^{(t_{AB})}(0)}{\Gamma\left(M_A \cdot M_B + M_R \cdot \min\{M_A, M_B\}\right)}. \tag{6.31}$$

As a consequence, high-SNR performance can be obtained as follows:

$$P_b = \frac{1}{\log_2(M)} \left((2b\rho_{AR} G_A)^{-d} + (2b\rho_{AR} G_B)^{-d} \right) + o\left(\rho_{AR}^{-d}\right) \tag{6.32}$$

$$d = M_R \cdot \min\{M_A, M_B\} + M_A \cdot M_B \tag{6.33}$$

$$G_A = \left(\frac{a 2^{d-1} \eta_A \Gamma\left(d + \frac{1}{2}\right)}{\sqrt{\pi} d} \right)^{-\frac{1}{d}} \tag{6.34}$$

$$G_B = \left(\frac{a 2^{d-1} \eta_B \Gamma\left(d + \frac{1}{2}\right)}{\sqrt{\pi} d} \right)^{-\frac{1}{d}}. \tag{6.35}$$

Note that the diversity order of all three two-way relay systems with direct links is $M_R \cdot \min\{M_A, M_B\} + M_A \cdot M_B$, and equations (6.32)-(6.35) provide sum-BER lower-bounds for all two-way relay protocols with direct links. Note also that equation (6.32) can be used to obtain equation (5.18) by removing contribution from direct links, $M_A \cdot M_B$, $f_{\lambda_{AB}}^{(t_{AB})}(0)$, and $f_{\lambda_{AB}}^{(t_{BA})}(0)$. Due to different diversity orders, equation (6.32) presents much better performance than equation (5.18) regardless of protocols.

6.4 Stochastic Ordering of AF MIMO BF Two-Way Relay Networks

In what follows, we compare performance of AF MIMO BF two-way relay networks with and without direct links using the theory of stochastic orders in terms of sum-BER and maximum sum-rate since the authors in [71] never consider MIMO and two-way relay systems. We start with stochastic ordering preliminaries.

6.4.1 Preliminaries

We explore "integral stochastic order", which can be used in communication systems. The integral stochastic order is defined as [75]

$$X \leq_{\Re} Y \Leftrightarrow \mathbb{E}\left[g(X)\right] \leq \mathbb{E}\left[g(Y)\right], \forall g(\cdot) \in \Re, \tag{6.36}$$

where X and Y are RVs and $\Re$ is a set of real valued functions such as $g(\cdot) : \mathbb{R}^+ \rightarrow \mathbb{R}$, which is a generator of the integral stochastic order, $\leq_{\Re}$. Since there are more than one generator, we show a few of them herein.

For the first example, the magnitude of two RVs can be compared by the "usual stochastic order", which is defined by

$$X \leq_{st} Y \Leftrightarrow F_X(x) \geq F_Y(x), \forall x, \tag{6.37}$$

where $F_X(x)$ and $F_Y(x)$ are CDFs of X and Y, respectively. This order means that comparing X and Y with respect to $\leq_{st}$ corresponds to comparing their outage probabilities for all thresholds. The generator for the usual stochastic order in equation (6.36) is the set of increasing functions [75].

For the second example, the "convex ordering" denoted as $X \leq_{cx} Y$ is presented, where the generator in equation (6.36) is the set of convex functions. Since $\mathbb{E}[X] = \mathbb{E}[Y]$ when X and Y are convex ordered and $\leq_{cx}$ gives us a measure of variability, $X \leq_{cx} Y$ means X is less variable than Y even though the RVs have same mean value. Actually, convex ordering of two RVs can provide a qualitative measure of average performance because many performance metrics such as channel capacity and error rates are convex or concave functions of instantaneous SNRs.

For the third example, the "Laplace transform order" is considered as

$$X \leq_{Lt} Y \Leftrightarrow \mathbb{E}\left[\exp\left(-\rho X\right)\right] \geq \mathbb{E}\left[\exp\left(-\rho Y\right)\right], \forall \rho \geq 0. \tag{6.38}$$

In this case, the generator in equation (6.36) is the set of $-\exp\left(-\rho x\right), \forall \rho \geq 0$. More generally, when $g(x)$ is a *completely monotonic* (*c.m.*) function, $(-1)^n d^n g(x)/dx^n \geq 0$ for $x > 0$ and $n = 0, 1, 2, \ldots$, equation (6.38) becomes

$$X \leq_{Lt} Y \Leftrightarrow \mathbb{E}\left[g\left(X\right)\right] \geq \mathbb{E}\left[g\left(Y\right)\right]. \tag{6.39}$$

Furthermore, when $g(x)$ is a *completely monotonic derivative* (*c.m.d.*) function, $(-1)^n d^n (dg(x)/dx)/dx^n \geq 0$ for $x > 0$ and $n = 0, 1, 2, \ldots$, equation (6.38) becomes

$$X \leq_{Lt} Y \Leftrightarrow \mathbb{E}\left[g\left(X\right)\right] \leq \mathbb{E}\left[g\left(Y\right)\right]. \tag{6.40}$$

Based on careful investigations, it is beneficial to recognize that $X \leq_{cx} Y \Rightarrow Y \leq_{Lt} X$ and $X \leq_{st} Y \Rightarrow X \leq_{Lt} Y$ for any of two RVs, X and Y.

6.4.2 Stochastic Ordering

Using the Laplace transform order, we compare sum-BER and maximum sum-rate of two-way AF MIMO BF relay networks with and without direct links. Without loss of generality, we assume $\rho = \rho_{AR} = \rho_{BR} = \rho_{RA} = \rho_{RB} = \rho_{AB} = \rho_{BA} \geq 0$ for transmit SNRs at each node in two-way relay networks. Therefore, all RVs for two-way relay networks in Chapters 5 and 6 can be written as $\gamma_{AR} = \gamma_{RA} = \rho\lambda_{AR}$, $\gamma_{BR} = \gamma_{RB} = \rho\lambda_{BR}$, and $\gamma_{AB} = \gamma_{BA} = \rho\lambda_{AB}$ for simplicity. As an example, $g(x)$ using the unified received SNR representations at A and B for two-way AF MIMO BF relay networks without direct links, equations (5.1) and (5.2), can be rewritten as

$$g_{BRA}(\mathbf{x}) = \frac{A_{BRA}x_1x_2}{B_{BRA}x_1 + C_{BRA}x_2 + \frac{1}{\rho}} \tag{6.41}$$

$$g_{ARB}(\mathbf{x}) = \frac{A_{ARB}x_1x_2}{B_{ARB}x_2 + C_{ARB}x_1 + \frac{1}{\rho}}, \tag{6.42}$$

where $\mathbf{x} := [x_1\ x_2]$, RVs $X_1 := \lambda_{BR}$ and $X_2 := \lambda_{AR}$ are statistically independent, and A_{ARB}, B_{ARB}, C_{ARB}, A_{BRA}, B_{BRA}, and C_{BRA} are non-negative constants in Table 5.2.

When multiple RVs are considered, reference [71] provides the following mathematical tool:

Theorem 6.1. *Let RVs $X_1, X_2, \ldots, X_N$ be statistically independent and RVs $Y_1, Y_2, \ldots, Y_N$ be also statistically independent. If $X_n \leq_{Lt} Y_n$ for $n = 1, 2, \ldots, N$, then $g(X_1, X_2, \ldots, X_N) \leq_{Lt} g(Y_1, Y_2, \ldots, Y_N)$ for $g(\cdot) : \mathbb{R}^m \to \mathbb{R}^+$ such that $\partial g(x_1, x_2, \ldots, x_N)/\partial x_n$ is c.m. for $n = 1, 2, \ldots, N$ when all other variables are fixed.*

Since $\partial g_{BRA}(\mathbf{x})/\partial x_n$ and $\partial g_{ARB}(\mathbf{x})/\partial x_n$ using equations (6.41) and (6.42) are c.m. for $n = 1, 2$ (i.e. as seen by taking multiple derivatives) based on **Theorem 6.1** given by [71], we can say that $g_{BRA}(\mathbf{X}) \leq_{Lt} g_{BRA}(\mathbf{Y})$ and $g_{ARB}(\mathbf{X}) \leq_{Lt} g_{ARB}(\mathbf{Y})$ if $X_n \leq_{Lt} Y_n$ for $n = 1, 2$, where $\mathbf{X} := [X_1\ X_2]$ and $\mathbf{Y} := [Y_1\ Y_2]$.

Similar to the previous example, we can apply the Laplace transform order to two-way AF MIMO BF relay networks with direct link as well. If we consider the relay networks illustrated in Figure 6.1, unified instantaneous received SNR expressions in equations (6.1) and (6.2) can be rewritten as follows:

$$g_A(\mathbf{x}) = \frac{A_{BRA}x_1x_2}{B_{BRA}x_1 + C_{BRA}x_2 + \frac{1}{\rho}} + x_3 \tag{6.43}$$

$$g_B(\mathbf{x}) = \frac{A_{ARB}x_1x_2}{B_{ARB}x_2 + C_{ARB}x_1 + \frac{1}{\rho}} + x_3, \tag{6.44}$$

where $\mathbf{x} := [x_1\ x_2\ x_3]$, and RVs $X_1 := \lambda_{BR}$, $X_2 := \lambda_{AR}$, and $X_3 := \lambda_{AB}$ are statistically independent. Based on **Theorem 6.1** given by [71], since $\partial g_A(\mathbf{x})/\partial x_n$ and $\partial g_B(\mathbf{x})/\partial x_n$ using equations (6.43) and (6.44) are c.m. for $n = 1, 2, 3$ (i.e. as seen by taking multiple derivatives), we can say that $g_A(\mathbf{X}) \leq_{Lt} g_A(\mathbf{Y})$ and $g_B(\mathbf{X}) \leq_{Lt} g_B(\mathbf{Y})$ if $X_n \leq_{Lt} Y_n$ for $n = 1, 2, 3$, where $\mathbf{X} := [X_1\ X_2\ X_3]$ and $\mathbf{Y} := [Y_1\ Y_2\ Y_3]$.

Since we are interested in sum-BER and maximum sum-rate, we consider the following metrics:

$$P_b = \frac{a}{\log_2(M)}\left(\mathbb{E}\left[Q\left(\sqrt{2b\rho g_A(\mathbf{X})}\right) + Q\left(\sqrt{2b\rho g_B(\mathbf{X})}\right)\right]\right) \tag{6.45}$$

$$R = \frac{1}{T}\left(\mathbb{E}\left[\log_2\left(1 + \rho g_A(\mathbf{X})\right) + \log_2\left(1 + \rho g_B(\mathbf{X})\right)\right]\right), \tag{6.46}$$

where T is the number of time slots used. By comparing $g_A(\mathbf{X})$ and $g_A(\mathbf{Y})$, and $g_B(\mathbf{X})$ and $g_B(\mathbf{Y})$, separately, using the Laplace transform order, we can obtain the following theorem:

Theorem 6.2. *Let RVs $X_1, X_2, \ldots, X_N$ be statistically independent and RVs $Y_1, Y_2, \ldots, Y_N$ be also statistically independent, and let $\mathbf{X} := [X_1\ X_2\ \ldots\ X_N]$ and $\mathbf{Y} := [Y_1\ Y_2\ \ldots\ Y_N]$. If $X_n \leq_{Lt} Y_n$ for $n = 1, 2, \ldots, N$, then*

$$\mathbb{E}\left[P_b\left(\rho g_A\left(\mathbf{X}\right)\right) + P_b\left(\rho g_B\left(\mathbf{X}\right)\right)\right] \geq \mathbb{E}\left[P_b\left(\rho g_A\left(\mathbf{Y}\right)\right) + P_b\left(\rho g_B\left(\mathbf{Y}\right)\right)\right] \tag{6.47}$$

$$\mathbb{E}\left[R\left(\rho g_A\left(\mathbf{X}\right)\right) + R\left(\rho g_B\left(\mathbf{X}\right)\right)\right] \leq \mathbb{E}\left[R\left(\rho g_A\left(\mathbf{Y}\right)\right) + R\left(\rho g_B\left(\mathbf{Y}\right)\right)\right] \tag{6.48}$$

for $g(\cdot) : \mathbb{R}^m \rightarrow \mathbb{R}^+$ such that $\partial g\left(x_1, x_2, \ldots, x_N\right)/\partial x_n$ is c.m. for $n = 1, 2, \ldots, N$ when all other variables are fixed.

Proof. Since $P_b(\rho x) := Q\left(\sqrt{2b\rho x}\right)$ is c.m. and $R(\rho x) := \log_2\left(1 + \rho x\right)$ is c.m.d. [71], if $g_A\left(\mathbf{X}\right) \leq_{Lt} g_A\left(\mathbf{Y}\right)$ and $g_B\left(\mathbf{X}\right) \leq_{Lt} g_B\left(\mathbf{Y}\right)$ when $X_n \leq_{Lt} Y_n$ for $n = 1, 2, \ldots, N$, $\mathbb{E}\left[P_b\left(\rho g_A\left(\mathbf{X}\right)\right)\right] \geq \mathbb{E}\left[P_b\left(\rho g_A\left(\mathbf{Y}\right)\right)\right]$ and $\mathbb{E}\left[P_b\left(\rho g_B\left(\mathbf{X}\right)\right)\right] \geq \mathbb{E}\left[P_b\left(\rho g_B\left(\mathbf{Y}\right)\right)\right]$ based on equation (6.39), and $\mathbb{E}\left[R\left(\rho g_A\left(\mathbf{X}\right)\right)\right] \leq \mathbb{E}\left[R\left(\rho g_A\left(\mathbf{Y}\right)\right.\right.$ $\left.\left.\right)\right]$ and $\mathbb{E}\left[R\left(\rho g_B\left(\mathbf{X}\right)\right)\right] \leq \mathbb{E}\left[R\left(\rho g_B\left(\mathbf{Y}\right)\right)\right]$ based on equation (6.40). Therefore, **Theorem 6.2** is proved when above relevant expectations are added. □

The same result can be obtained for AF MIMO BF two-way relay networks without direct link using the Laplace transform order. For example, if we consider the number of relay antennas in Rayleigh fading, $X \leq_{Lt} Y$ if $M_R^X \leq M_R^Y$, where large M_R presents better performance in sum-BER and sum-rate, which can be easily seen based on our average performance in closed-form. As another example, if we consider Rician fading, the average sum-BER and sum-rate improve as the line of sight (LoS) parameter K increases [71]. Therefore, we can say that $X \leq_{Lt} Y$ if $K^X \leq K^Y$, which means large K provides better performance in sum-BER and sum-rate, as illustrated in Section 6.5. Note that we can compare two average quantities using the Laplace transform order even though the average performance of sum-BER and sum-rate is not tractable in closed-form for Rician fading.

6.5 Numerical and Simulation Results

In Monte-Carlo simulations, the transmitted symbol is QPSK, 8-QAM, or 16-QAM modulated for two-slot, three-slot, four-slot protocols, respectively, for rate normalization. The two-slot protocol without direct links is included as a benchmark. Zero mean and unit variance are used to model the Rayleigh or Rician block fading channel. The distance between A and R is set as a reference d_0 whereas the distance between A and B is d. Therefore, once d_0 is determined, $10\log_{10}(\rho_{BR}) = 10\log_{10}(\rho_{AR}) - 10\gamma\log_{10}((1-d_0)/d_0)$, where γ is the path-loss exponent of the simplified path-loss model in [7]. We also consider strong and weak direct links using a scaling factor in simulations. Note that average transmit SNR is normalized in unified received SNR expressions for fair comparison among all protocols.

6.5.1 Accuracy of Analysis

This subsection shows the accuracy of our analysis in equations (6.7), (6.11), (6.14), (6.15), (6.32), and the analysis using equations (6.18)-(6.21). Figures 6.3 and 6.4 show $1 \times 1 \times 1$ and $2 \times 2 \times 2$ AF two-way relay network performance in sum-BER when the path-loss exponent $\gamma = 3$ and both average transmit SNRs are balanced (i.e. $\rho_{AR} = \rho_{BR}$ due to $d_0 = 0.5$), respectively. All simulation curves in Figure 6.3 are from Monte-Carlo simulations while all simulation curves in Figure 6.4 are from numerical simulations. All analytical curves of three protocols in Figure 6.3 are from equation (6.7) with proper constants given in Table 6.1, but all analytical curves of three protocols in Figure 6.4 are from using equations (6.18)-(6.21) with proper constants given in Table 6.2. All high-SNR analytical curves in Figures 6.3 and 6.4 are from equations (6.11) and (6.32), respectively. Our high-SNR analysis matches exactly with

Monte-Carlo simulations at high-SNR, and our analysis is within 0.2 dB in Figures 6.3 and 6.4. Note that sum-BER performance in equations (6.7) and using equations (6.18)-(6.21) provides tight approximations to equation (6.3). Note also that performance using the first four-slot protocol is exactly same as that using the second four-slot protocol in Figure 6.3.

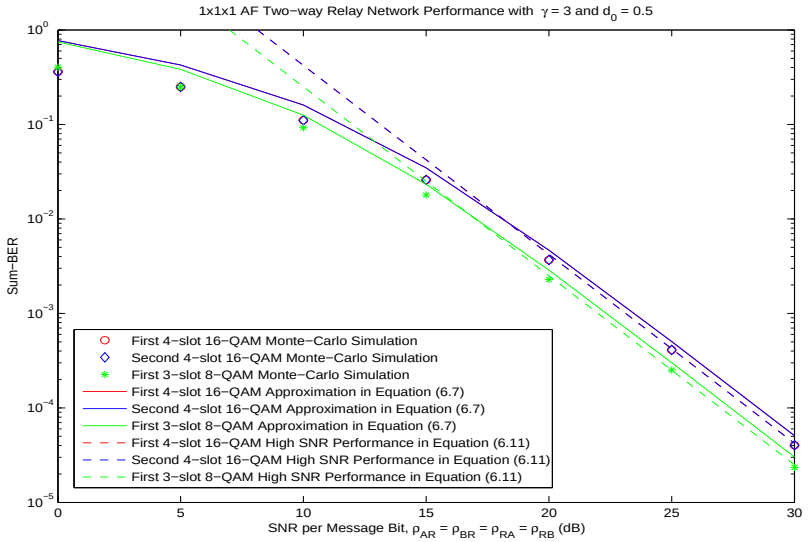

Figure 6.3: $1 \times 1 \times 1$ AF Two-Way Relay Network Performance in Sum-BER when $\gamma = 3$ and $d_0 = 0.5$.

Figure 6.5 shows the optimal average β^2 for the first three-slot and second four-slot protocols at high-SNR using equation (6.11) for $1 \times 1 \times 1$ AF two-way relay network performance with $\rho_{AR} = \rho_{RA} = \rho_{RB} = 40$ dB when average transmit SNRs are unbalanced (i.e. $\rho_{AR} \neq \rho_{BR}$ due to $d_0 = 0.3$). Using the same setup, analytical results in equations (6.14) and (6.15) present $\beta^2 = 0.82915$ and $\beta^2 = 0.85159$ for the first three-slot and second four-slot protocols, respectively.

Figure 6.6 shows $1 \times 1 \times 1$ AF two-way relay network performance in sum-BER when average transmit SNRs are unbalanced. All simulation curves

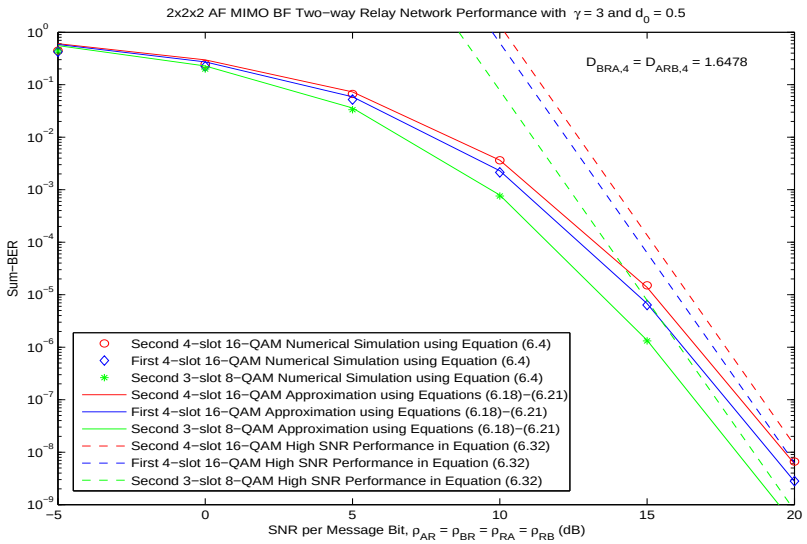

Figure 6.4: $2 \times 2 \times 2$ AF Two-Way Relay Network Performance in Sum-BER when $\gamma = 3$ and $d_0 = 0.5$.

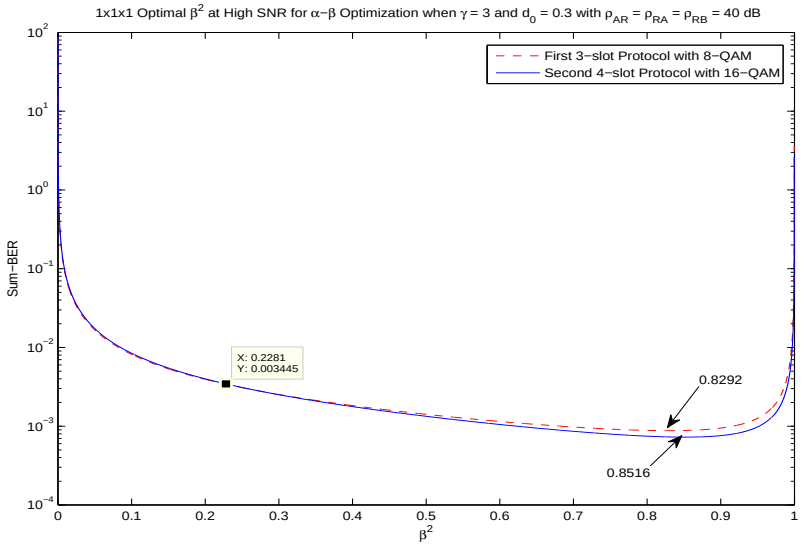

Figure 6.5: Optimal β^2 at High-SNR for $1 \times 1 \times 1$ AF Two-Way Relay Network Performance with $\rho_{AR} = 40$ dB when $\gamma = 3$ and $d_0 = 0.3$.

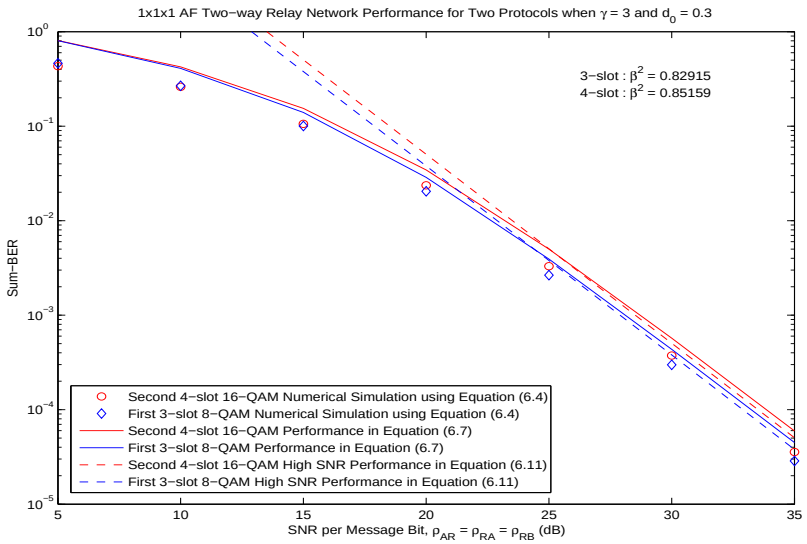

Figure 6.6: $1 \times 1 \times 1$ AF Two-Way Relay Network Performance in Sum-BER when $\gamma = 3$ and $d_0 = 0.3$.

in Figure 6.6 are from numerical simulations using equation (6.4), where the optimal βs are selected based on instantaneous channel realization. All analytical curves of two protocols are from equation (6.7) with proper constants. All high-SNR analytical curves are from equation (6.11) with related constants. $\beta^2 = 0.82915$ and $\beta^2 = 0.85159$ are used for optimal values at high-SNR using equation (6.11) for the first three-slot and second four-slot protocols, respectively. The optimal βs are chosen to minimize average high-SNR performance in our analysis. Our analysis in equation (6.7) matches exactly with high-SNR analysis in equation (6.11). However, about 1 dB gaps exist between our analysis and numerical simulations at high-SNR due to choice of optimal βs.

6.5.2 Comparisons of Protocols

This subsection compares sum-BER performance among three relaying protocols. Note that α-β optimization is performed when average transmit SNRs are unbalanced, for the first three-slot and second four-slot protocols.

Figure 6.7 shows $1 \times 1 \times 1$ AF two-way relay network performance comparison when $\gamma = 3$ and $d_0 = 0.3$. All simulation curves are from numerical simulations using equation (6.4) with α-β optimization. All analytical curves are from equation (6.7) with proper constants. Note that the first three-slot and second four-slot protocols need to find optimal α and β satisfying $\alpha^2 + \beta^2 = 1$ for instantaneous minimum sum-BER. The first three-slot protocol with optimal α and β and normalized rate outperforms other protocols at high-SNR in Figure 6.7.

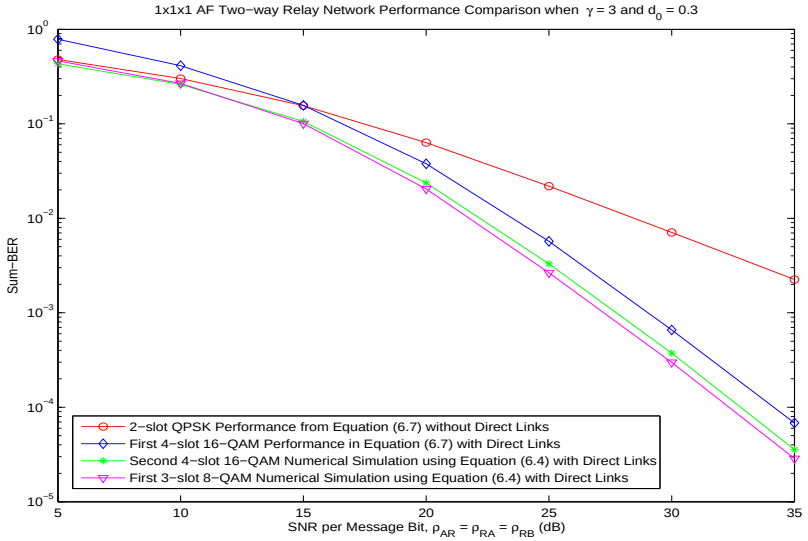

Figure 6.7: $1 \times 1 \times 1$ AF Two-Way Relay Network Performance Comparison in Sum-BER when $\gamma = 3$ and $d_0 = 0.3$.

Figure 6.8 shows $2 \times 2 \times 2$ AF MIMO BF two-way relay network performance comparison when $\gamma = 3$, $\rho_{AB} = \rho_{BA} = \rho_{AR}/10^6$, and $d_0 = 0.3$. All simulation curves are from numerical simulations using equation (6.4) with α-β optimization. All analytical curves are from using equations (6.18)-(6.21) with proper constants. Note that the first three-slot and second four-slot protocols need to find optimal α and β satisfying $\alpha^2 + \beta^2 = 1$ for instantaneous

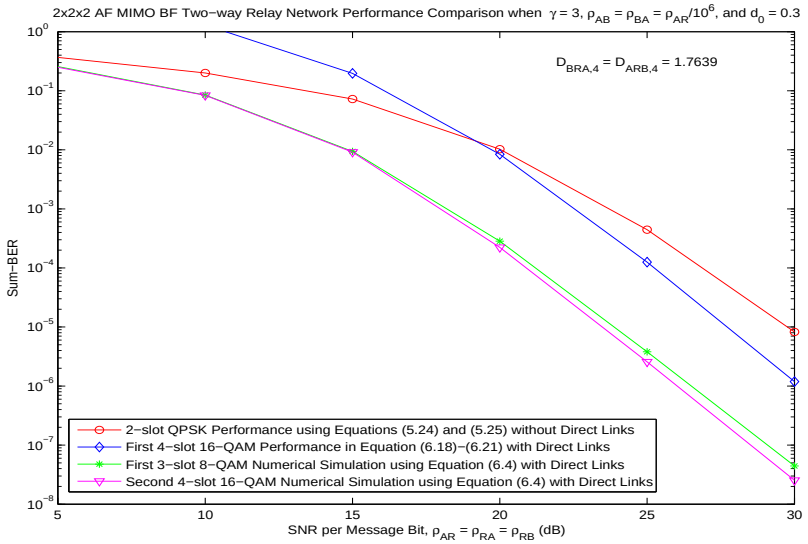

Figure 6.8: $2 \times 2 \times 2$ AF Two-Way Relay Network Performance Comparison in Sum-BER when $\gamma = 3$, $\rho_{AB} = \rho_{BA} = \rho_{AR}/10^6$, and $d_0 = 0.3$.

minimum sum-BER. The second four-slot protocol with optimal α and β and normalized rate outperforms other protocols at high-SNR in Figure 6.8.

Based on simulations, note that all protocols with direct links outperform the two-slot protocol without direct links for all scenarios. The second four-slot protocol dominates other protocols when direct links hardly help the total performance (i.e. $\rho_{AB} = \rho_{BA} = \rho_{AR}/10^6$), whereas the first three-slot dominates other protocols otherwise.

6.5.3 Stochastic Ordering

This subsection illustrates stochastic ordering of sum-BER and maximum sum-rate for two-way relay protocols with and without direct links presented in Section 6.4.2. We use Rician fading with the LoS parameters $K^X = 1$ and $K^Y = 3$ to show the usefulness of stochastic ordering since the average performance of sum-BER and sum-rate is not tractable in closed-form for Ri-

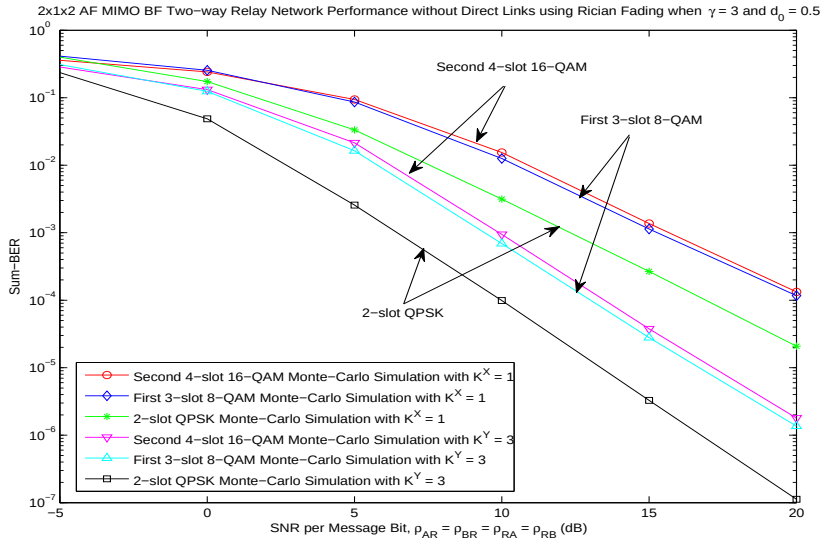

Figure 6.9: $2 \times 1 \times 2$ AF MIMO BF Two-Way Relay Network Performance in Sum-BER without Direct Links when $\gamma = 3$ and $d_0 = 0.5$.

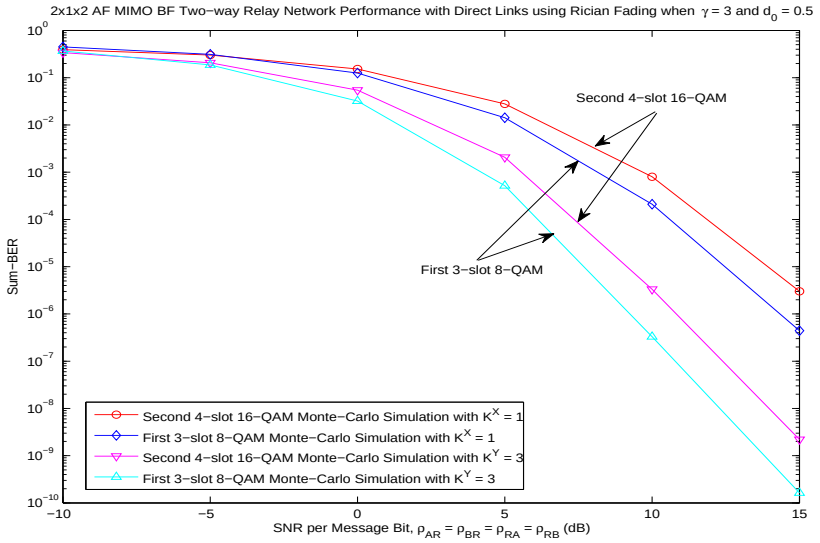

Figure 6.10: $2 \times 1 \times 2$ AF MIMO BF Two-Way Relay Network Performance in Sum-BER with Direct Links when $\gamma = 3$ and $d_0 = 0.5$.

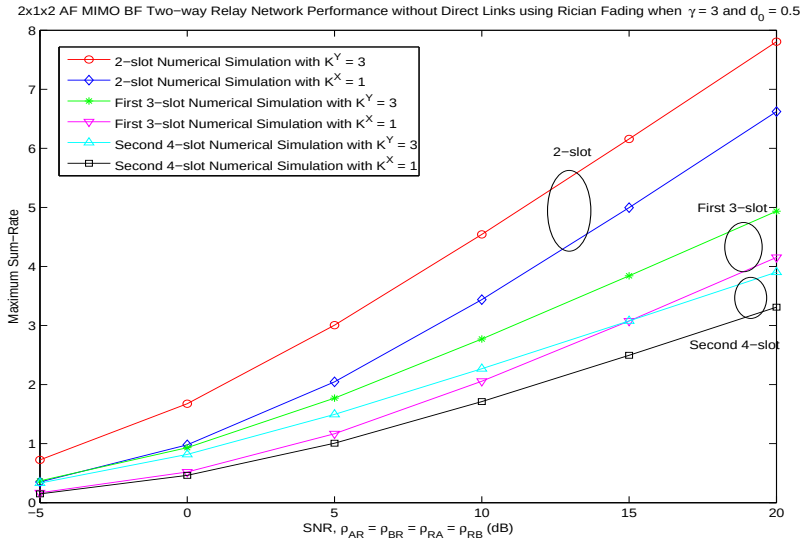

Figure 6.11: $2 \times 1 \times 2$ AF MIMO BF Two-Way Relay Network Performance in Sum-Rate without Direct Links when $\gamma = 3$ and $d_0 = 0.5$.

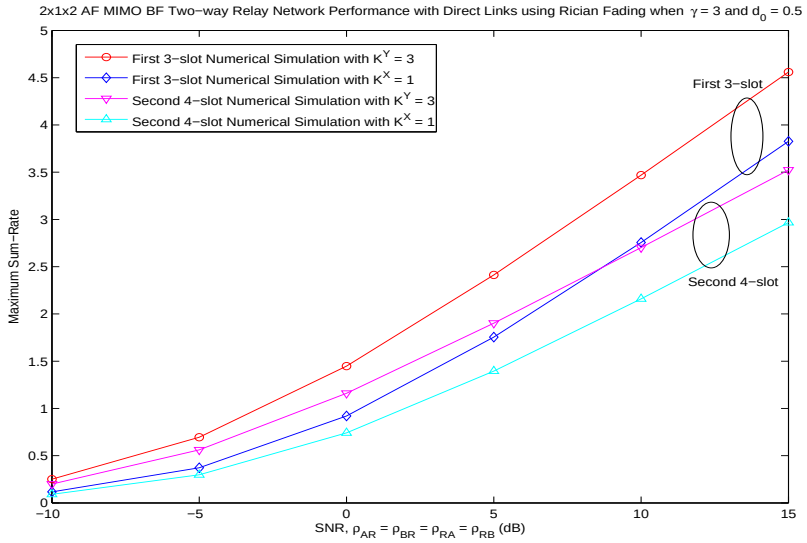

Figure 6.12: $2 \times 1 \times 2$ AF MIMO BF Two-Way Relay Network Performance in Sum-Rate with Direct Links when $\gamma = 3$ and $d_0 = 0.5$.

cian fading. Figures 6.9 and 6.10 show $2 \times 2 \times 2$ AF MIMO BF two-way relay network performance in sum-BER with and without direct links, respectively, when $\gamma = 3$ and $d_0 = 0.5$. From Figures 6.9 and 6.10, large K (i.e. K^Y) provides better performance in sum-BER for all protocols regardless of direct links, which matches with results in Section 6.4.2.

Figures 6.11 and 6.12 show $2 \times 2 \times 2$ AF MIMO BF two-way relay network performance in sum-rate with and without direct links, respectively, when $\gamma = 3$ and $d_0 = 0.5$. From Figures 6.11 and 6.12, large K (i.e. K^Y) provides better performance in sum-rate for all protocols regardless of direct links, which matches with results in Section 6.4.2 as well.

6.6 Chapter Summary

Unified performance analysis and stochastic ordering have been conducted for AF MIMO BF two-way relay networks with direct links using three different relaying protocols. After introducing the two-way relaying protocols with direct links, novel closed-form unified sum-BER expressions have been presented with corresponding closed-form unified CDFs. Furthermore, new closed-form unified high-SNR performance expressions have been provided for simplicity and mathematical tractability. Stochastic ordering of sum-BER and maximum sum-rate is also provided using the unified expressions of AF MIMO BF two-way relay networks with and without direct links.

Based on analytical and simulation results, we have investigated the performance of three different protocols with three or four time slots using the sum-BER metric. As a result, we can conclude that all protocols with direct links dominate the two-slot protocol without direct links, and the three-slot protocol outperforms other protocols at high-SNR when direct links are con-

sidered, while the four-slot protocol outperforms other protocols at high-SNR when direct links cannot contribute much to the total performance if average transmit SNRs are unbalanced. Finally, stochastic ordering can compare two average quantities even when the average performance is not tractable in closed-form, and it is shown that a large Los parameter K can provide better performance in sum-BER and sum-rate for all two-way relay protocols.

Chapter 7

Conclusions

The combined performance is analyzed for AF/DF two-hop MIMO beamforming relay networks using one-way relay protocols. Since the solution for optimal BF coefficients not only is difficult to implement, it also does not lend itself to performance analysis because the optimal BF coefficients cannot be expressed in closed-form when beamforming to both relay and destination, the suboptimal strong-path BF and new selection relaying with strong-path BF are considered under the different CSI assumptions. In addition to presenting novel selection relaying, the performance analysis including high SNR analysis for strong-path BF is conducted in BERs/SERs for the first time. When 4 antennas are used for the source and destination and one antenna is used for the relay, simulations show that strong-path BF slightly outperforms the optimized BF performance and selection relaying with strong-path BF performance is about 1 dB away from the optimized BF performance at the reasonable error rate. Note that full CSI is available for strong-path BF and the optimized BF but partial CSI is known for selection relaying with strong-path BF.

Novel lower-bounds of AF/DF MIMO BF relay networks are presented with known CSI of the relay link at the source and destination. It is shown that the lower-bound is achievable at the expense of a rate penalty, and the achievable scheme using three time slots is also analyzed for AF/DF MIMO BF fixed two-hop relay networks for the first time. When the CSI of the relay link is not available at the source and destination, selection relaying is considered, in which the optimal SNR threshold is used. New high SNR performance is

also analyzed for AF relay networks to simplify the lower-bound via diversity and array gain expressions. Simulations show that lower-bounds are about 1 dB better than the optimized BF performance and AF relaying performance is better than DF relaying performance at high SNR. The availability or the CSI at the source and destination is crucial in BER/SER performance.

Novel average BER/SER bounds are obtained for systems with instantaneous SNRs given by a sum of N statistically independent non-negative RVs using the AM and GM inequality. Their tightness is quantified analytically at high SNR by calculating the SNR gap, and shown to be within $O(1/N)$ of the true value for large N. The bounds are most useful when the distribution of the sum is intractable, since they do not require finding the combined PDFs or CDFs of the sum. The bounds are illustrated with the MRC, the combined average performance for AF relay networks using multiple relays, and AF MIMO single relay systems with BF using multiple antennas at the source, relay, and destination. In addition, applicability of the bounds to non-Gaussian noise is addressed, and the tightness of the bounds is confirmed graphically. Simulations show that the bounds are tight at high SNR for all examples even when the RVs are spread out.

Unified performance analysis is conducted for AF MIMO BF two-way relay networks with five different relaying protocols. Two novel relaying protocols are introduced using three and four time slots suitable for BF. Unified CDFs and PDFs are provided and the closed-form sum-BER expression is obtained as a result. Due to simplicity and mathematical tractability, high SNR performance expressions are presented for sum-BER and the analytical high-SNR gap expression is provided. BF optimization is also discussed for sum-BER since multiple antennas are used at all nodes. We investigate the

performance of the five protocols with two, three, or four time slots using the metrics of sum-BER, and show that the proposed three-slot and four-slot protocols outperform the existing two-slot, three-slot, four-slot protocols in sum-BER for some practical scenarios with beamforming, while the two-slot scheme is better than the proposed protocols when a single relay antenna is used with balanced transmit powers. Therefore, the proposed protocols give a excellent comprise with the two-slot protocol in sum-BER.

Finally, unified performance analysis and stochastic ordering have been conducted for AF MIMO BF two-way relay networks with direct links using three different relaying protocols. After introducing the two-way relaying protocols with direct links, novel closed-form unified sum-BER expressions have been presented with corresponding closed-form unified CDFs. Furthermore, new closed-form unified high-SNR performance expressions have been provided for simplicity and mathematical tractability. Stochastic ordering of sum-BER and sum-rate is also provided using the unified expressions of AF MIMO BF two-way relay networks with and without direct links. In this case, we can say that all protocols with direct links dominate the two-slot protocol without direct links, and the four-slot protocol outperforms other protocols at high-SNR when direct links cannot contribute much to the total performance if average transmit SNRs are unbalanced, whereas the three-slot protocol outperforms other protocols at high-SNR otherwise. Stochastic ordering can compare two average quantities even when the average performance is not tractable in closed-form, and it is shown that a large Los parameter K can provide better performance in sum-BER and sum-rate for all two-way relay protocols.

REFERENCES

[1] A. J. Paulraj, D. A. Gore, R. U. Nabar, and H. Bolcskei, "An overview of MIMO communications - A key to gigabit wireless." *Proceedings of the IEEE*, vol. 92, no. 2, pp. 198–218, 2004.

[2] J. H. Winters, "On the capacity of radio communications systems with diversity in Rayleigh fading environments." *IEEE Journal on Selected Areas in Communications*, vol. 5, no. 5, pp. 871–878, 1987.

[3] G. L. Stuber, J. R. Barry, S. W. McLaughlin, Y. Li, M. A. Ingram, and T. G. Pratt, "Broadband MIMO-OFDM wireless communications." *Proceedings of the IEEE*, vol. 92, no. 2, pp. 271–294, 2004.

[4] Q. Li, G. Li, W. Lee, M. Lee, D. Mazzarese, B. Clerckx, and Z. Li, "MIMO techniques in WiMAX and LTE: a feature overview." *IEEE Communications Megazine*, vol. 48, no. 5, pp. 86–92, 2010.

[5] L. Eastwood, S. Migaldi, Q. Xie, and V. Gupta, "Mobility using IEEE 802.21 in a heterogeneous IEEE 802.16/802.11-based, IMT-advanced (4G) network." *IEEE Wireless Communications*, vol. 15, no. 2, pp. 26–34, 2008.

[6] T. K. Y. Lo, "Maximum ratio transmission." *IEEE Transactions on Communications*, vol. 47, no. 10, pp. 1458–1461, 1999.

[7] A. Goldsmith, *Wireless Communications.* Cambridge University Press, 2005.

[8] C. Lu, F. H. P. Fitzek, P. C. F. Eggers, O. K. Jensen, G. F. Pedersen, and T. Larsen, "Terminal-embedded beamforming for wireless local area networks." *IEEE Wireless Communications*, vol. 15, no. 2, pp. 82–91, 2008.

[9] E. Matskani, N. D. Sidiropoulos, Z. Luo, and L. Tassiulas, "Efficient batch and adaptive approximation algorithms for joint multicast beamforming and admission control." *IEEE Transactions on Signal Processing*, vol. 57, no. 12, pp. 4882–4894, 2009.

[10] Z. Chen, M. Peng, W. Wang, and H. H. Chen, "Cooperative base station beamforming in WiMAX systems." *IET Communications*, vol. 4, no. 9, pp. 1049–1058, 2010.

[11] J. N. Laneman, D. N. C. Tse, and G. W. Wornell, "Cooperative diversity in wireless networks: Efficient protocols and outage behavior." *IEEE Transactions on Information Theory*, vol. 50, no. 12, pp. 3062–3080, 2004.

[12] A. Sendonaris, E. Erkip, and B. Aazhang, "User cooperation diversity-Part I: System description." *IEEE Transactions on Communications*, vol. 51, no. 11, pp. 1927–1938, 2003.

[13] ——, "User cooperation diversity-Part II: Implementation aspects and performance analysis." *IEEE Transactions on Communications*, vol. 51, no. 11, pp. 1939–1948, 2003.

[14] T. Saito, Y. Tanaka, and T. Kato, "Trends in LTE/WiMAX systems." *Fujitsu Scientific and Technical Journal*, vol. 45, no. 4, pp. 355–362, 2009.

[15] Y. Yang, H. Hu, J. Xu, and G. Mao, "Relay technologies of WiMAX and LTE-advanced mobile systems." *IEEE Communications Magazine*, vol. 47, no. 10, pp. 100–105, 2009.

[16] J. Sydir and R. Taori, "An evolved cellular system architecture incorporating relay stations." *IEEE Communications Magazine*, vol. 47, no. 6, pp. 115–121, 2009.

[17] A. Ghosh, R. Ratasuk, B. Mondal, and N. Mangalvedhe, "LTE-advanced: next-generation wireless broadband technology." *IEEE Wireless Communications*, vol. 17, no. 3, pp. 10–22, 2010.

[18] M. Salem, A. Adinoyi, M. Rahman, H. Yanikomeroglu, D. Falconer, and Y. Kim, "Fairness-aware radio resource management in downlink OFDMA cellular relay networks." *IEEE Transactions on Wireless Communications*, vol. 9, no. 5, pp. 1628–1639, 2010.

[19] P. Popovski and H. Yomo, "Wireless network coding by amplify-and-forward for bi-directional traffic flows." *IEEE Communications Letters*, vol. 11, no. 1, pp. 16–18, 2007.

[20] Q. Li, S. H. Ting, A. Pandharipande, and Y. Han, "Adaptive two-way relaying and outage analysis." *IEEE Transactions on Wireless Communications*, vol. 8, no. 6, pp. 3288–3299, 2009.

[21] R. H. Y. Louie, Y. Li, and B. Vucetic, "Practical physical layer network coding for two-way relay channels: Performance analysis and comparison." *IEEE Transactions on Wireless Communications*, vol. 9, no. 2, pp. 764–777, 2010.

[22] S. W. Peters, A. Y. Panah, K. T. Truong, and R. W. Heath Jr., "Relay architectures for 3GPP LTE-advanced." *EURASIP Journal on Wireless Communications and Networking*, vol. 2009, article ID 618787, 14 pages, doi:10.1155/2009/618787, 2009.

[23] S. W. Peters and R. W. Heath Jr., "The future of WiMAX: multihop relaying with IEEE 802.16j." *IEEE Communications Magazine*, vol. 47, no. 1, pp. 104–111, 2009.

[24] J. G. Proakis, *Digital Communications.* McGraw Hill, 2000.

[25] M. K. Simon and M. S. Alouini, *Digital Communication over Fading Channels.* Wiley-IEEE Press, 2005.

[26] M. K. Simon, *Probability Distributions Involving Gaussian Random Variables.* Springer, 2006.

[27] M. K. Simon and M. S. Alouini, *Digital Communication over Fading Channels: A Unified Approach to Performance Analysis.* Wiley, 2005.

[28] T. M. Duman and A. Ghrayeb, *Coding for MIMO Communication Systems.* Wiley, 2007.

[29] R. H. Y. Louie, Y. Li, and B. Vucetic, "Performance analysis of beamforming in two hop amplify and forward relay networks." *Proceedings of ICC*, pp. 4311–4315, 2008.

[30] P. A. Dighe and R. K. Mallik, "Analysis of transmit-receive diversity in Rayleigh fading." *IEEE Transactions on Communications*, vol. 51, no. 4, pp. 694–703, 2003.

[31] B. Khoshnevis, W. Yu, and R. Adve, "Grassmannian beamforming for MIMO amplify-and-forward relaying." *IEEE Journal on Selected Areas on Communications*, vol. 26, no. 8, pp. 1397–1407, 2008.

[32] S. M. Kay, *Fundamentals of Statistical Signal Processing: Detection Theory.* Prentice Hall, 1998.

[33] T. Wang, A. Cano, G. B. Giannakis, and J. N. Laneman, "High-performance cooperative demodulation with decode-and-forward relays." *IEEE Transactions on Communications*, vol. 55, no. 7, pp. 1427–1438, 2007.

[34] Z. Wang and G. B. Giannakis, "A simple and general parameterization quantifying performance in fading channels." *IEEE Transactions on Communications*, vol. 51, no. 8, pp. 1389–1398, 2003.

[35] R. H. Y. Louie, Y. Li, H. A. Suraweera, and B. Vucetic, "Performance analysis of beamforming in two hop amplify and forward relay networks with antenna correlation." *IEEE Transactions on Wireless Communications*, vol. 8, no. 6, pp. 3132–3141, 2009.

[36] D. J. Love. Grassmannian Subspace Packing. [Online]. Available: http://cobweb.ecn.purdue.edu/∼djlove/grass.html

[37] I. S. Gradshteyn and I. M. Ryzhik, *Table of Integrals, Series, and Products.* Academic Press, 2007.

[38] A. Papoulis and S. U. Pillai, *Probability, Random Variables, and Stochastic Processes.* McGraw Hill, 2002.

[39] J. B. Kim and D. Kim, "Performance of dual-hop amplify-and-forward beamforming and its equivalent systems in Rayleigh fading channels." *IEEE Transactions on Communications*, vol. 58, no. 3, pp. 729–732, 2010.

[40] Y. Rong and F. Gao, "Optimal beamforming for non-generative MIMO relays with direct link." *IEEE Communications Letters*, vol. 13, no. 12, pp. 926–928, 2009.

[41] D. Chen and J. N. Laneman, "Cooperative diversity for wireless fading channels without channel state information." *Proceedings of Asilomar Conference*, pp. 1307–1312, 2004.

[42] H. Kim and C. Tepedelenlioğlu, "Performance analysis in AF/DF relay networks with beamforming." *Proceedings of Asilomar Conference*, pp. 534–538, 2009.

[43] ——, "Performance analysis in AF/DF relay networks with strong-path beamforming." *Proceedings of ICASSP*, pp. 3262–3265, 2010.

[44] M. R. McKay, A. J. Grant, and I. B. Collings, "Performance analysis of MIMO-MRC in double-correlated Rayleigh environments." *IEEE Transactions on Communications*, vol. 55, no. 3, pp. 497–507, 2007.

[45] H. Kim and C. Tepedelenlioğlu, "Performance analysis of MIMO beamforming AF relay networks using multiple relay antennas." *Proceedings of Asilomar Conference*, pp. 1874–1878, 2010.

[46] Y. Chen and C. Tellambura, "Distribution functions of selection combiner output in equally correlated Rayleigh, Rician, and Nakagami-m fading channels." *IEEE Transactions on Communications*, vol. 52, no. 11, pp. 1948–1956, 2004.

[47] P. A. Anghel and M. Kaveh, "Exact symbol error rate probability of a cooperative network in a Rayleigh-fading environment." *IEEE Transactions on Wireless Communications*, vol. 3, no. 5, pp. 1416–1421, 2004.

[48] S. Atapattu, N. Rajatheva, and C. Tellambura, "Performance analysis of TDMA relay protocols over Nakagami-m fading." *IEEE Transactions on Vehicular Technology*, vol. 59, no. 1, pp. 93–104, 2003.

[49] J. B. Kim and D. Kim, "Performance of dual-hop amplify-and-forward beamforming and its equivalent systems in Rayleigh fading channels." *IEEE Transactions on Communications*, vol. 58, no. 3, pp. 729–732, 2010.

[50] N. H. Vien and H. H. Nguyen, "Performance analysis of fixed-gain amplify-and-forward relaying with MRC." *IEEE Transactions on Vehicular Technology*, vol. 59, no. 3, pp. 1544–1552, 2010.

[51] T. Q. Duong, H. J. Zepernick, and V. N. Q. Bao, "Symbol error probability of hop-by-hop beamforming in Nakagami-m fading." *IET Electornics Letters*, vol. 45, no. 20, pp. 1042–1044, 2009.

[52] G. K. Karagiannidis, T. A. Tsiftsis, and N. C. Sagias, "A closed-form upper-bound for the distribution of the weighted sum of Rayleigh variates." *IEEE Communications Letters*, vol. 9, no. 7, pp. 589–591, 2005.

[53] G. K. Karagiannidis, T. A. Tsiftsis, and R. K. Mallik, "Bounds for multihop relayed communications in Nakagami-m fading." *IEEE Transactions on Communications*, vol. 54, no. 1, pp. 18–22, 2006.

[54] C. Tepedelenlioğlu and P. Gao, "On diversity reception over fading channels with impulsive noise." *IEEE Transactions on Vehicular Technology*, vol. 54, no. 6, pp. 2037–2047, 2005.

[55] S. G. Samko, A. A. Kilbas, and O. I. Marichev, *Fractional Integrals and Derivatives: Thoery and Applications.* Taylor and Francis, 1993.

[56] D. J. Love and R. W. Heath Jr., "Grassmannian beamforming for multiple-input multiple-output wireless systems." *IEEE Transactions on Information Theory*, vol. 49, no. 10, pp. 2735–2747, 2003.

[57] B. Rankov and A. Wittneben, "Spectral efficient protocols for half-duplex fading relay channels." *IEEE Journal on Selected Areas in Communications*, vol. 25, no. 2, pp. 379–389, 2007.

[58] P. Popovski and H. Yomo, "Physical network coding in two-way wireless relay channels." in *Proc. IEEE International Conference on Communications*, Glasgow, Scotland, 2007, pp. 707–711.

[59] Y. Han, S. H. Ting, C. K. Ho, and W. H. Chin, "Performance bounds for two-way amplify-and-forwar relaying." *IEEE Transactions on Wireless Communications*, vol. 8, no. 1, pp. 432–439, 2009.

[60] H. Guo, J. Ge, and H. Ding, "Symbol error probability of two-way amplify-and-forward relaying." *IEEE Communications Letters*, vol. 15, no. 1, pp. 22–24, 2011.

[61] H. Guo and L. Wang, "Performance analysis of two-way amplify-and-forward relaying with beamforming over Nakagami-m fading channels." in *Proc. IEEE WiCOM*, Wuhan, China, 2011, pp. 1–4.

[62] N. Lee, H. Park, and J. Chun, "Linear precoder and decoder design for two-way AF MIMO relaying system." in *Proc. IEEE Vehicular Technology Conference*, Barcelona, Spain, 2008, pp. 1221–1225.

[63] N. Lee, C. B. Chae, O. Simeone, and J. Kang, "On the optimization of two-way AF MIMO relay channel with beamforming." in *Proc. IEEE Asilomar Conference*, Pacific Grove, CA, 2010, pp. 918–922.

[64] X. Wang and X. D. Zhang, "Optimal beamforming in MIMO two-way relay channels." in *Proc. IEEE Global Telecommunications Conference*, Miami, FL, 2010, pp. 1–5.

[65] A. Y. Panah and J. R. W. Heath, "MIMO two-way amplify-and-forward relaying with imperfect receiver CSI." *IEEE Transactions on Vehicular Technology*, vol. 59, no. 9, pp. 4377–4387, 2010.

[66] H. Kim and C. Tepedelenlioğlu, "Performance bounds on average error rates using the AM-GM inequality and their applications in relay networks." *IEEE Transactions on Wireless Communications*, vol. PP, no. 99, pp. 1–10, 2012.

[67] S. Boyd and L. Vandenberghe, *Convex Optimization.* Cambridge University Press, 2004.

[68] H. Shen, B. Li, M. Tao, and X. Wang, "Mse-based transceiver designs for the MIMO interference channel." *IEEE Transactions on Wireless Communications*, vol. 9, no. 11, pp. 3480 – 3489, 2010.

[69] J. C. Park, J. S. Wang, and Y. H. Kim, "Rate and outage performance of non-regenerative two-way relaying protocols with direct link." in *Proc. IEEE Vehicular Technology Conference*, San Francisco, CA, 2011, pp. 1–5.

[70] H. Ding, J. Ge, D. B. da Costa, and Z. Jiang, "Two birds with one stone: Exploiting direct link for multiuser two-way relaying systems." *IEEE Transactions on Wireless Communications*, vol. 11, no. 1, pp. 54–59, 2012.

[71] C. Tepedelenlioğlu, A. Rajan, and Y. Zhang, "Applications of stochastic ordering ot wireless communications." *IEEE Transactions on Wireless Communications*, vol. 10, no. 12, pp. 4249–4257, 2011.

[72] M. Shaked and J. G. Shanthikumar, *Stochastic Orders and Their Applications.* Academic Press, 1994.

[73] D. Tse, R. Yates, and Z. Li, "Fading broadcast channels with state information at the receivers." in *Proc. IEEE Allerton Conference*, Monticello, IL, 2008, pp. 221–227.

[74] N. Levy, O. Somekh, S. Sharmai, and O. Zeitouni, "On certain large random Hermitian Jacobi matrices with applications to wireless communications." *IEEE Transactions on Information Theory*, vol. 55, no. 4, pp. 1534–1554, 2009.

[75] A. Müller and D. Stoyan, *Comparison Methods for Stochastic Models and Risks.* Wiley, 2002.